

A DOSIMETRIC MODEL FOR SMALL-FIELD ELECTRON RADIATION
THERAPY

A CREATIVE PROJECT (3 SEMESTER HOURS)
SUBMITTED TO THE GRADUATE SCHOOL
IN PARTIAL FULFILLMENT OF THE REQUIREMENTS
FOR THE DEGREE
MASTER OF ARTS
BY
GREGORY K. POLSTON

DEPARTMENT OF PHYSICS
ADVISOR: DR. THOMAS H. ROBERTSON
BALL STATE UNIVERSITY
MUNCIE, INDIANA
NOVEMBER 2008

Table of Contents

Abstract	ii
List of Figures	iii
List of Tables	iv
Acknowledgements	v
Chapter 1: Introduction	1
Chapter 2: Literature Review	3
2.1. Dose Measurements	3
2.2. MapCHECK vs Ionization Chambers	4
2.3. MapCHECK vs Film Dosimetry	6
Chapter 3: Experimental Methods	8
3.1. MapCHECK Calibrations	8
3.2. Experimental Variables	9
3.3. Setup Parameters	9
Chapter 4: Experimental Results	11
4.1 Cutout Factors	11
4.2. Beam Profiles	13
4.2.1. Square and Rectangular Beam Profiles	13
4.2.2. Circular Beam Profiles	21
Chapter 5: Summary and Conclusions	28
References	30
Appendix A	31
Appendix B	68
Appendix C	105

Research: A Dosimetric Model for Small-Field Electron Radiation Therapy
Paper

Student: Gregory K. Polston

Degree: Master of Arts

College: Sciences and Humanities

Date: November, 2008

Pages: 141

The collection of patient specific dosimetric data is a time consuming but necessary process for radiation therapy treatments using small-electron fields. This paper presents data that has been measured for specific field shapes and sizes that closely approximate many of those used clinically. The data presents cutout factors and beam profiles constructed from measurements obtained with a 2-D array. For use clinically, the patient's field will be compared to that of one of the small-electron fields created in this research. Use of the beam profiles will allow the clinicians to optimally design small-electron fields knowing the radiation field width and beam penumbras. The penumbras ranged from 5.75 mm for a 3-cm x 3-cm 100-cm SSD 15-MeV square to 15.75 mm for a 3-cm 110-cm SSD 6-MeV circle. This data matches the theory for penumbra characteristics for electron fields.

List of Figures

Figure 1: Beam's Eye View of MapCHECK	3
Figure 2: Farmer-type Ionization Chamber	4
Figure 3: Parallel-Plate Ionization Chamber.....	4
Figure 4: Film artifacts created by misalignment of the film in the phantom. The effects of (A) air gaps between the film and the phantom, (B) film edge extending beyond the phantom, and (C) film edge recessed within the phantom (Dutreix, 1969).....	6
Figure 5: Solid Water Phantom.....	9
Figure 6: Comparison of depth dose curves measured with a diode and an ion chamber (Khan, 2003)	10
Figure 7: 3-cm x 3-cm 100-cm SSD 6-MeV Profile	14
Figure 8: 3-cm x 3-cm 105-cm SSD 6-MeV Profile	15
Figure 9: 3-cm x 3-cm 110-cm 6-MeV Profile	15
Figure 10: 3-cm x 3-cm 100-cm SSD 6-MeV Profile	16
Figure 11: 3-cm x 3-cm 100-cm 9-MeV Profile	17
Figure 12: 3-cm x 3-cm 100-cm SSD 12-MeV Profile	17
Figure 13: 3-cm x 3-cm 100-cm 15-MeV Profile	18
Figure 14: 3-cm x 3-cm 100-cm SSD 6-MeV Profile	19
Figure 15: 4-cm x 4-cm 100-cm SSD 6-MeV Profile	19
Figure 16: 5-cm x 5-cm 100-cm SSD 6-MeV Profile	20
Figure 17: 3-cm 100-cm SSD 6-MeV Profile	21
Figure 18: 3-cm 105-cm SSD 6-MeV Profile	22
Figure 19: 3-cm 110-cm SSD 6-MeV Profile	22
Figure 20: 3-cm 100-cm SSD 6-MeV Profile	23
Figure 21: 3-cm 100-cm SSD 9-MeV Profile	24
Figure 22: 3-cm 100-cm SSD 12-MeV Profile	24
Figure 23: 3-cm 100-cm SSD 15-MeV Profile	25
Figure 24: 3-cm 100-cm SSD 6-MeV Profile	26
Figure 25: 4-cm 100-cm SSD 6-MeV Profile	26
Figure 26: 5-cm 100-cm SSD 6-MeV Profile	27

List of Tables

Table 1: Cutout Factors for 100-cm SSD, 105-cm SSD, and 110-cm SSD Squares	12
Table 2: Cutout Factors for 100-cm SSD, 105-cm SSD, and 110-cm SSD Rectangles...	13
Table 3: Cutout Factors for 100-cm SSD, 105-cm SSD, and 110-cm SSD Circles.....	13

Acknowledgements

I would like to thank Al Foster and Joe Butts for their patience, guidance, and friendship during my time as a student at Ball Memorial Hospital. Also, I would like to thank the dosimetrists and therapists for their patience with all my questioning. Lastly, I'd like to thank Dr. David Ober for admitting me as a graduate student when I'm not sure that others would have been so gracious.

Chapter 1

Introduction

Electron beam therapy is a well established clinical radiation therapy modality that has been around since the early 1950s. At first, the therapy was limited to a few institutions that had betatrons and Van de Graaff generators. Its clinical use became more widely used in the 1970s with the commercial production of the linear accelerator with a retractable x-ray target. This allowed one linear accelerator to be used for photon and electron therapy treatments. It was discovered that electrons had some significant advantages over that of photons. Possibly its greatest advantage was that electrons did not penetrate as far into healthy tissue as photons and therefore could be used to treat more superficial lesions with less worry about the dose to underlying tissues. Today, electrons are primarily used for the treatment of superficial lesions such as skin and lip cancers and for dose boosts to lymph nodes and breast scars.

Electron fields can be divided into two distinct characteristic field sizes: broad fields and small fields. Broad fields are defined as fields that have exceeded the range of lateral scatter equilibrium (LSE). LSE occurs when the distance between the point of measurement and the edge of the field is shorter than the range of the laterally scattered electrons (Kahn, 2003). Dose distribution in a broad field is only dependent on the

source-to-surface distance (SSD) and the energy. This makes using broad fields more desirable in a clinical setting.

Small fields are defined as those fields that have not exceeded LSE and this causes the dose to be dependent on the field size as well as the energy and SSD. The reason for the field size dependence is due to the radial spread of the electron pencil beam upon incidence with the surface of a patient. The dose distribution can vary significantly with these small field sizes. Thus predicting the dose becomes impossible and causes major problems in the calculation of monitor units.

The goal of this project was to create a library of beam profiles and cutout factors constructed from relative dose measurements for a series of small fields that include circles, rectangles, and squares. In this study, a small field was defined as any rectangle or square with sides ≥ 3 cm and ≤ 5 cm and circles with the same diameter parameters. A 2-D diode array was used to measure dose given by a linear accelerator.

Chapter 2

Literature Review

2.1. Dose Measurements

There are three commonly used methods for measuring dose: ionization chambers, film, and diodes. This section presents these methods, discusses the advantages and disadvantages that each method would present, and then explains why a 2-D diode array was chosen. The 2-D diode array used for this project is known as MapCHECK and is manufactured by Sun Nuclear. MapCHECK is 2-D array of 445 radiation-hardened p-n junction diode

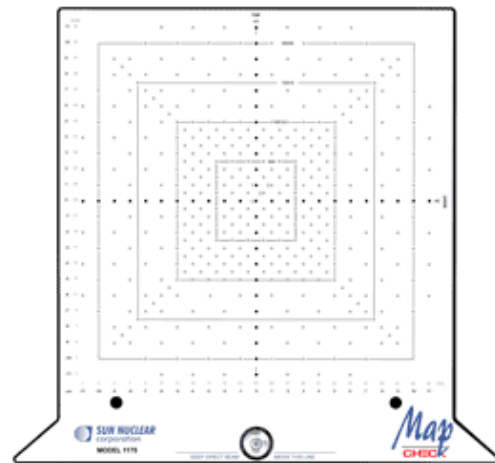


Figure 1: Beam's Eye View of MapCHECK

detectors. These diodes are arranged in a 22-cm octagonal pattern with the highest concentration of diodes in the 10.0-cm x 10.0-cm array. The area of importance for this project was the center 5.0-cm x 5.0-cm array. In this array, there are 61 diodes with adjacent spacing of 1.0 mm and diagonal spacing of 7.07 mm. MapCHECK has an inherent buildup of 2.0 g/cm² with the physical position of the diodes lying 1.35 cm below the surface of the array (MapCHECK User Guide).

2.2. MapCHECK vs. Ionization Chambers

Ionization Chambers are routinely used for dose measurements. These chambers come in two common types: a Farmer-type cylindrical chamber and parallel-plate chamber. When properly calibrated, ionization chambers are very accurate at determining



Figure 2: Farmer-type Ionization Chamber



Figure 3: Parallel-Plate Ionization Chamber

dose for a specific point within a field. This is advantageous for central axis dose measurements and single point measurements. However, this project necessitates that dose be measured at multiple points along an X and Y axis to give the data required to construct beam profiles perpendicular to the direction of the beam. Using an ionization chamber would involve moving the phantom and chamber to multiple locations along both axes to get the required data. The 2-D array solves this problem. The layout of the diodes allows for multiple measurements with the delivery of a single beam.

Another disadvantage is that ionization chambers have a relatively large active detector size and are not as accurate for small field measurements. These chambers are considered accurate as long as the field is no smaller than 4.0 cm x 4.0 cm (Amerio, 2004). The fields that were used for this project ranged from 3.0 cm x 3.0 cm to 5.0 cm x 5.0 cm with the majority of the fields being smaller than 4.0 cm x 4.0 cm. The active detector size of the 2-D array is 0.8 cm x 0.8 cm and by comparison, the active area of a

PTW PinPoint ionization chamber is 2.0-mm in diameter (PTW-Freiburg). Due to the large detector size, ionization chambers consistently over estimate the penumbra region of smaller fields (Sun Nuclear Corporation). This is significant because over estimation of the penumbra region can lead to under dosage of the tumor because of concerns of dose to the underlying and adjacent tissues.

The diode from the 2-D array has an active volume of 0.000019 cm^3 which is small in size when compared to a PTW PinPoint ionization chamber with its volume of 0.015 cm^3 (PTW-Freiburg). Despite the small size of these diodes, they have an incredibly high sensitivity when compared to ionization chambers (Kahn, 1991). This sensitivity is due to the silicon p-n junction diodes that are in the range of 18,000 times more sensitive than ionization chambers (Sun Nuclear Corporation). The diode sensitivity displayed by the 2-D array leads to more accurate dose readings for smaller field sizes.

In summary, the 2-D array allows for the recording of multiple measurements with the delivery of a single beam and also eliminates the need for volume averaging because of its miniscule detector size. These advantages make a 2-D array preferable to any ionization chamber.

2.3. MapCheck vs. Film Dosimetry

Film dosimetry can also be useful in making dosimetric measurements. Complete sets of isodose curves, practical ranges, and beam flatness can all be determined by one exposure. Relative dose measurements are also easily obtained and interpreted by a densitometer. Film has been shown to have a close agreement with ion chambers in measuring relative dose. Film is valued for its high spatial resolution and is only limited

by the ability of the user to calibrate the densitometer and interpret its results. However, film is not as useful for obtaining absolute dose measurements for electrons. Therefore, it is restricted to relative dose measurements only (Kahn, 2003). Film is extremely sensitive to processor conditions and the characteristics of each film can cause frequent, time consuming calibrations. On the other hand, when calibrated correctly, MapCHECK can record both absolute and relative dose measurements, thus, making it a more efficient process.

Figure 4 shows artifacts that can occur from the improper setup of film. Improper setup can occur when care is not taken to assure that there is no air gap between the film and the phantom. A phantom is a QA tool used to simulate a real patient. Phantoms have electron densities similar to that of tissue or water. Other common setup errors happen when the film overlaps the phantom or is recessed in to the phantom.

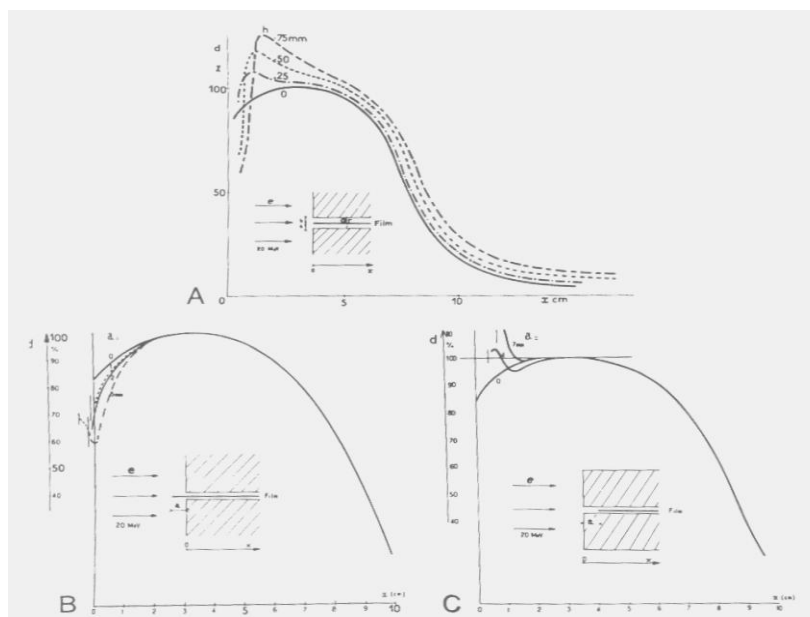


Figure 4: Film artifacts created by misalignment of the film in the phantom. The effects of (A) air gaps between the film and the phantom, (B) film edge extending beyond the phantom, and (C) film edge recessed within the phantom (Dutreix, 1969).

Film has long been used as a QA tool as well. Before the introduction of the 2-D array, film was used in the QA process of IMRT plans. A single film would be exposed to field generated from a treatment planning system. This film would then be analyzed and compared to the intensity map created by the treatment system. The actual and theoretical fields were then compared by the relative intensities, and it was then determined as to whether there was an agreement between the planned field and the field delivered by the linear accelerator. This process was then done for every field. Now that MapCHECK has become more popular, it has begun to phase out film as the sole QA tool for IMRT plans.

Chapter 3

Experimental Methods

3.1 MapCHECK Calibrations

MapCHECK was initially designed to be a quality assurance (QA) tool used for Intensity Modulated Radiation Therapy (IMRT). IMRT is an external beam photon radiation therapy that uses dynamic multileaf collimators (MLC) to modulate the intensity of the beams in order to create an optimal dose distribution (Kahn, 2003).

However, MapCheck can be used for acquiring multiple dose measurements in one exposure which is beneficial in constructing beam profiles. Calibration for the diode array for electrons is the same process as that used for photon calibration with one exception. For electron calibrations, care must be taken to use the correct buildups because as depth increases the energy of the electron beam decreases as it moves through any scattering medium (MapCHECK User Guide). The percent depth dose (PDD) rapidly decreases for electron beams due to multiple Coulomb interactions. PDD is defined as the quotient of the absorbed dose at any depth, d , to the absorbed dose at a fixed reference depth, d_0 . This reference depth can be any depth but generally it is the depth of maximum dose, d_{\max} .

Background readings are recorded before calibration. MapCHECK then has two parameters that should be calibrated for all beam energies. There is an array calibration that compares the relative sensitivities of each detector to the other detectors and when applied during a measurement eliminates the response differences between detectors (MapCHECK User Guide). The other calibration is an absolute dose calibration. This is performed for all beam energies, and the correction factor produced is applied to all diodes (MapCHECK User Guide).

3.2 Experimental Variables

Three shapes were used to closely approximate fields that are commonly used in electron therapy treatments: squares, rectangles, and circles. These fields are common in treatments of skin lesions, breast scars, and intraoral cancers. Table 1 shows all the field shapes and sizes that were used. Each field was exposed to 6-, 9-, 12-, and 15-MeV energies. Three source-to-surface distances (SSD) were used, the standard 100-cm SSD and two extended SSDs at 105 cm and 110 cm. As for all electron treatments, the SSD is determined as the distance from the electron source to the surface of the patient.

3.3 Setup Parameters

A Varian 21EX linear accelerator was used for all measurements. This accelerator has five available electron energies, and as previously mentioned four were used for this project. 5 mm of solid water buildup



Figure 5: Solid Water Phantom

were used for this project. 5 mm of solid water buildup was added to the 12- and 15-MeV energies while no buildup was needed for the 6- and 9-

MeV energies (Reference MedPhysFiles Spreadsheet). A buildup material is a type of medium that has a similar electron density to that of water or tissue. The buildups were determined by defining the d_{\max} of all energies. d_{\max} is the depth of maximum dose and is dependent on the beam's energy. Electron energies have a buildup effect that causes dose to accumulate to a maximum within a medium and then falls off with a steep gradient. Figure 6 shows the buildup effect measured by an ionization chamber and a diode detector.

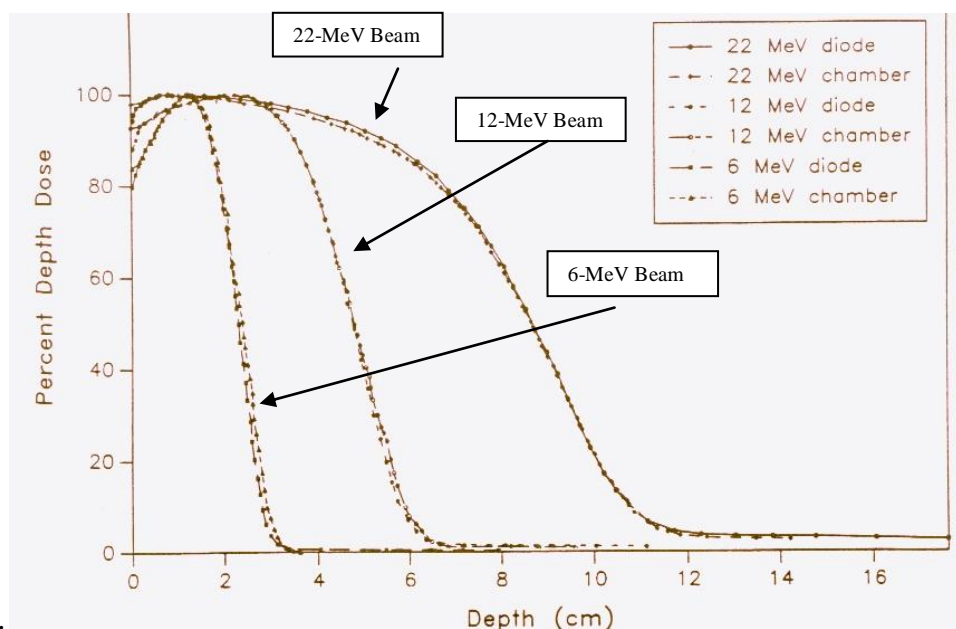


Figure 6: Comparison of depth dose curves measured with a diode and an ion chamber (Khan, 2003)

Chapter 4

Experimental Results

The data that was gathered was used to create beam profiles and cutout factors. The beam profiles are perpendicular to the beam and the cutout factors are a ratio of two dose readings, blocked field to open field. The blocked field dose measurement was one concentration of this project. The open field was given by the standard 6.0-cm x 6.0-cm electron applicator.

4.1. Cutout Factors

Cutout factors are used in the calculation of monitor units for electron fields. Monitor units are a value related to the on time of the linear accelerator. Generally, the more monitor units that are needed corresponds to higher dose treatments. The equation used for the monitor unit (MU) calculation is,

$$MU = \frac{Rx}{(Cutout\ Factor) * (Cone\ Factor) * (PDD\ or\ Isodose\ Line)} \quad (4.1) \text{ where MU stands for}$$

the number of monitor units, Rx is the dose prescription, and PDD is the percent depth dose. The cone factor is a value that is dependent on the electron applicator being used and has units of $\frac{cGy}{MU}$. The absolute cone factor is the value for a 10-cm x 10-cm electron

applicator. All other applicators are relative to this one. The cutout factor is a unit less value given by the equation,

$$\textit{Cutout Factor} = \frac{\textit{Blocked Field}}{\textit{Open Field}} \quad (4.2)$$

where the open field reading is energy dependent and the blocked field is dependent on the field shape, size, and the source-to-surface distance (SSD). The open field measurements were taken for the 6-, 9-, 12-, and 15-MeV beam energies at 100-cm SSD.

Cutout Factors were created for all fields at 6, 9, 12, and 15 MeV and 100-cm, 105-cm, and 110-cm SSDs. They can be looked at as the percentage of dose that is not blocked by the electron cone insert. As seen in Eq. 4.1, the lower the cutout factor the higher the number of monitor units needed to deliver the prescribed dose. Below are the cutout factors for all the small electron fields that were used.

Cutout Factors for all Squares												
	100-cm SSD				105-cm SSD				110-cm SSD			
Sizes (cm)	6 MeV	9 MeV	12 MeV	15 MeV	6 MeV	9 MeV	12 MeV	15 MeV	6 MeV	9 MeV	12 MeV	15 MeV
3 x 3	0.927	0.947	0.979	0.990	0.750	0.789	0.844	0.856	0.542	0.653	0.740	0.753
4 x 4	0.969	0.968	0.940	0.990	0.823	0.853	0.830	0.876	0.688	0.747	0.730	0.773
5 x 5	1.000	1.000	0.990	1.010	0.865	0.863	0.870	0.887	0.740	0.768	0.770	0.784

Table 1: Cutout Factors for 100-cm SSD, 105-cm SSD, and 110-cm SSD Squares

Cutout Factors for all Rectangles												
	100-cm SSD				105-cm SSD				110-cm SSD			
Sizes (cm)	6 MeV	9 MeV	12 MeV	15 MeV	6 MeV	9 MeV	12 MeV	15 MeV	6 MeV	9 MeV	12 MeV	15 MeV
3 x 4	0.958	0.947	0.950	0.990	0.781	0.821	0.840	0.876	0.615	0.695	0.730	0.773
3 x 5	0.948	0.958	0.960	1.000	0.813	0.832	0.850	0.876	0.635	0.705	0.740	0.763
4 x 5	1.000	0.989	0.990	1.010	0.844	0.863	0.860	0.897	0.719	0.758	0.770	0.794

Table 2: Cutout Factors for 100-cm SSD, 105-cm SSD, and 110-cm SSD Rectangles

Cutout Factors for all Circles												
	100-cm SSD				105-cm SSD				110-cm SSD			
Radii (cm)	6 MeV	9 MeV	12 MeV	15 MeV	6 MeV	9 MeV	12 MeV	15 MeV	6 MeV	9 MeV	12 MeV	15 MeV
1.5	0.917	0.937	0.950	0.990	0.677	0.758	0.790	0.835	0.521	0.632	0.680	0.742
2.0	0.948	0.958	0.950	0.979	0.802	0.821	0.840	0.856	0.646	0.716	0.740	0.773
2.5	0.990	0.989	0.990	1.010	0.854	0.863	0.860	0.876	0.740	0.768	0.780	0.794

Table 3: Cutout Factors for 100-cm SSD, 105-cm SSD, and 110-cm SSD Circles

4.2. Beam Profiles

The beam profile data was collected perpendicular to the beam. Perpendicular profile data shows isodose lines for a given depth. The depth was assumed to be the depth of maximum dose, d_{\max} , for this project. Thus, the beam profiles show the width of the isodose lines at d_{\max} . The beam profiles were constructed from relative dose measurements acquired with the 2-D array.

4.2.1. Square and Rectangular Beam Profiles

The square and rectangular beam profiles were analyzed by comparing the penumbra region as the SSD, energy, and field size change. The penumbra is the region

at the edge of a radiation field where the dose changes rapidly as a function of distance from the beam axis (Kahn, 2003). The penumbra region is measured by the distance between the 20%-80% isodose lines.

The 3-cm x 3-cm beam profiles at 6 MeV was used to compare the changes in penumbra with the SSD increasing from 100 cm to 110 cm. The 3-cm x 3-cm data was used as a representative sample of all the data and was used to illustrate comparisons and analysis.

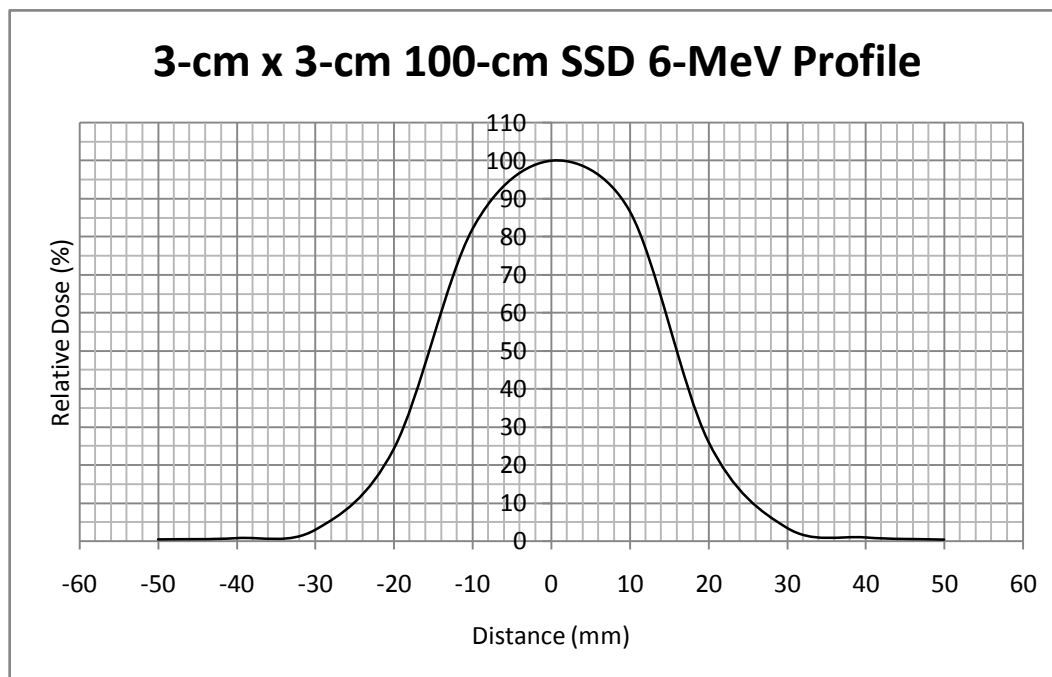


Figure 7: 3-cm x 3-cm 100-cm SSD 6-MeV Profile

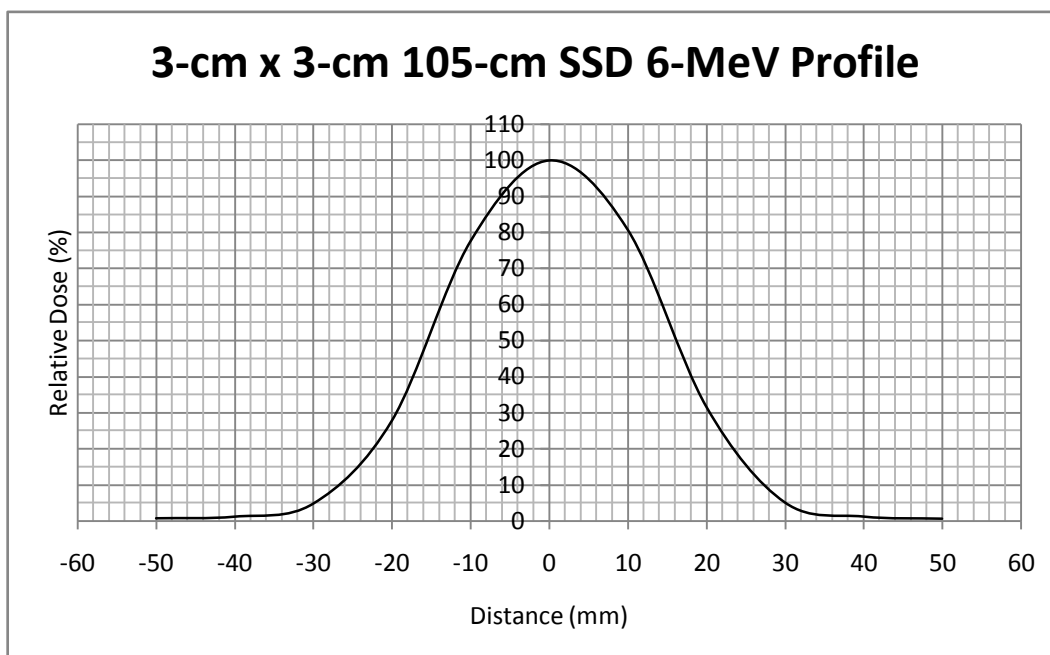


Figure 8: 3-cm x 3-cm 105-cm SSD 6-MeV Profile

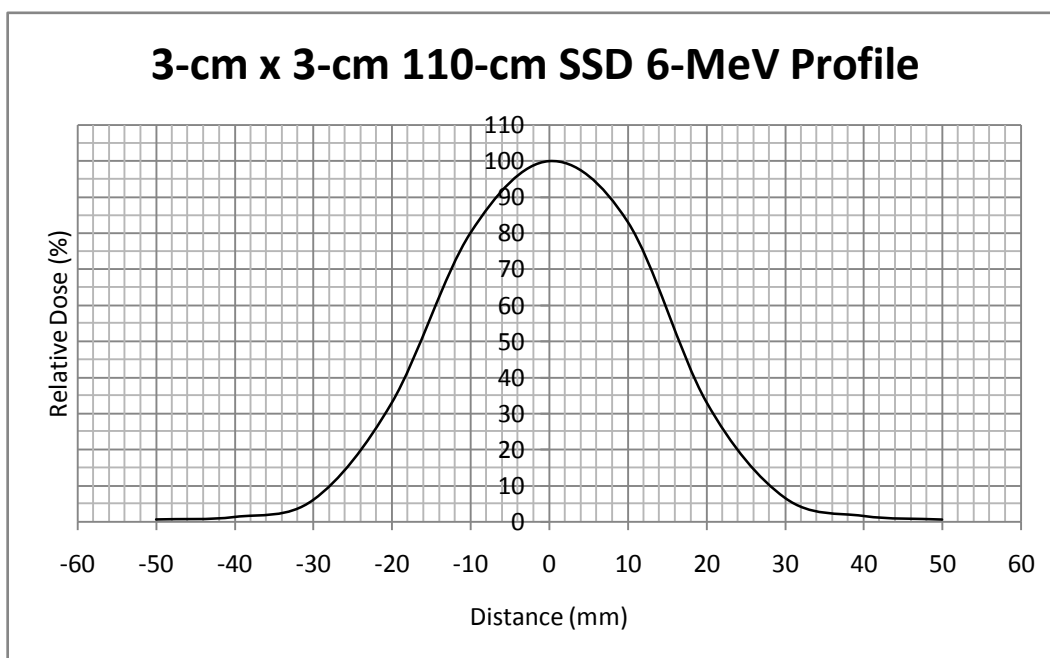


Figure 9: 3-cm x 3-cm 110-cm 6-MeV Profile

As seen in Fig. 7, the 3-cm x 3-cm 100-cm SSD 6-MeV profile has an average penumbra of 10.75 mm whereas the 3-cm x 3-cm 110-cm SSD 6-MeV profile in Fig. 9 has an average penumbra of 13.75 mm. This shows that the penumbra increases with the

increase in SSD. The greater distance between the source and the surface of the patient gives rise to greater electron scatter in the air causing an increase in the penumbra region. The field width, defined at the 50% isodose line, is 3.2 cm x 3.2 cm, and this is the same for all projected 3.0-cm x 3.0-cm squares for 6 MeV. The 50% isodose line is the field width at d_{\max} . Knowing the field width helps to determine the projected field size needed to adequately cover the tumor.

For comparison of penumbras within the same SSD set of data, the 3-cm x 3-cm beam profiles at 100-cm SSD were used for analysis.

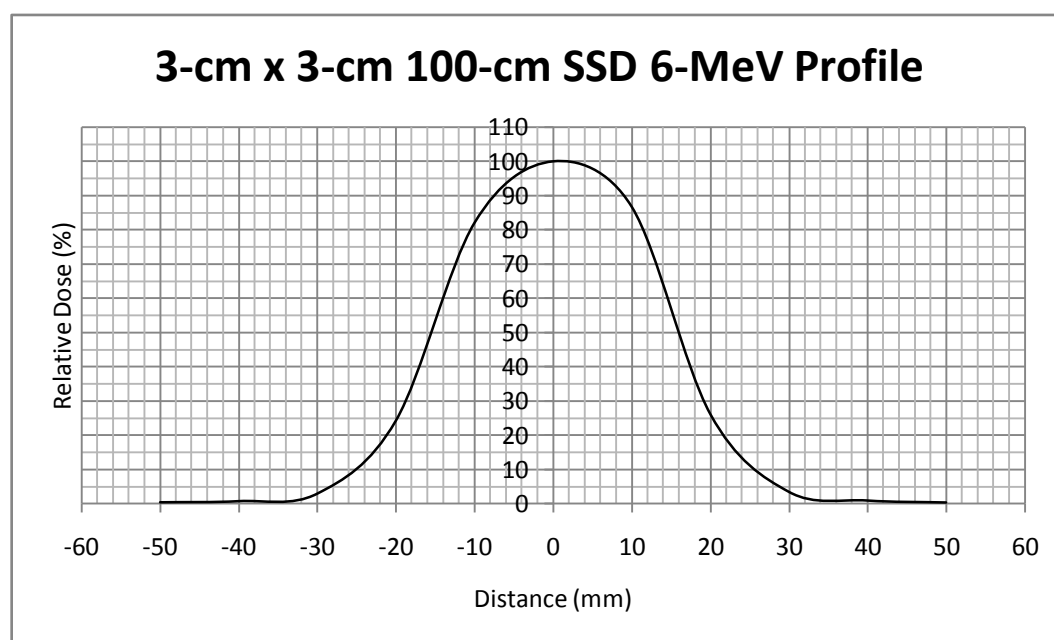


Figure 10: 3-cm x 3-cm 100-cm SSD 6-MeV Profile

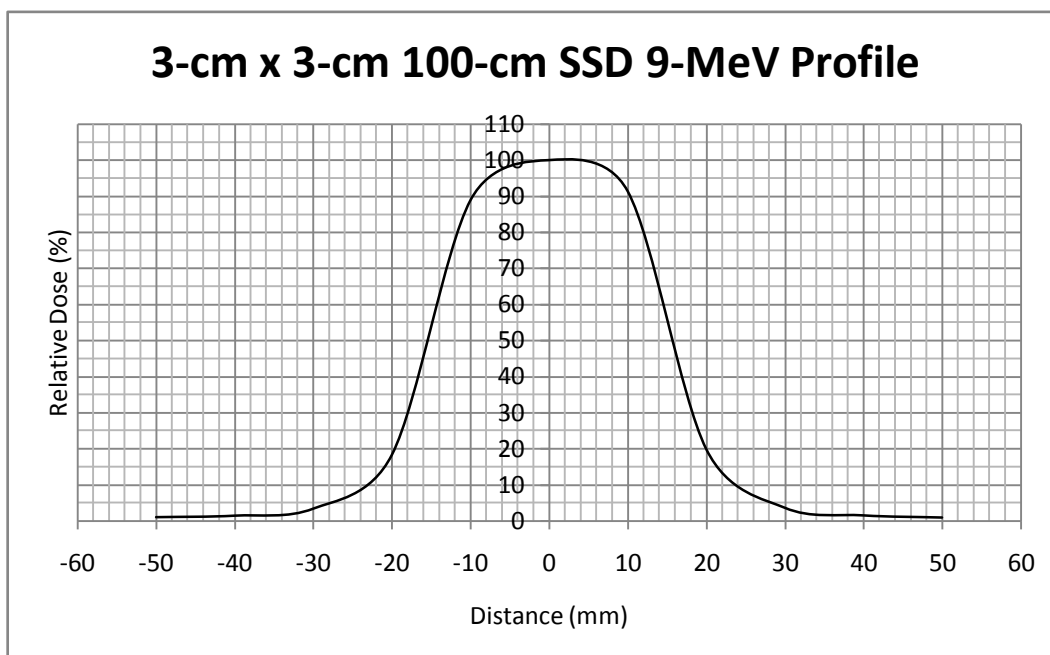


Figure 11: 3-cm x 3-cm 100-cm 9-MeV Profile

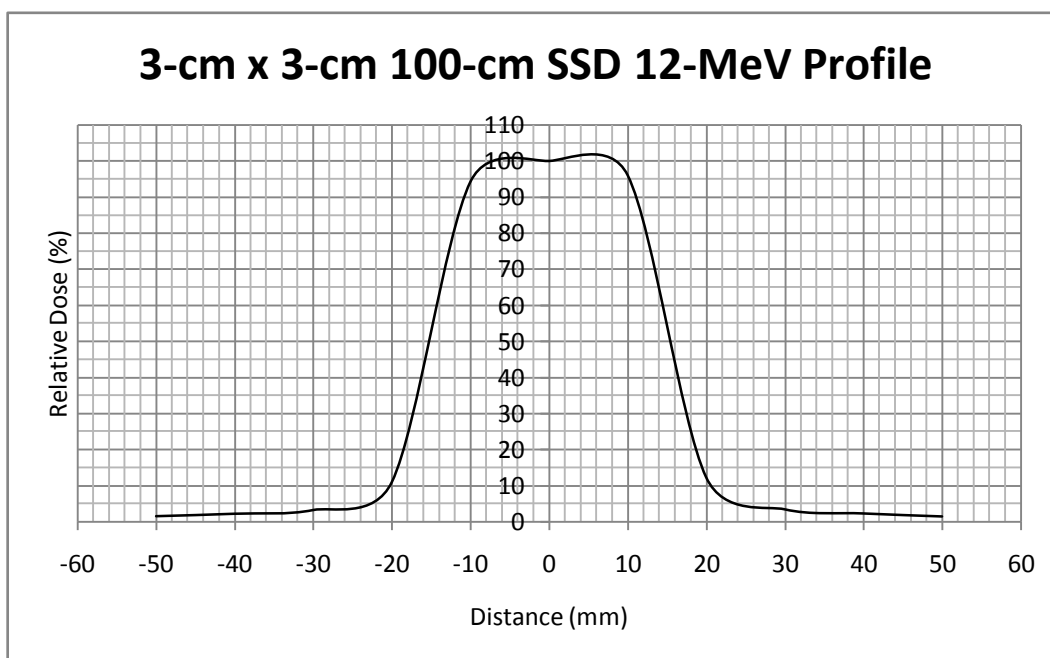


Figure 12: 3-cm x 3-cm 100-cm SSD 12-MeV Profile

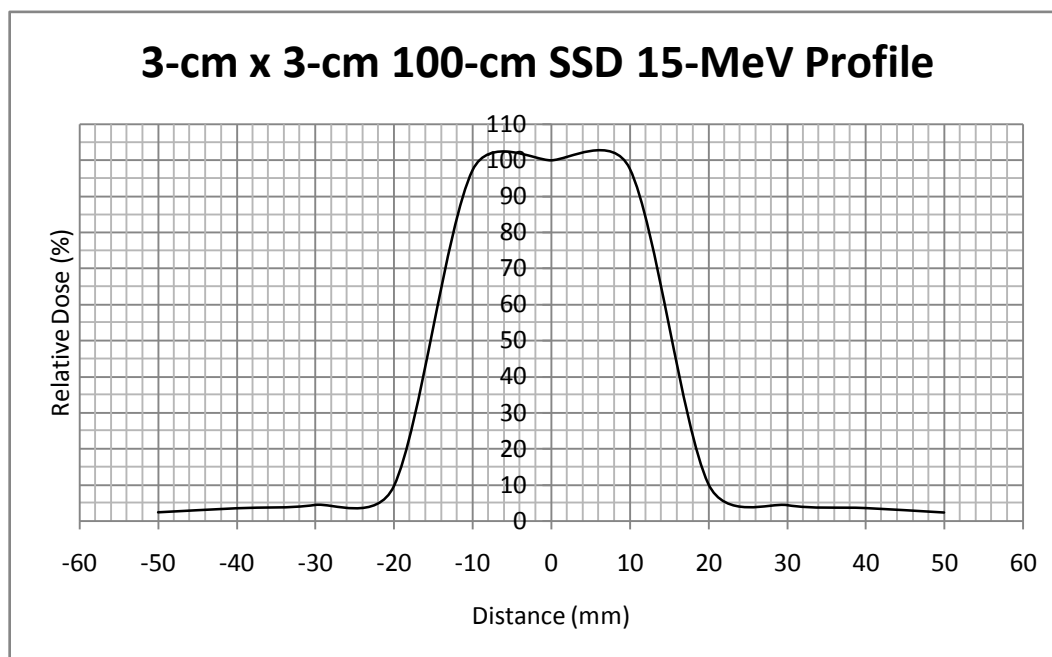


Figure 13: 3-cm x 3-cm 100-cm 15-MeV Profile

As seen in Fig. 10, the 3-cm x 3-cm 100-cm SSD 6-MeV profile has an average penumbra of 10.75 mm and the 3-cm x 3-cm 100-cm SSD 15-MeV profile in Fig. 13 has an average penumbra of 5.75 mm. The penumbra decreases as the energy increases within a set SSD. The higher energies are scattered more forward than the lower energies; therefore, the penumbras are smaller at higher energies, however, the field width at the 50% isodose line is still 3.2 cm x 3.2 cm for all energies.

Lastly, the 6-MeV at 100-cm SSD beam profiles was used to analyze the change in penumbra with the increase in field size from 3 cm x 3 cm to 5 cm x 5 cm.

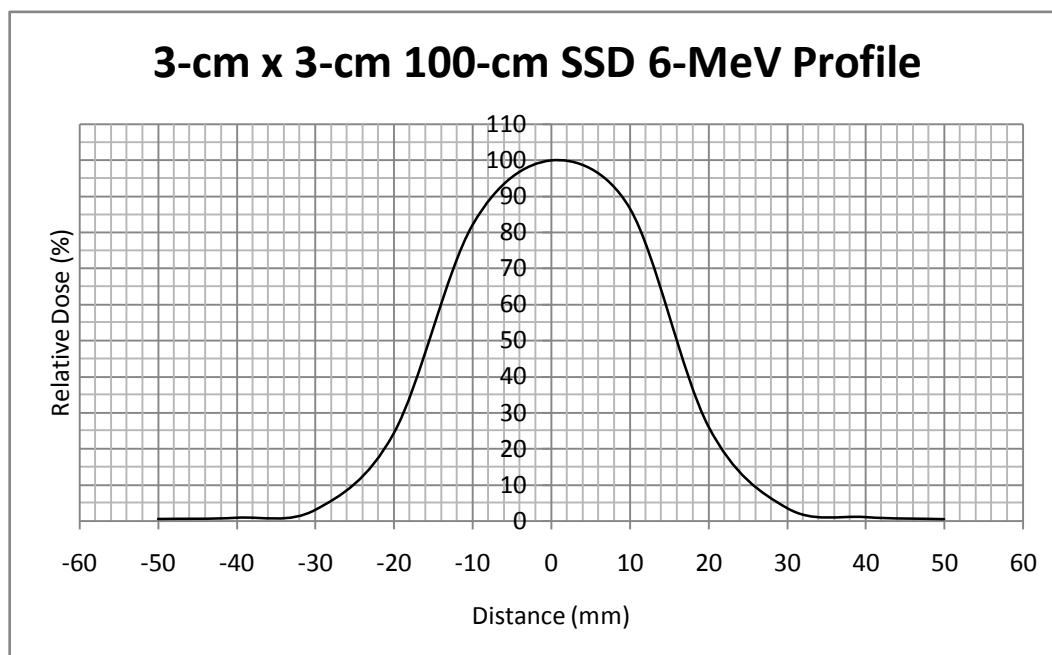


Figure 14: 3-cm x 3-cm 100-cm SSD 6-MeV Profile

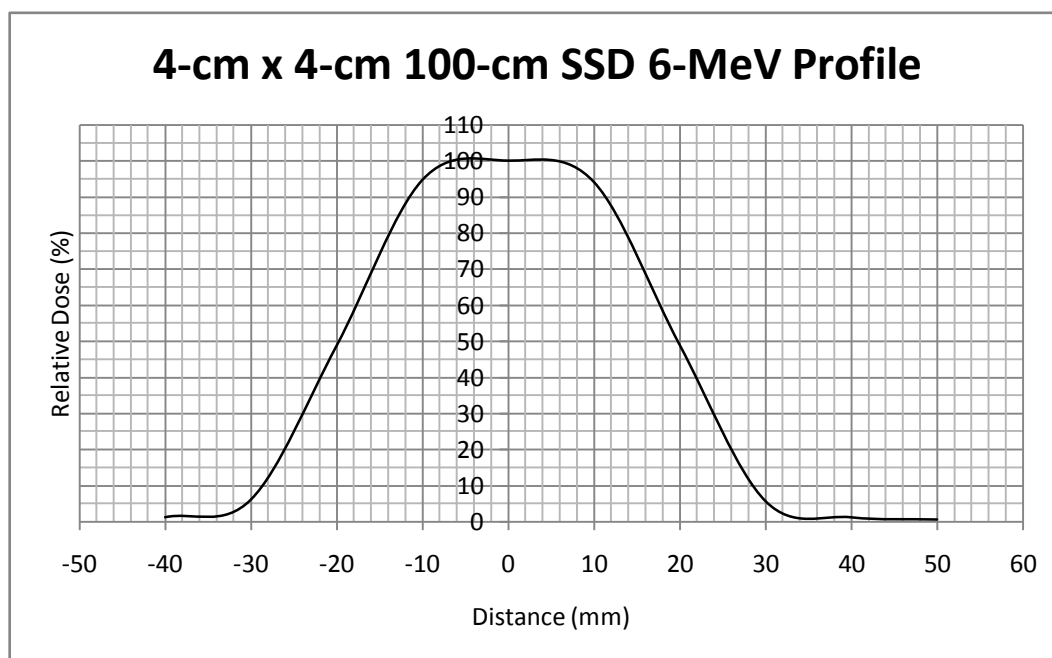


Figure 15: 4-cm x 4-cm 100-cm SSD 6-MeV Profile

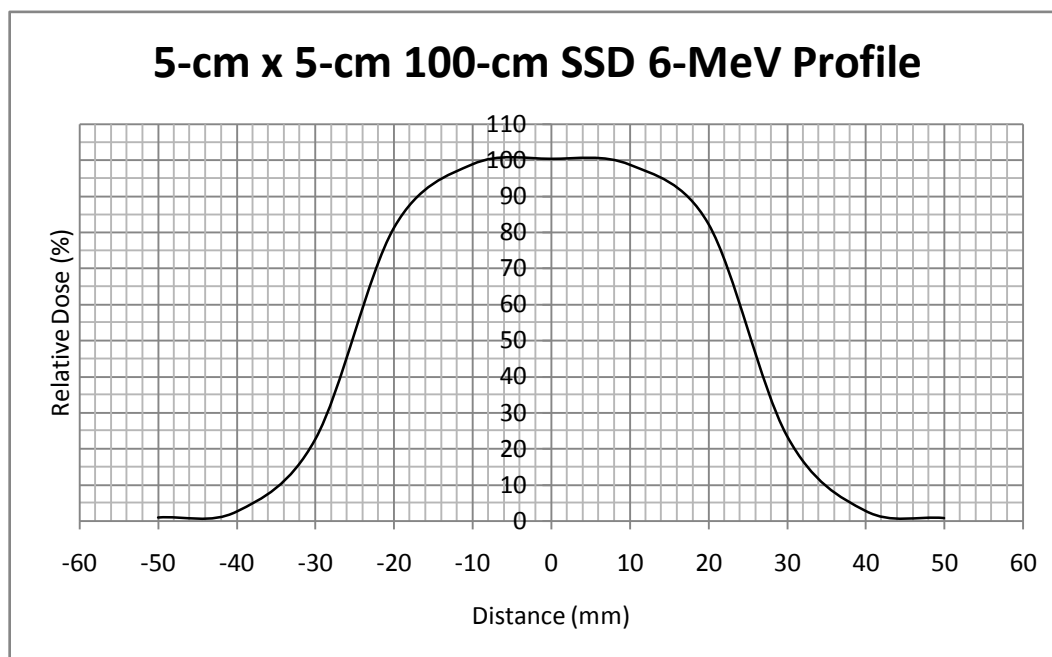


Figure 16: 5-cm x 5-cm 100-cm SSD 6-MeV Profile

As seen in Fig. 14, the 3-cm x 3-cm 100-cm SSD 6-MeV profile has an average penumbra of 10.75 mm and this is the same for the 5-cm x 5-cm 100-cm SSD 6-MeV profile in Fig. 16. However, Fig. 15 has a slightly larger penumbra region. It has an average penumbra of 12 mm. The penumbra should remain independent of the increase in field size as long as the energy and SSD remain the same.

The rectangular profiles were constructed from the square profiles; therefore, there will be no need for a separate analysis of rectangular data. Data for the beam profiles were taken for the rectangular fields, and it was found to be identical to the squares with the same sides. The remaining square and rectangular beam profiles can be seen in Appendices A and B, respectively.

4.2.2 Circular Beam Profiles

A similar analysis was done for the circular data as it was for the square and rectangular data. The 3.0-cm diameter circular profiles were a very good representation of the data for all the other circles. The following are the profiles for 3.0-cm 6-MeV for all three SSDs.

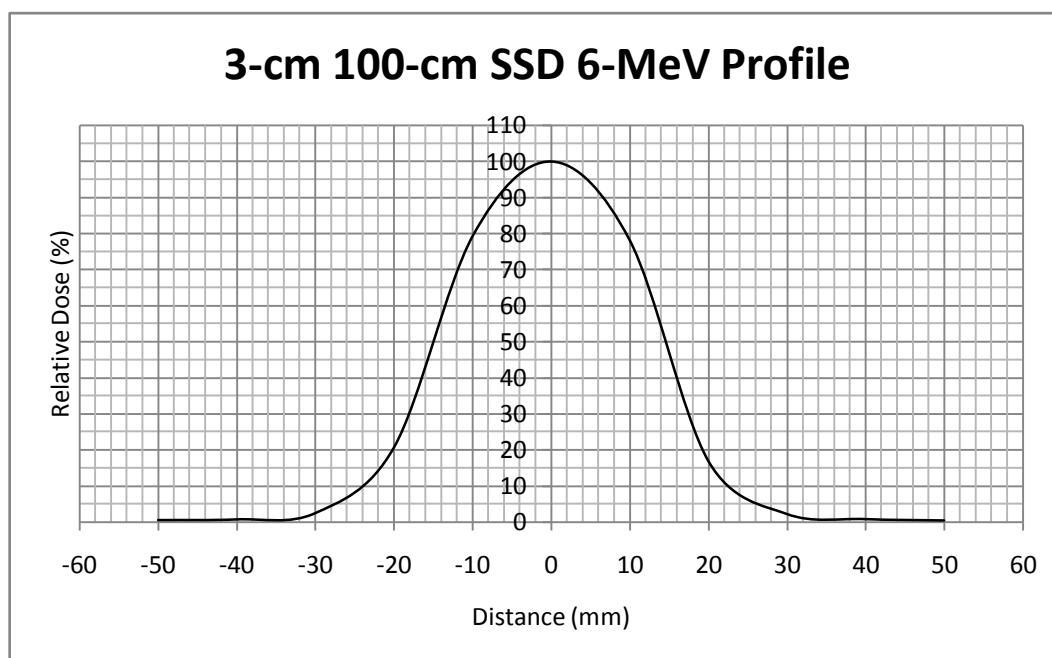


Figure 17: 3-cm 100-cm SSD 6-MeV Profile

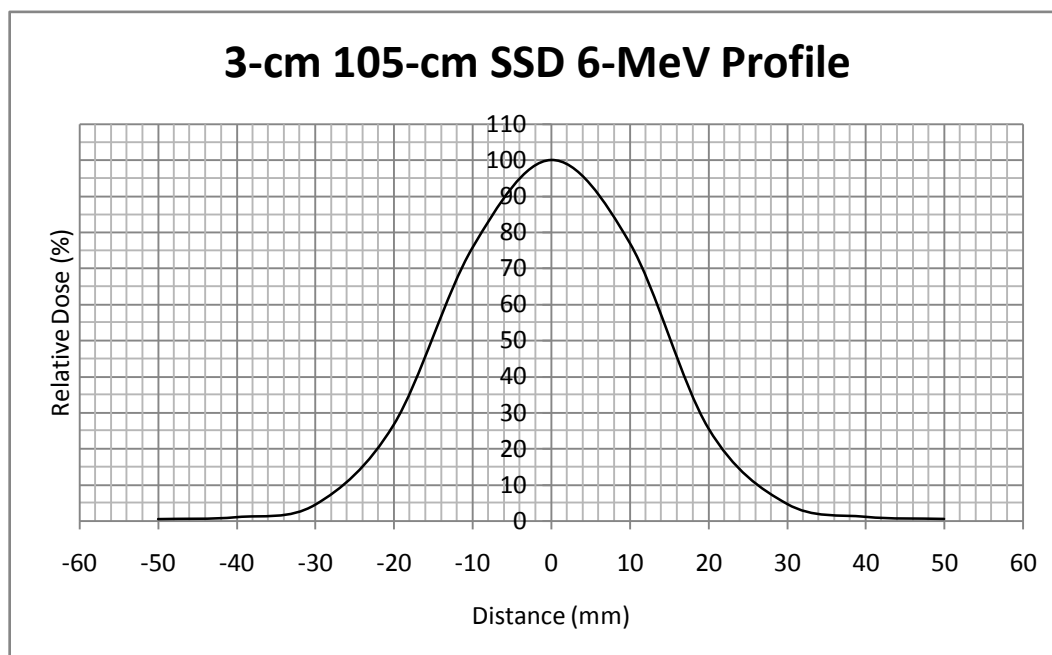


Figure 18: 3-cm 105-cm SSD 6-MeV Profile

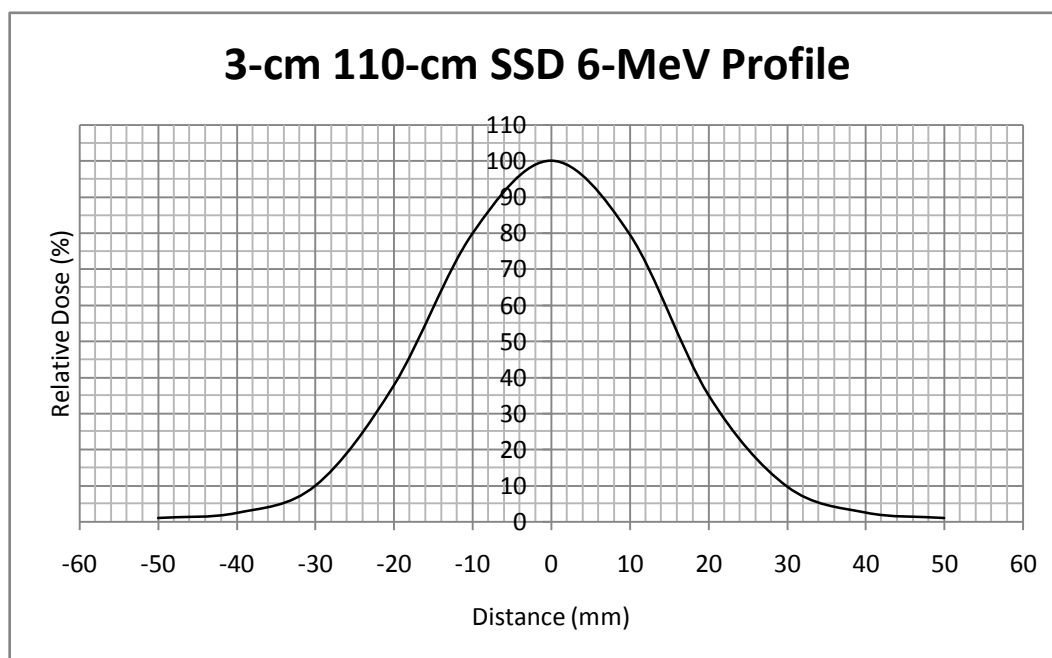


Figure 19: 3-cm 110-cm SSD 6-MeV Profile

The profiles for the circles were slightly different than they were for the squares and rectangles. The field width at d_{\max} gets larger as SSD increases. As seen in Fig. 17, the 3-cm 100-cm SSD 6-MeV profile has an average penumbra of 9.5 mm. By

comparison, the 3-cm 110-cm SSD 6-MeV profile in Fig. 19 has an average penumbra of 15.75 mm. The penumbra characteristic of increasing penumbra with increasing SSD is the same as it was for the squares.

The next set of beam profiles compares the change in penumbra with the increase in energy. The beam profiles for the 3.0-cm 100-cm SSD profiles of 6, 9, 12, and 15 MeV were used for analysis.

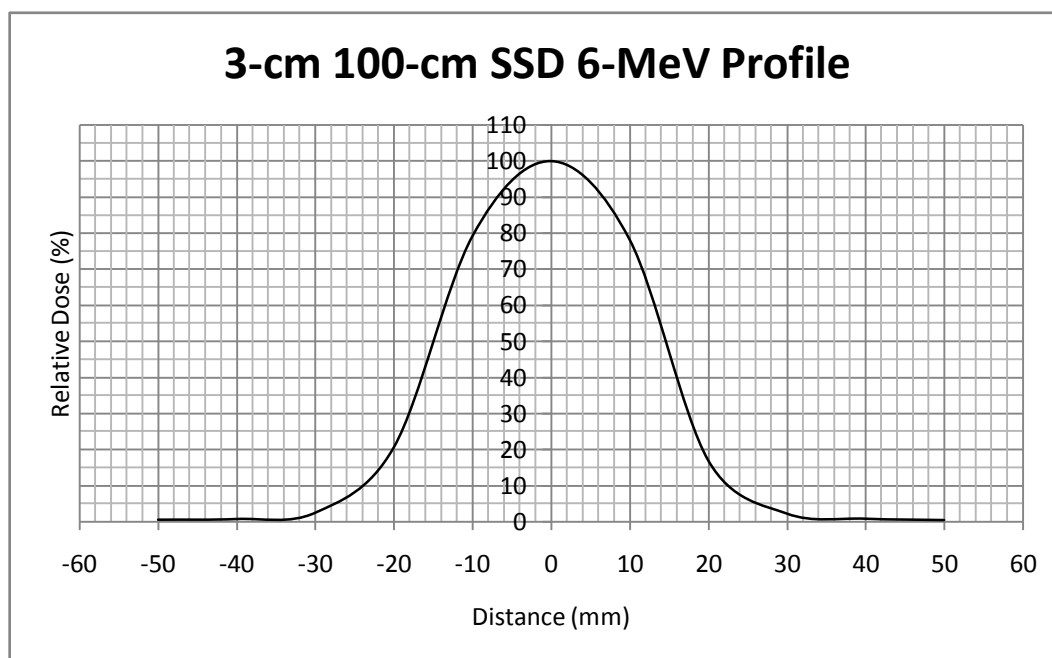


Figure 20: 3-cm 100-cm SSD 6-MeV Profile

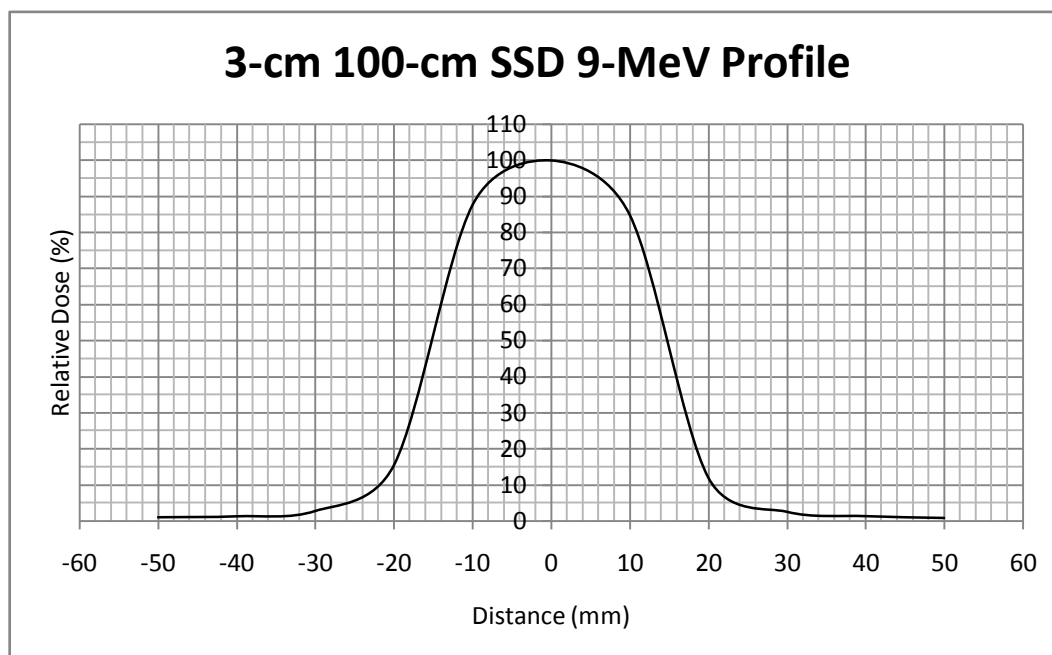


Figure 21: 3-cm 100-cm SSD 9-MeV Profile

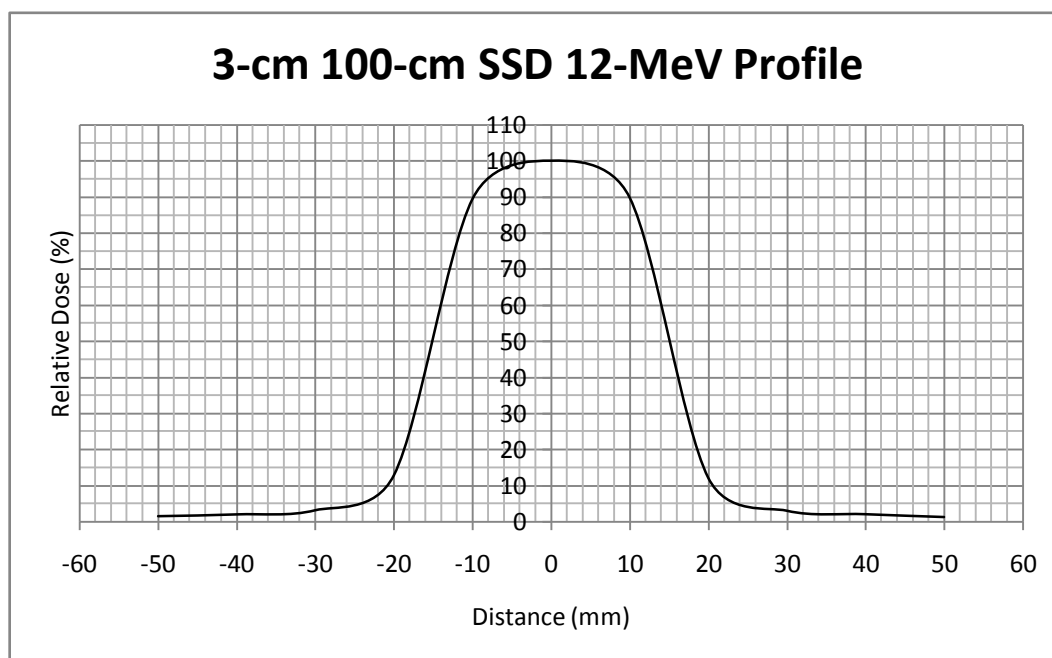


Figure 22: 3-cm 100-cm SSD 12-MeV Profile

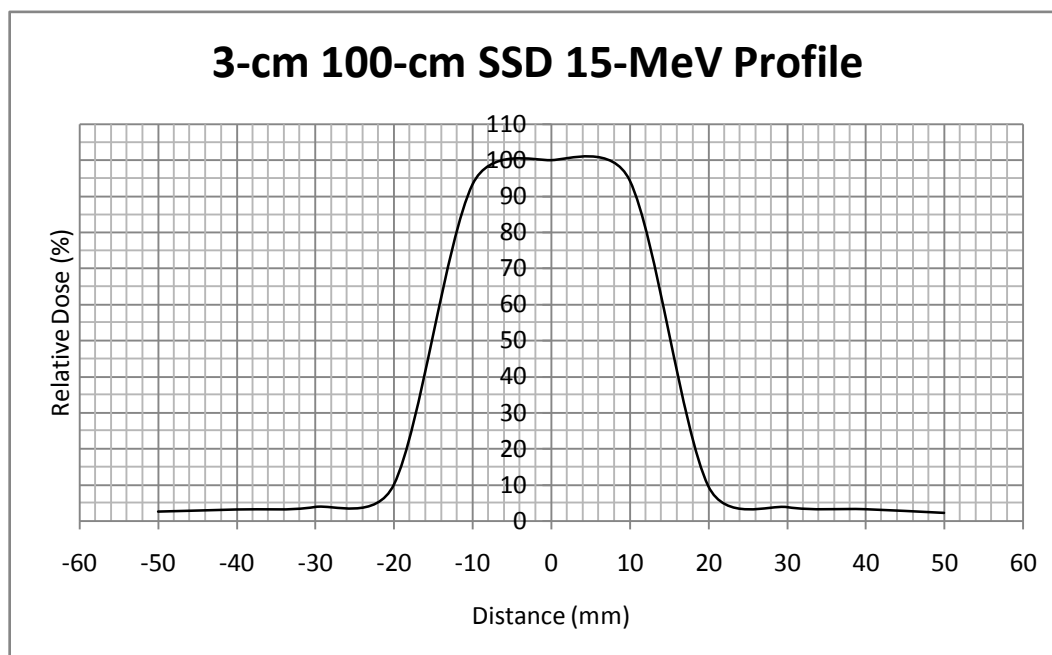


Figure 23: 3-cm 100-cm SSD 15-MeV Profile

Once again, the same characteristics are seen for the circles as they were for the squares and rectangles. As seen in Fig. 20, the 3-cm 100-cm SSD 6-MeV profile has an average penumbra of 9.5 mm whereas the 3-cm 100-cm SSD 15-MeV profile in Fig. 23 has an average penumbra of 6.0 mm. The penumbra for the circular profiles decreases with energy, but the field width remains the same. For the projected 3.0-cm circle, its field width is still approximately 3.0 cm.

The last comparison evaluated the change in penumbra with the increase in field size from 3.0 cm to 5.0 cm. The 6-MeV beam profiles at 100-cm SSD were analyzed.

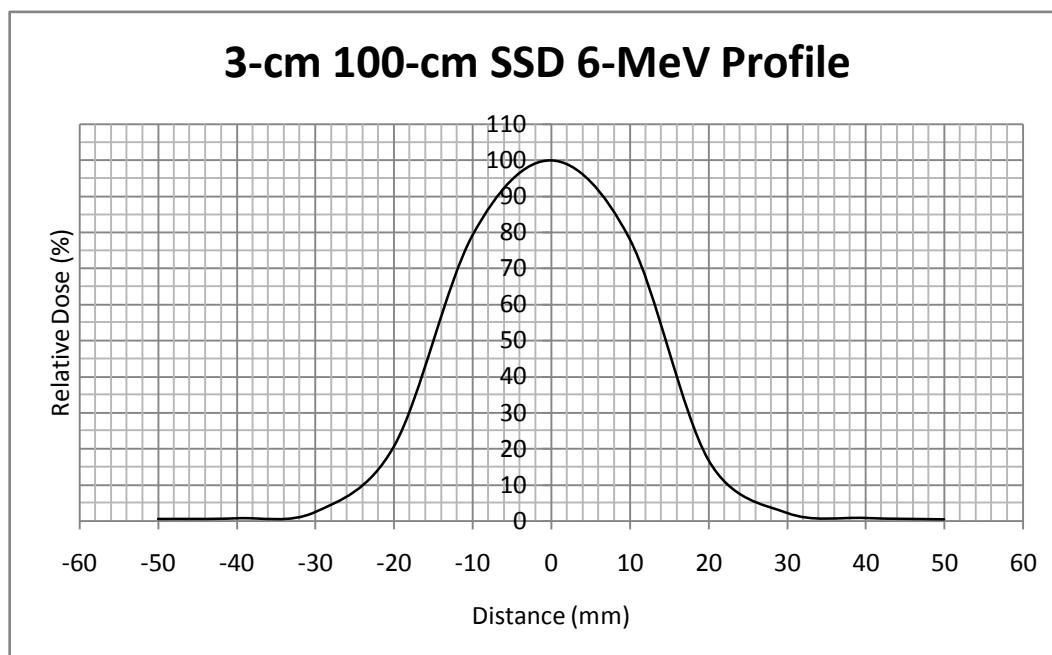


Figure 24: 3-cm 100-cm SSD 6-MeV Profile

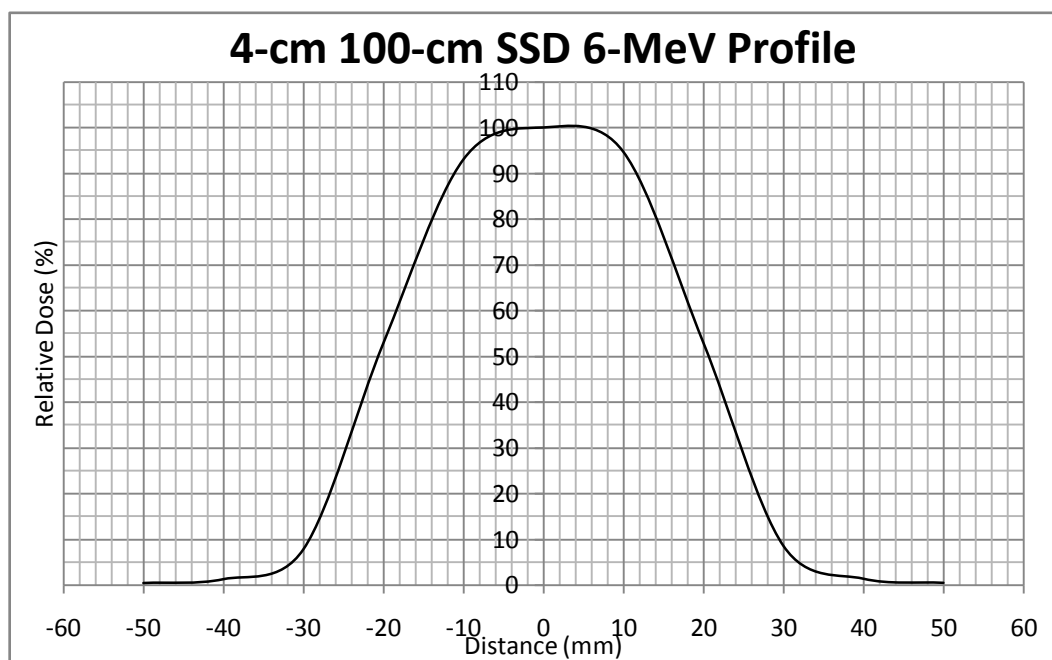


Figure 25: 4-cm 100-cm SSD 6-MeV Profile

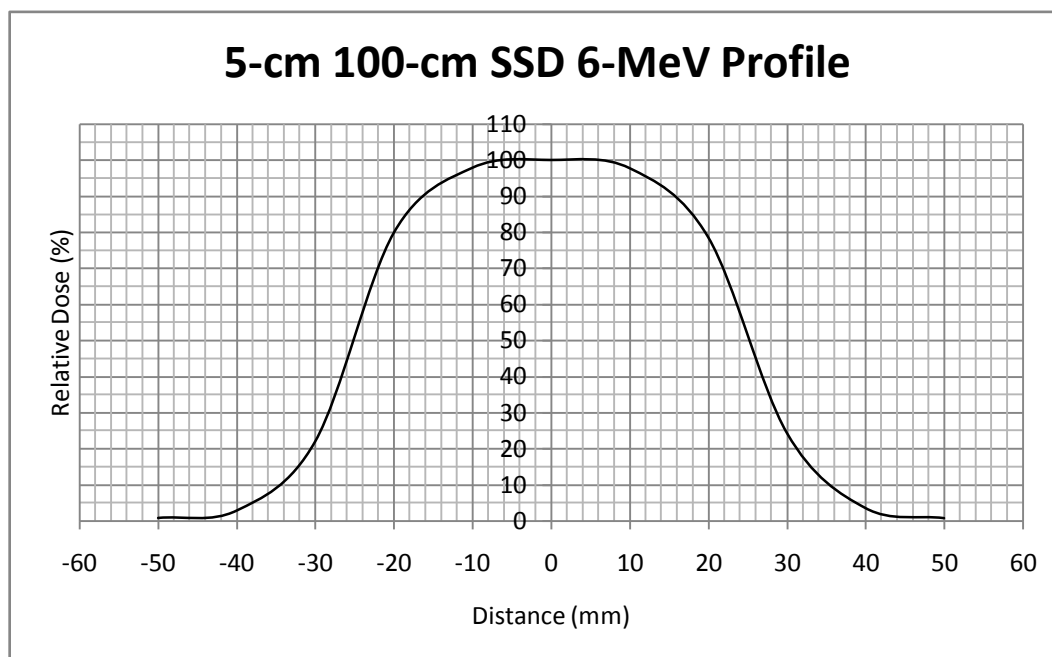


Figure 26: 5-cm 100-cm SSD 6-MeV Profile

The penumbras were comparable for the 3-cm and 5-cm circles, but it was slightly more than 2 mm larger for the 4-cm circle. The same difference occurs for the square and rectangular beam profiles as well. The reason for the difference is a physical characteristic of the 2-D array. Representative samples of circular beam profiles were used here; the rest of the circular profiles can be found in Appendix C.

Chapter 5

Summary and Conclusions

An index of tabulated data for small electron fields has been created for clinical use. The beam profiles can be used to more closely approximate the field size at d_{\max} for a given beam energy. The tabulated relative output factors can increase efficiency by eliminating the need for patient-specific dosimetry measurements. This new data should allow for a more accurate treatment of small, superficial tumors.

Field sizes with a side ≤ 2 cm were not pursued for this experiment. Initial investigation of these field sizes was found to have unreliable data. The cause of this can only be speculated, but it's believed that the inconsistent data was due to too few diodes being exposed to the beam. The beam profiles were shown to be inconsistent with the field width at d_{\max} for the three SSDs that were used. The 4-cm data did not conform to the expectations of the penumbra characteristics. The penumbra and field width were slightly larger than expected. This is because of the physical position of the diodes that were used to acquire the data. The edges of these fields were not centered on the diodes and this is a possible reason for the difference.

Further studies into small electron fields should be pursued. One possible study could make use of film to measure relative doses for beam profiles similar to what was done with the 2-D array. Another study could be to create Percent Depth Dose (PDD)

tables using a water tank. Because PDD decreases drastically for electrons with depth, having this data available would make for better accuracy for small-electron field calculations used for beam modeling on a treatment planning computer.

References

Dutreix, J., Dutreix, A. Film dosimetry of high energy electrons. *Ann. NY Acad. Sci.* 1969, 33, 161.

Khan, Faiz M., Doppke, K.P., Hogstrom, K. R., Kutcher, G. J., Nath, R., Prasad, S. C., Purdy, J. A., Rozenfeld, M., Werner, B.L. (1991). Clinical electron-beam dosimetry: Report of AAPM Radiation Therapy Committee Task Group No. 25. *Med. Phys.* Volume 18, Issue 1, 73-109.

Khan, F.M. (2003). *The Physics of Radiation Therapy*, 3rd edition. Philadelphia: Lippencott Williams & Wilkins.

PTW-Freiburg. PTW PinPoint Ionization Chamber Specifications.

http://www.ptw.de/pinpoint_chambers1.html

MapCHECK User Guide.

<http://www.sunnuclear.com/support/download/manuals/MapCHECK/MapCheckUsersGuide30500.pdf>

Sun Nuclear Corporation. Diodes versus Ion Chambers.

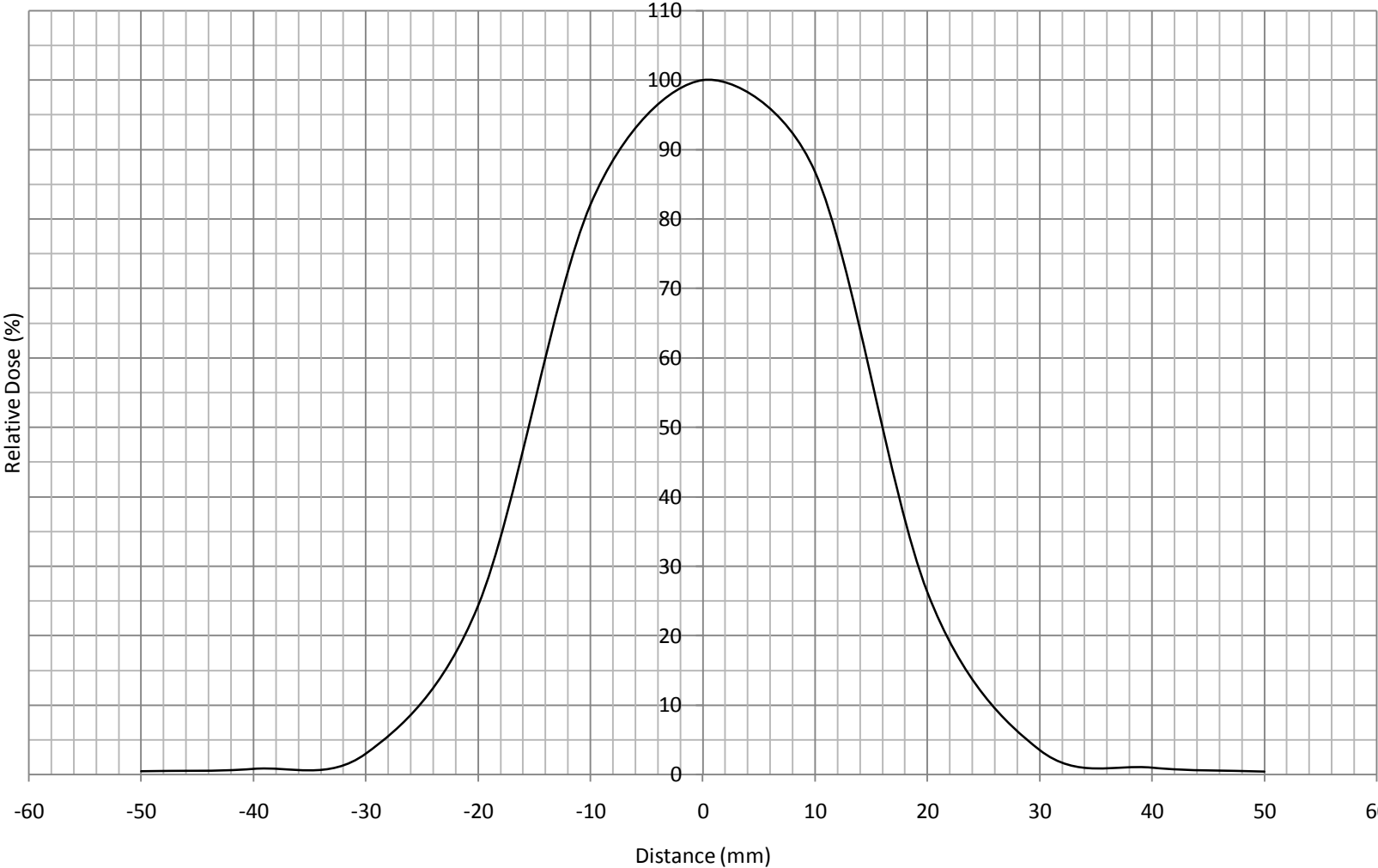
http://www.sunnuclear.com/documents/IonvsDiodes/IONvDiode_lo.pdf

S. Amerio et al. (2004). Dosimetric characterization of a larger area pixel-segmented ionization chamber. *Med. Phys.* Volume 31, Issue 2, 414-420.

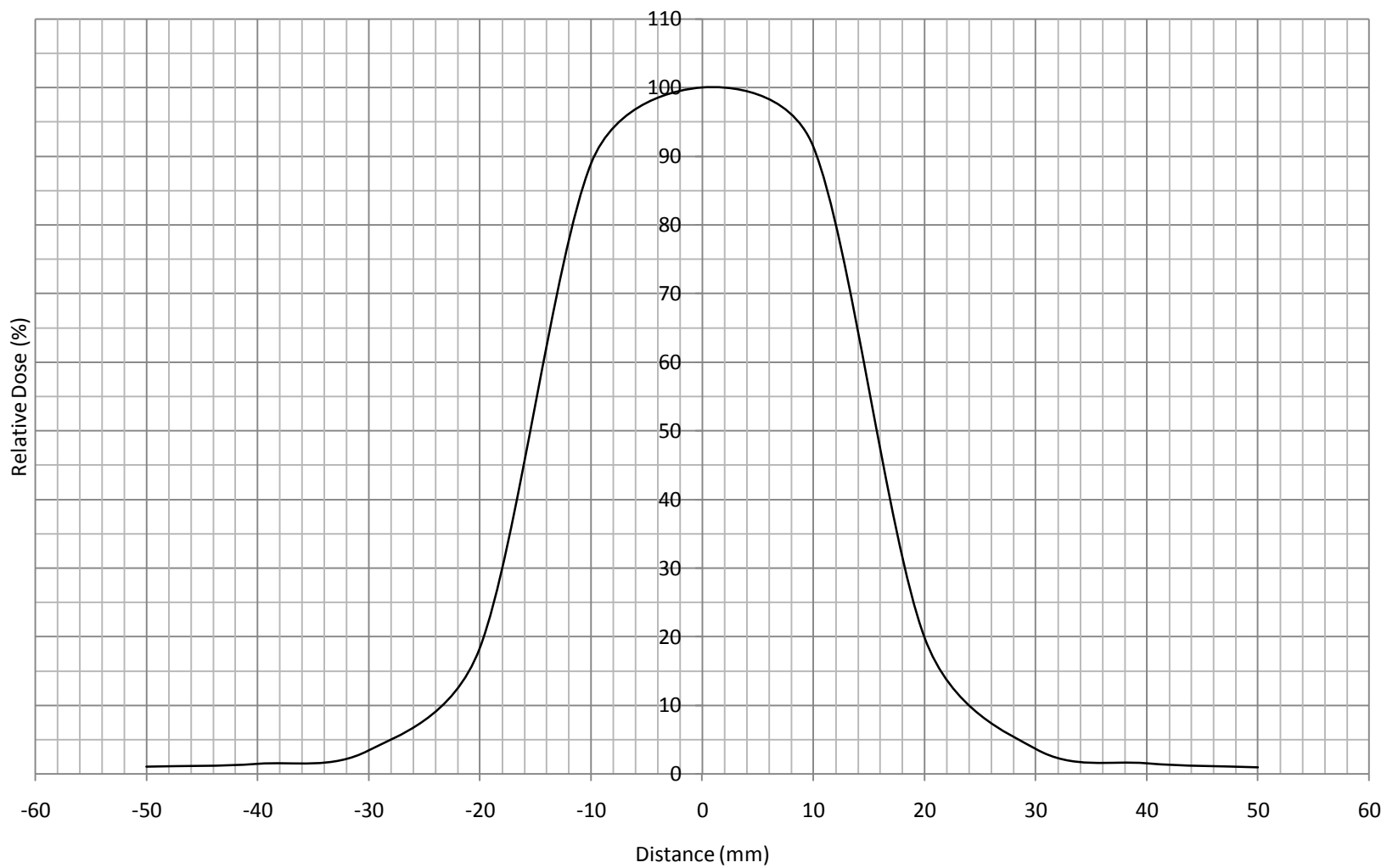
Appendix A

Beam Profiles of Small-Electron Square Fields

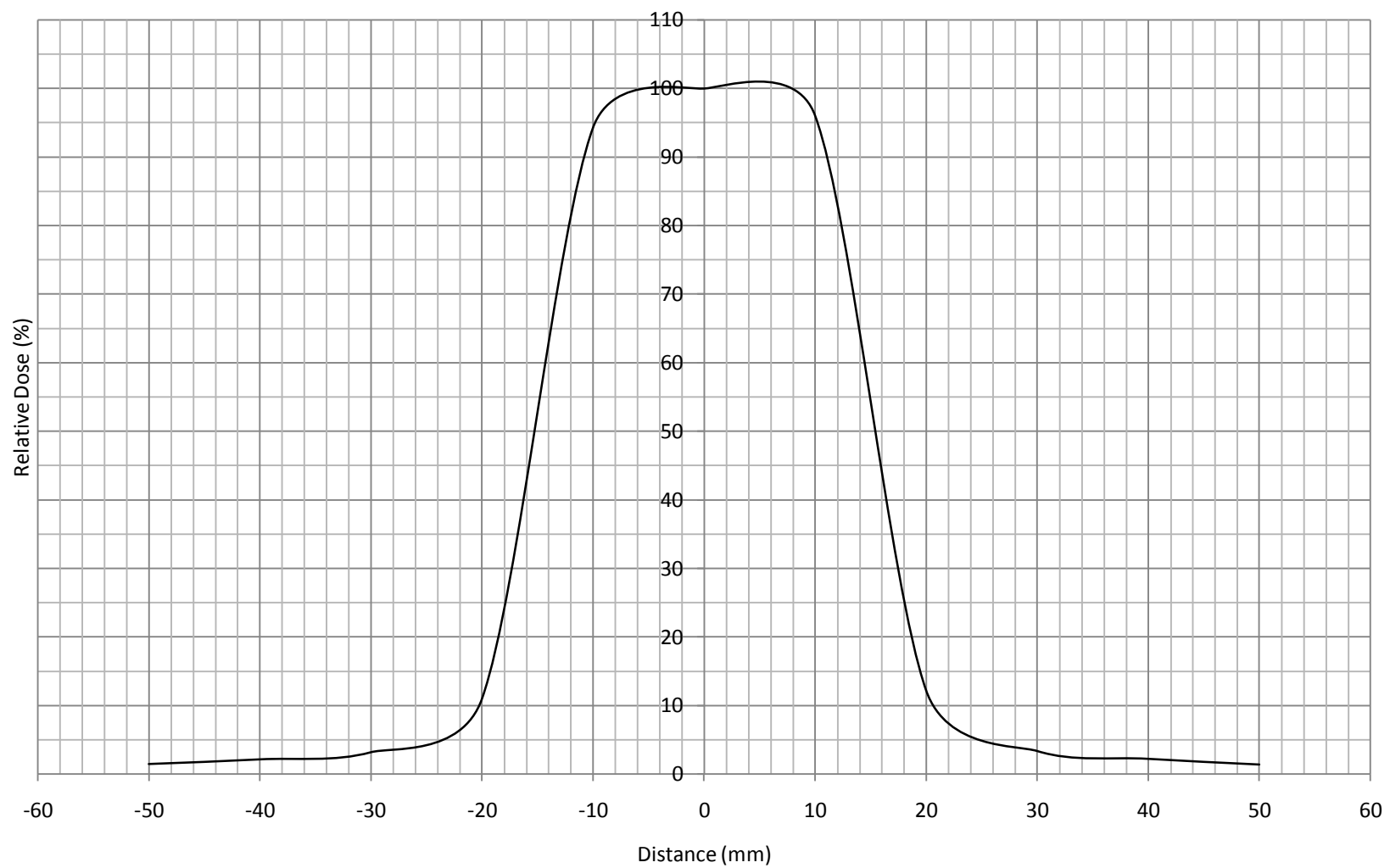
3-cm x 3-cm 100-cm SSD 6-MeV Profile



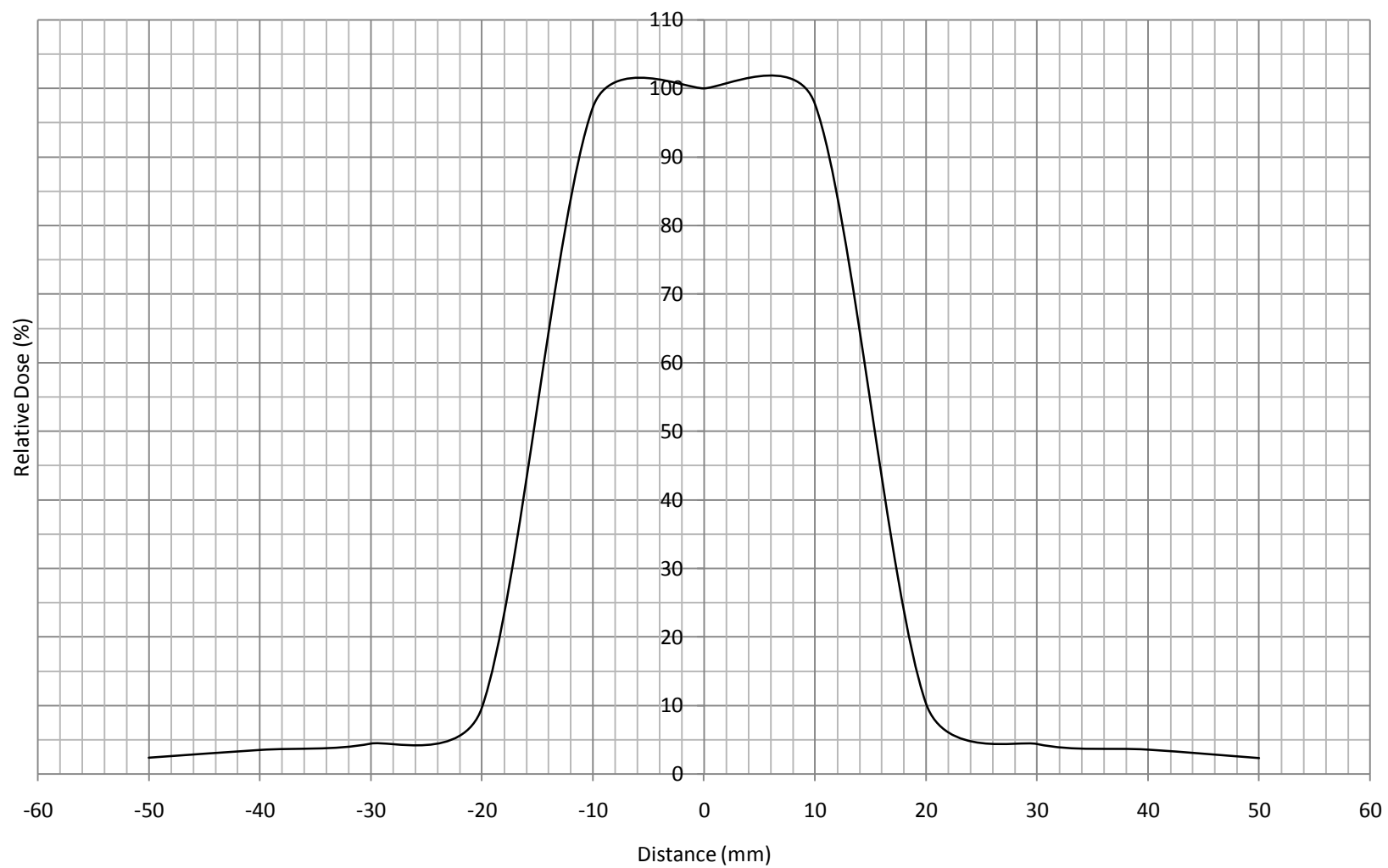
3-cm x 3-cm 100-cm SSD 9-MeV Profile



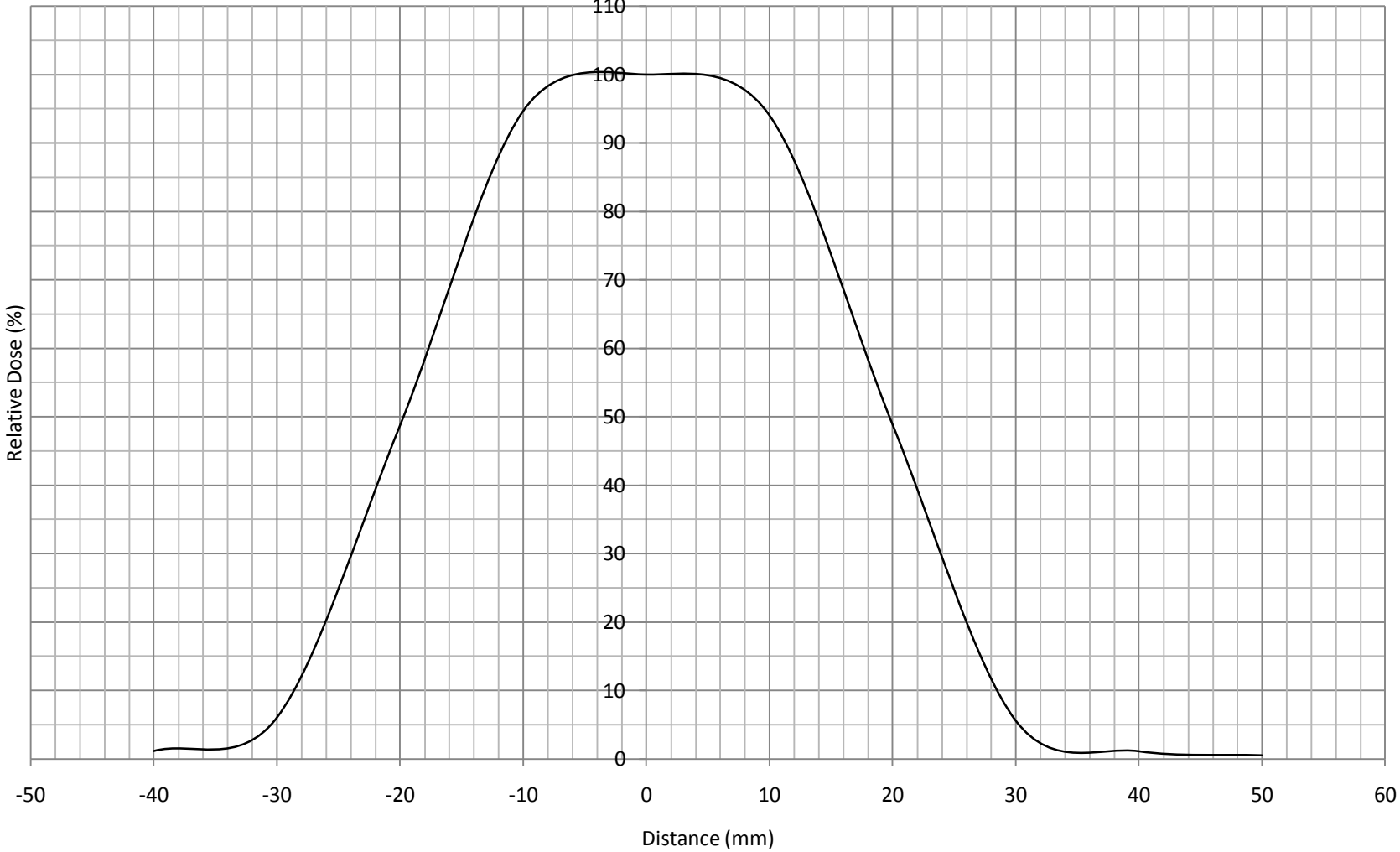
3-cm x 3-cm 100-cm SSD 12-MeV Profile



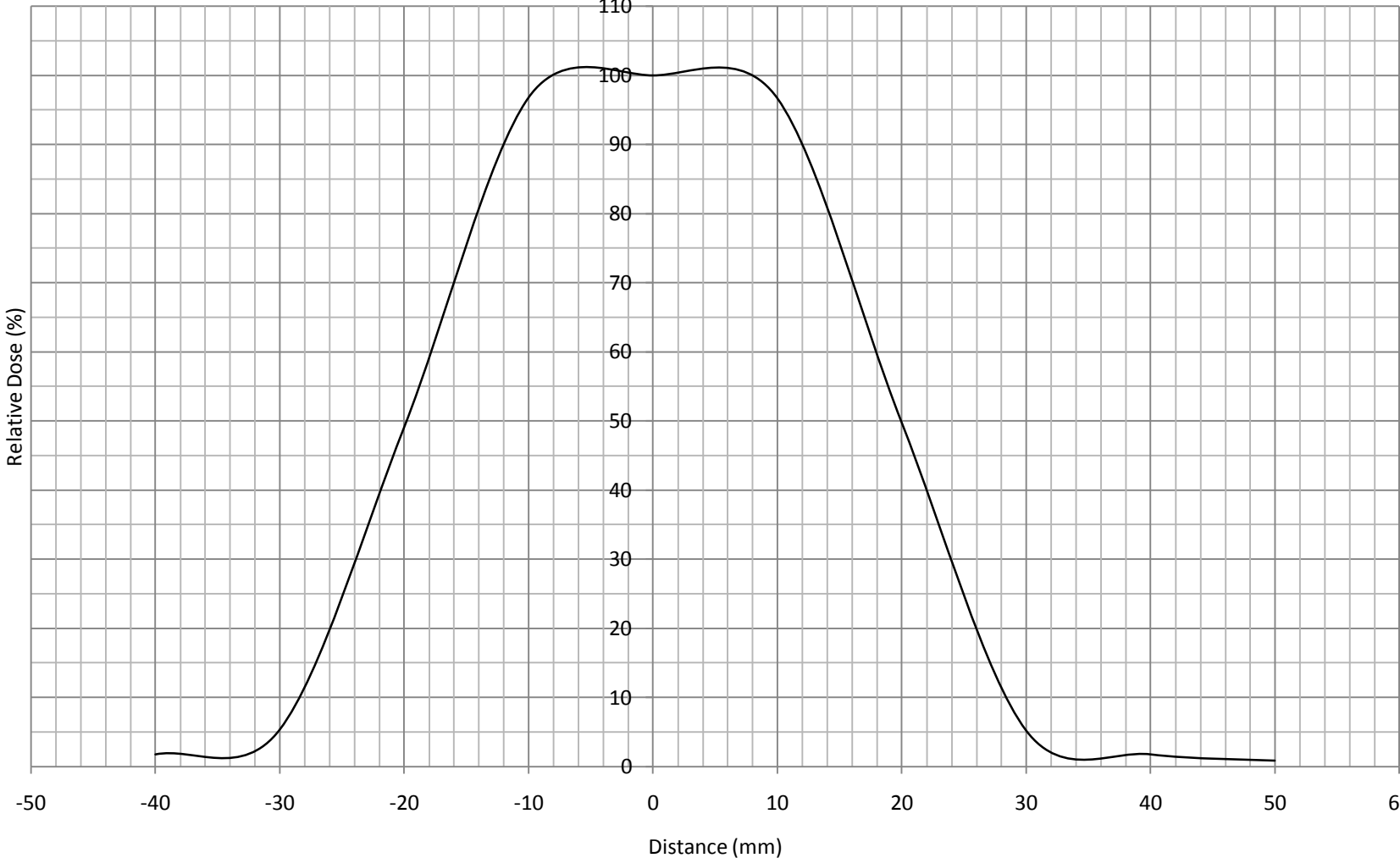
3-cm x 3-cm 100-cm SSD 15-MeV Profile



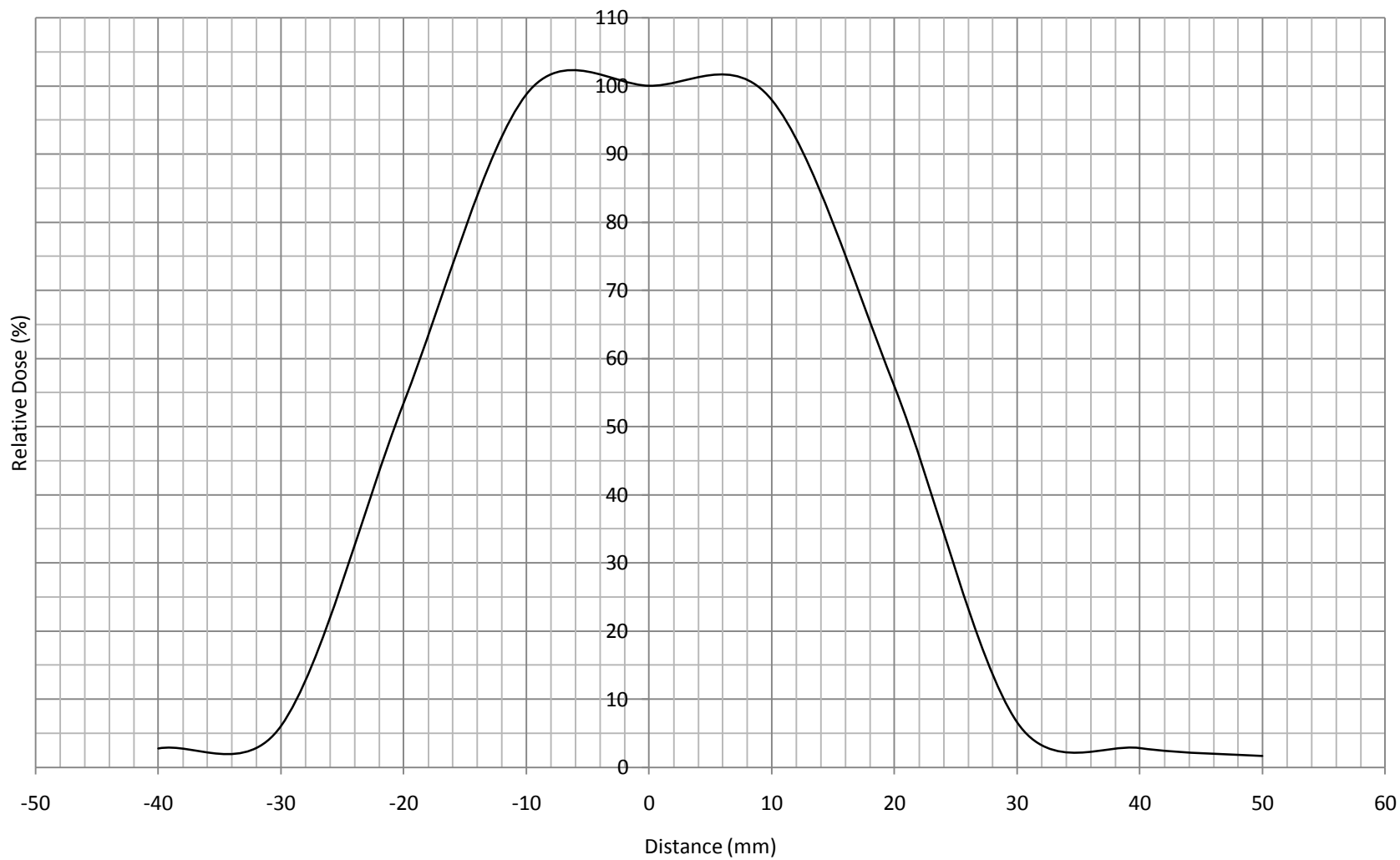
4-cm x 4-cm 100-cm SSD 6-MeV Profile



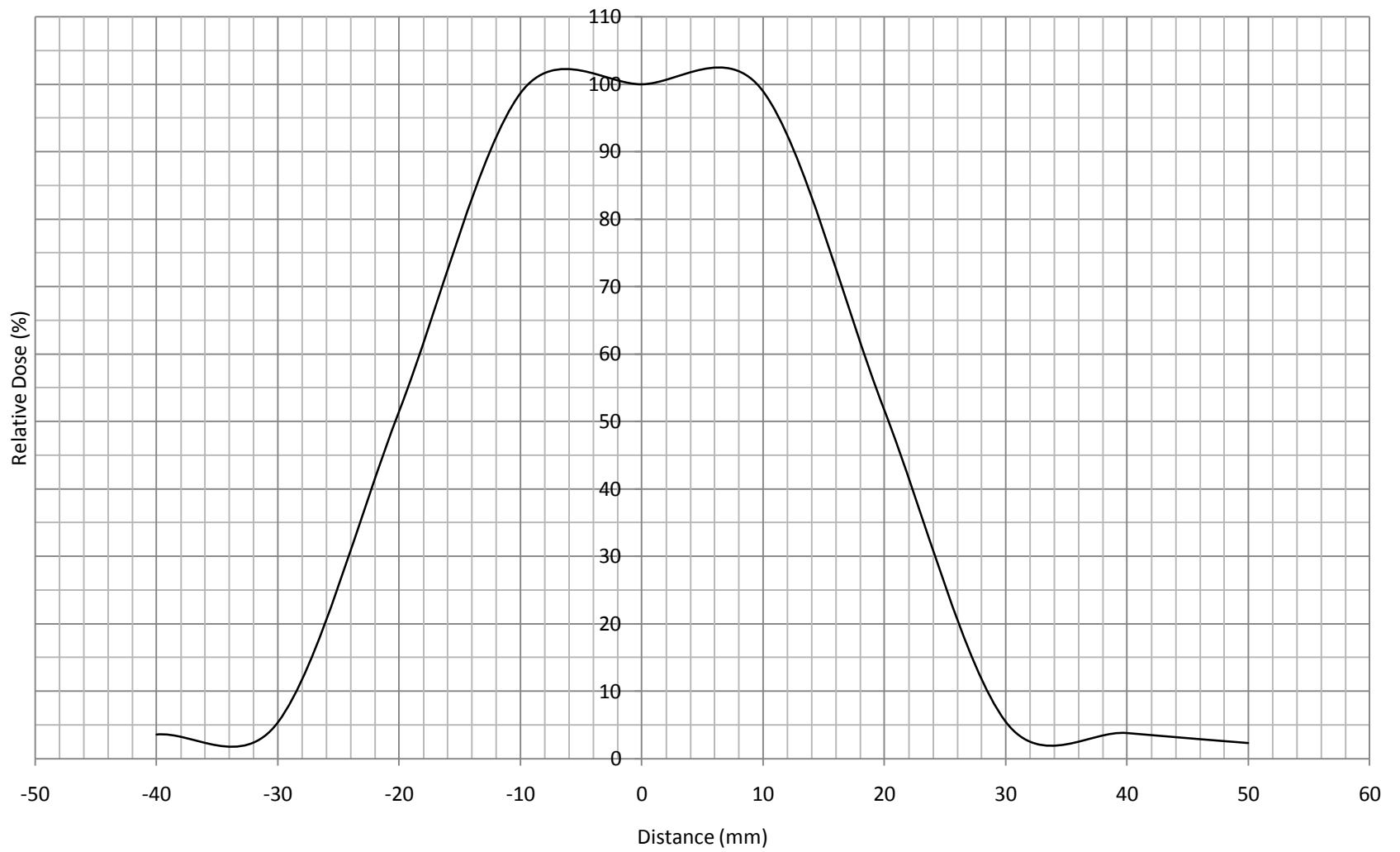
4-cm x 4-cm 100-cm SSD 9-MeV Profile



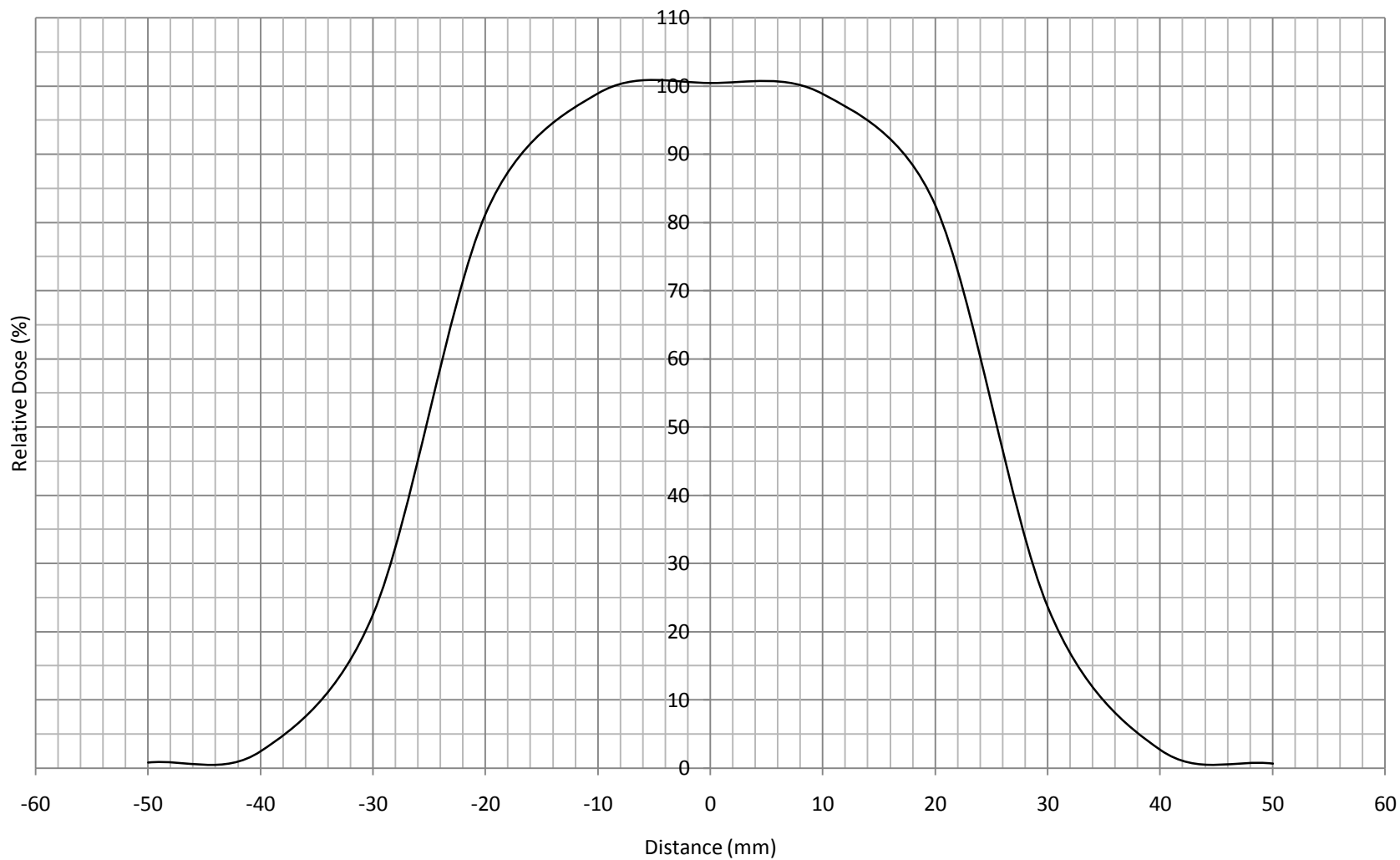
4-cm x 4-cm 100-cm SSD 12-MeV Profile



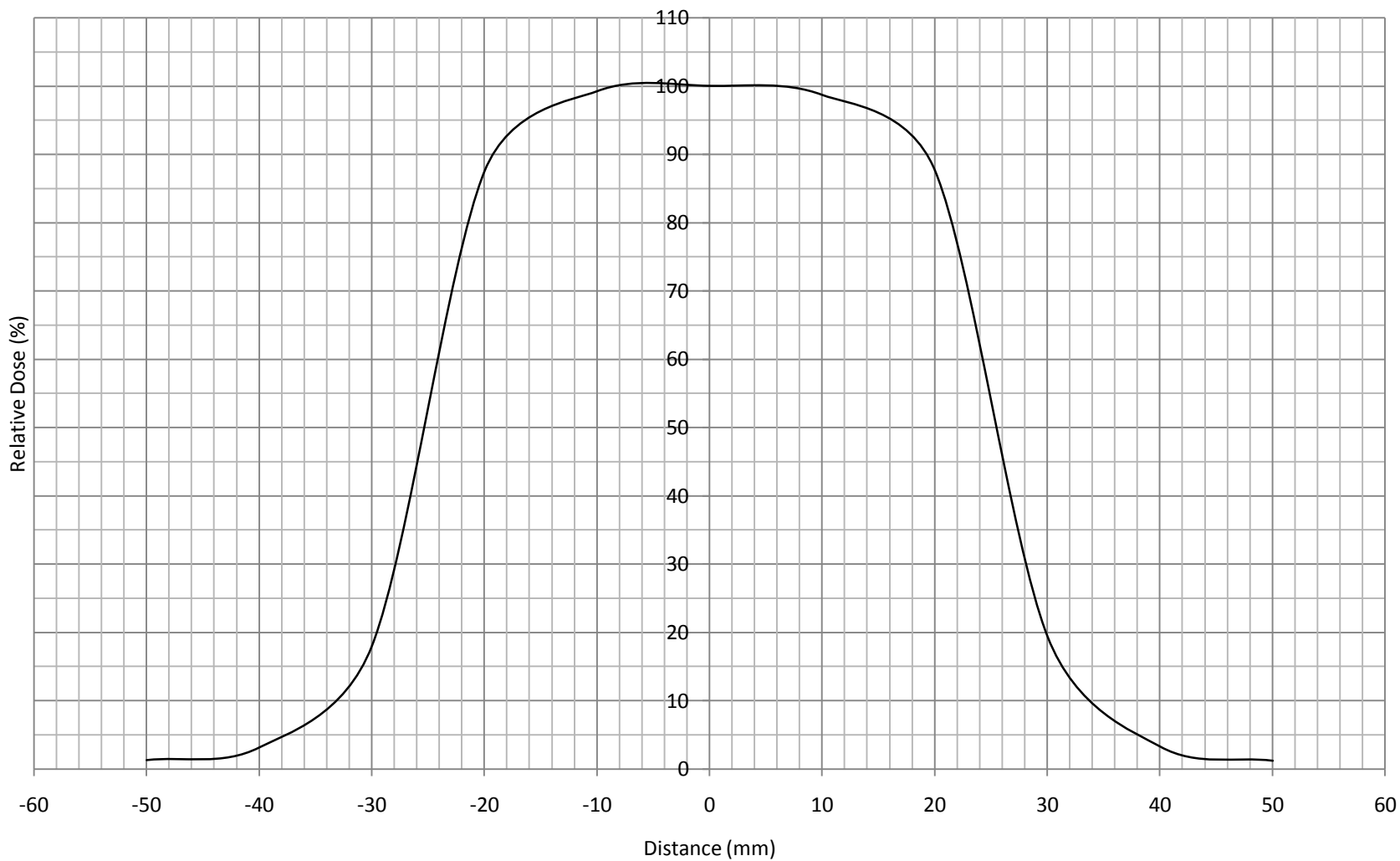
4-cm x 4-cm 100-cm SSD 15-MeV Profile



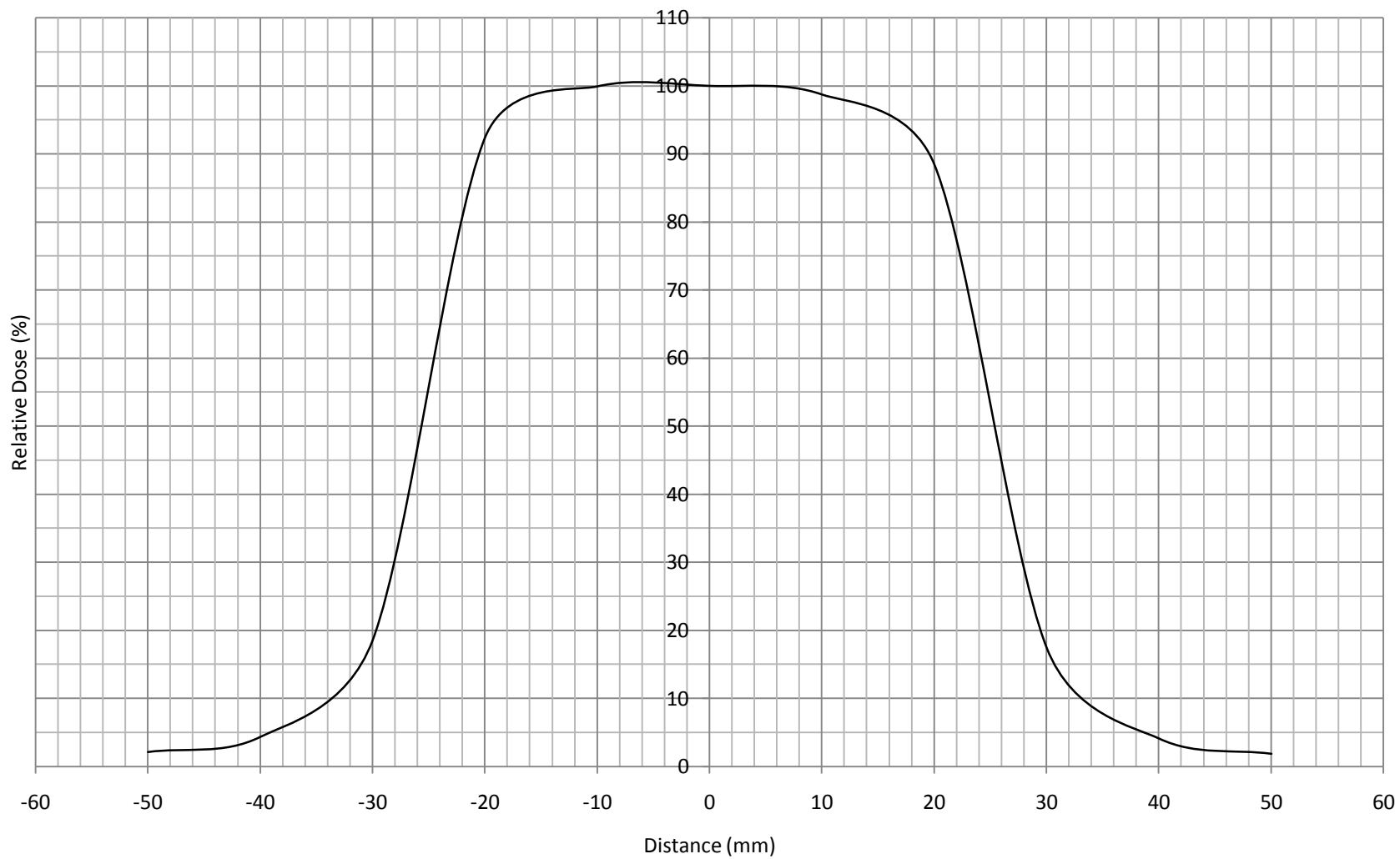
5-cm x 5-cm 100-cm SSD 6-MeV Profile



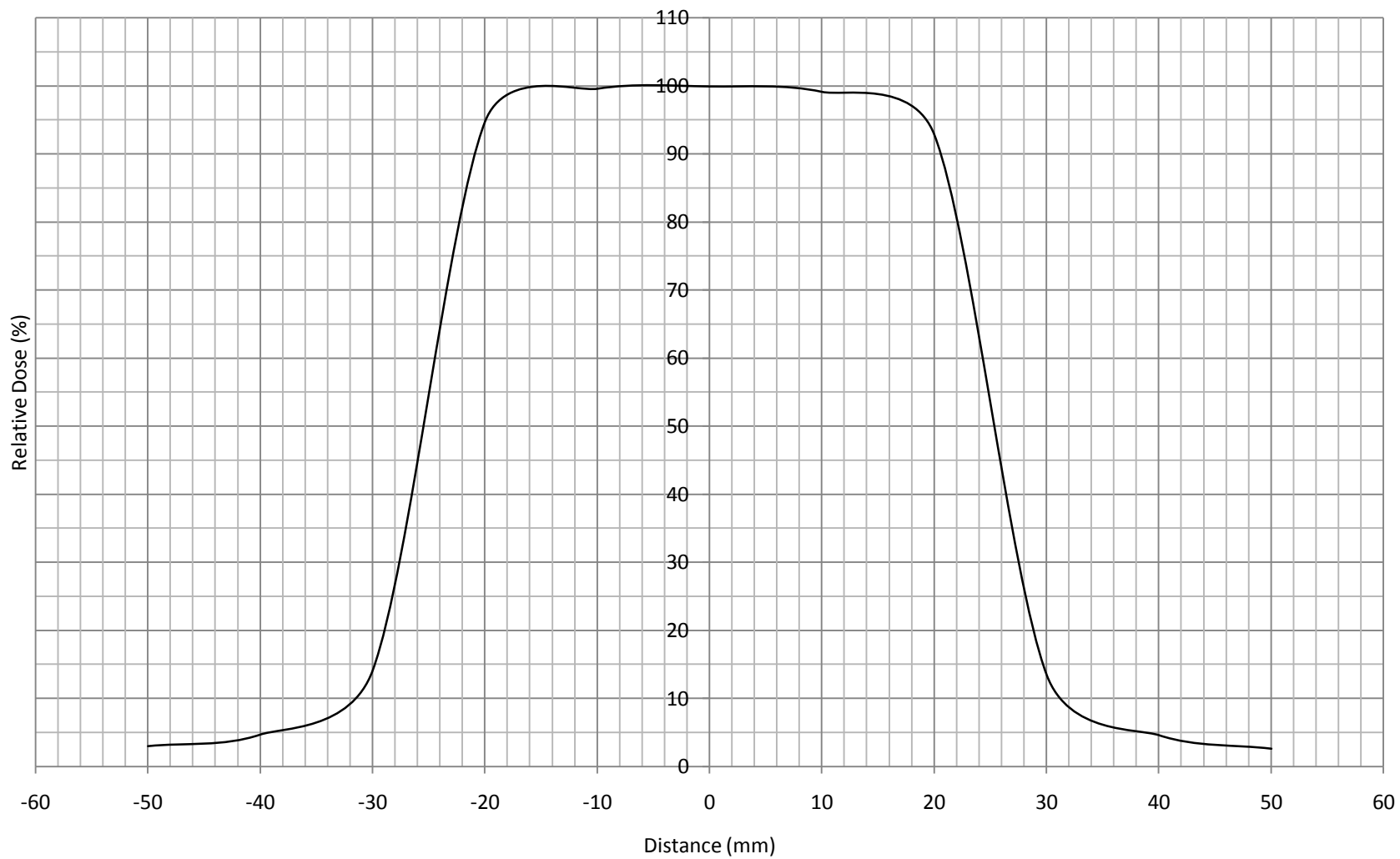
5-cm x 5-cm 100-cm SSD 9-MeV Profile



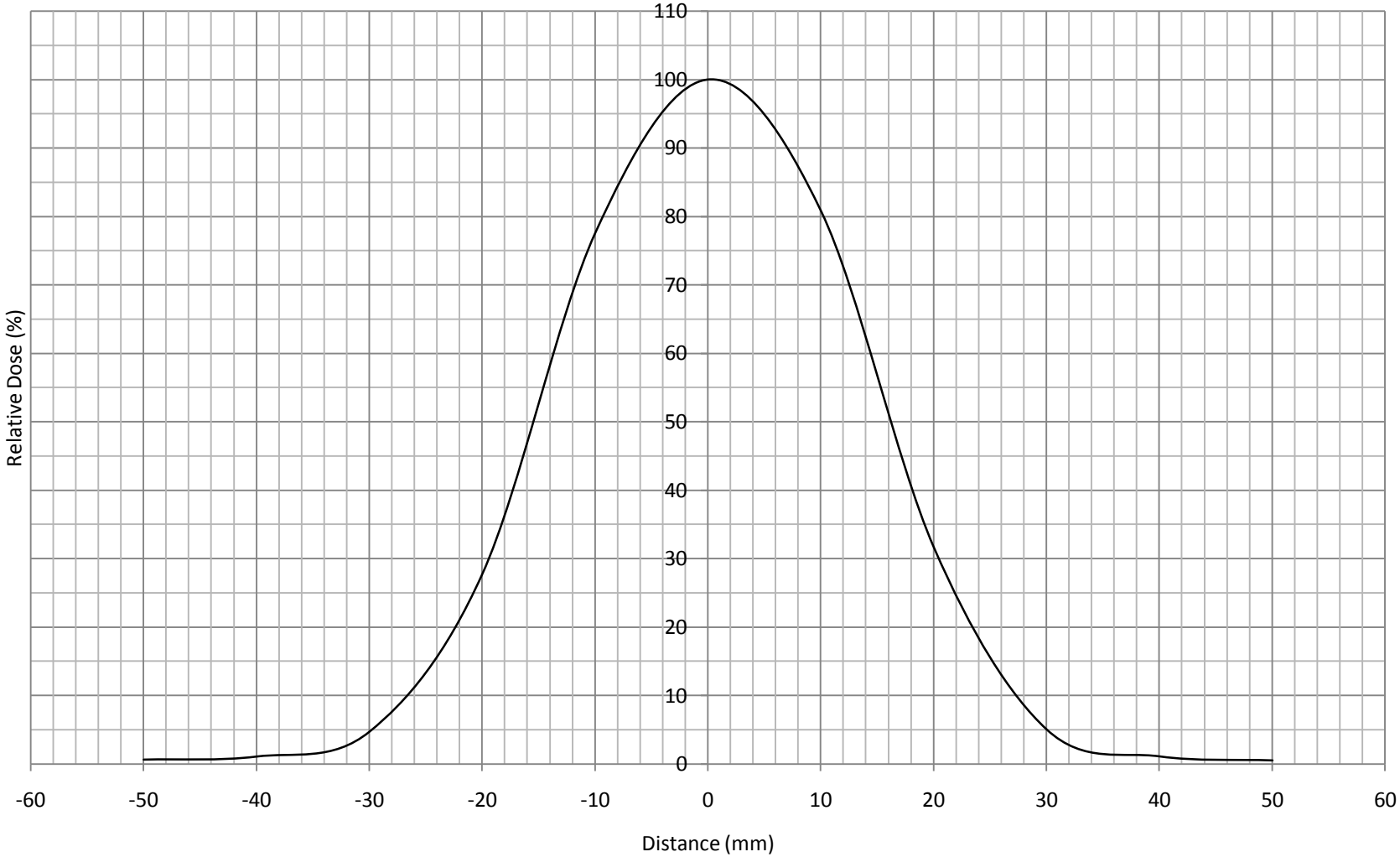
5-cm x 5-cm 100-cm SSD 12-MeV Profile



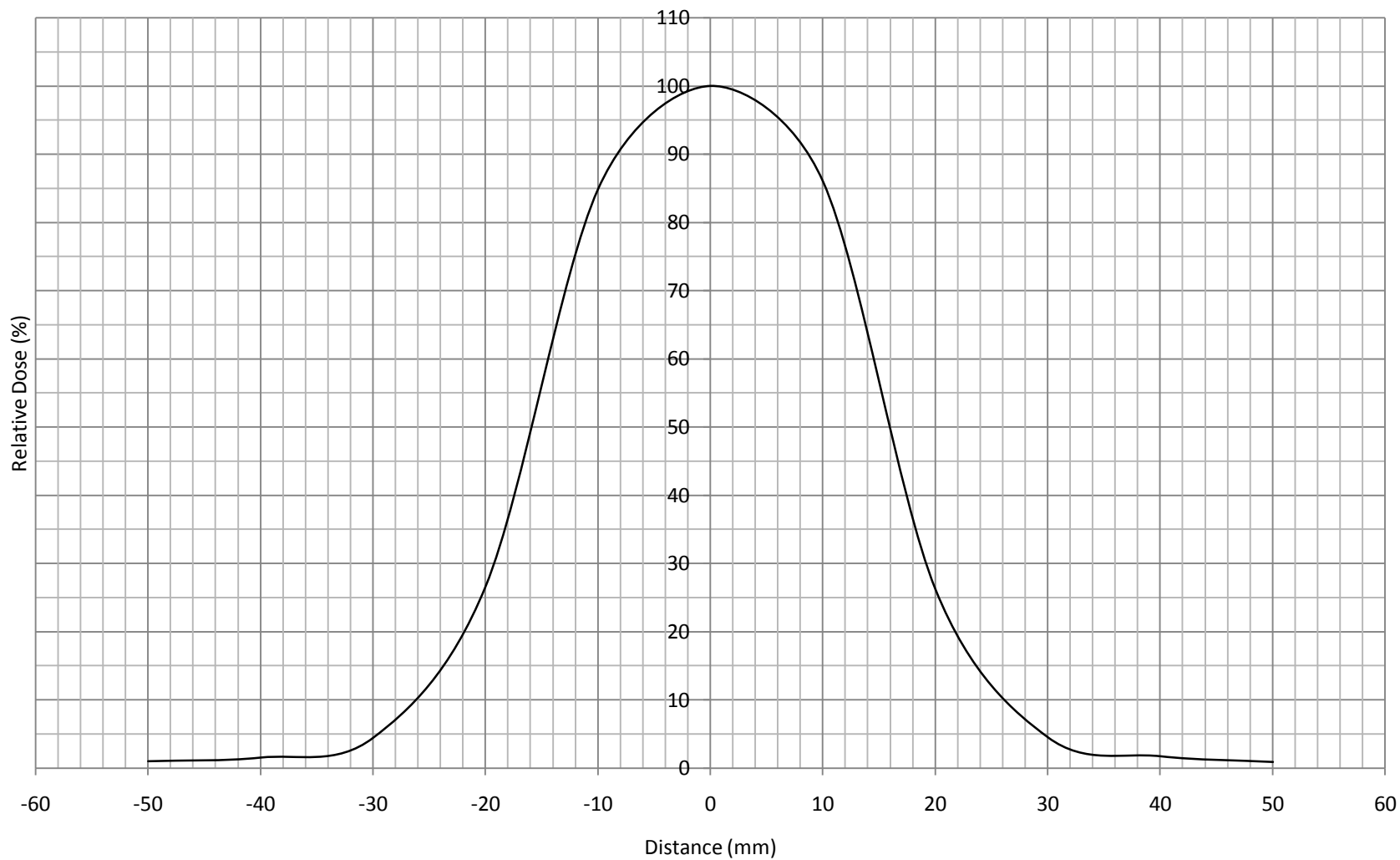
5-cm x 5-cm 100-cm SSD 15-MeV Profile



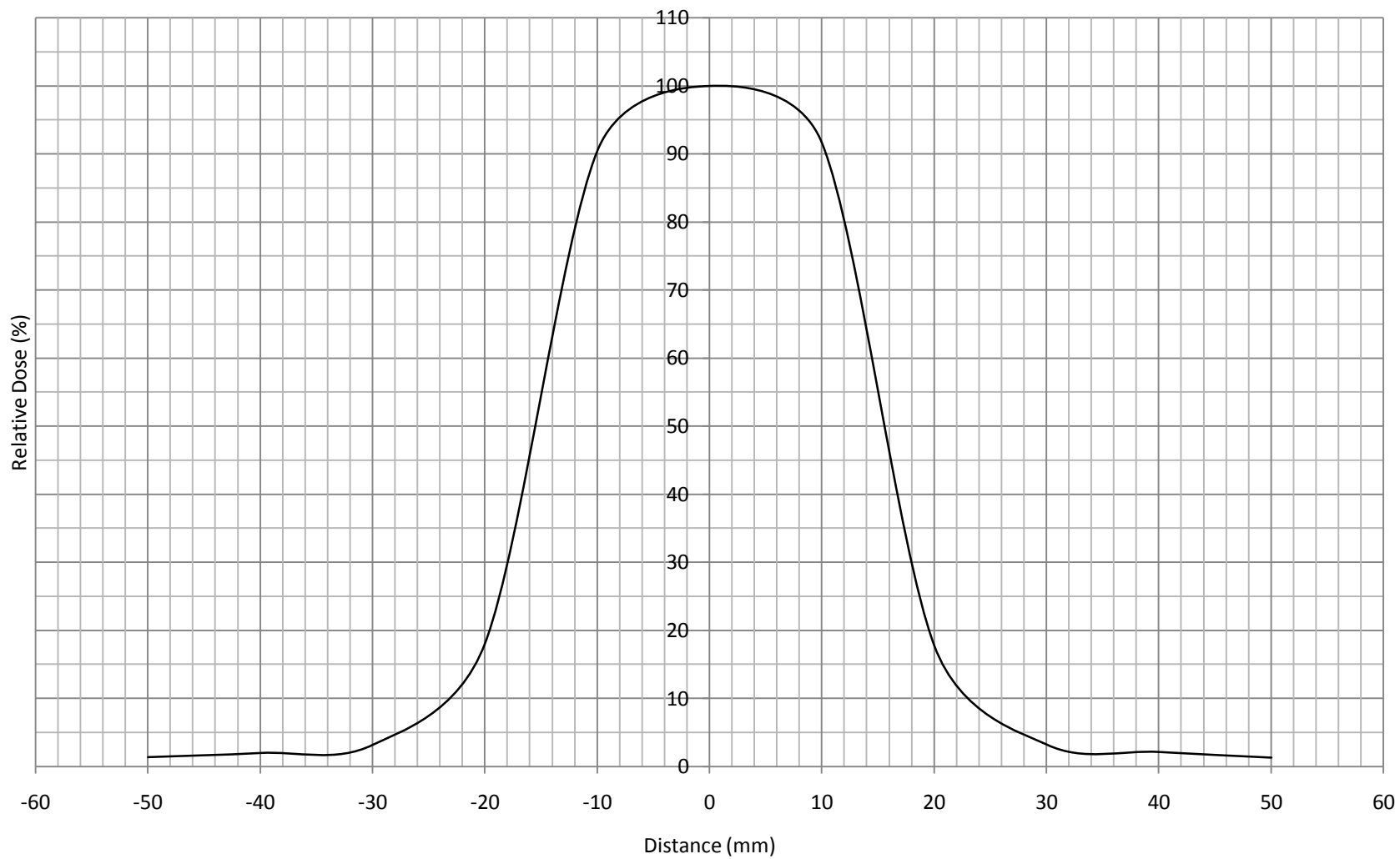
3-cm x 3-cm 105-cm SSD 6-MeV Profile



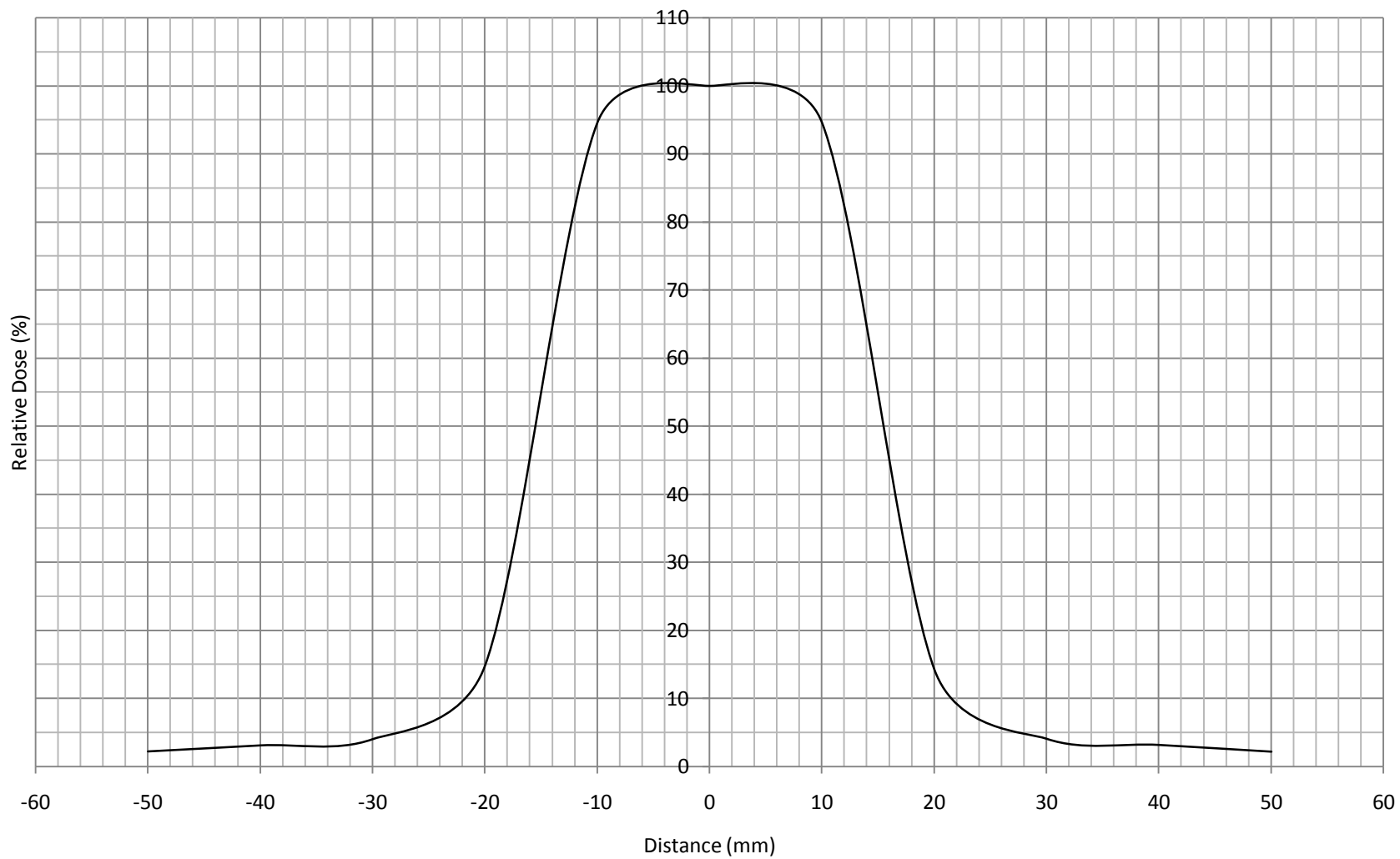
3-cm x 3-cm 105-cm SSD 9-MeV Profile



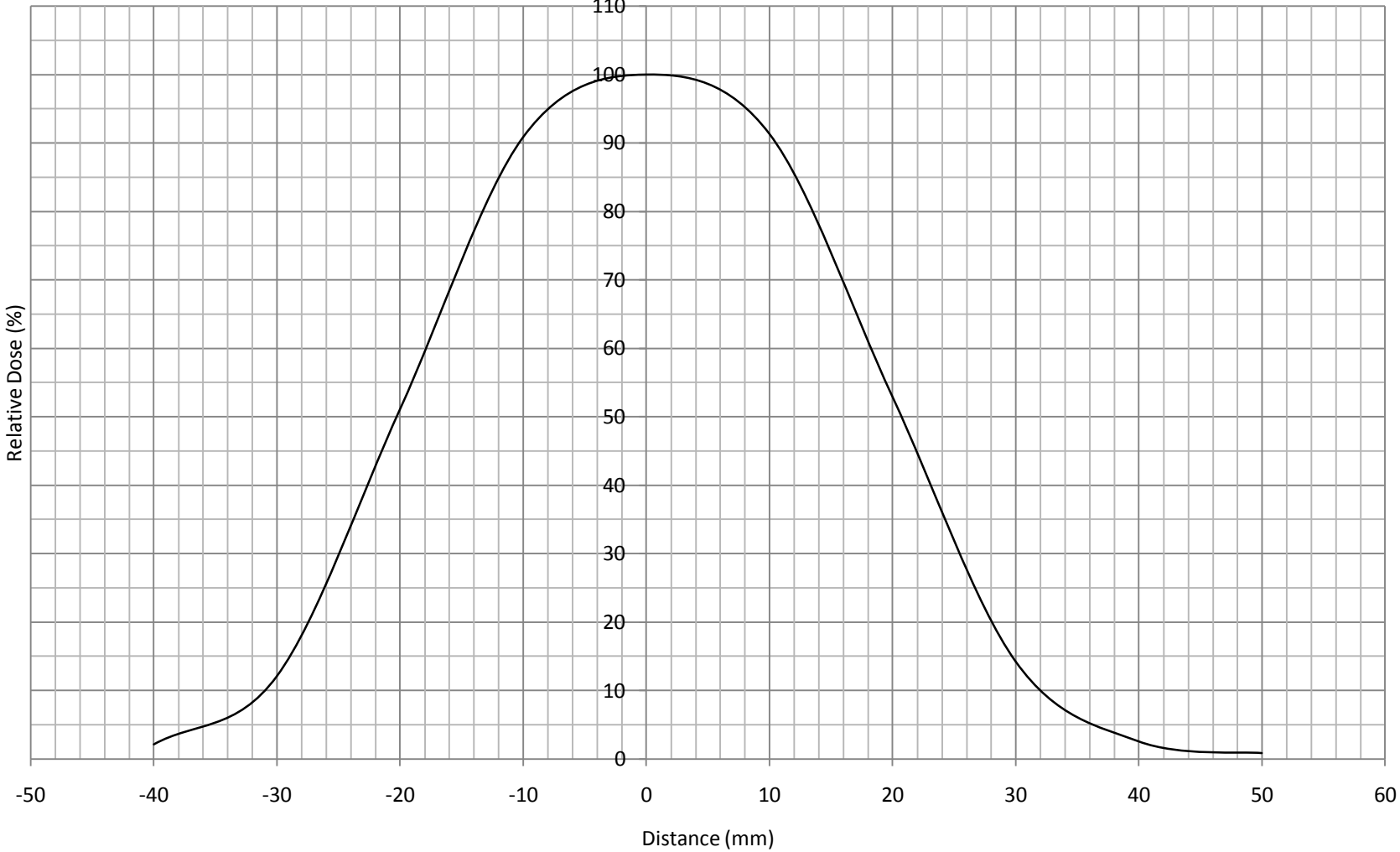
3-cm x 3-cm 105-cm SSD 12-MeV Profile



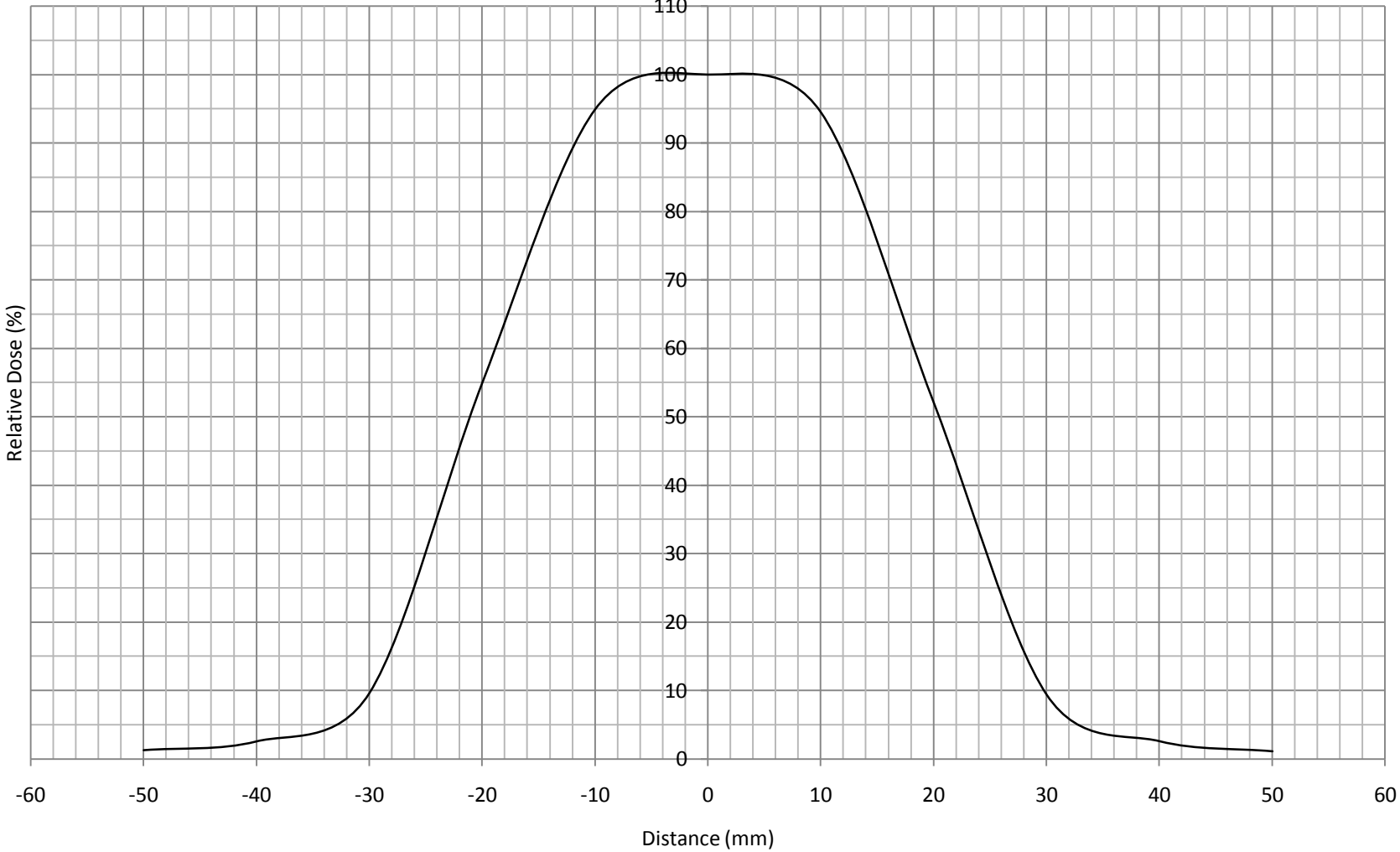
3-cm x 3-cm 105-cm SSD 15-MeV Profile



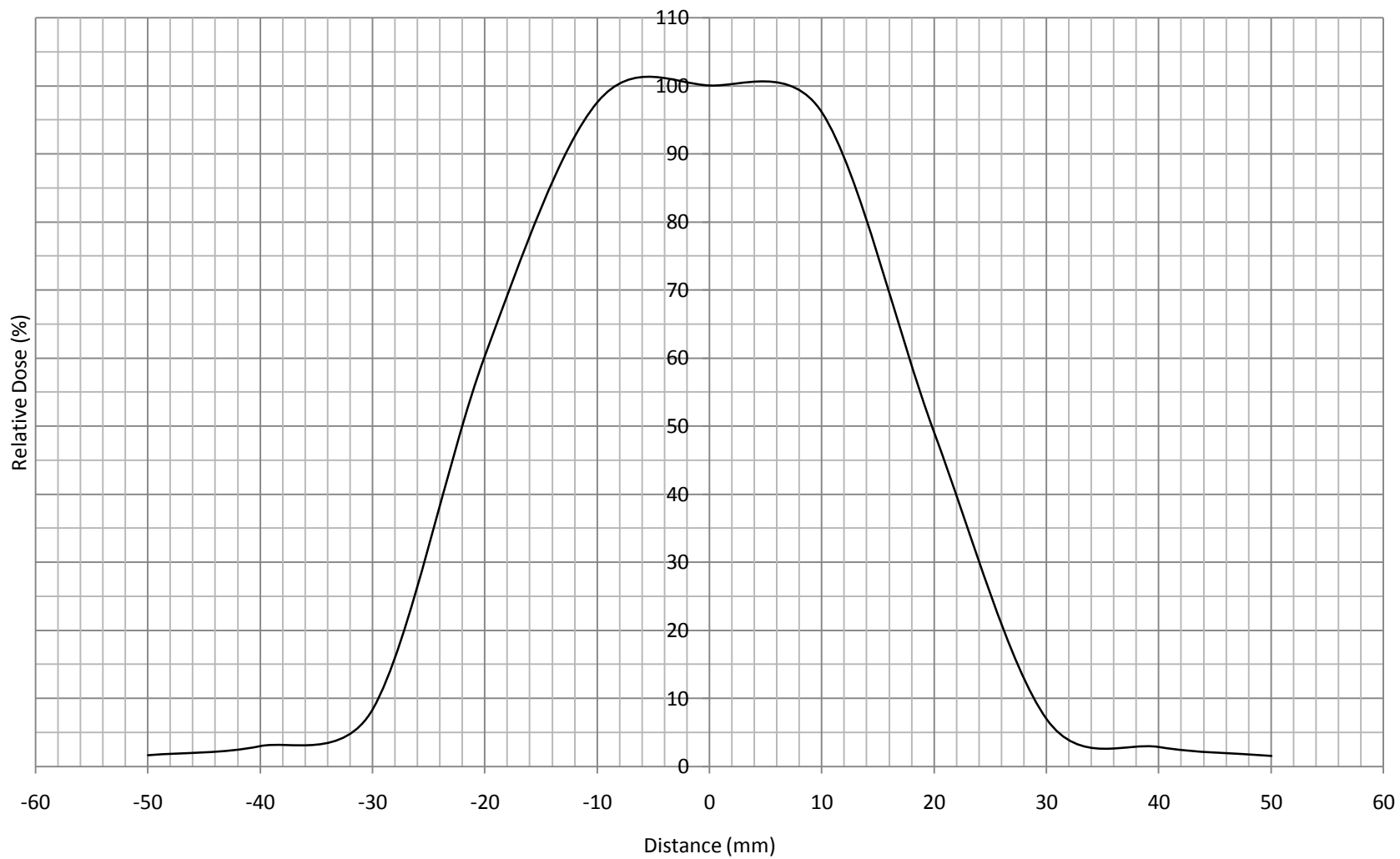
4-cm x 4-cm 105-cm SSD 6-MeV Profile



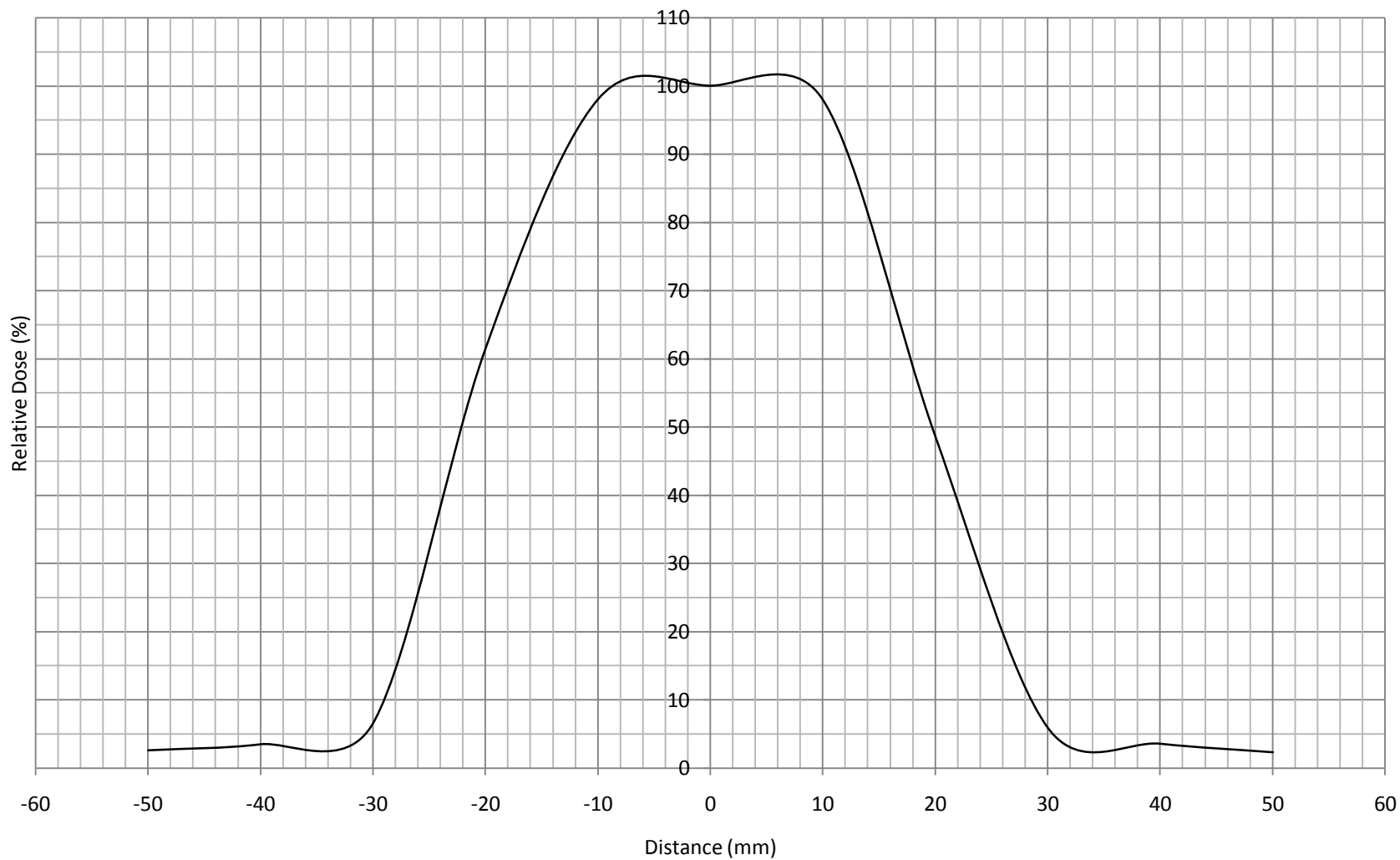
4-cm x 4-cm 105-cm SSD 9-MeV Profile



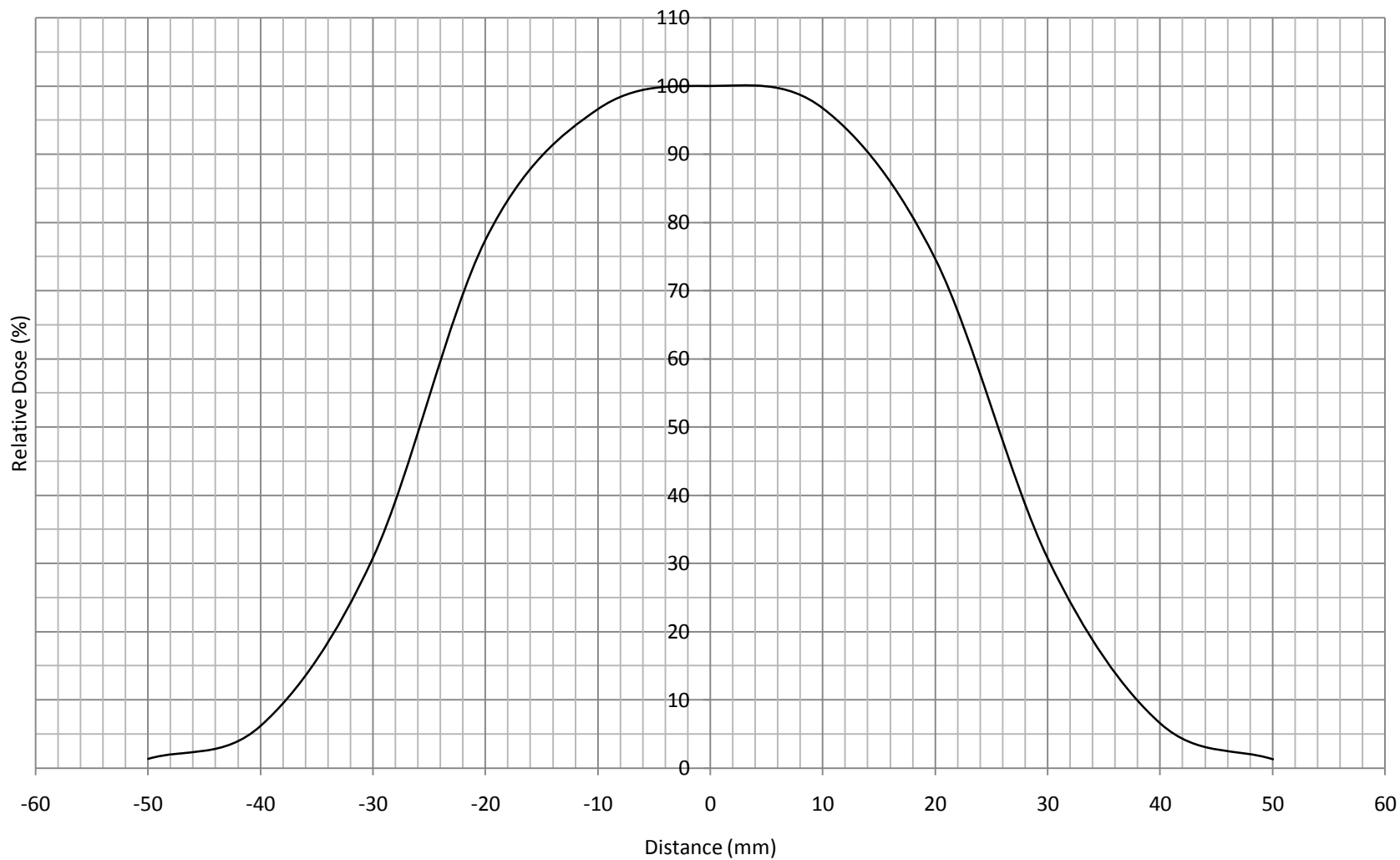
4-cm x 4-cm 105-cm SSD 12-MeV Profile



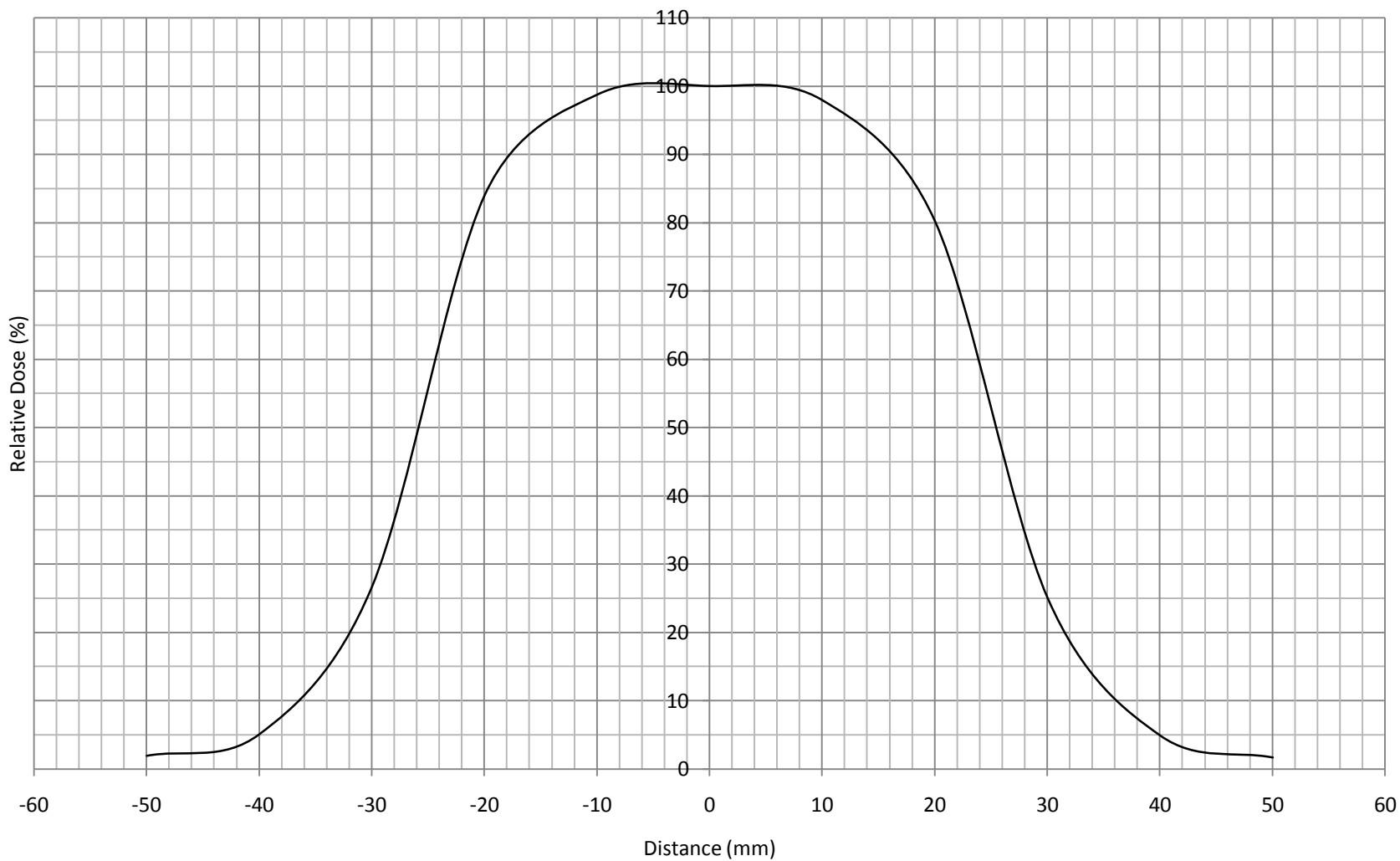
4-cm x 4-cm 105-cm SSD 15-MeV Profile



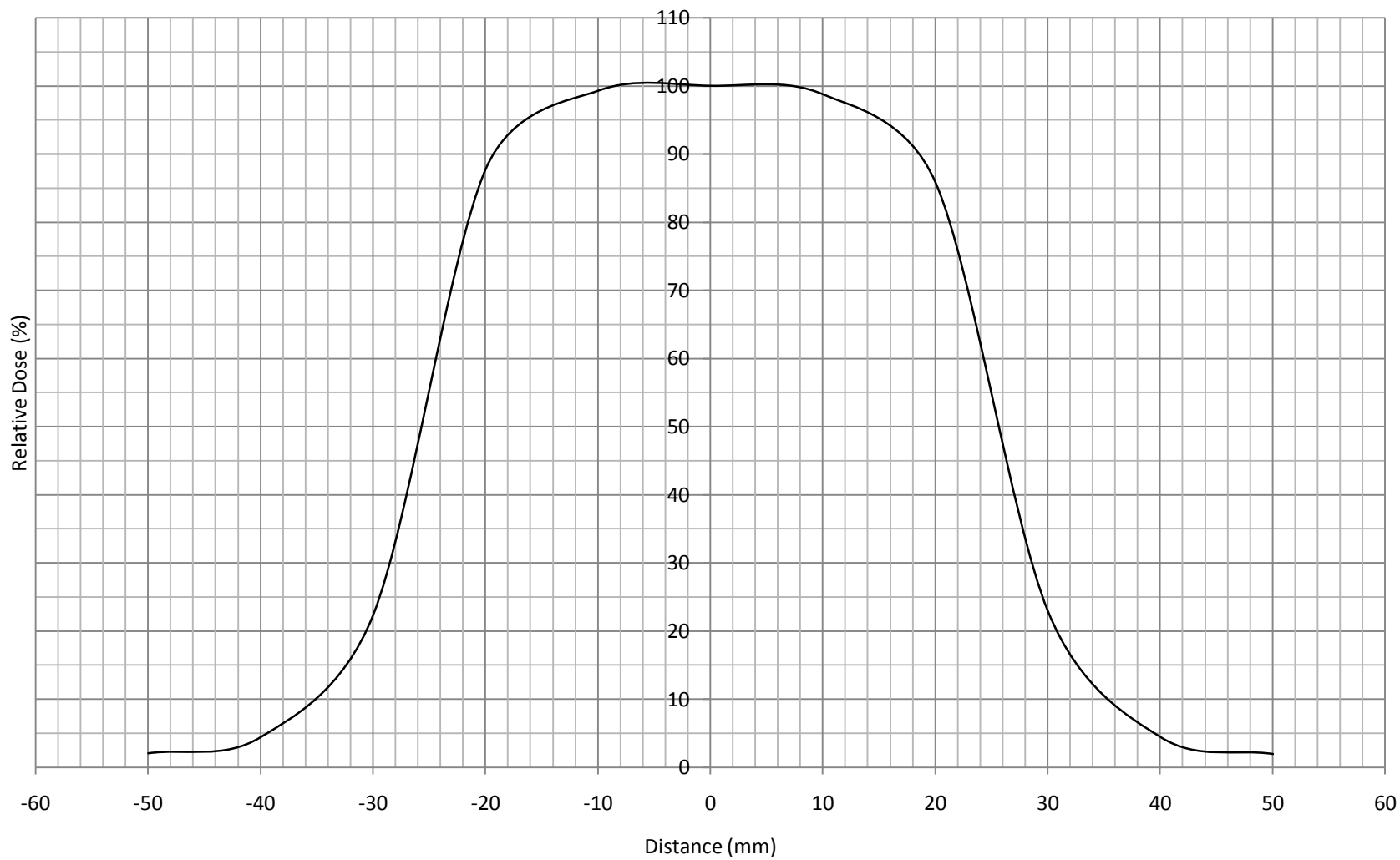
5-cm x 5-cm 105-cm SSD 6-MeV Profile



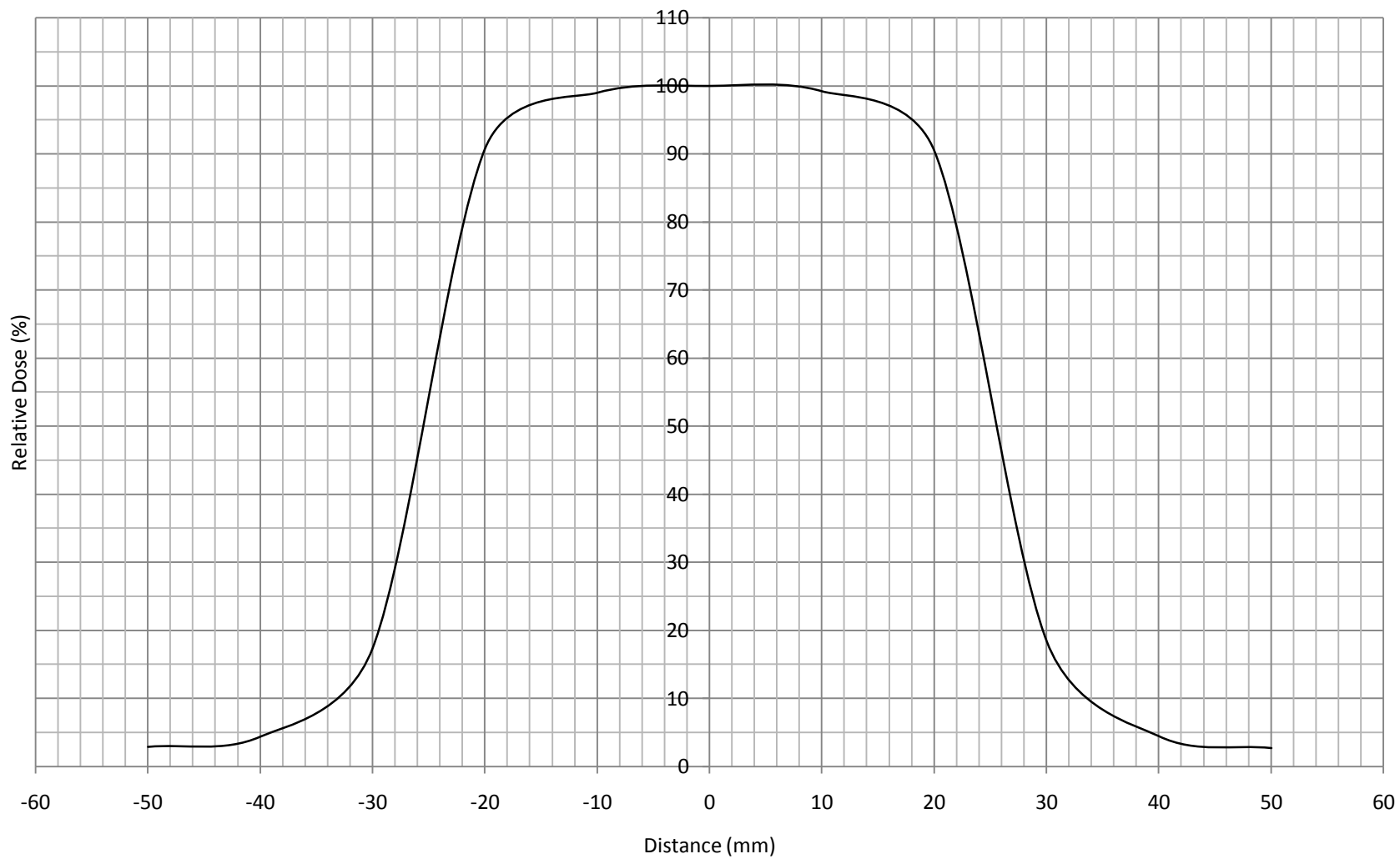
5-cm x 5-cm 105-cm SSD 9-MeV Profile



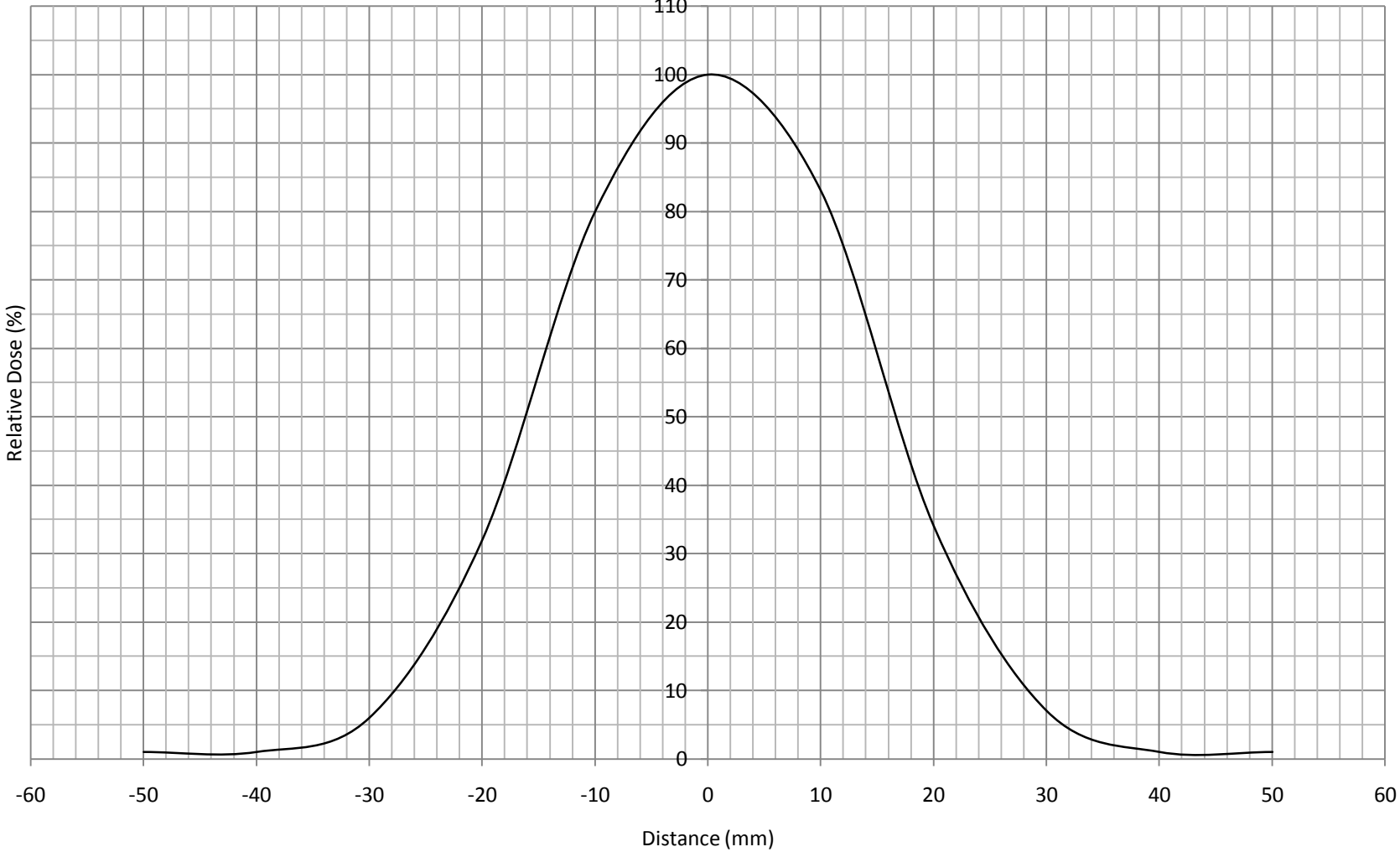
5-cm x 5-cm 105-cm SSD 12-MeV Profile



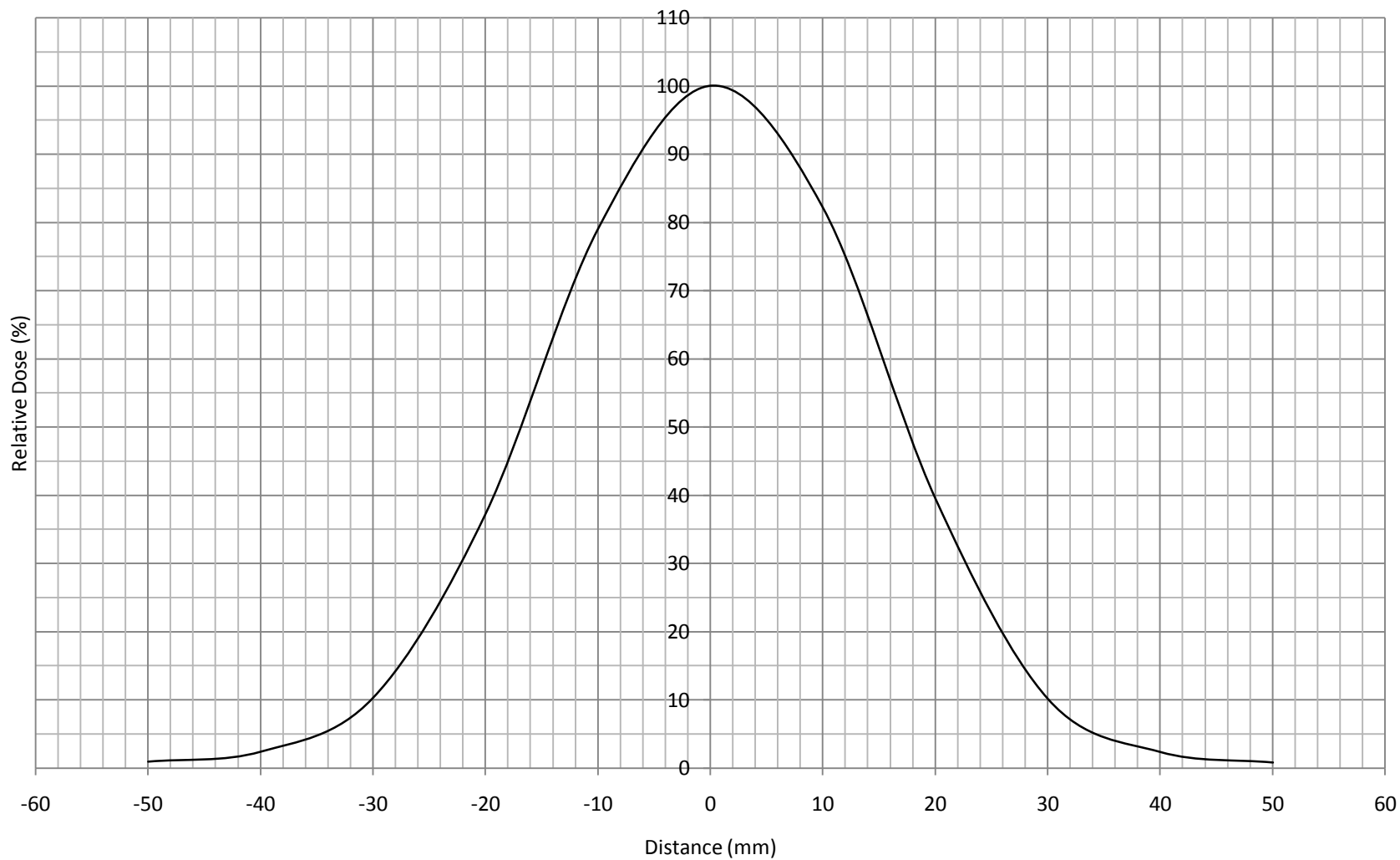
5-cm x 5-cm 105-cm SSD 15-MeV Profile



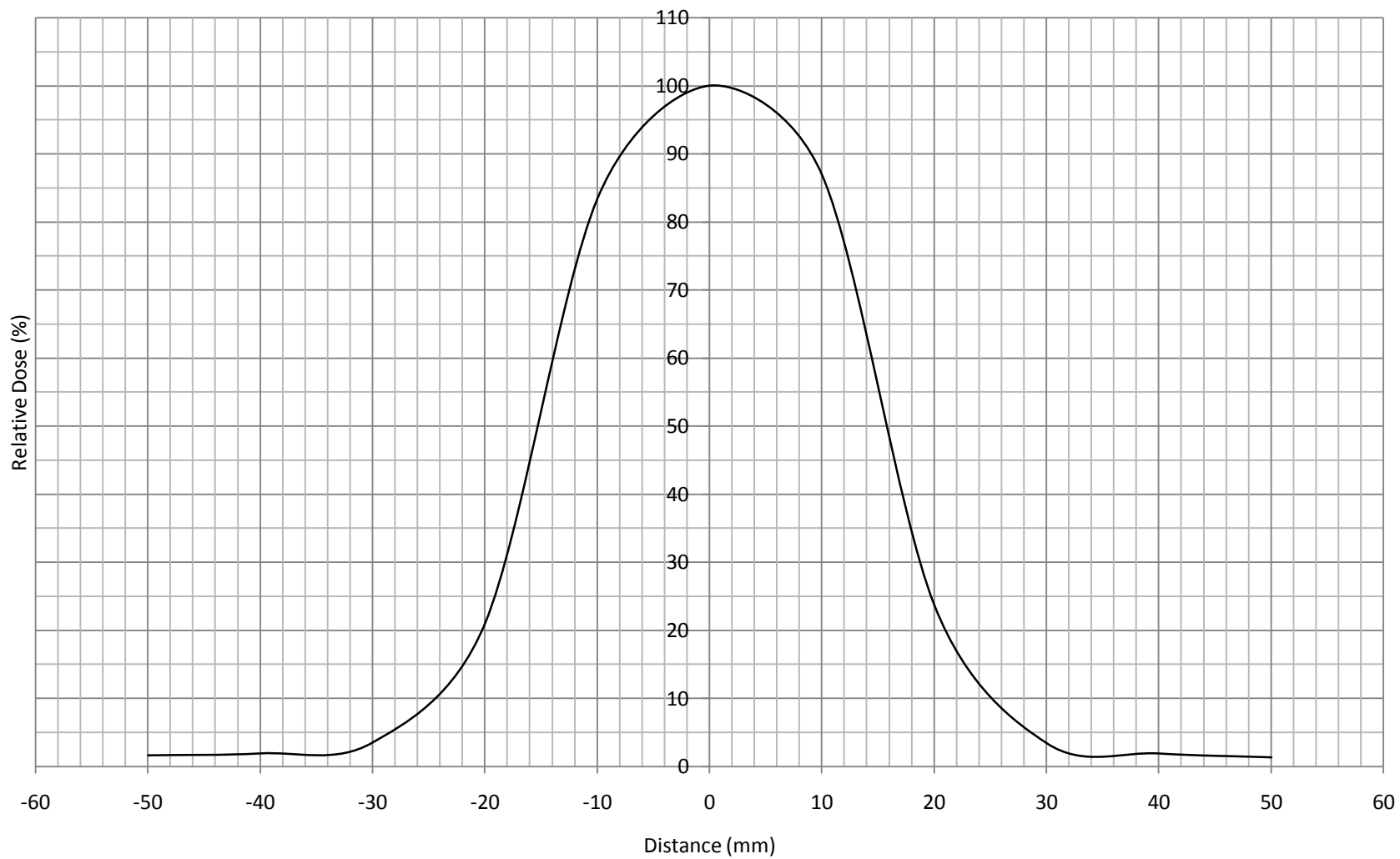
3-cm x 3-cm 110-cm SSD 6-MeV Profile



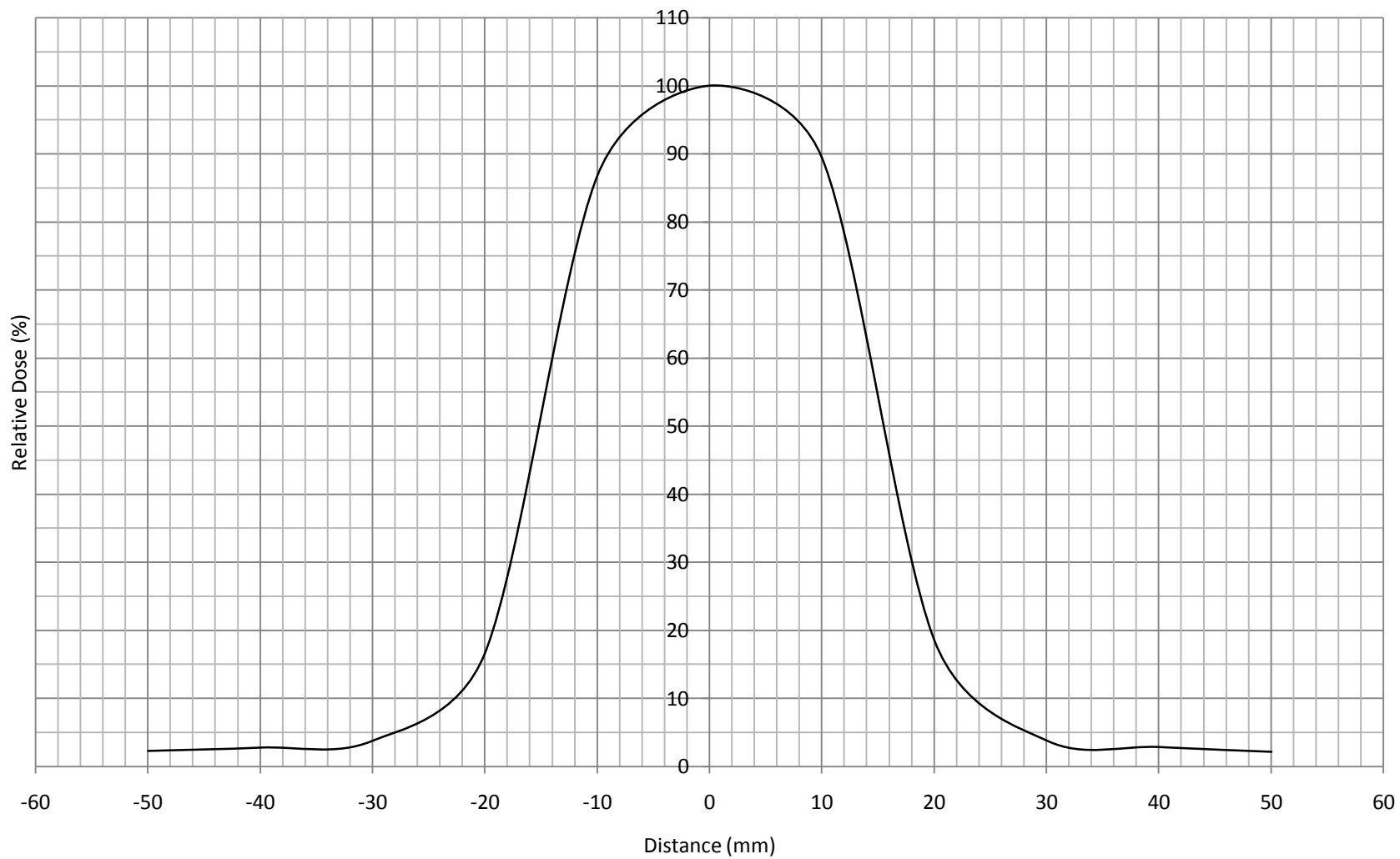
3-cm x 3-cm 110-cm SSD 9-MeV Profile



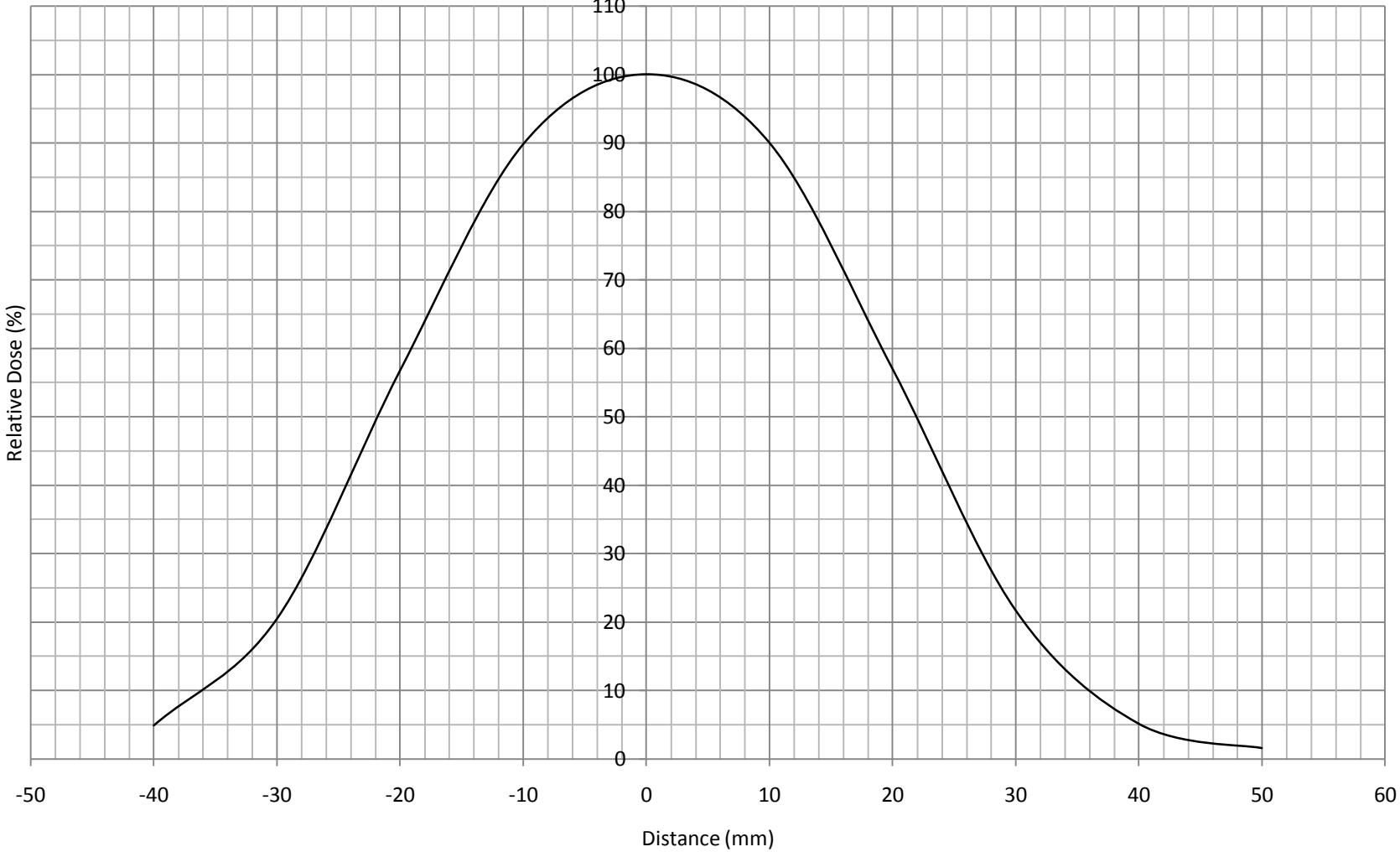
3-cm x 3-cm 110-cm SSD 12-MeV Profile



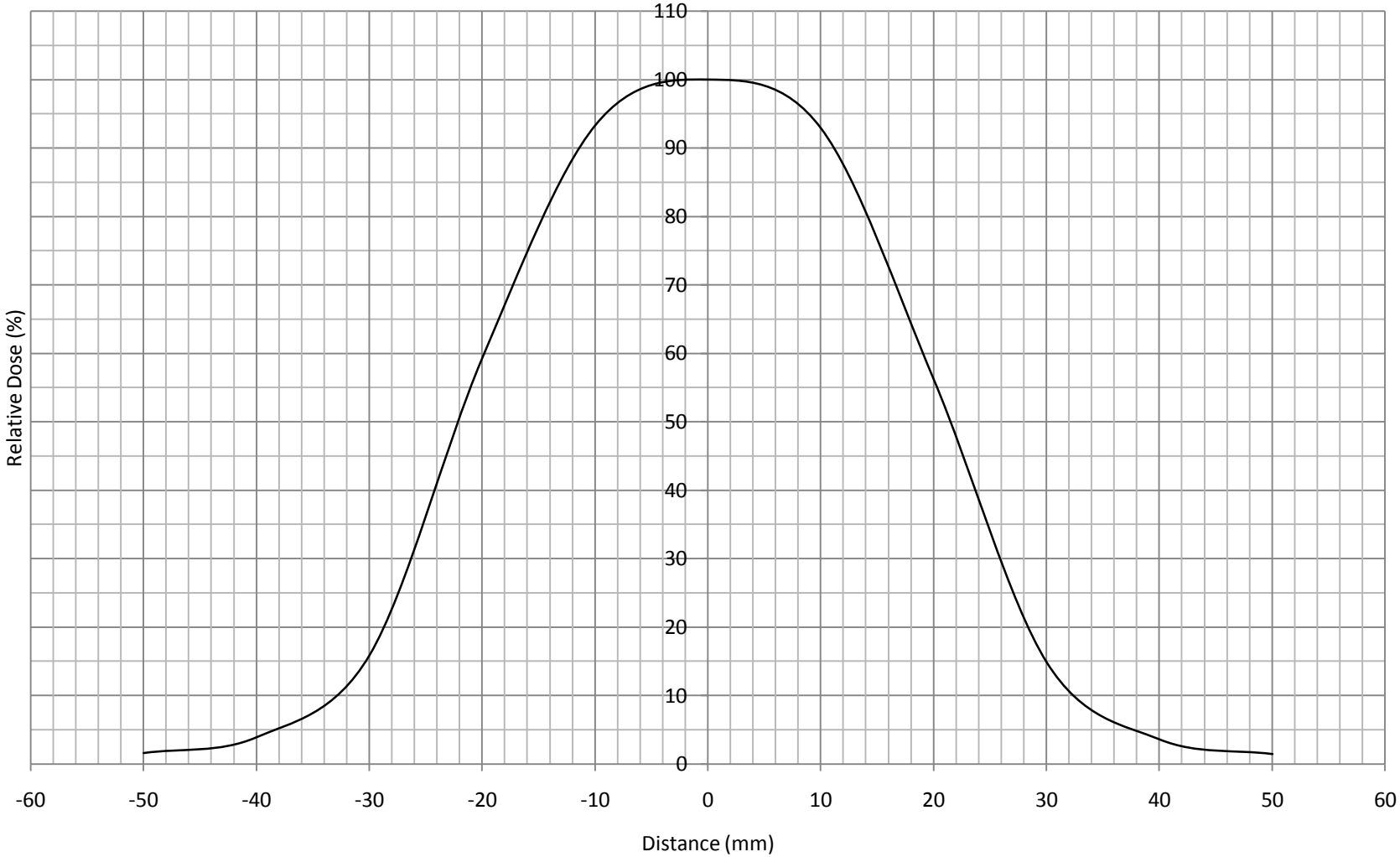
3-cm x 3-cm 110-cm SSD 15-MeV Profile



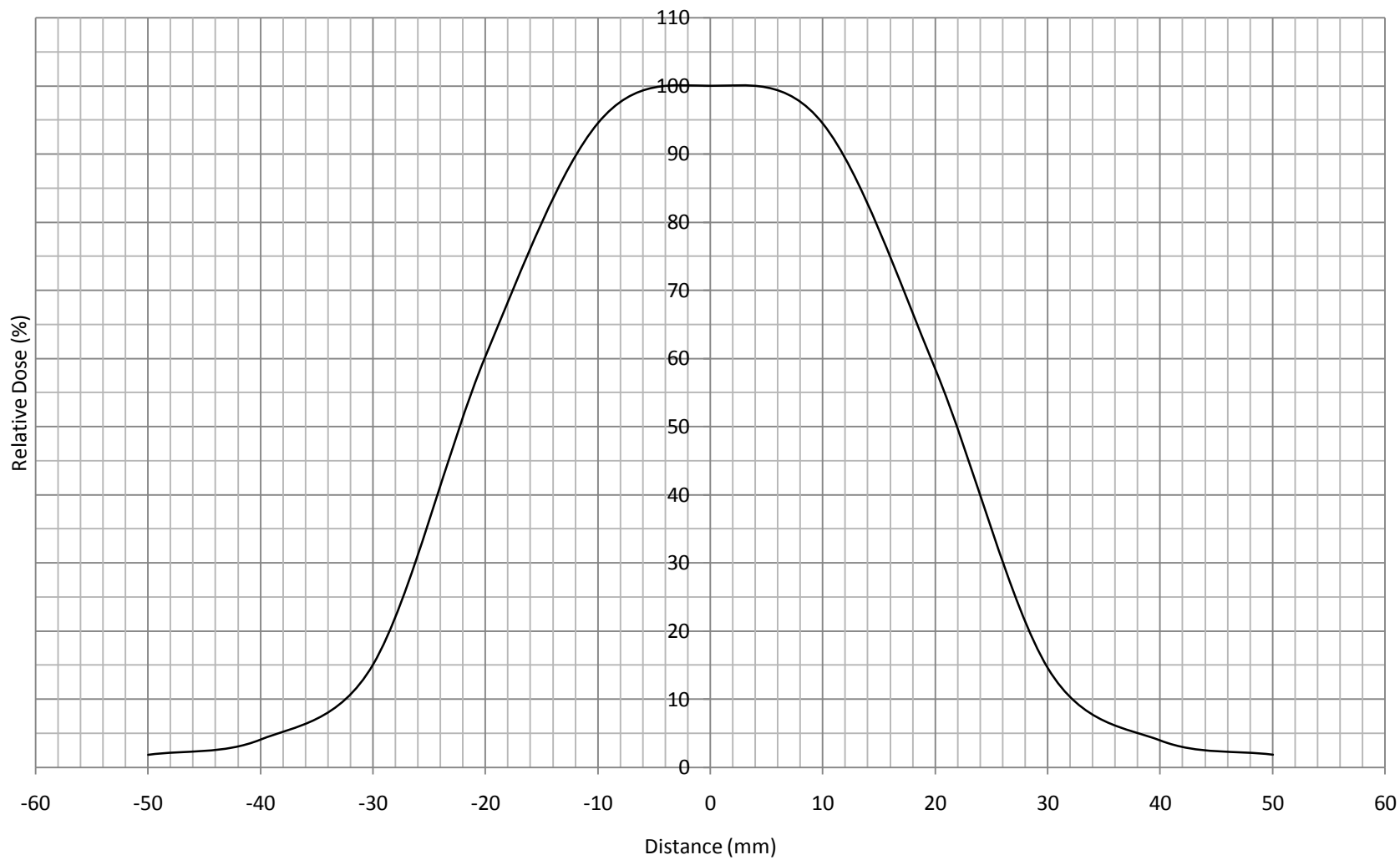
4-cm x 4-cm 110-cm SSD 6-MeV Profile



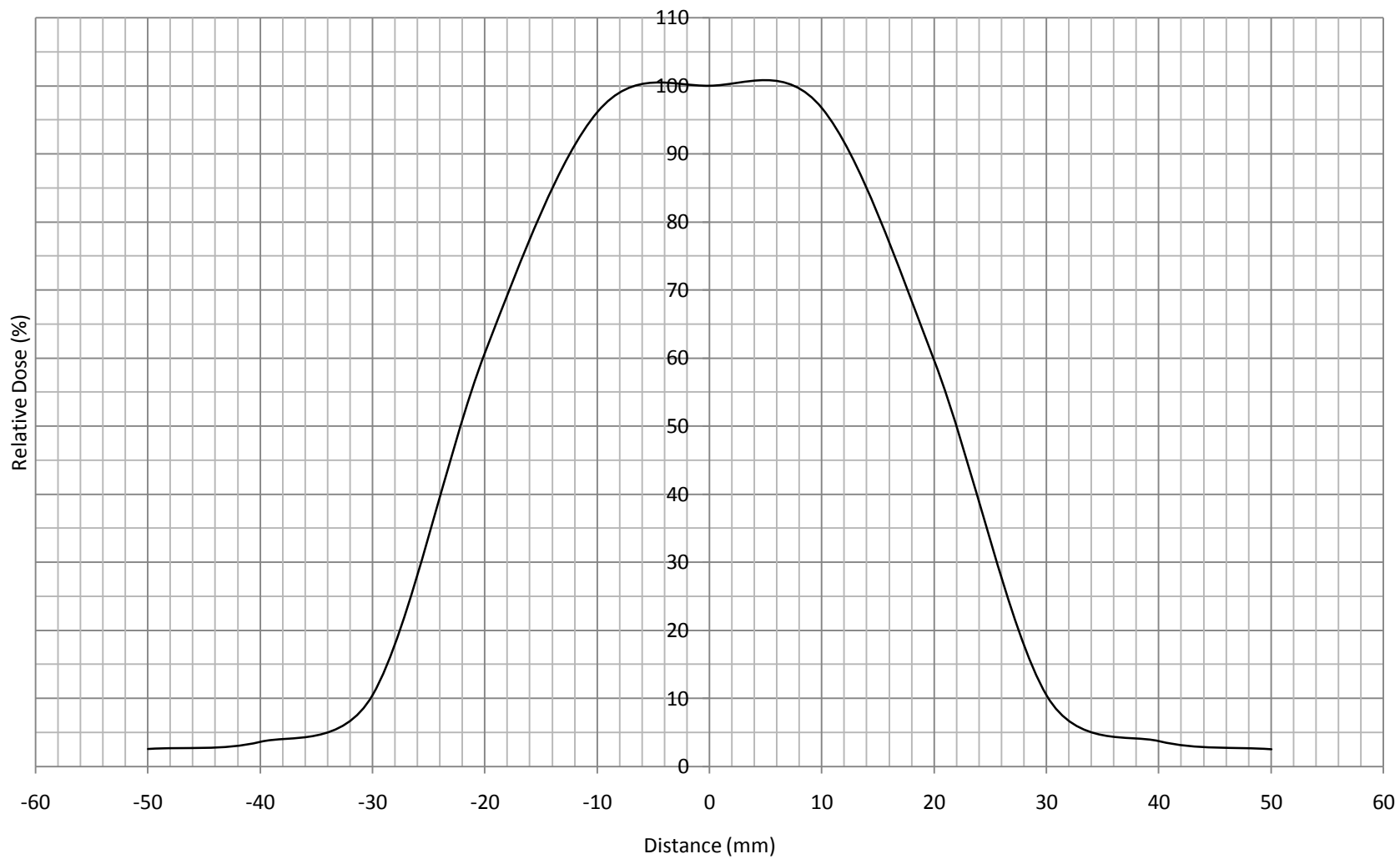
4-cm x 4-cm 110-cm SSD 9-MeV Profile



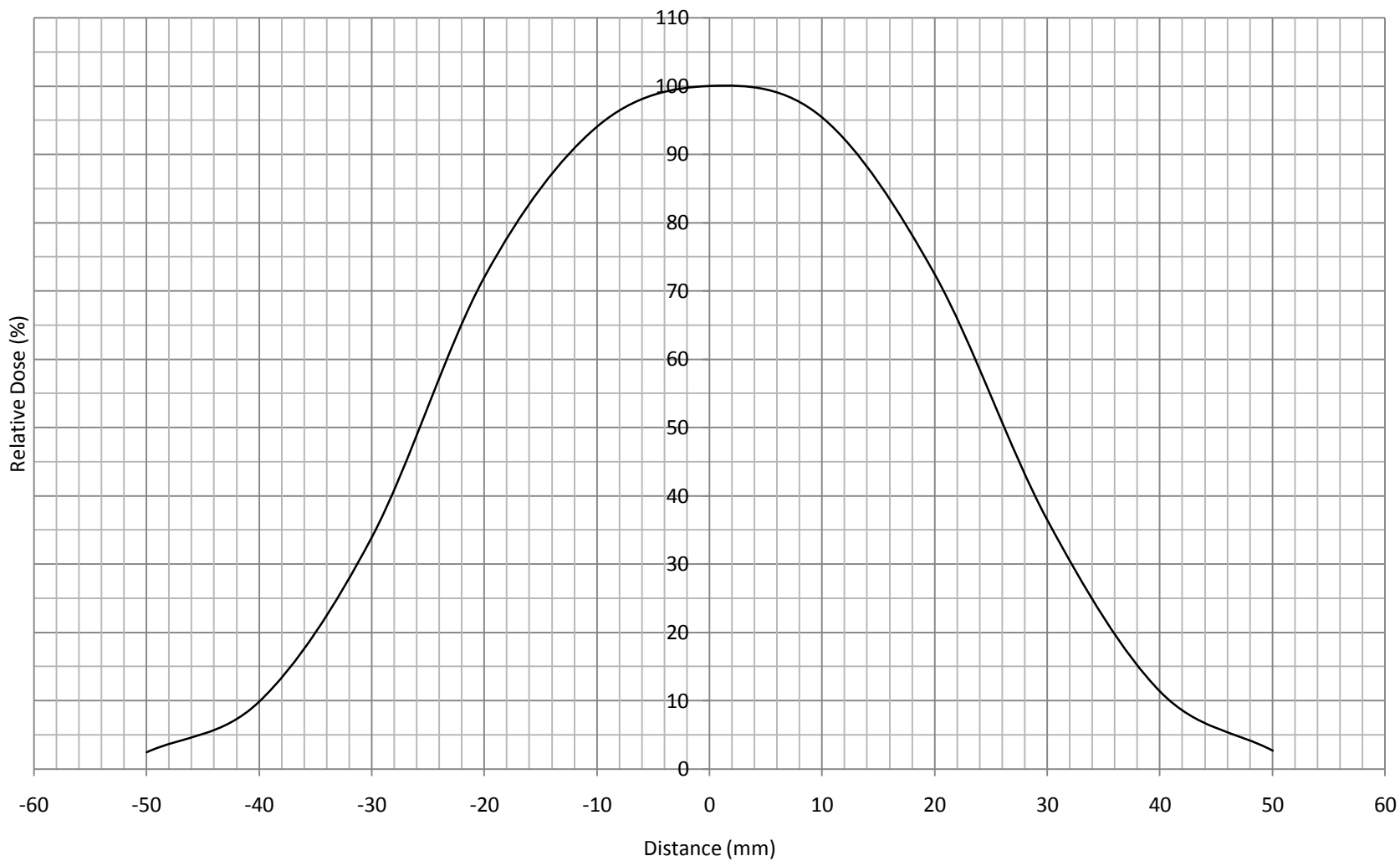
4-cm x 4-cm 110-cm SSD 12-MeV Profile



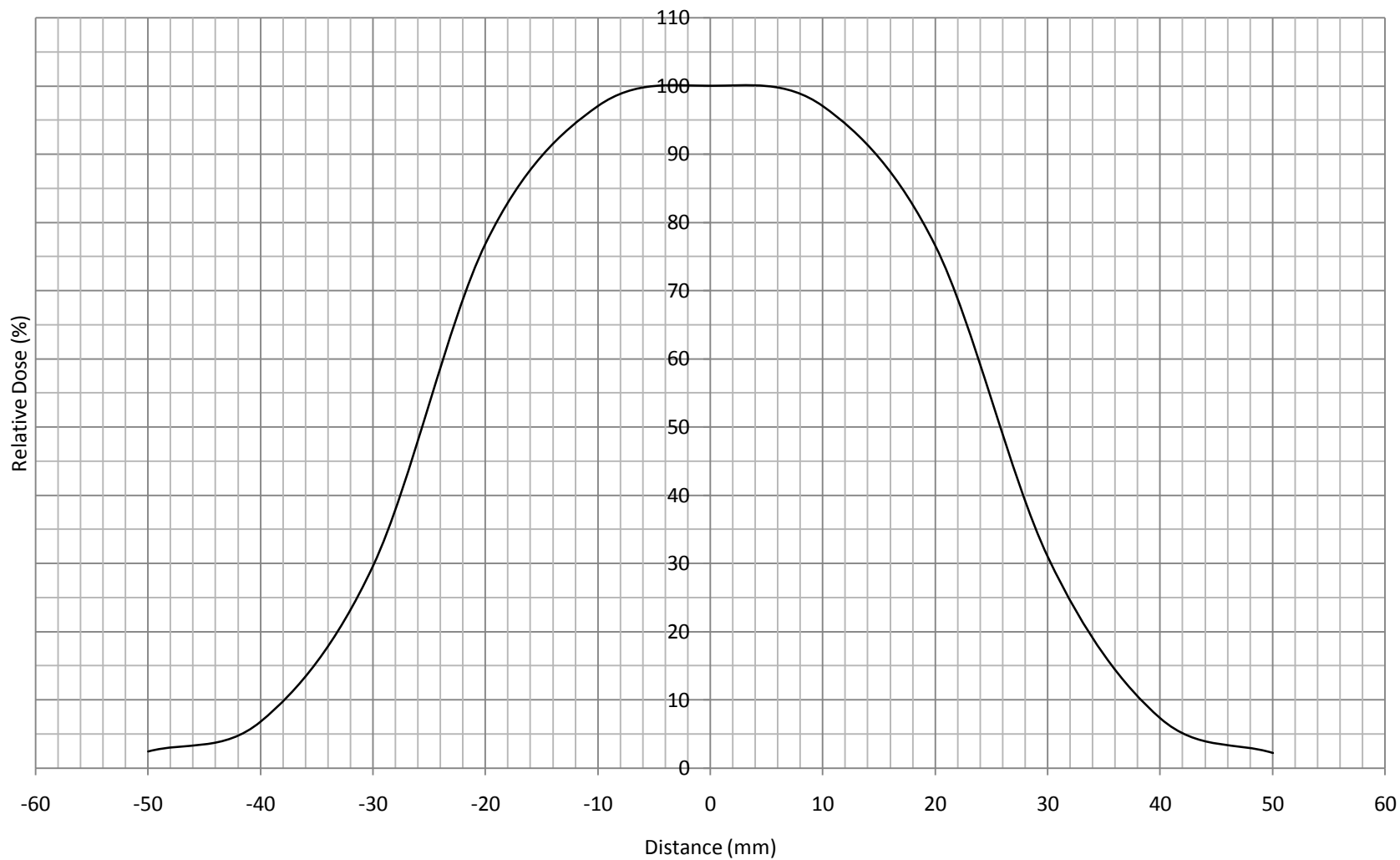
4-cm x 4-cm 110-cm SSD 15-MeV Profile



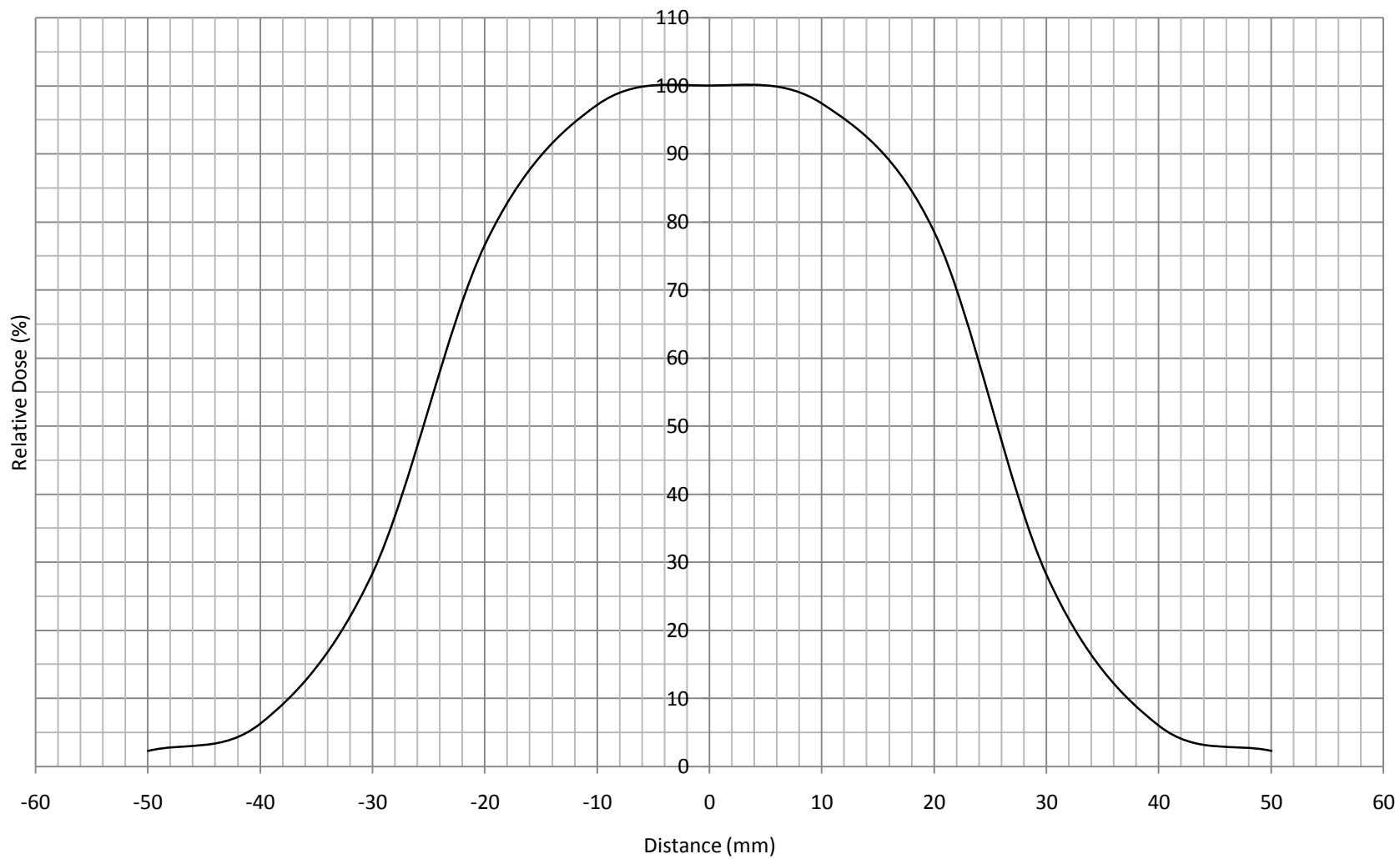
5-cm x 5-cm 110-cm SSD 6-MeV Profile



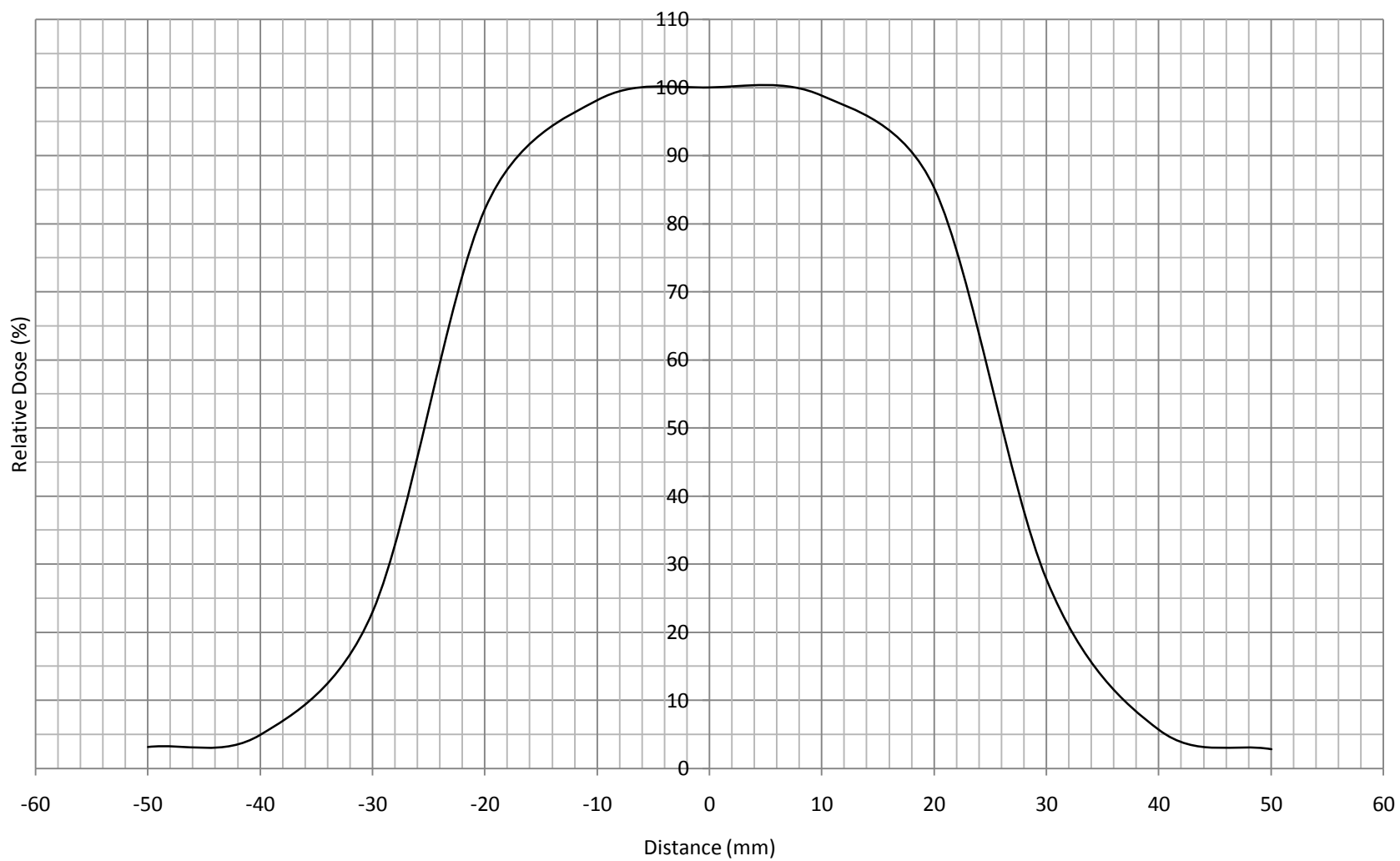
5-cm x 5-cm 110-cm SSD 9-MeV Profile



5-cm x 5-cm 110-cm SSD 12-MeV Profile



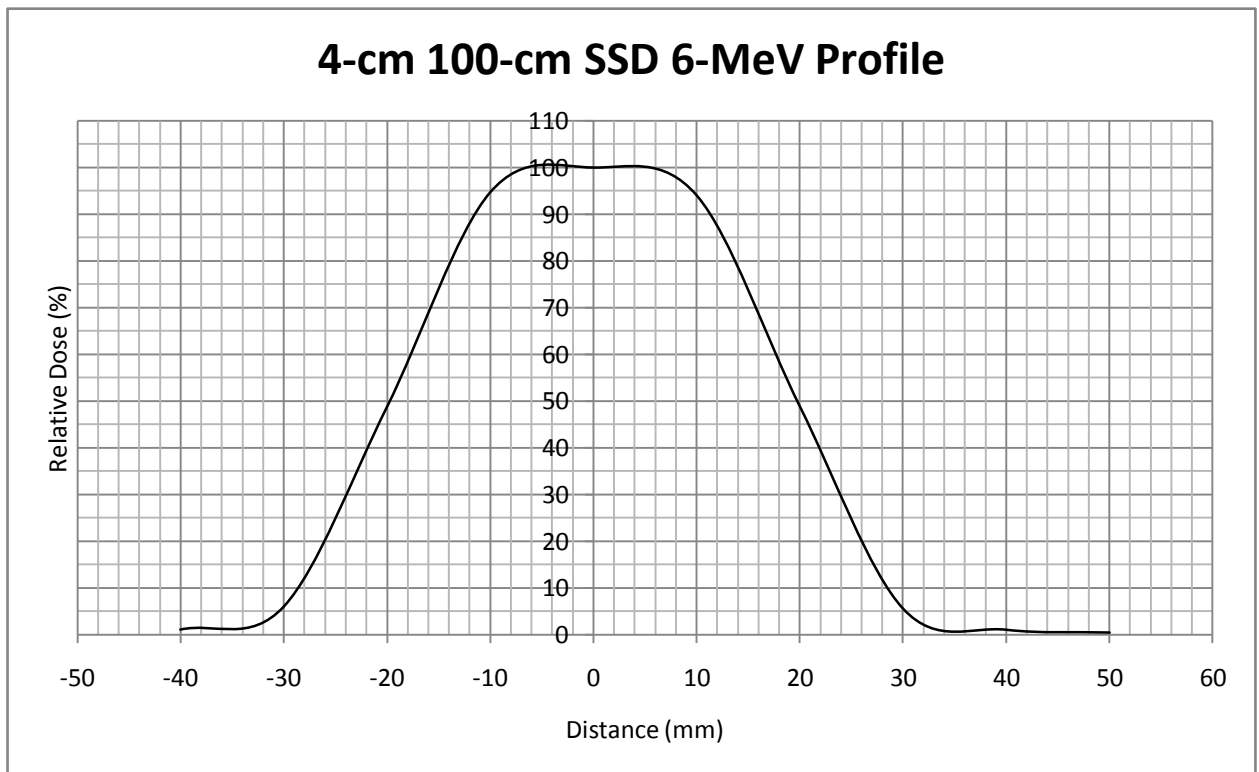
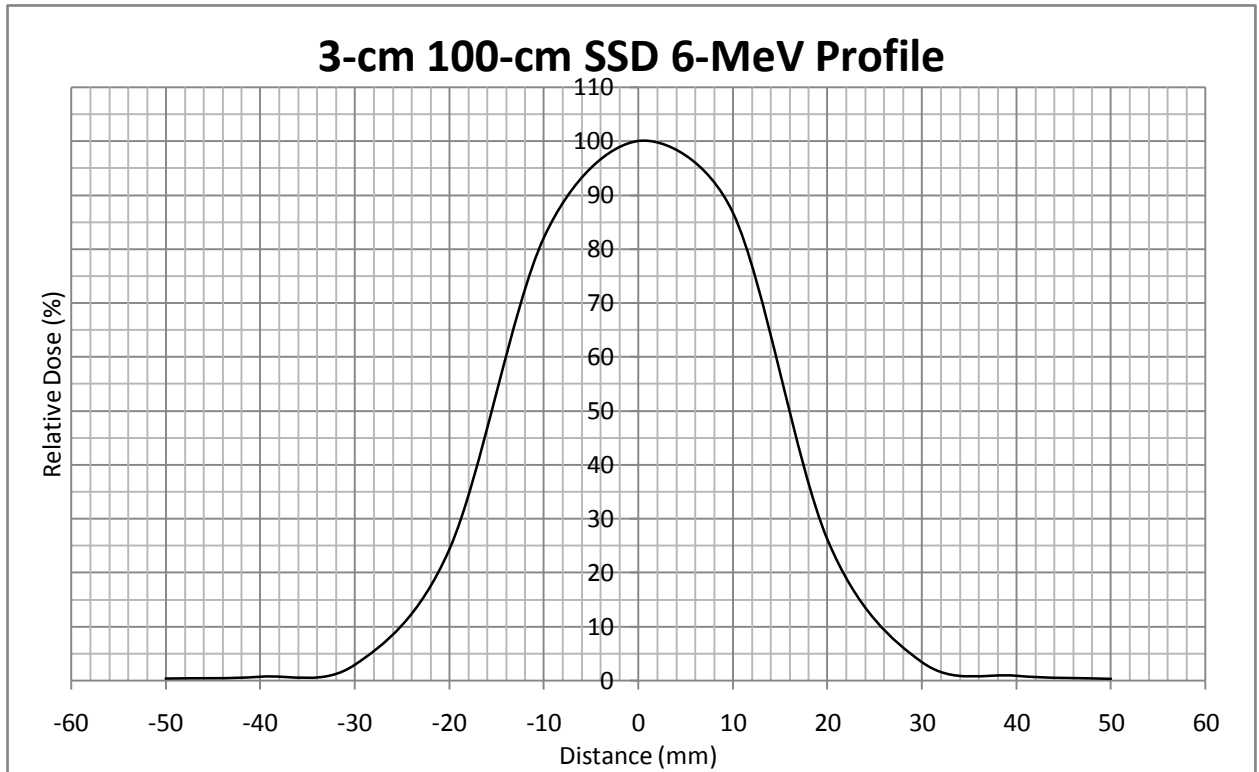
5-cm x 5-cm 110-cm SSD 15-MeV Profile



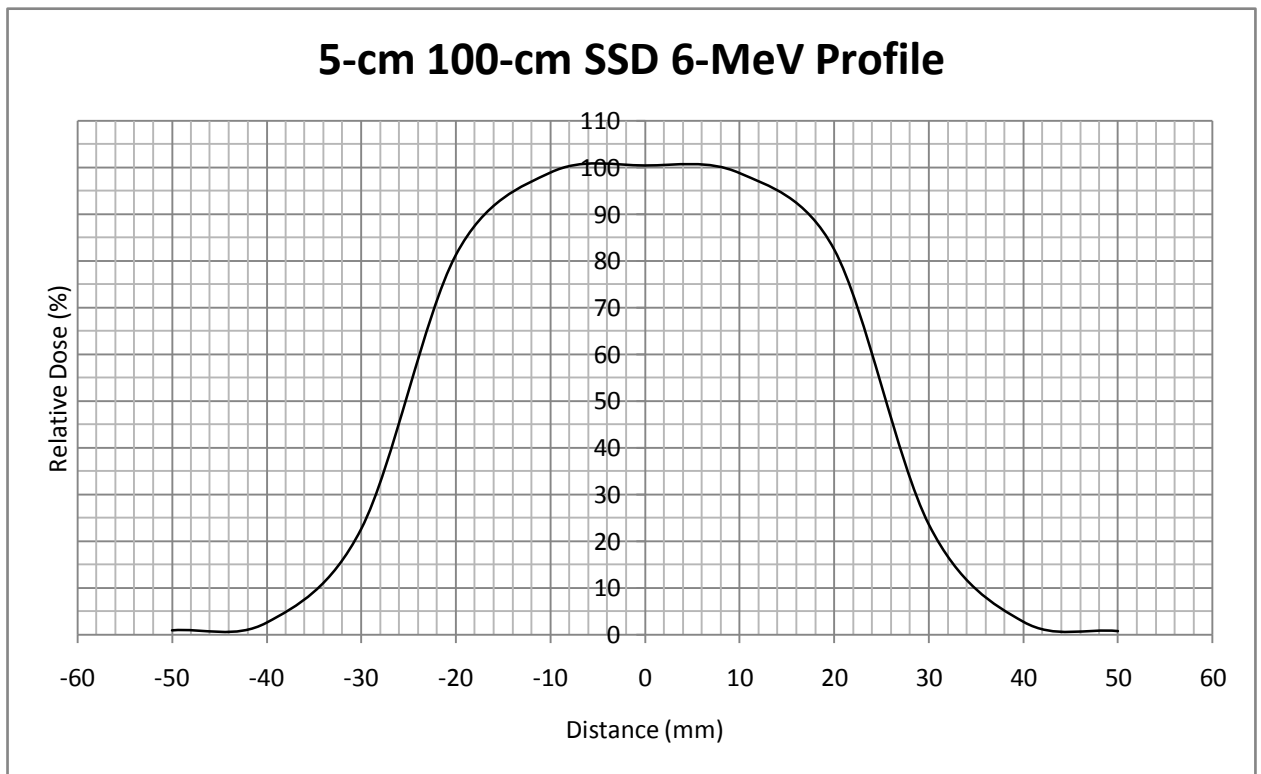
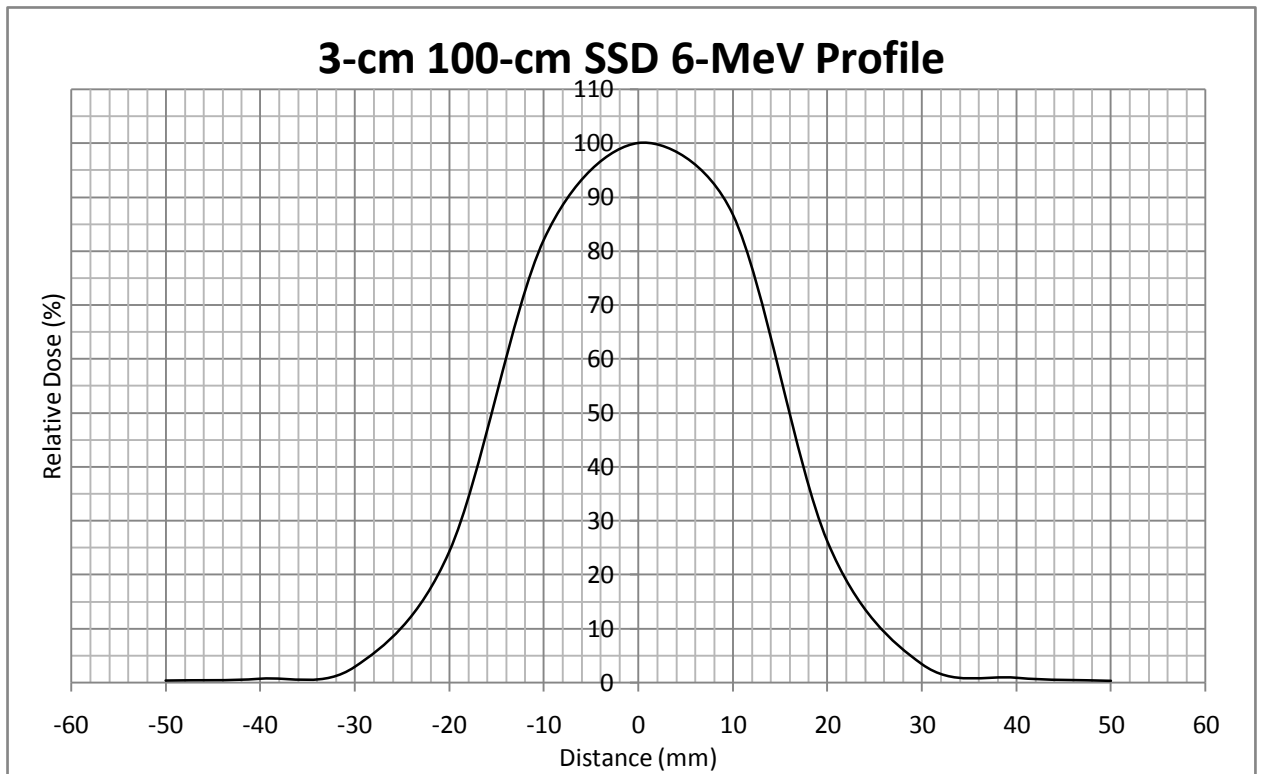
Appendix B

Beam Profiles of Small-Electron Rectangular Fields

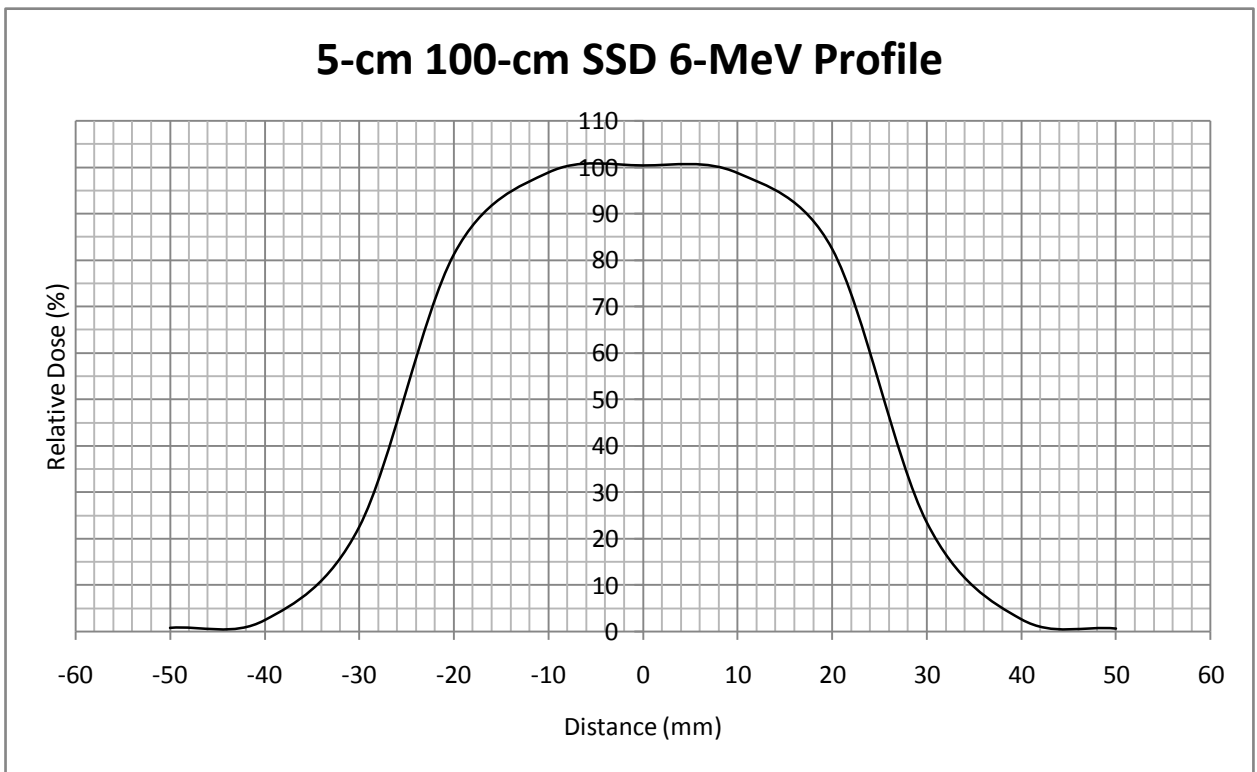
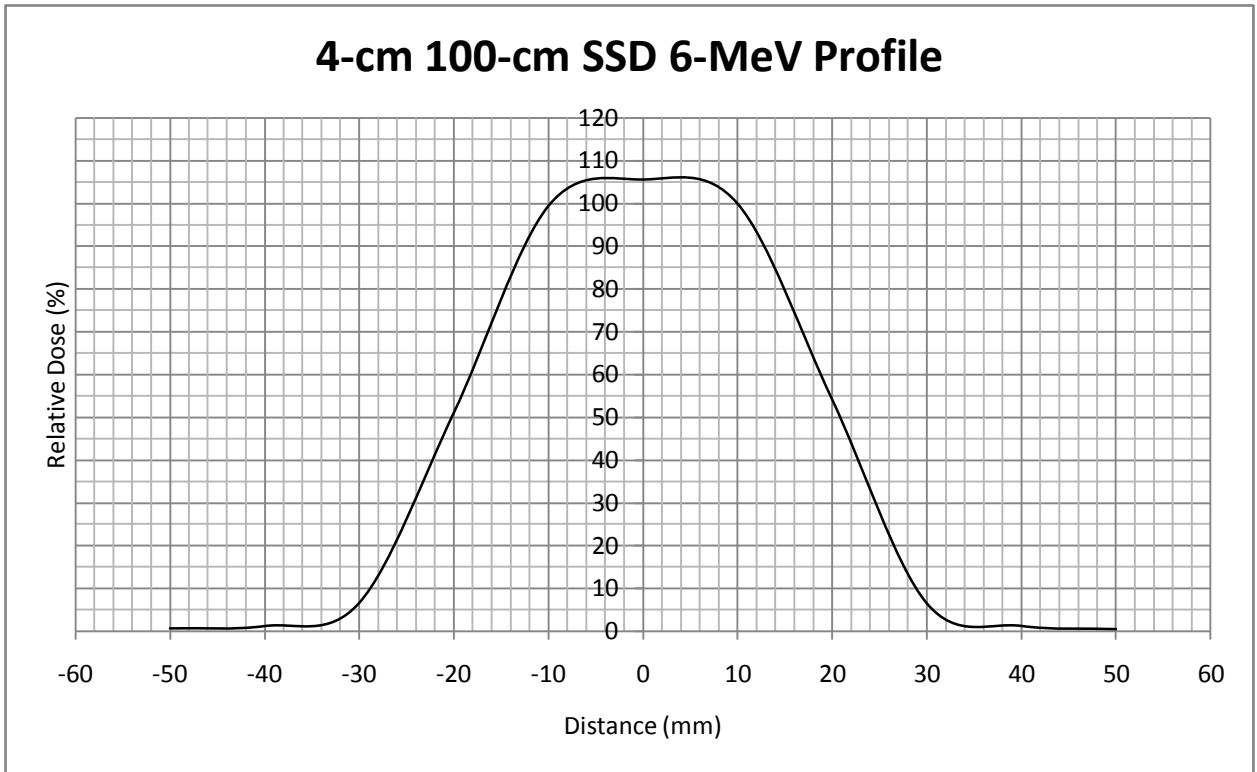
3-cm x 4-cm 100-cm SSD 6-MeV Profile



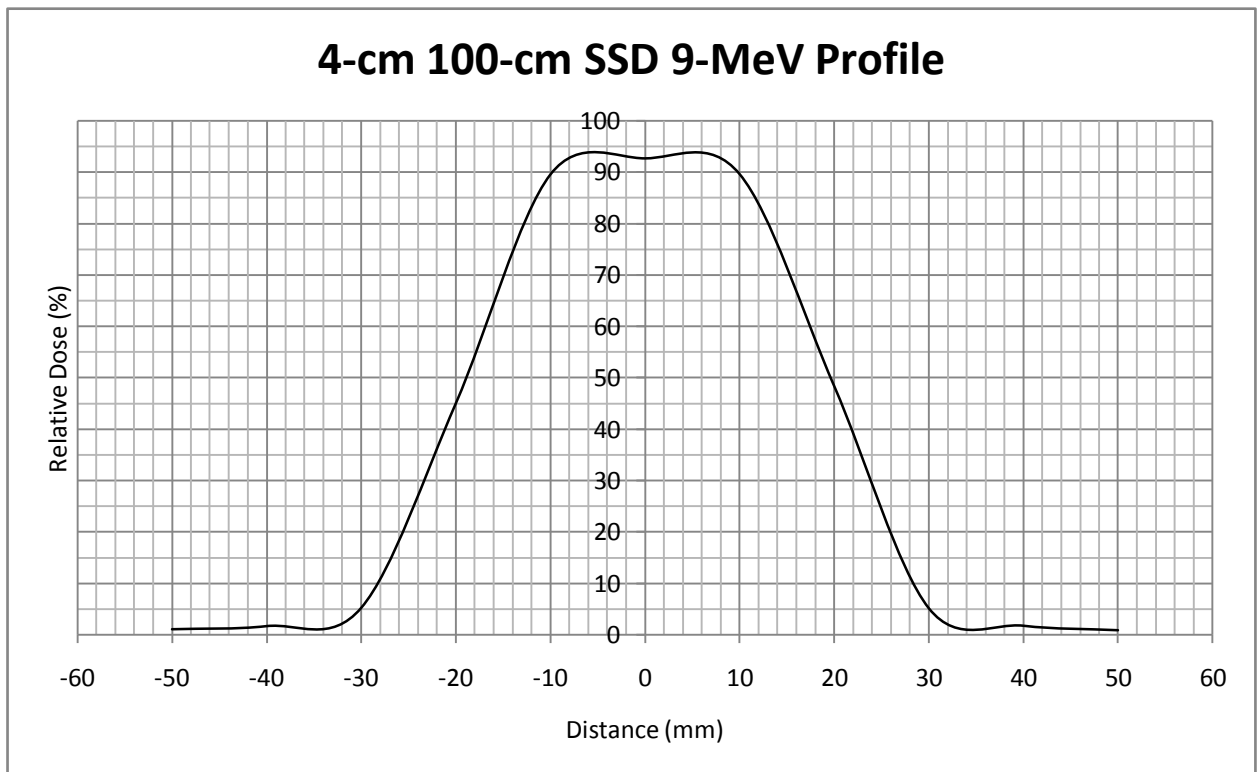
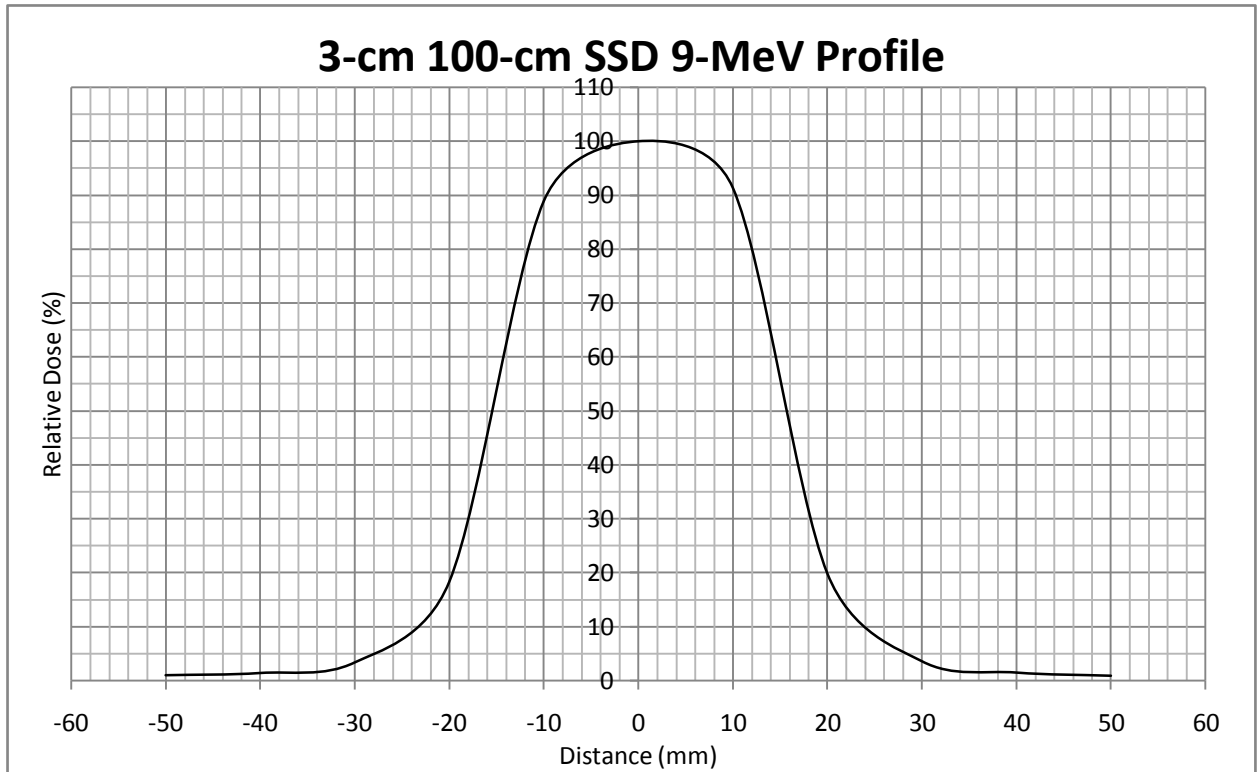
3-cm x 5-cm 100-cm SSD 6-MeV Profile



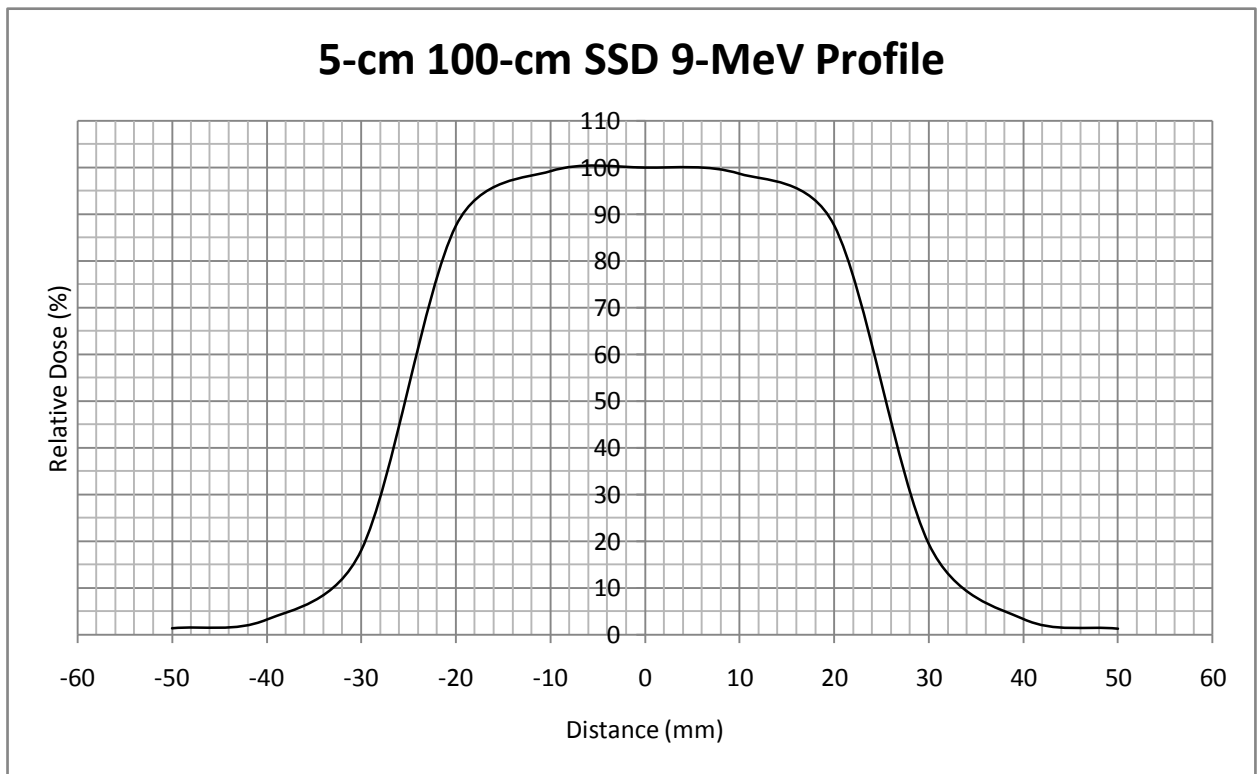
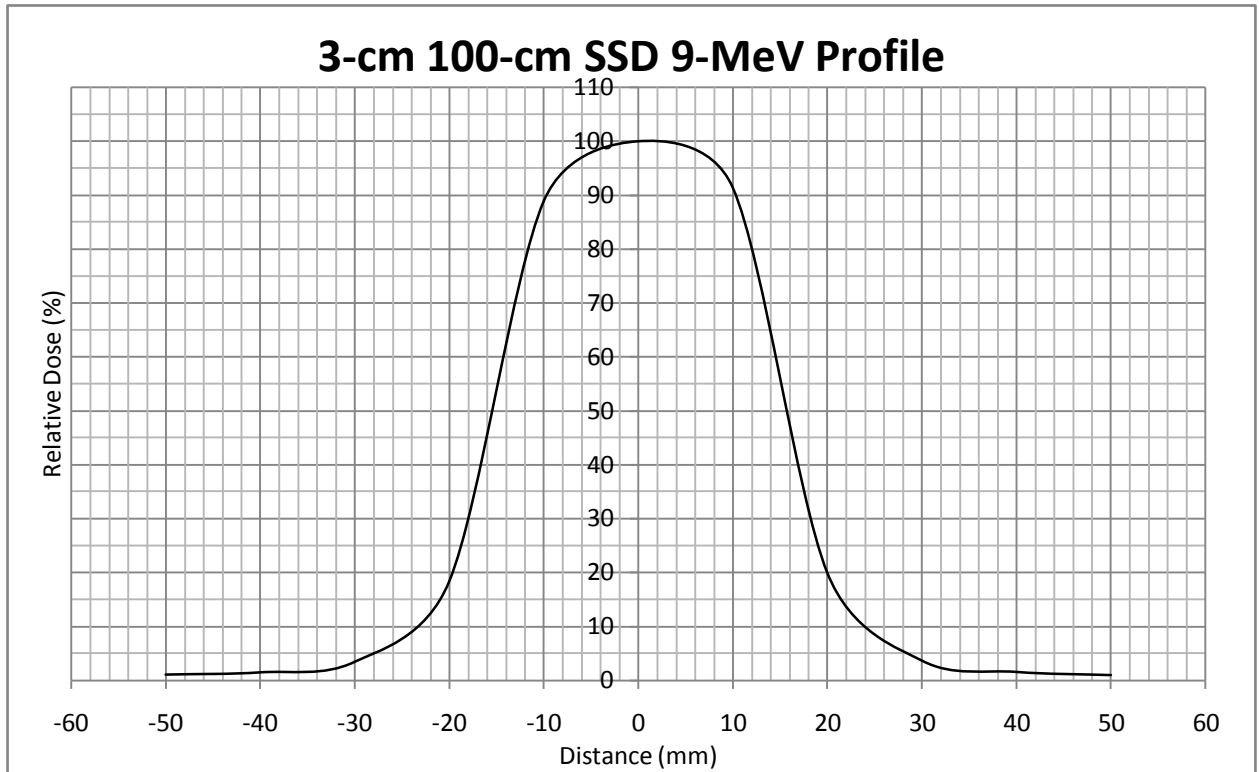
4-cm x 5-cm 100-cm SSD 6-MeV Profile



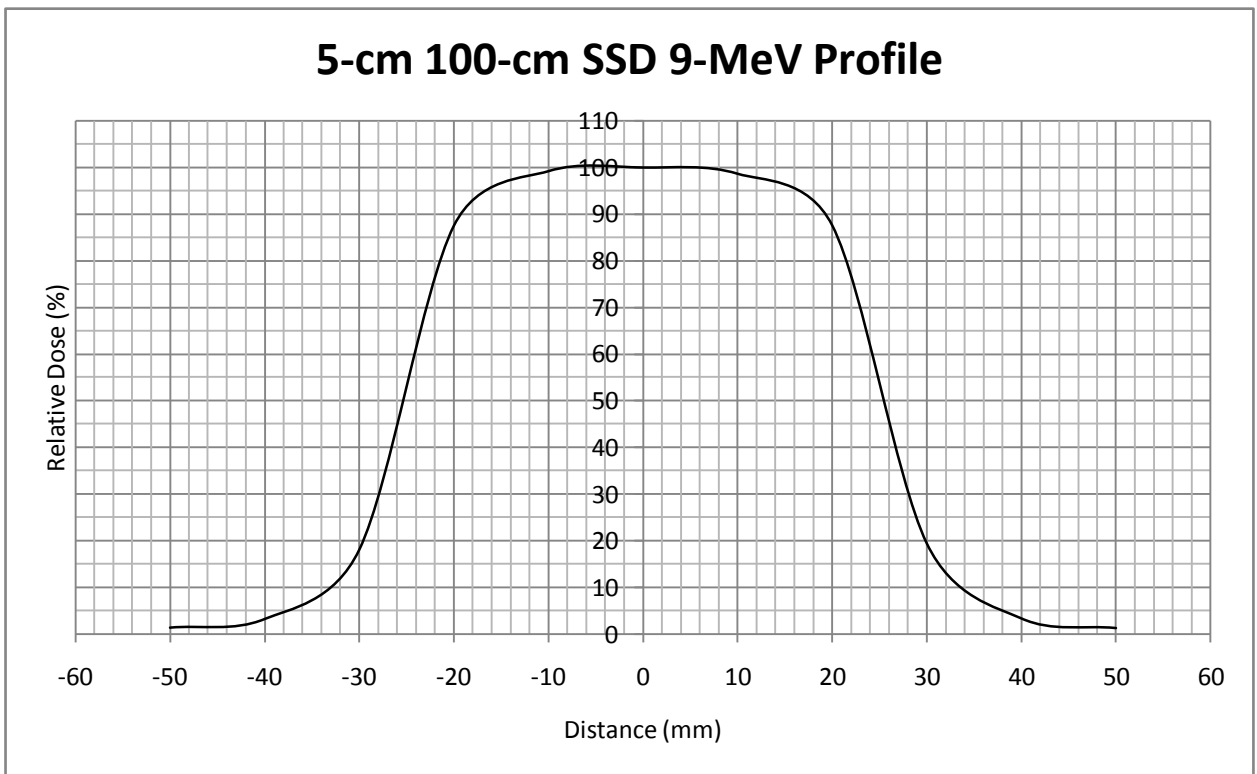
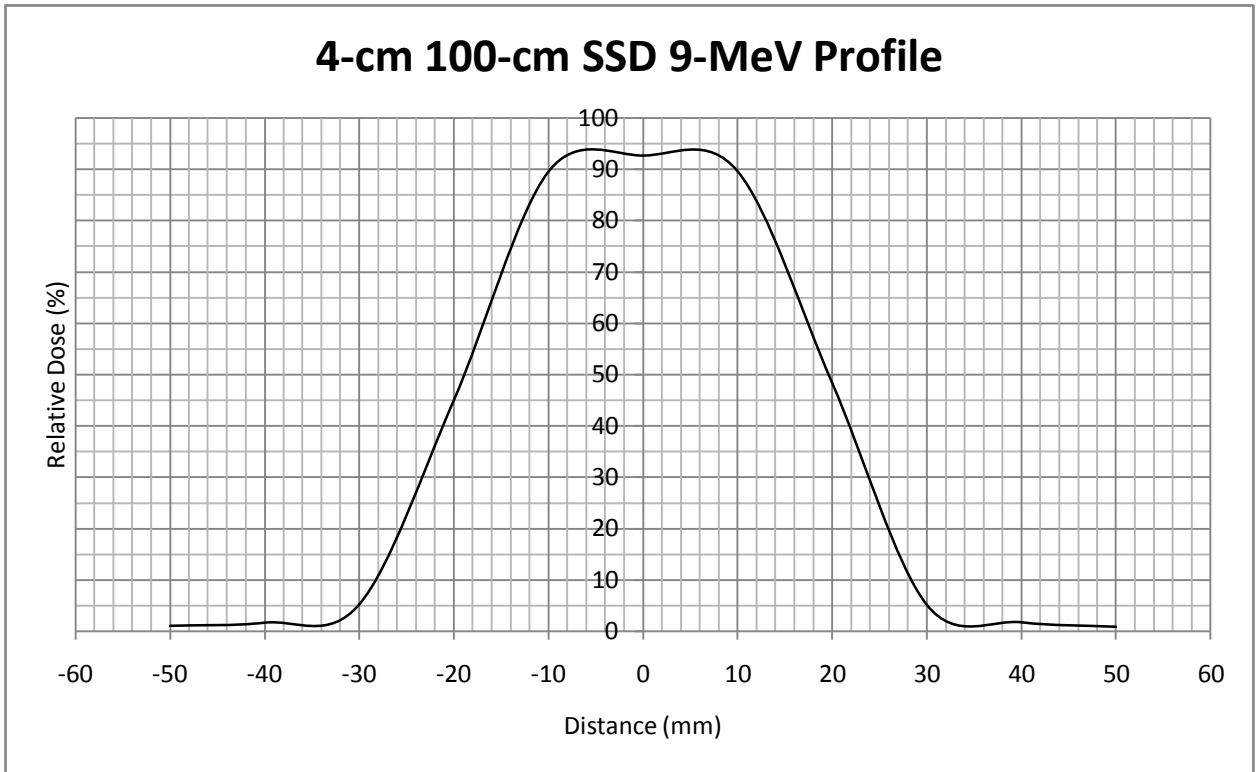
3-cm x 4-cm 100-cm SSD 9-MeV Profile



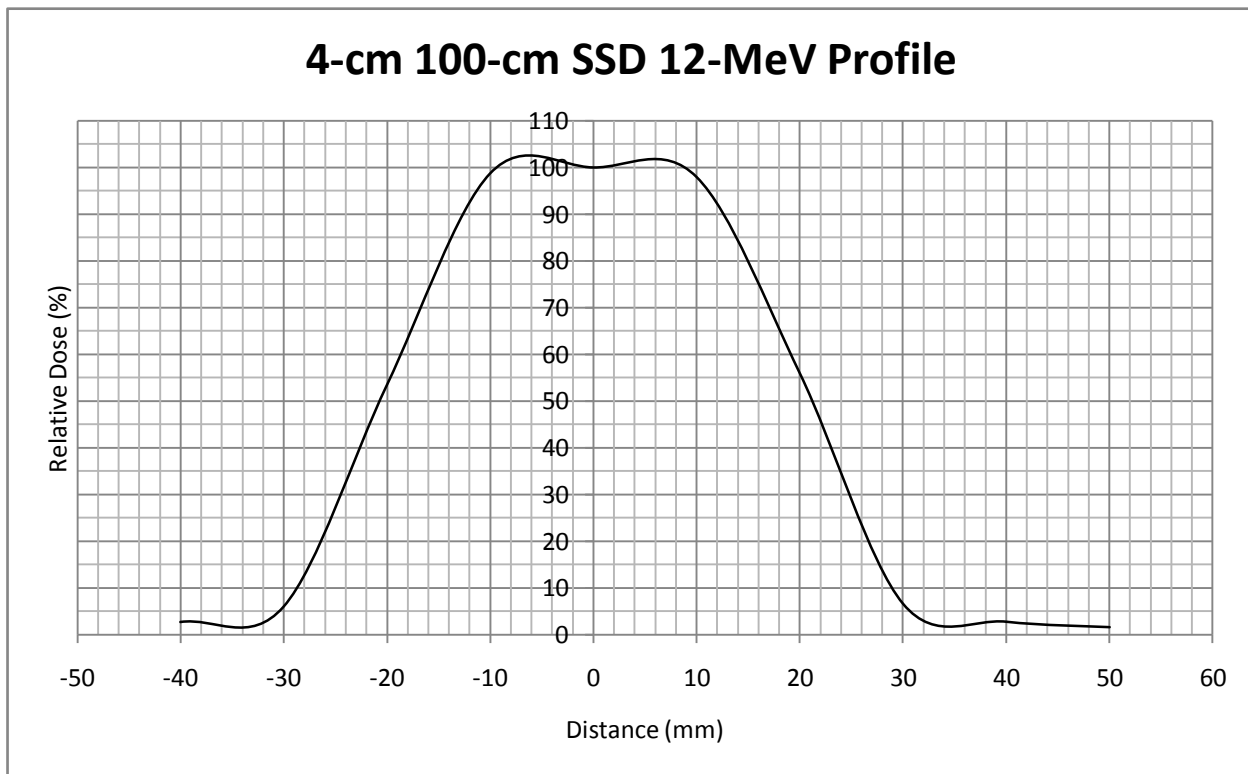
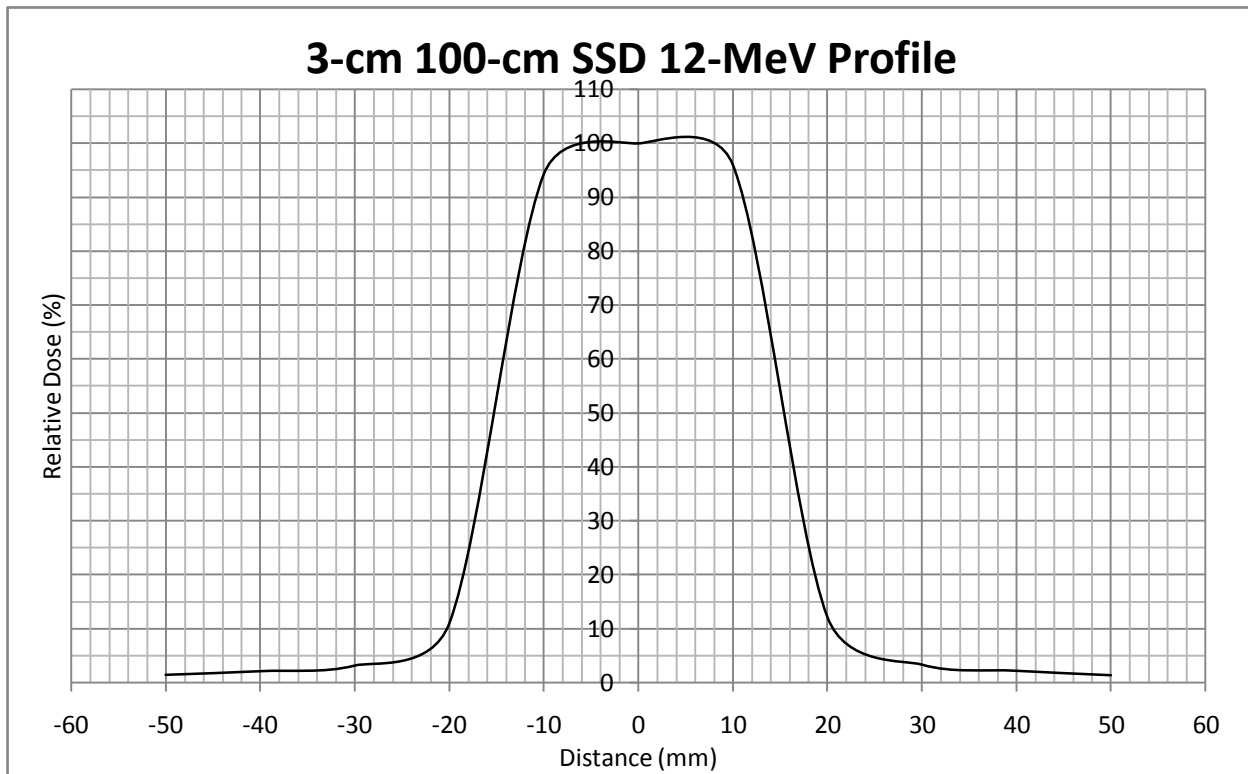
3-cm x 4-cm 100-cm SSD 9-MeV Profile



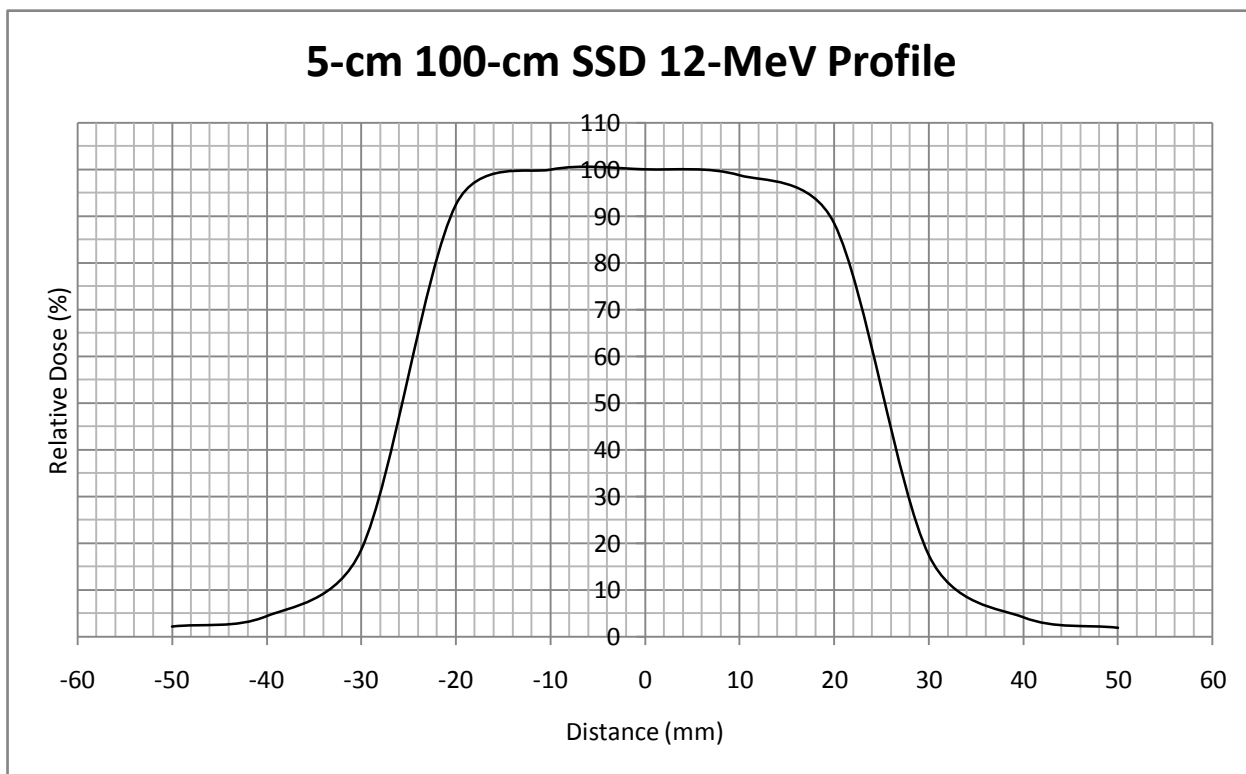
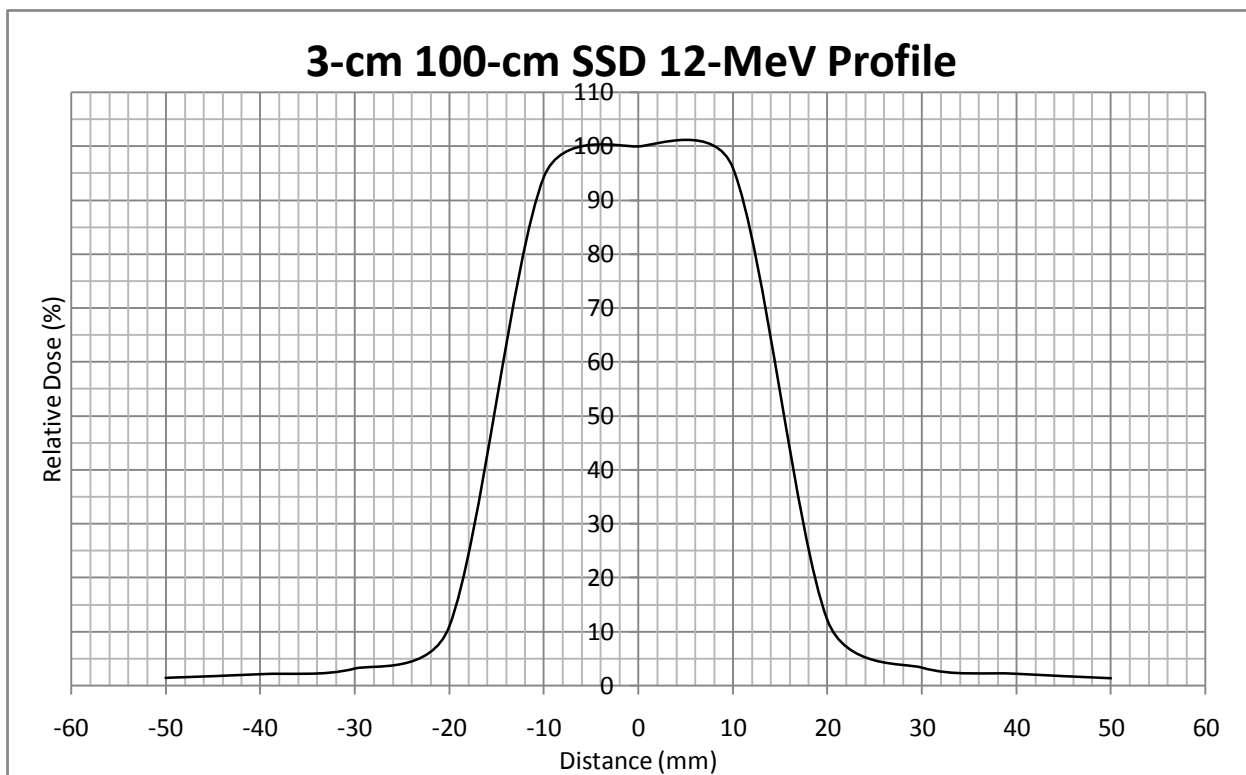
4-cm x 5-cm 100-cm SSD 9-MeV Profile



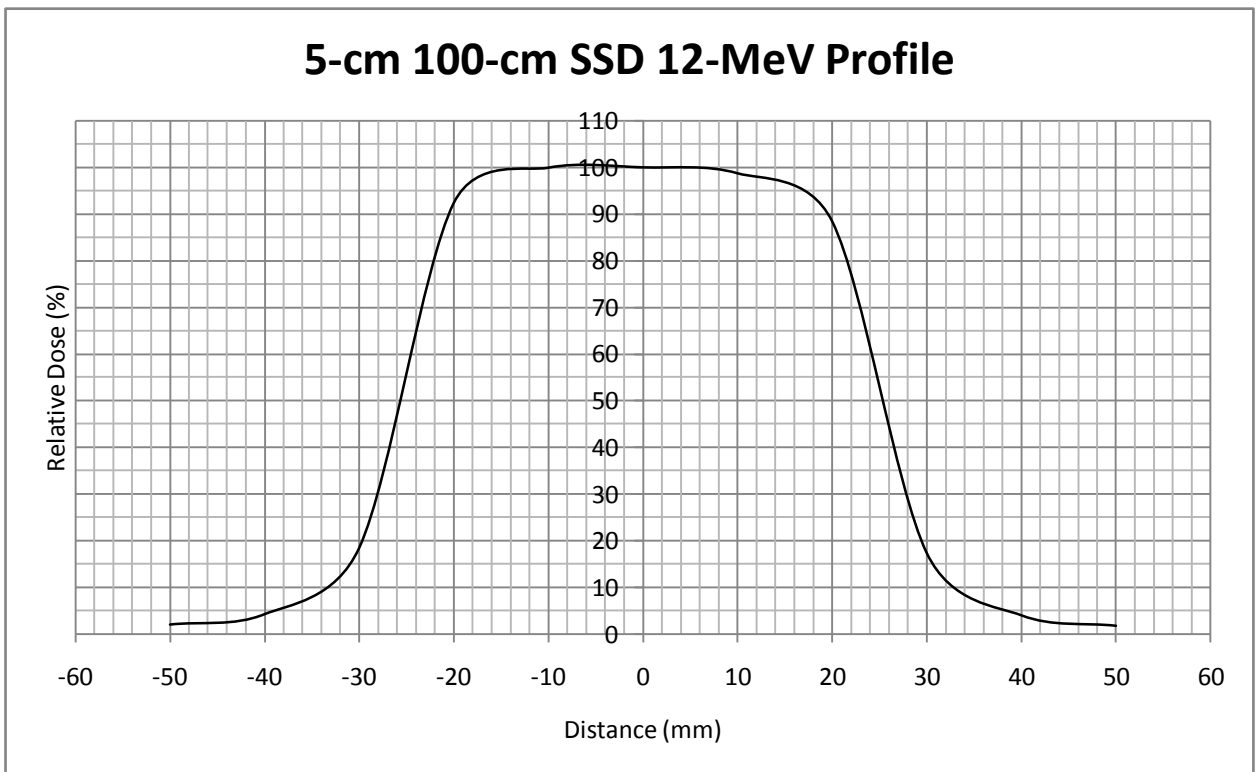
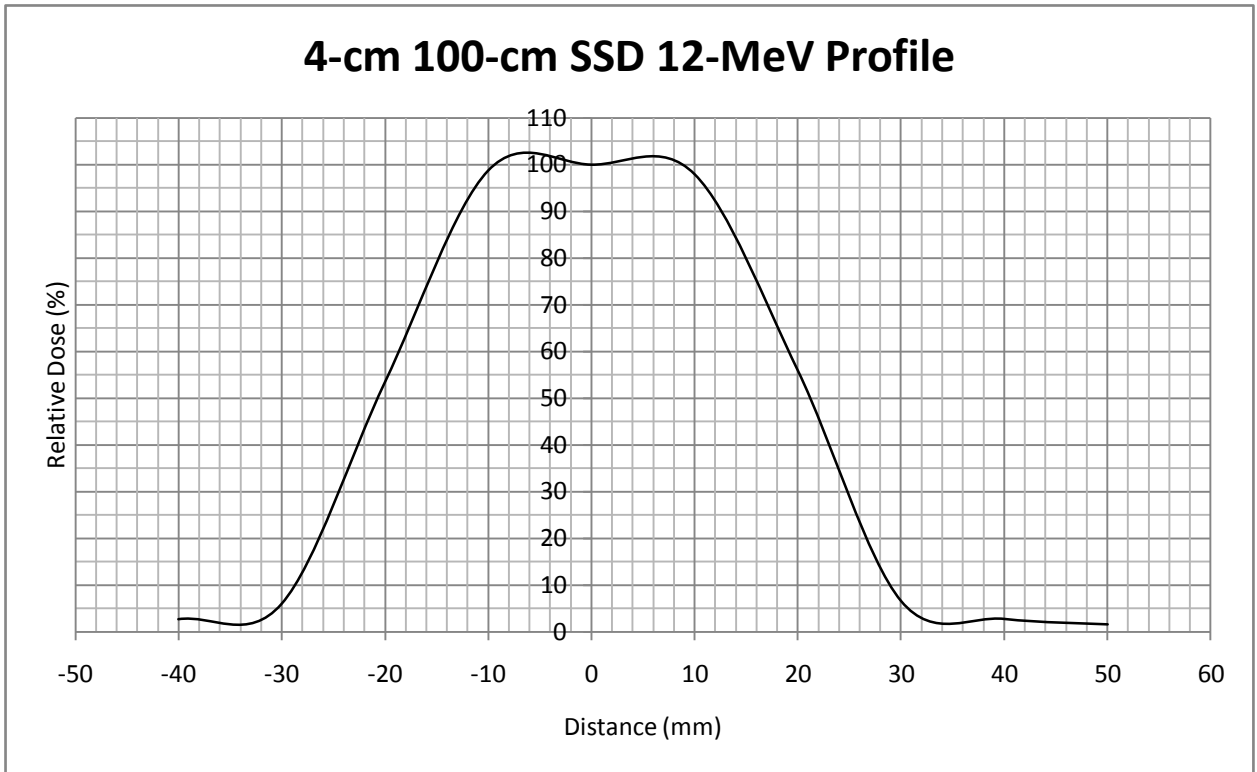
3-cm x 4-cm 100-cm SSD 12-MeV Profile



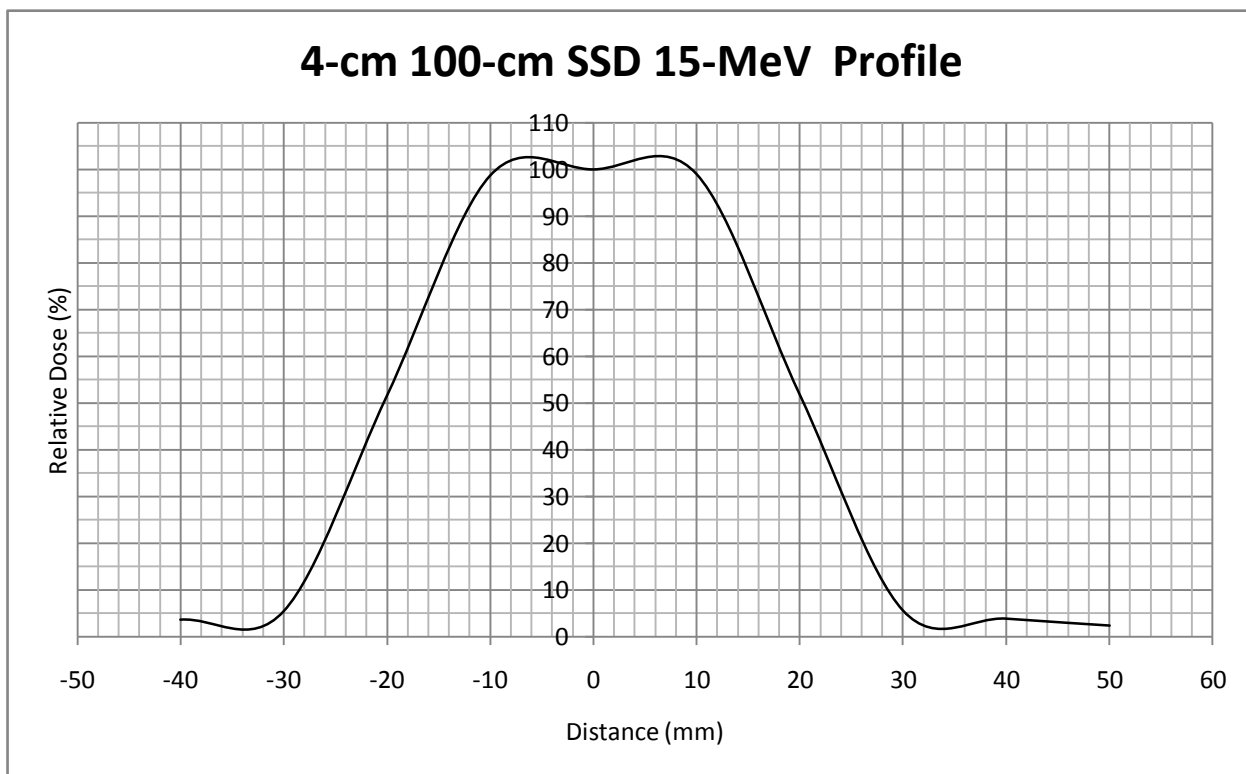
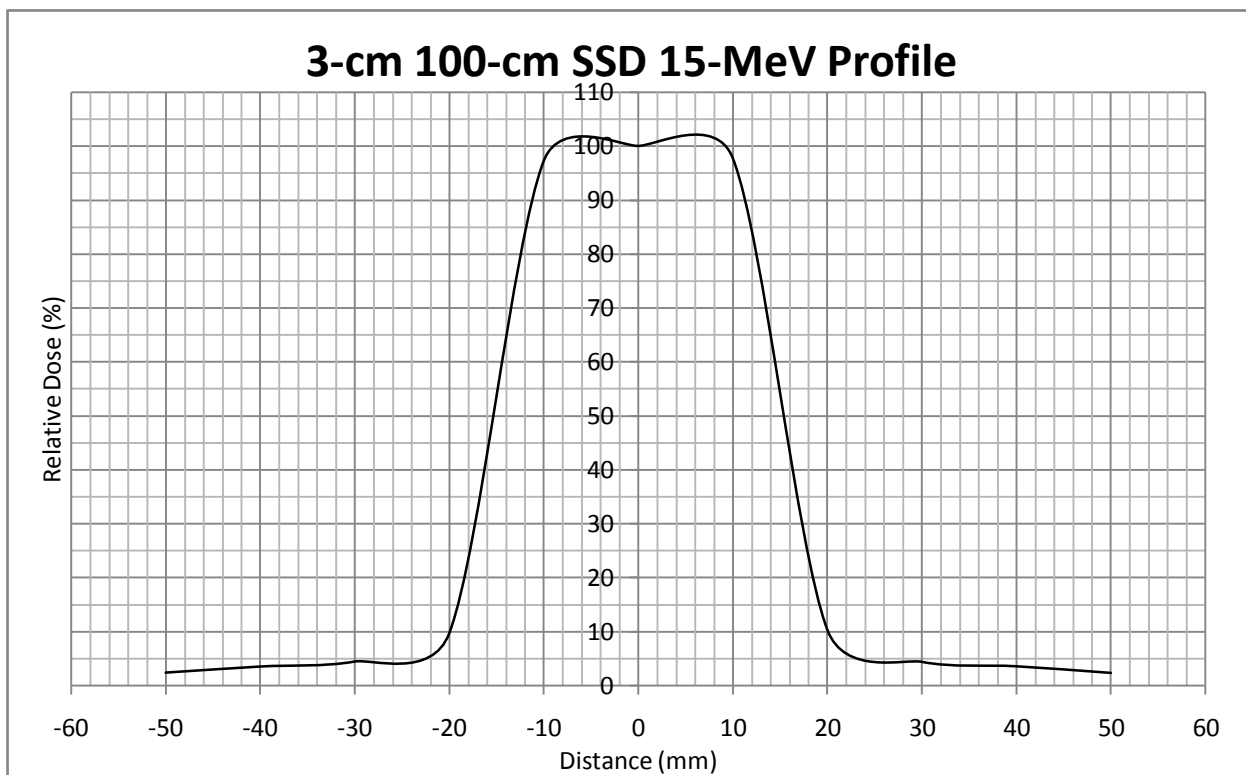
3 cm x 5 cm 100 cm SSD 12 MeV Profile



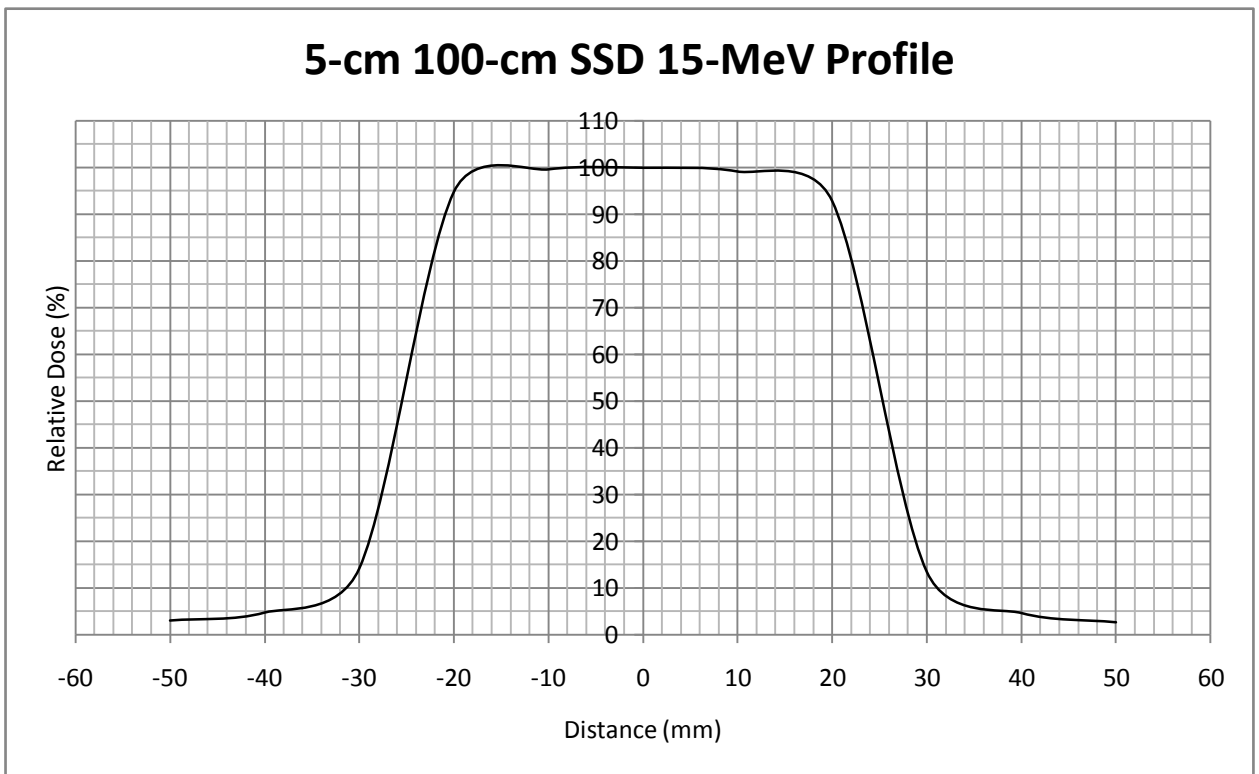
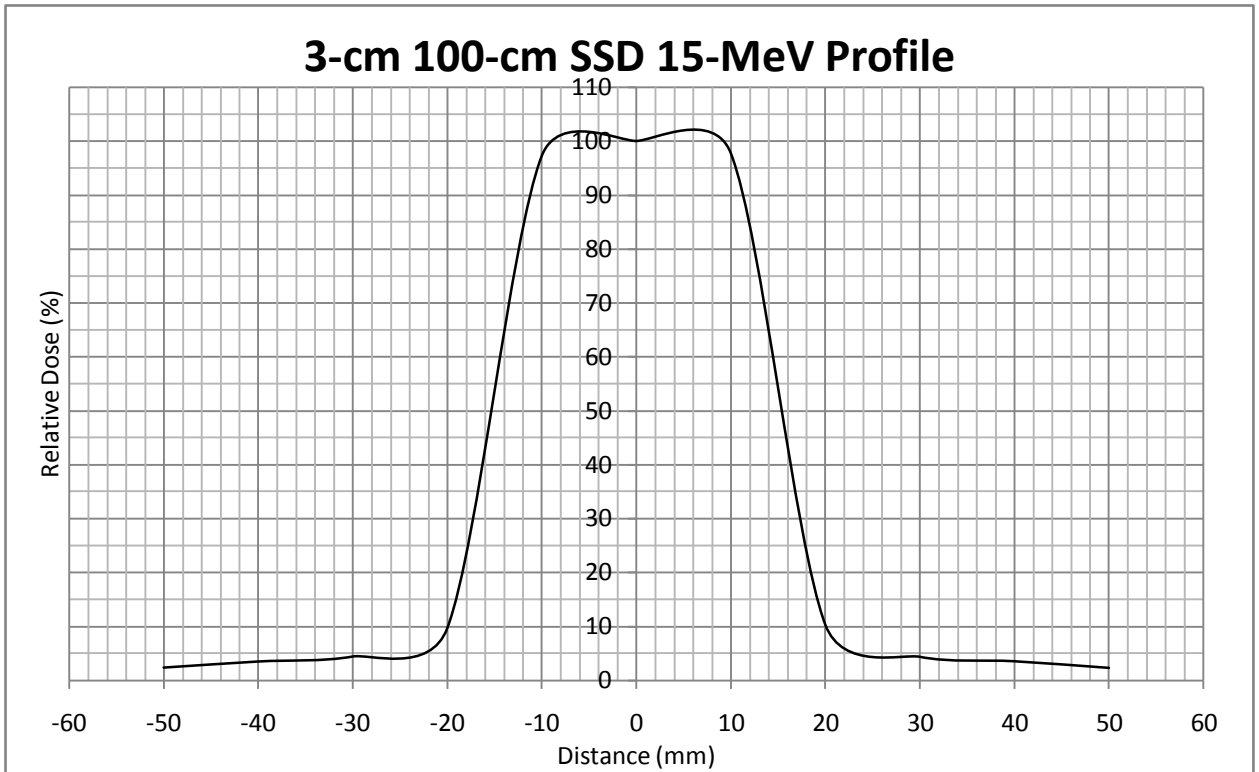
4-cm x 5-cm 100-cm SSD 15-MeV Profile



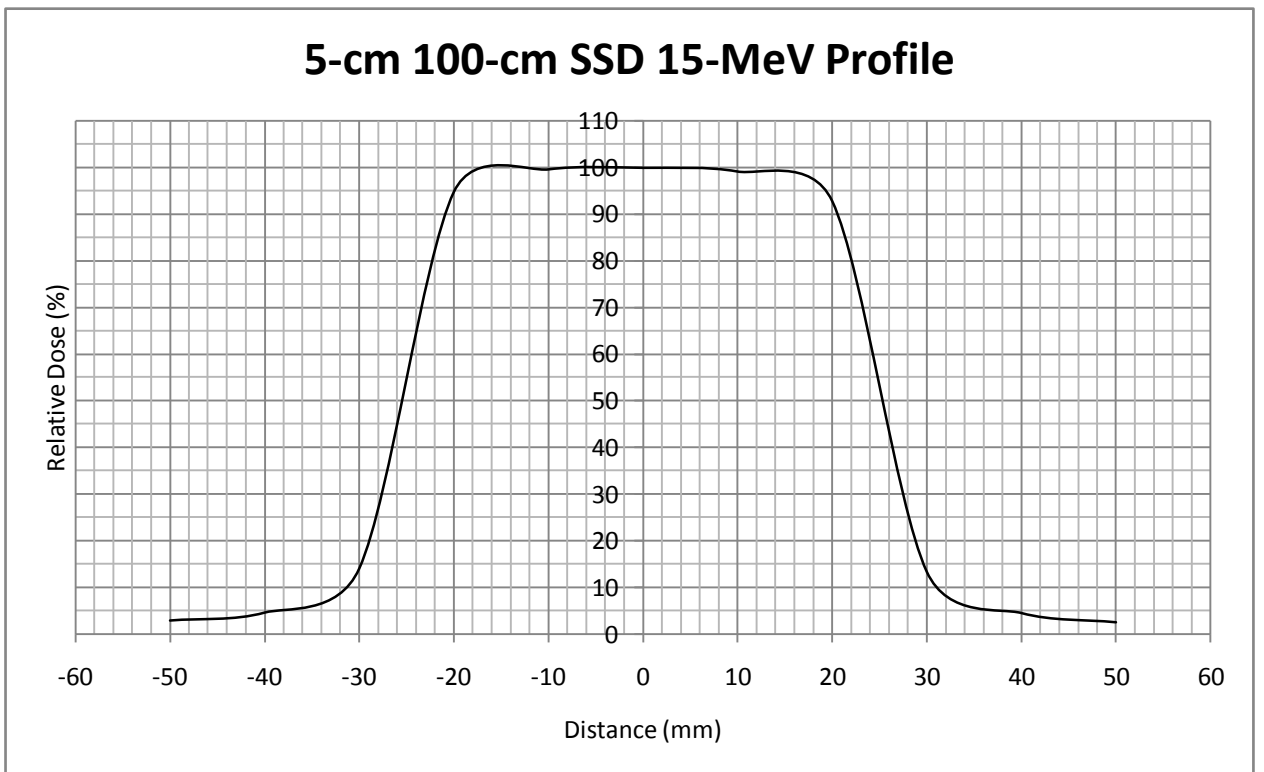
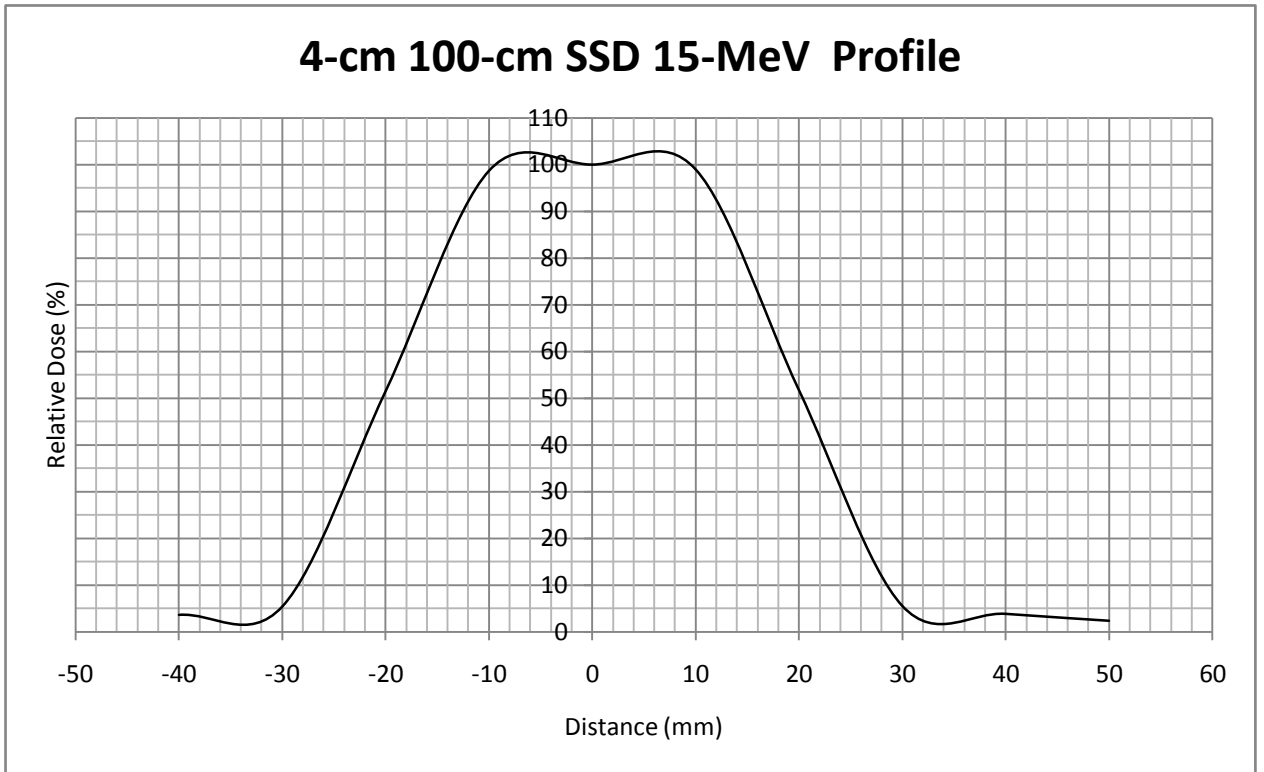
3-cm x 4-cm 100-cm SSD 15-MeV Profile



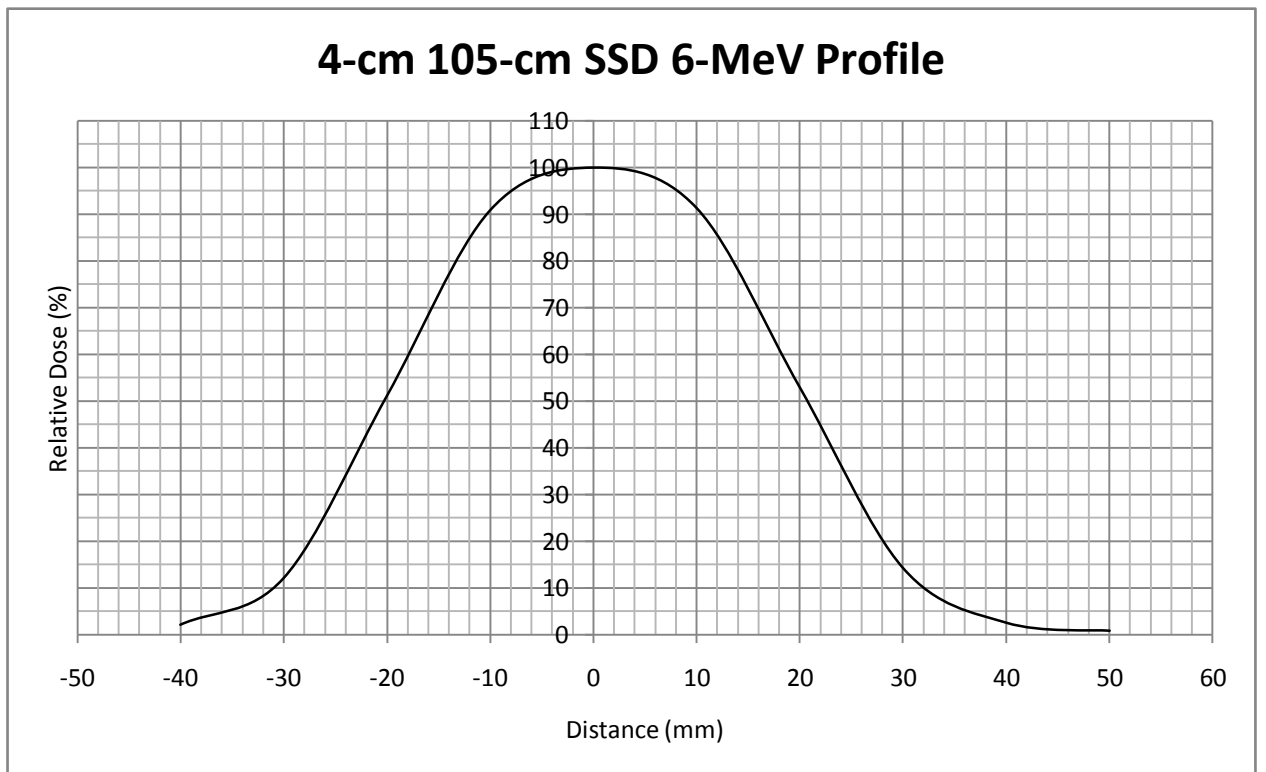
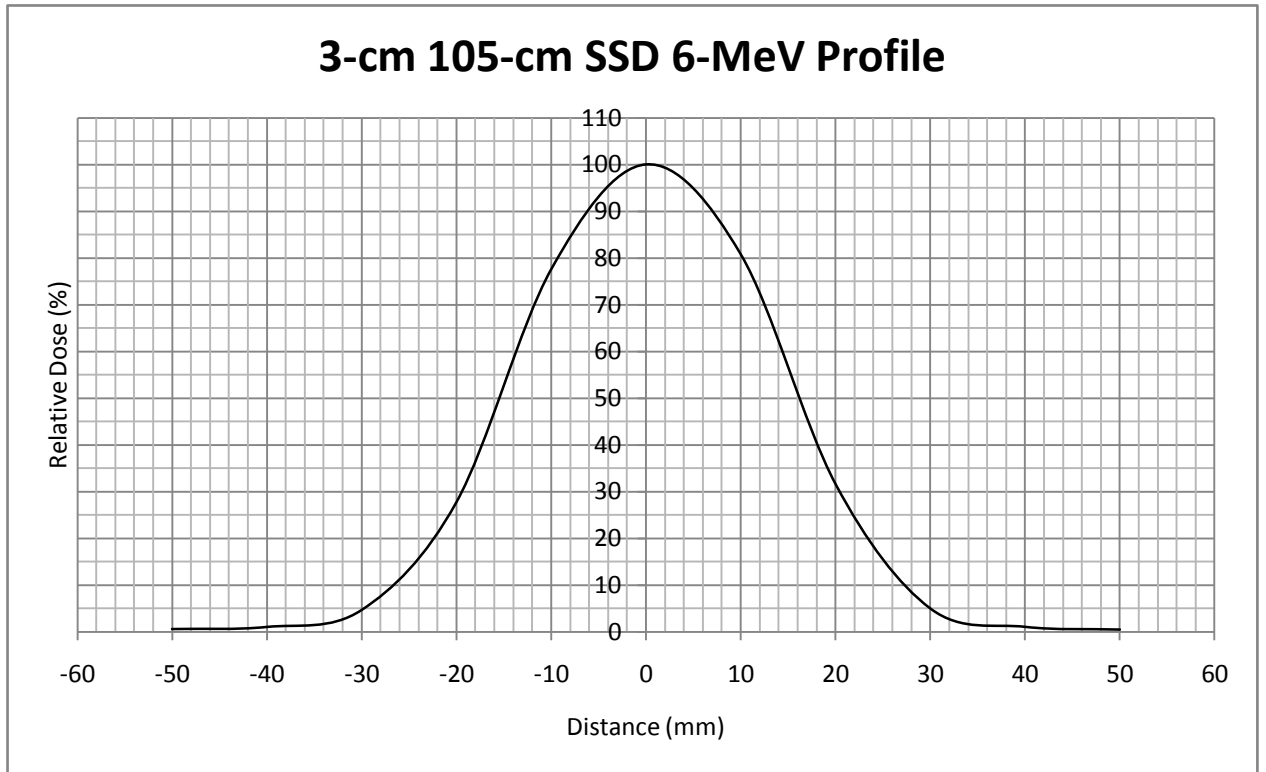
3-cm x 5-cm 100-cm SSD 15-MeV Profile



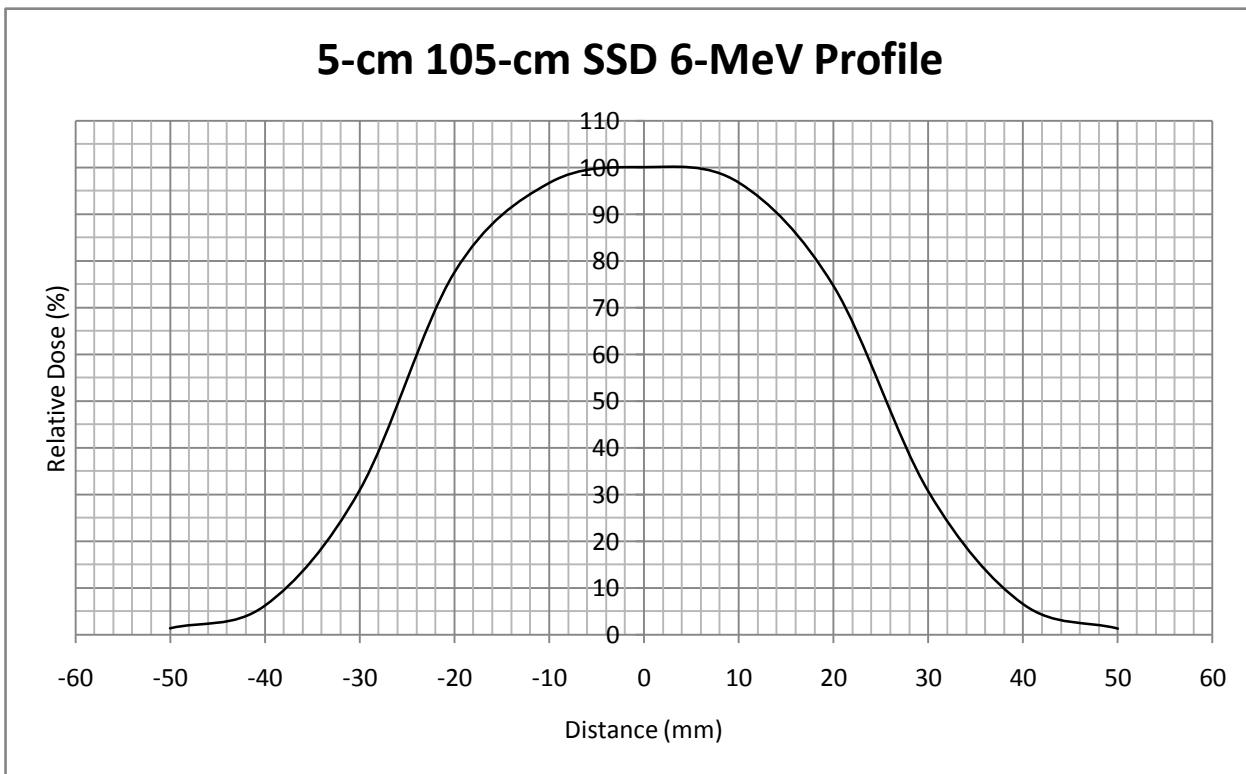
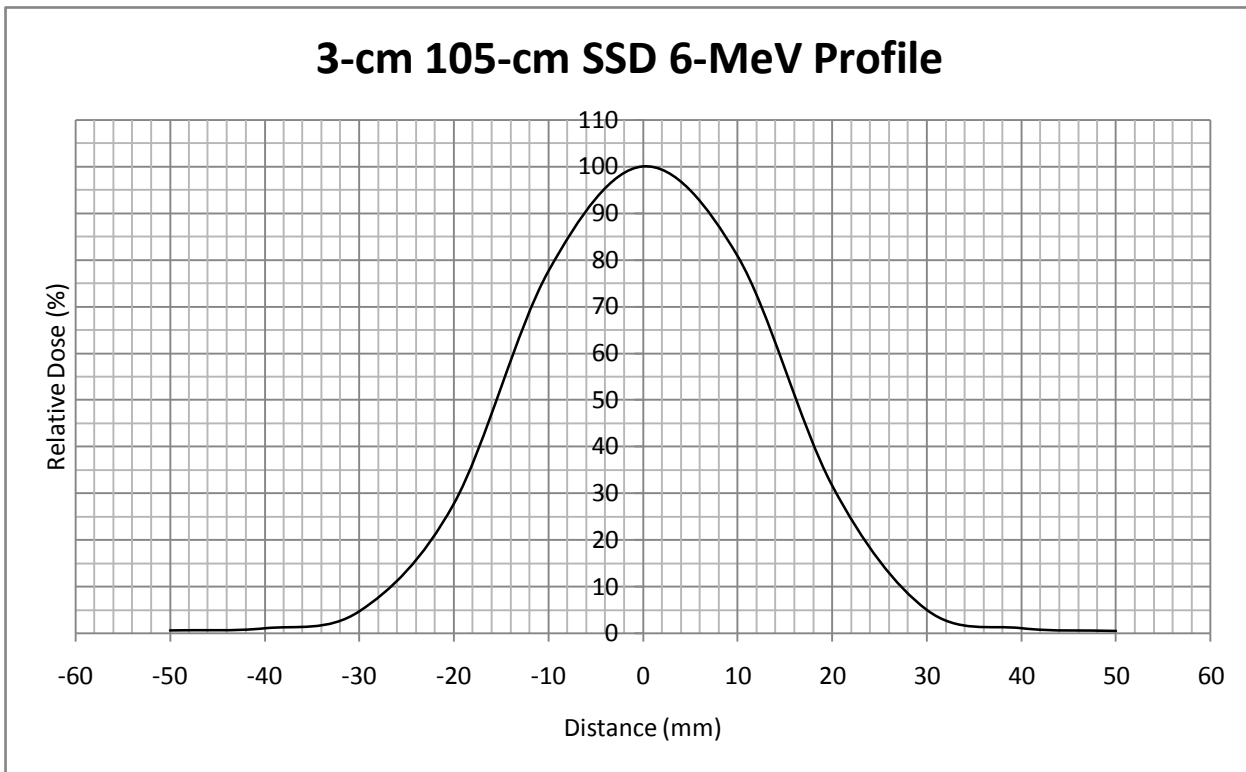
4-cm x 5-cm 100-cm SSD 15-MeV Profile



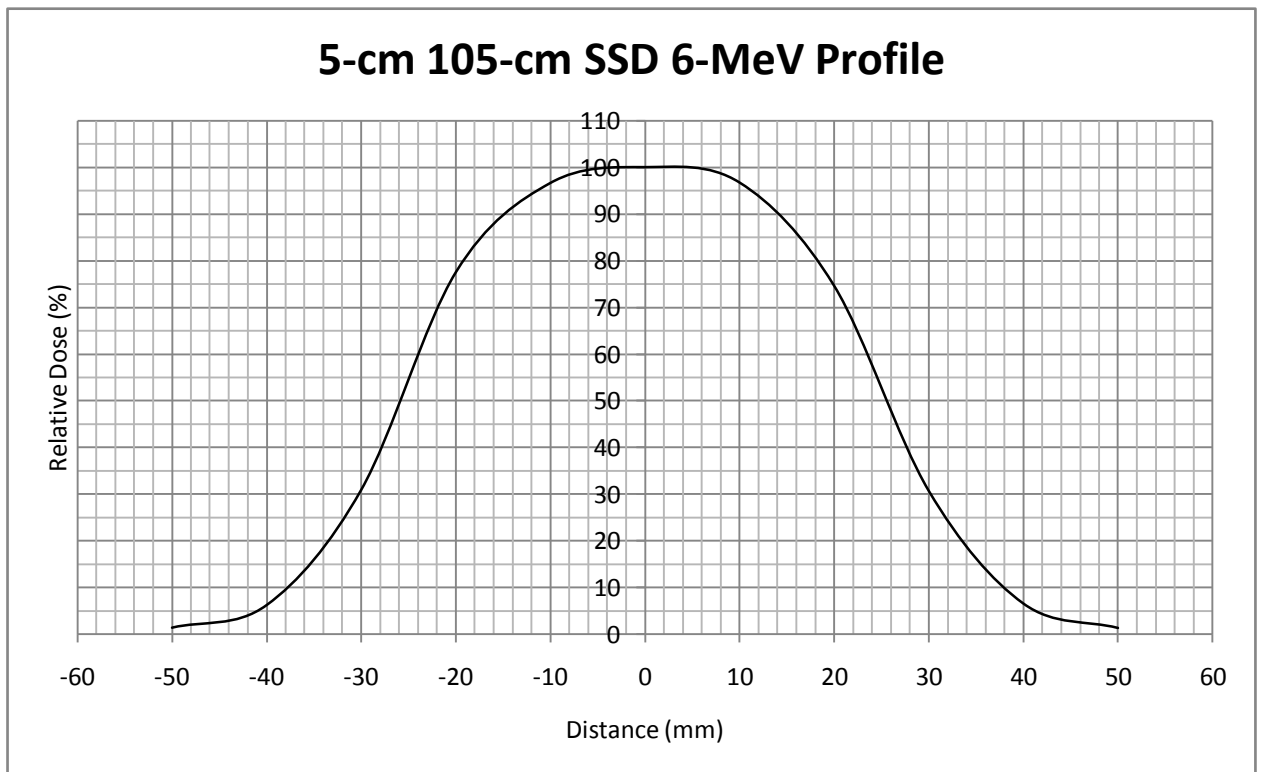
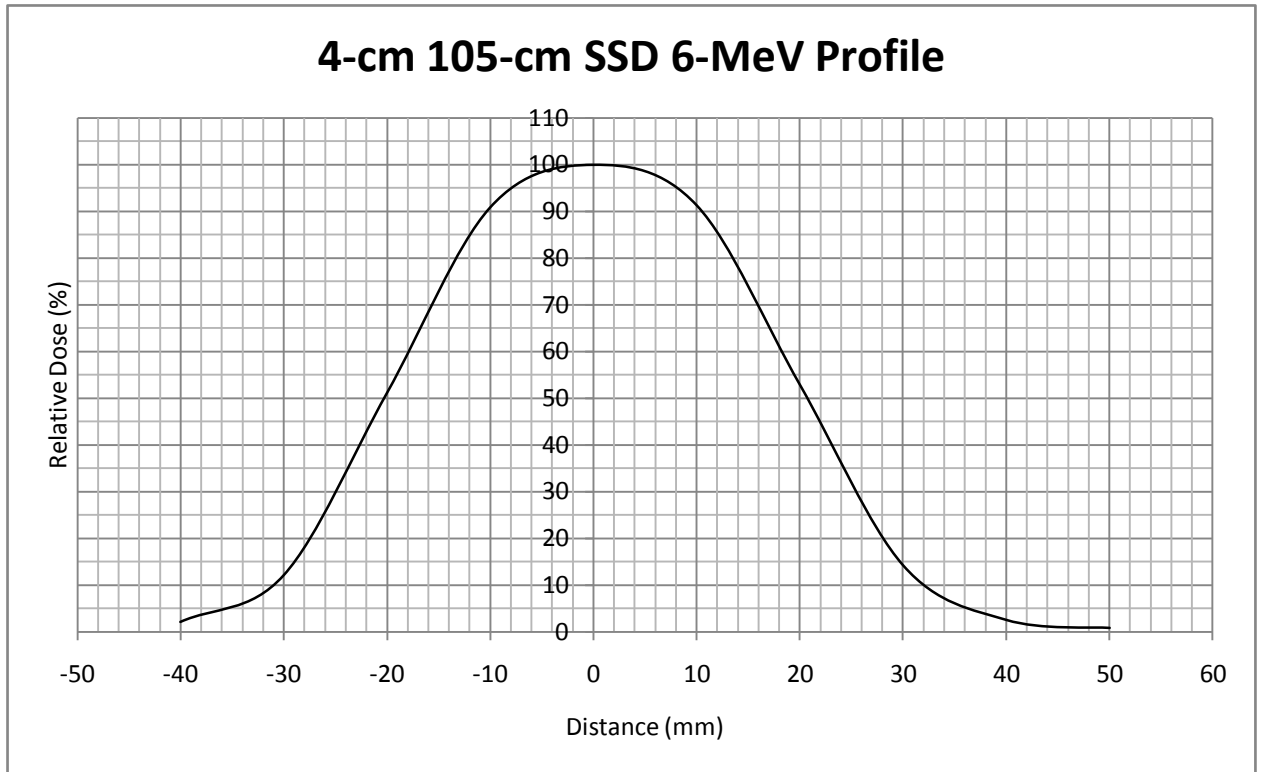
3-cm x 4-cm 105-cm SSD 6-MeV Profile



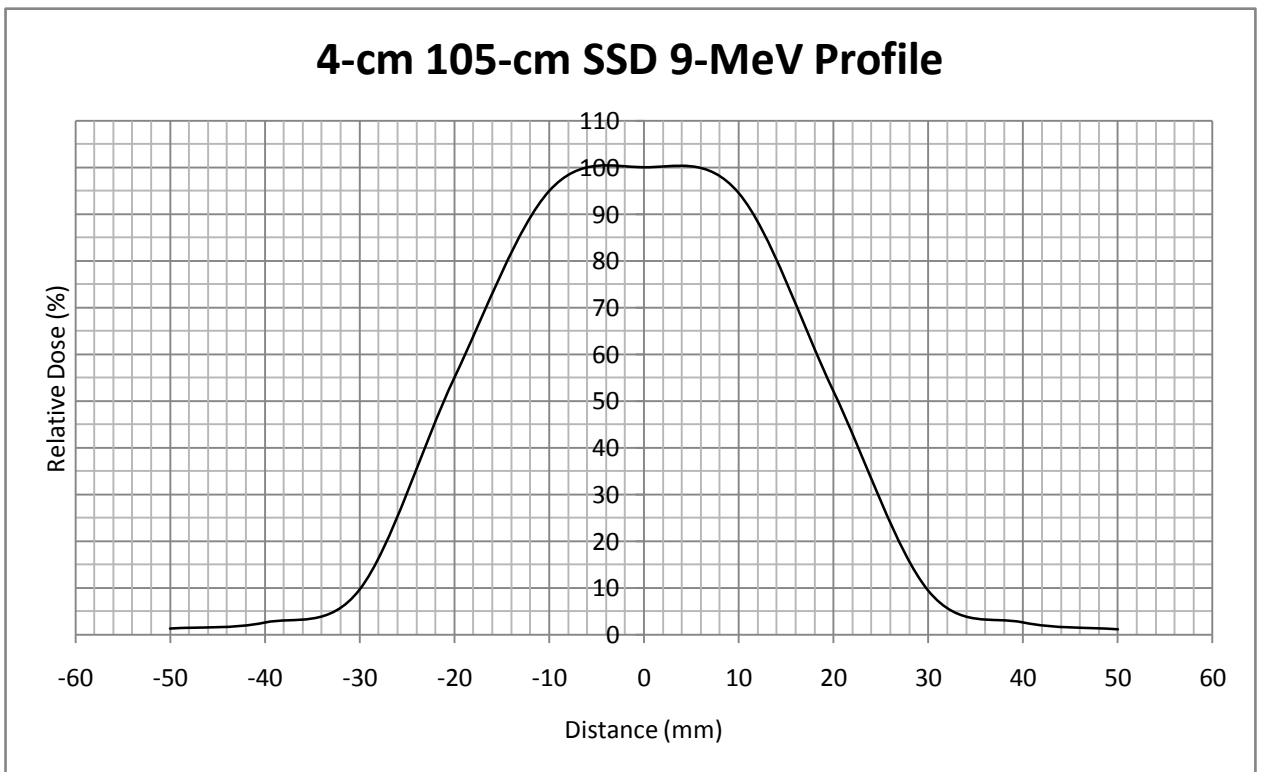
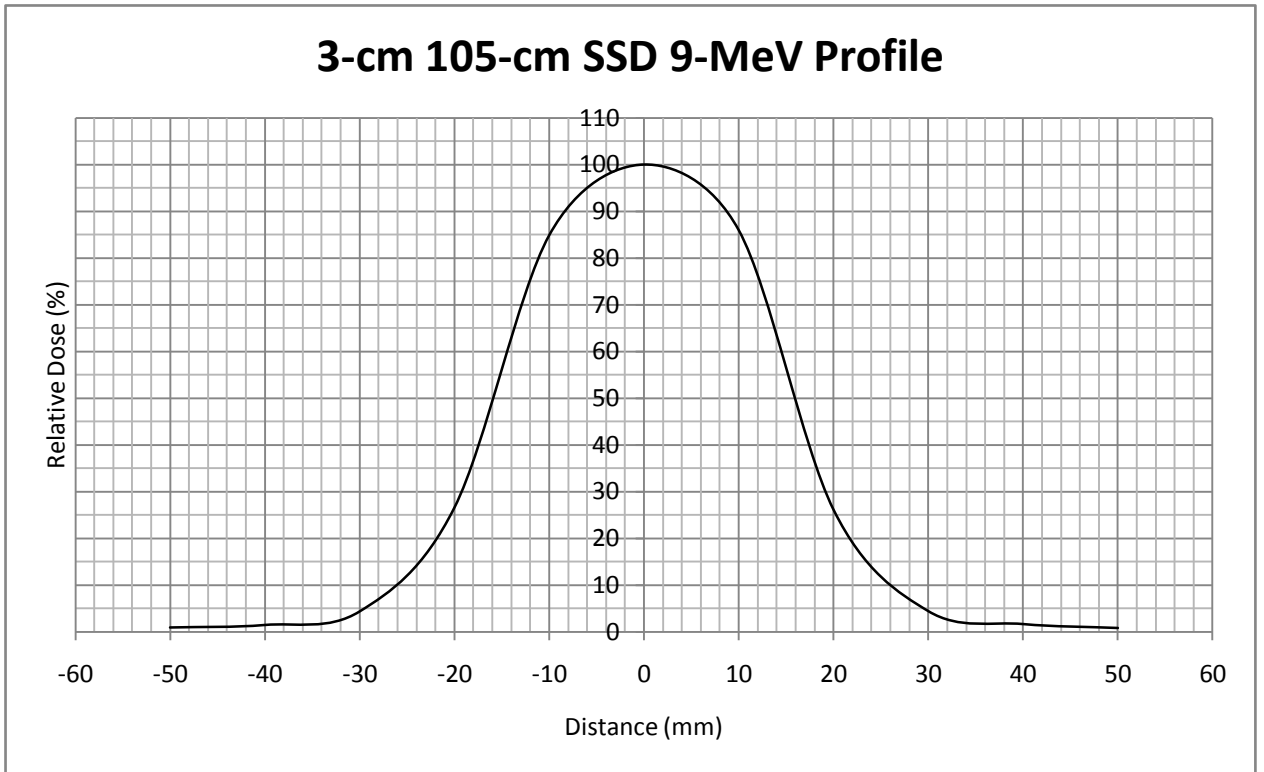
3-cm x 5-cm 105-cm 6-MeV Profile



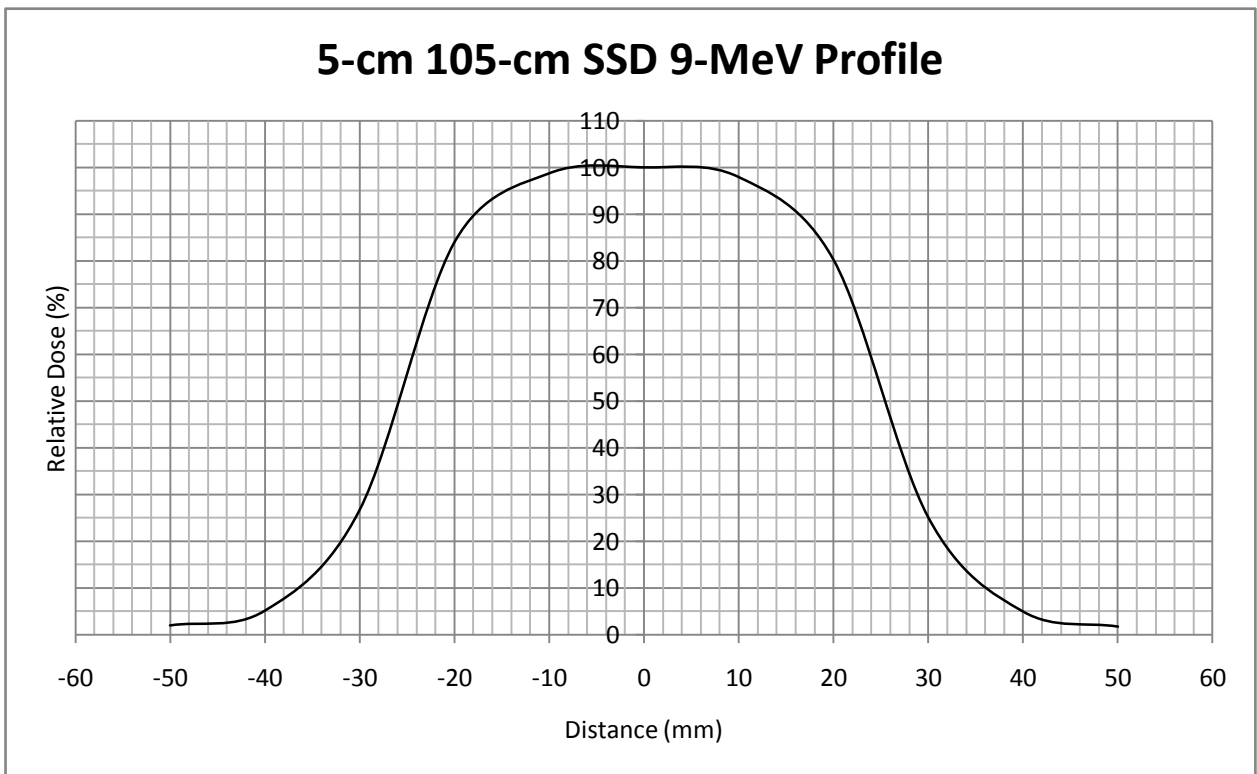
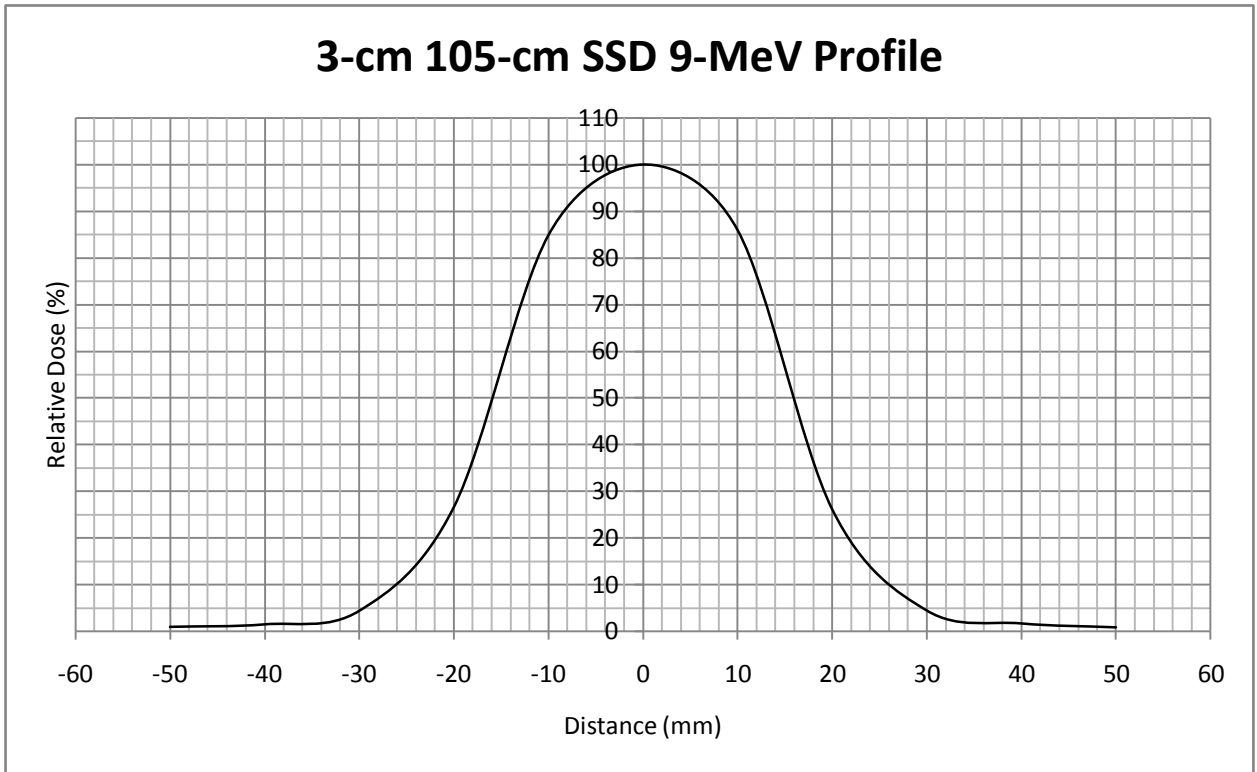
4-cm x 5-cm 105-cm SSD 6-MeV Profile



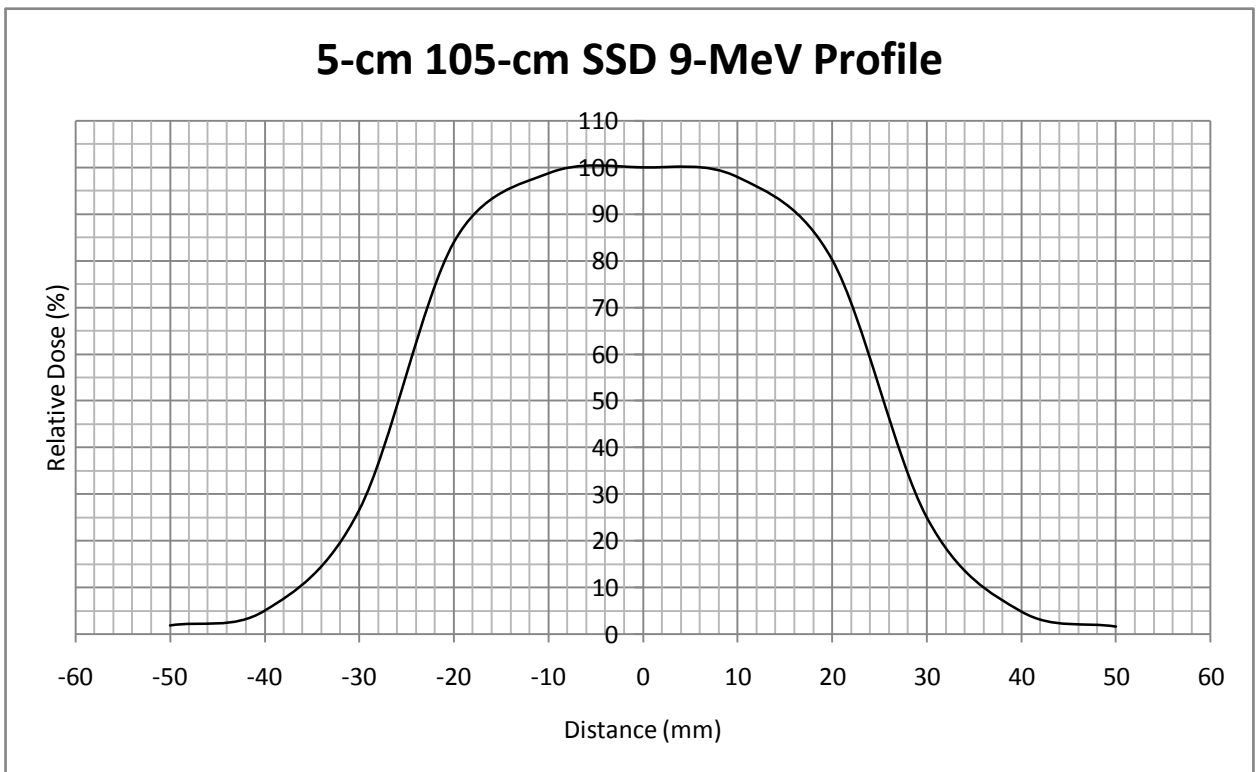
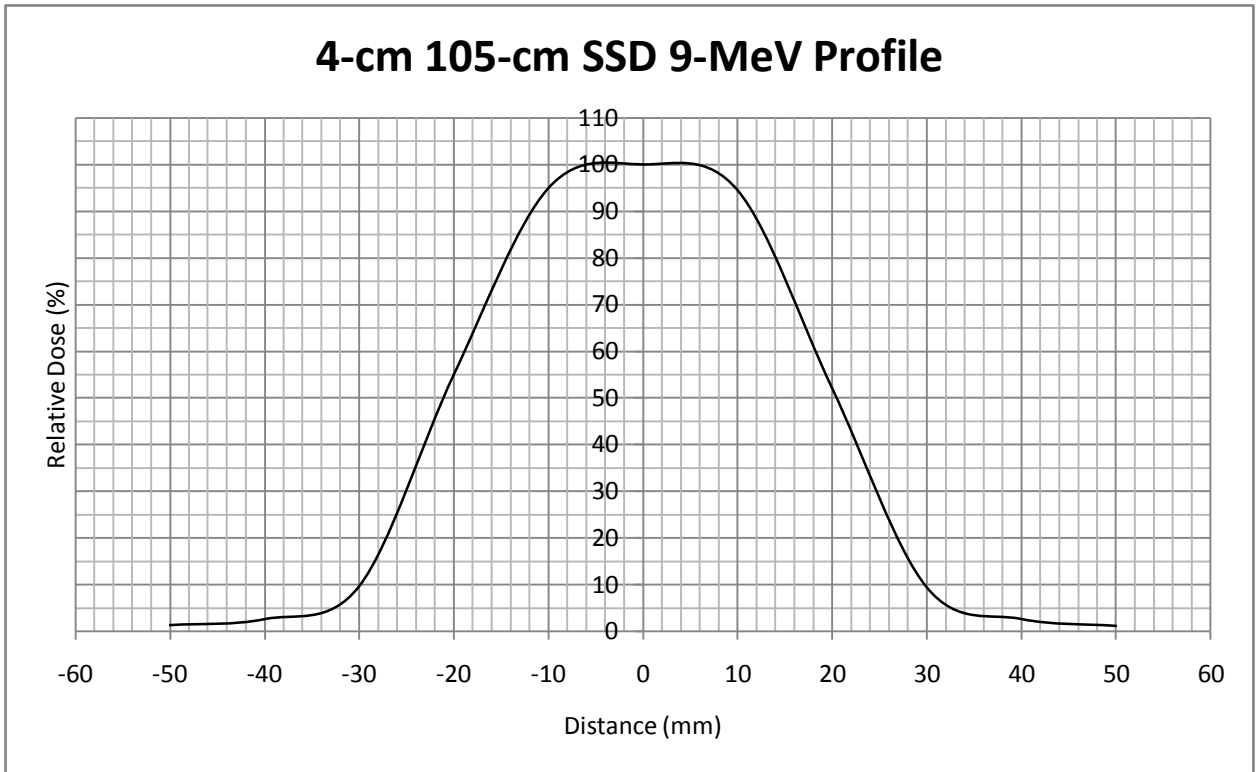
3-cm x 4-cm 105-cm SSD 9-MeV Profile



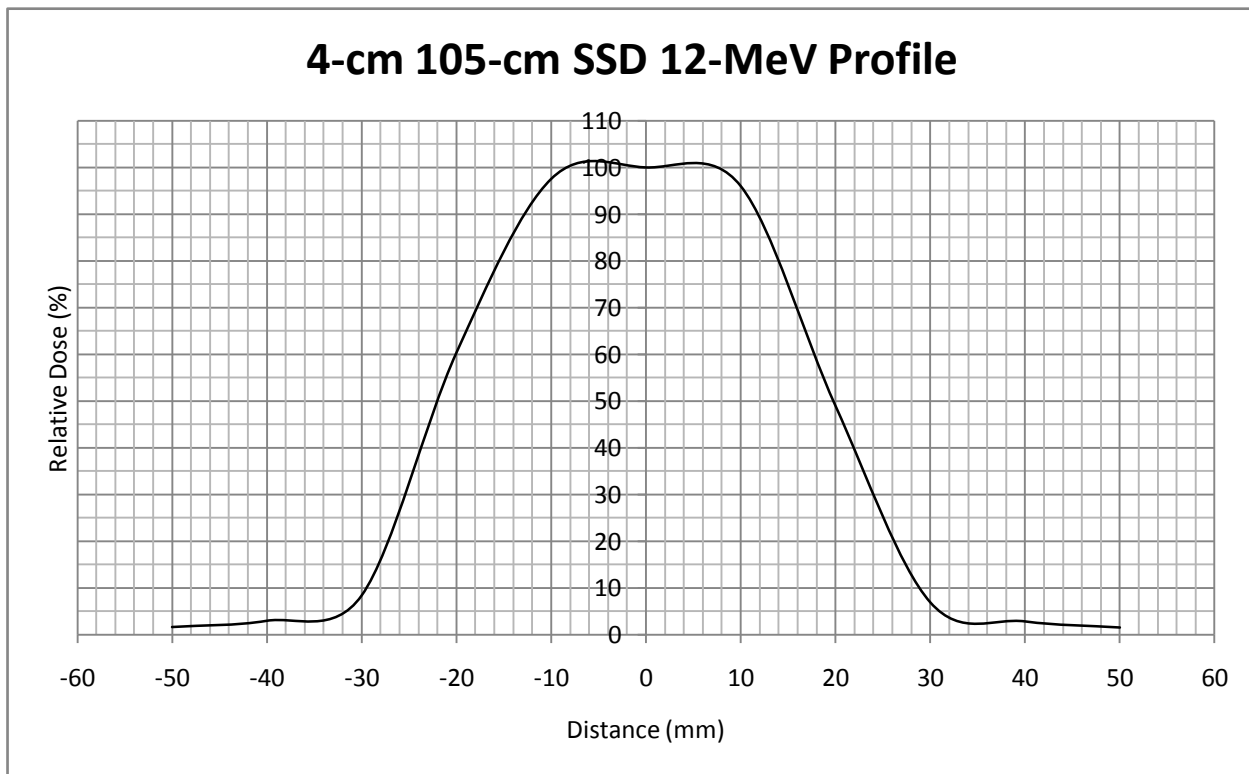
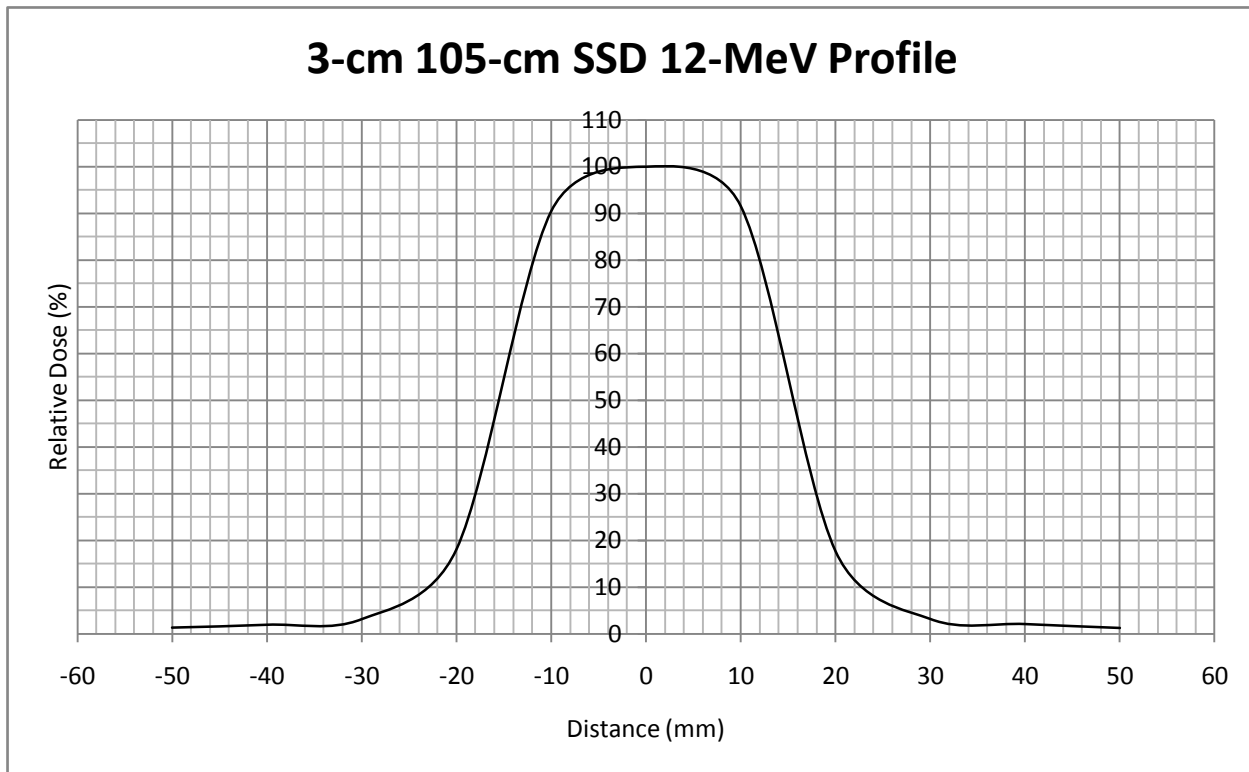
3-cm x 5-cm 105-cm SSD 9-MeV Profile



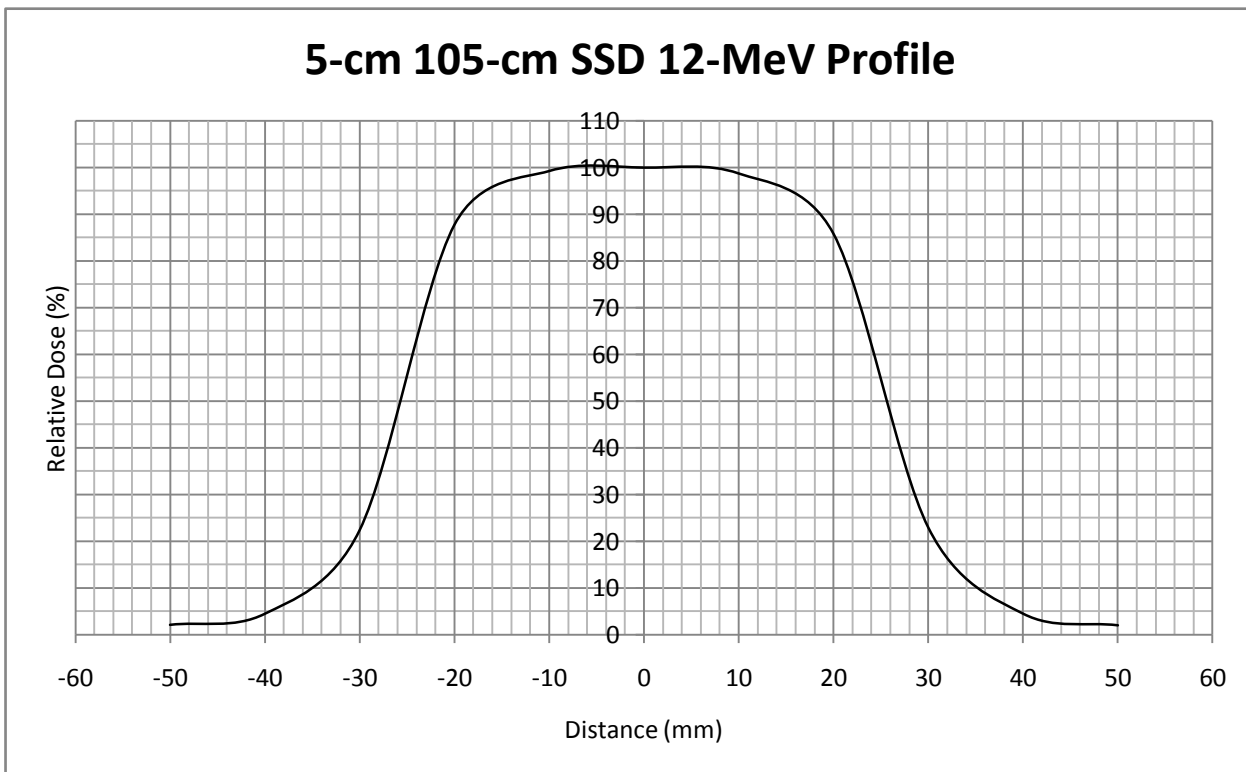
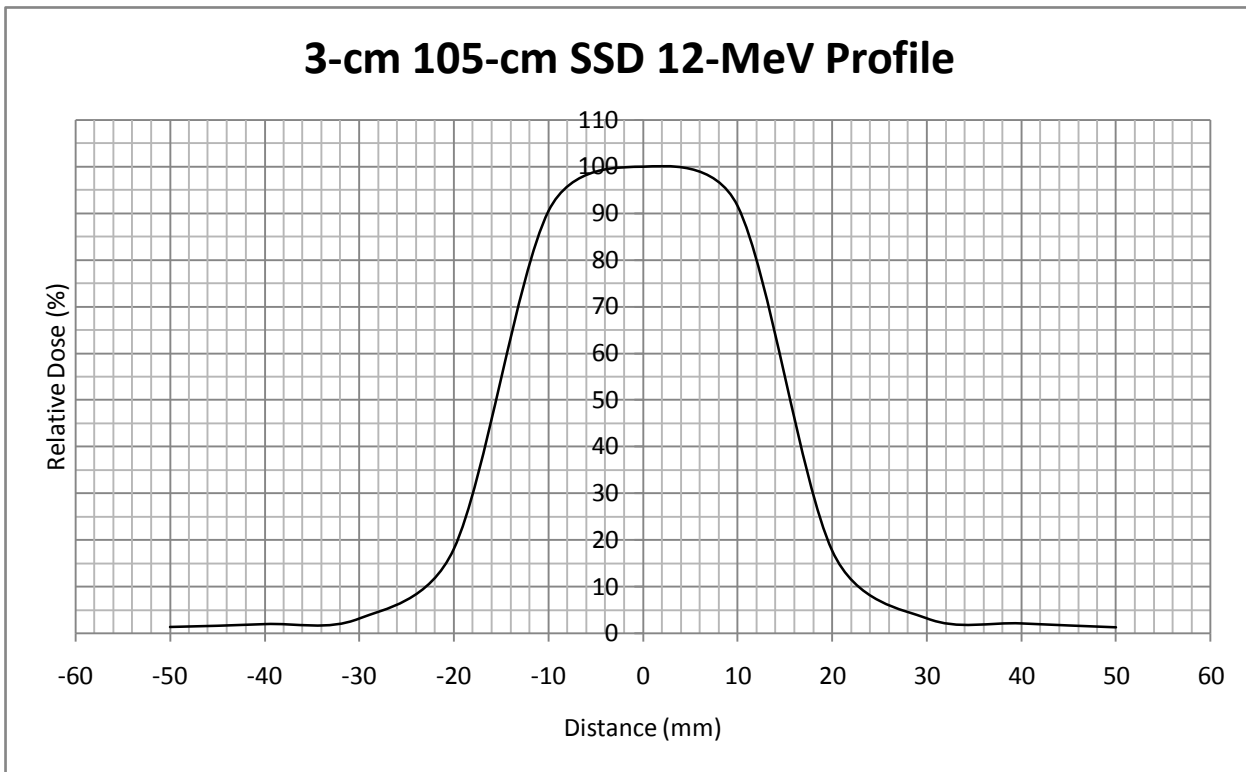
4-cm x 5-cm 105-cm SSD 9-MeV Profile



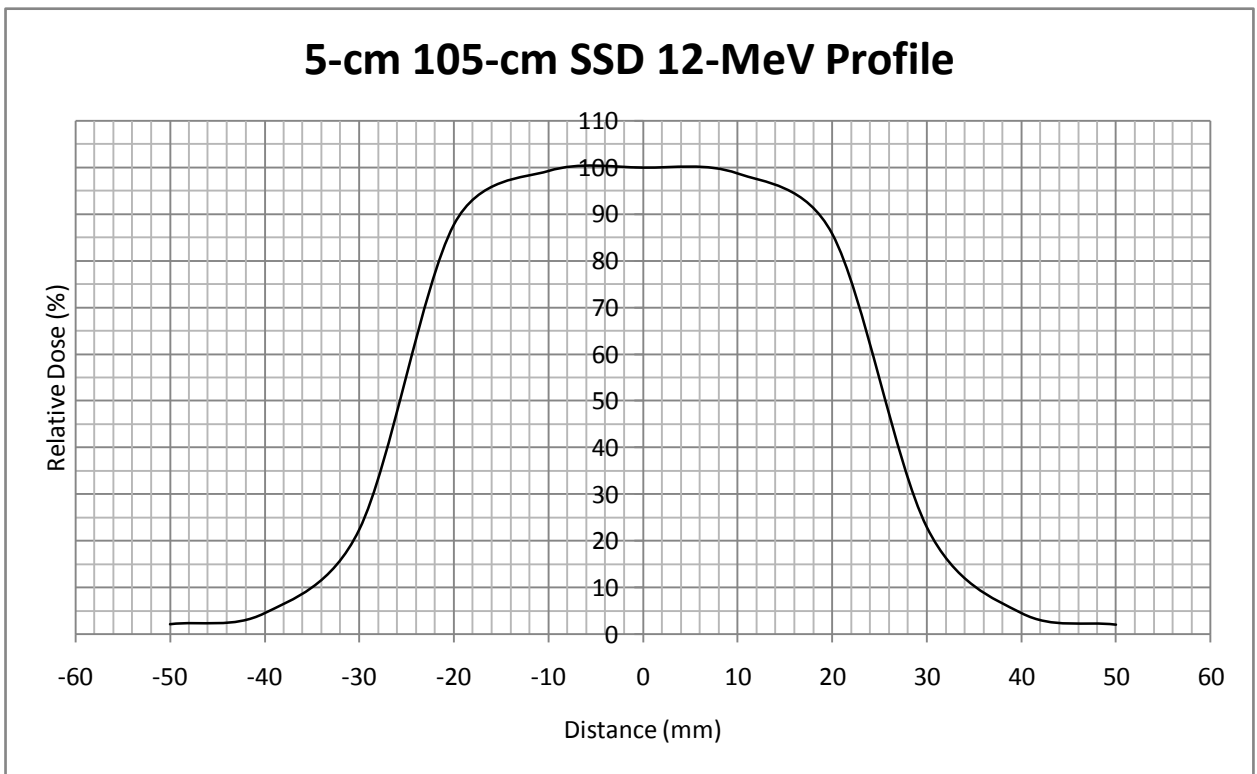
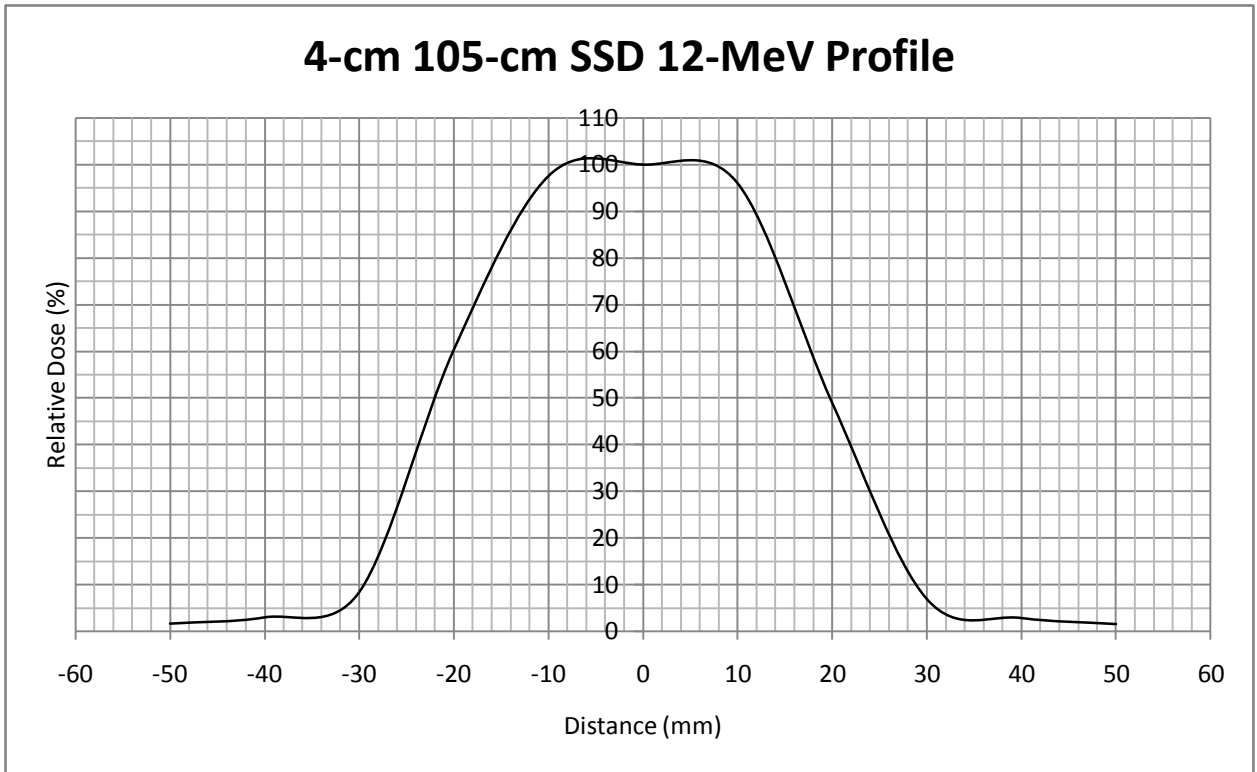
3-cm x 4-cm 105-cm SSD 12-MeV Profile



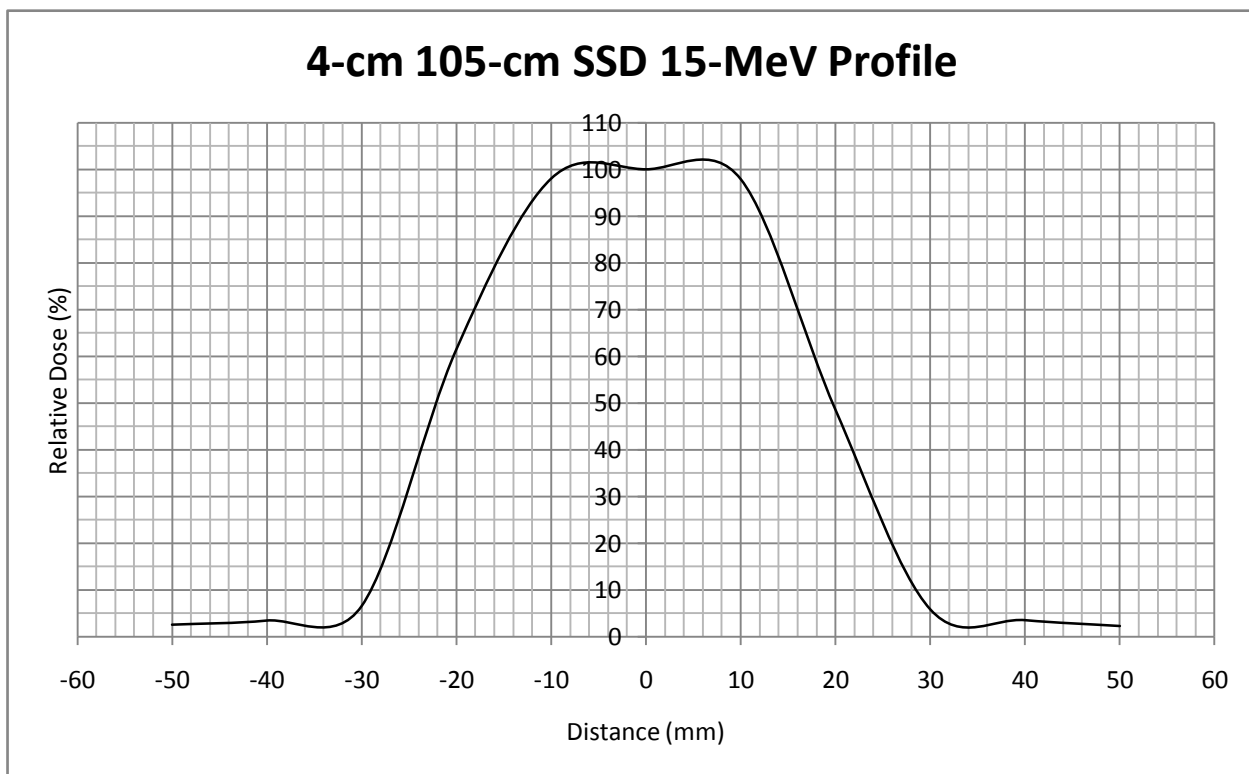
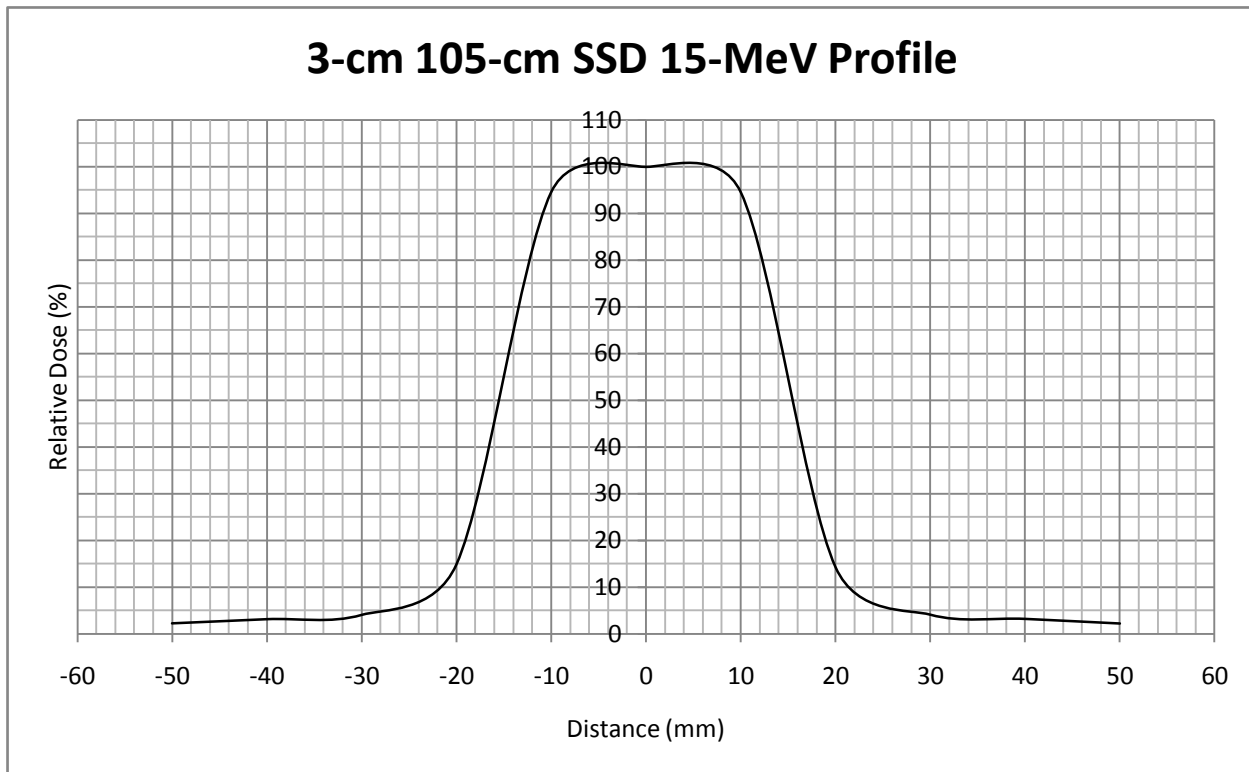
3-cm x 5-cm 105-cm SSD 12-MeV Profile



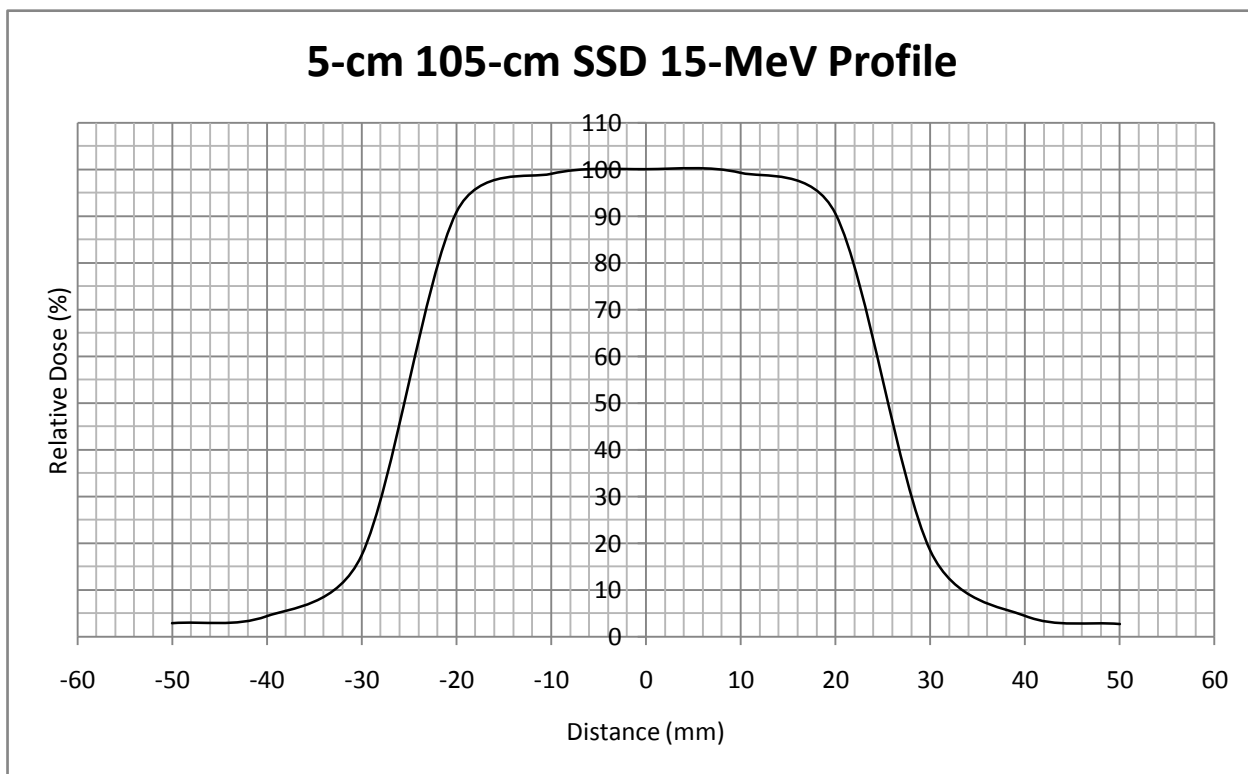
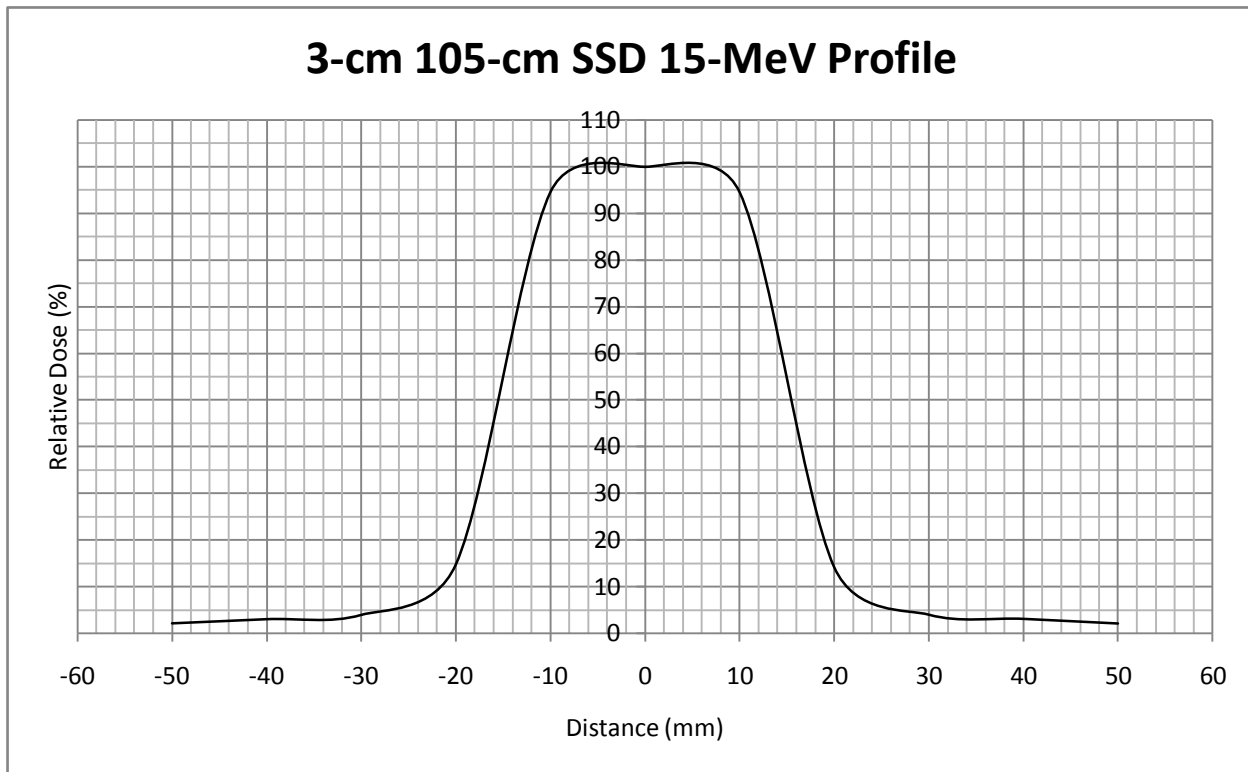
4-cm x 5-cm 105-cm SSD 12-MeV Profile



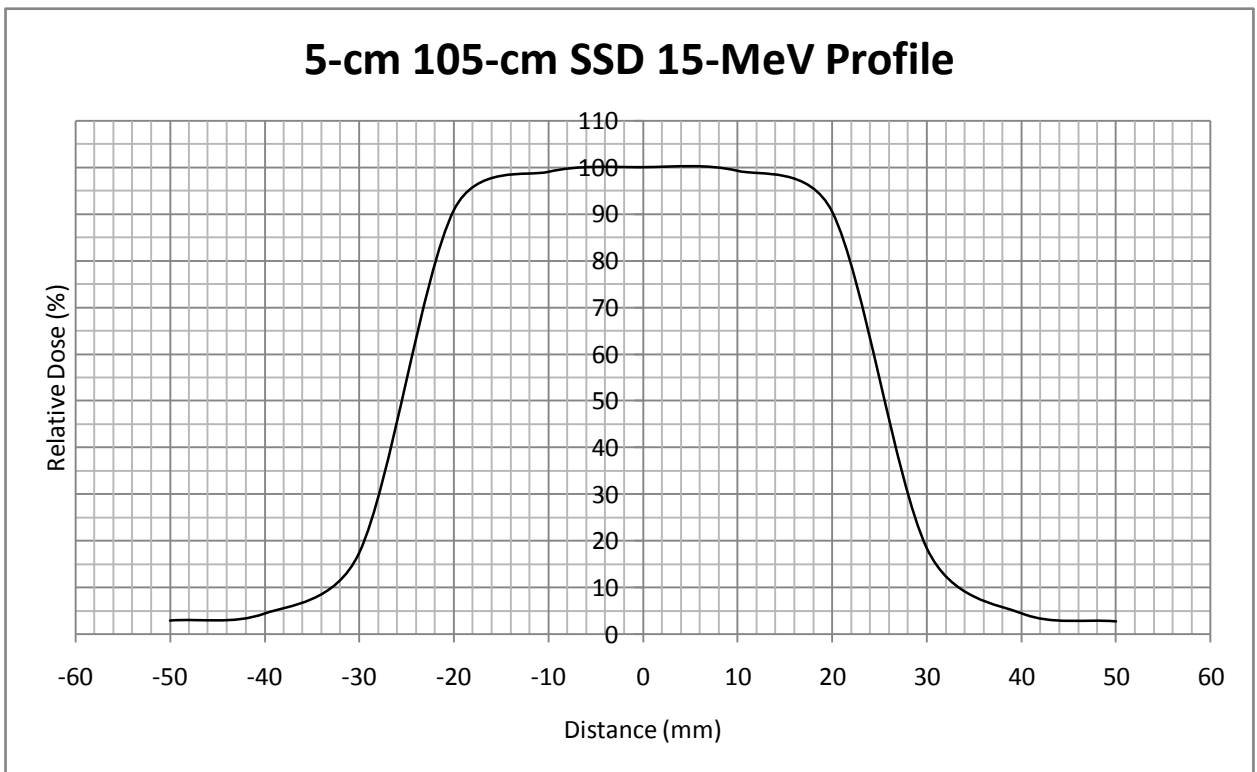
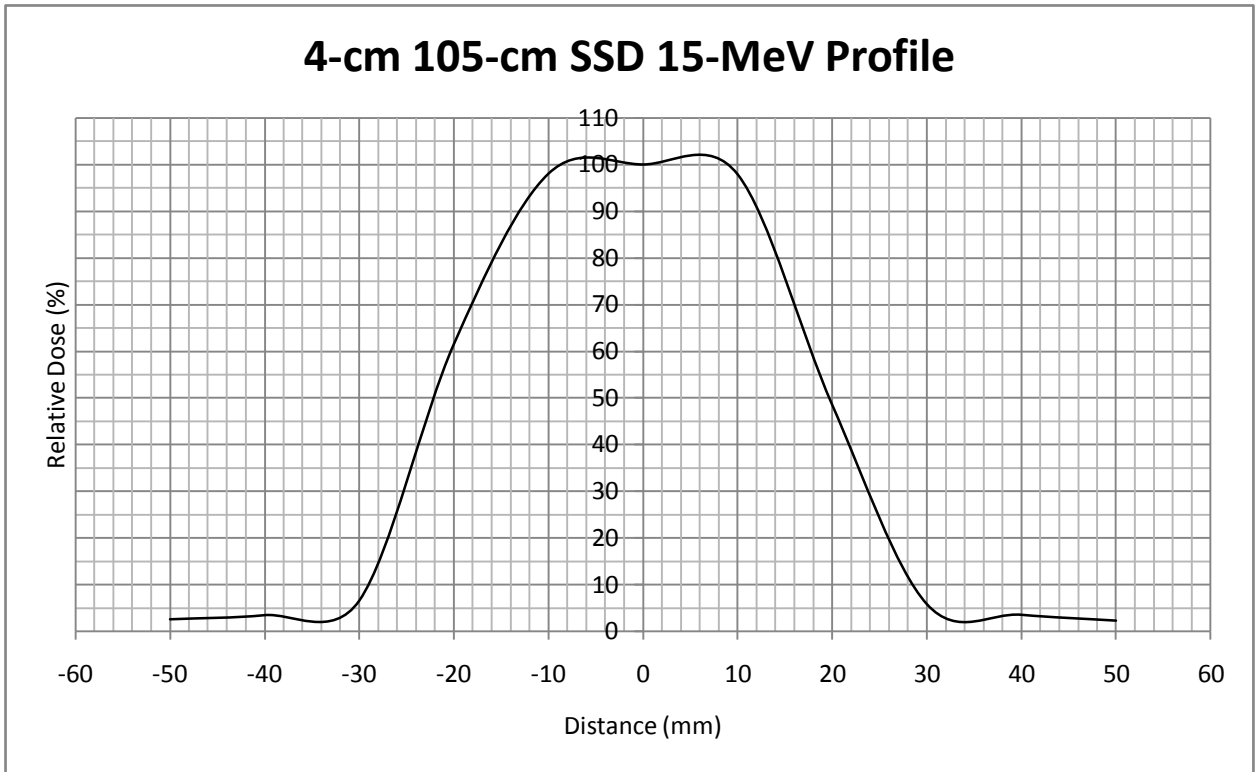
3-cm x 4-cm 105-cm SSD 15-MeV Profile



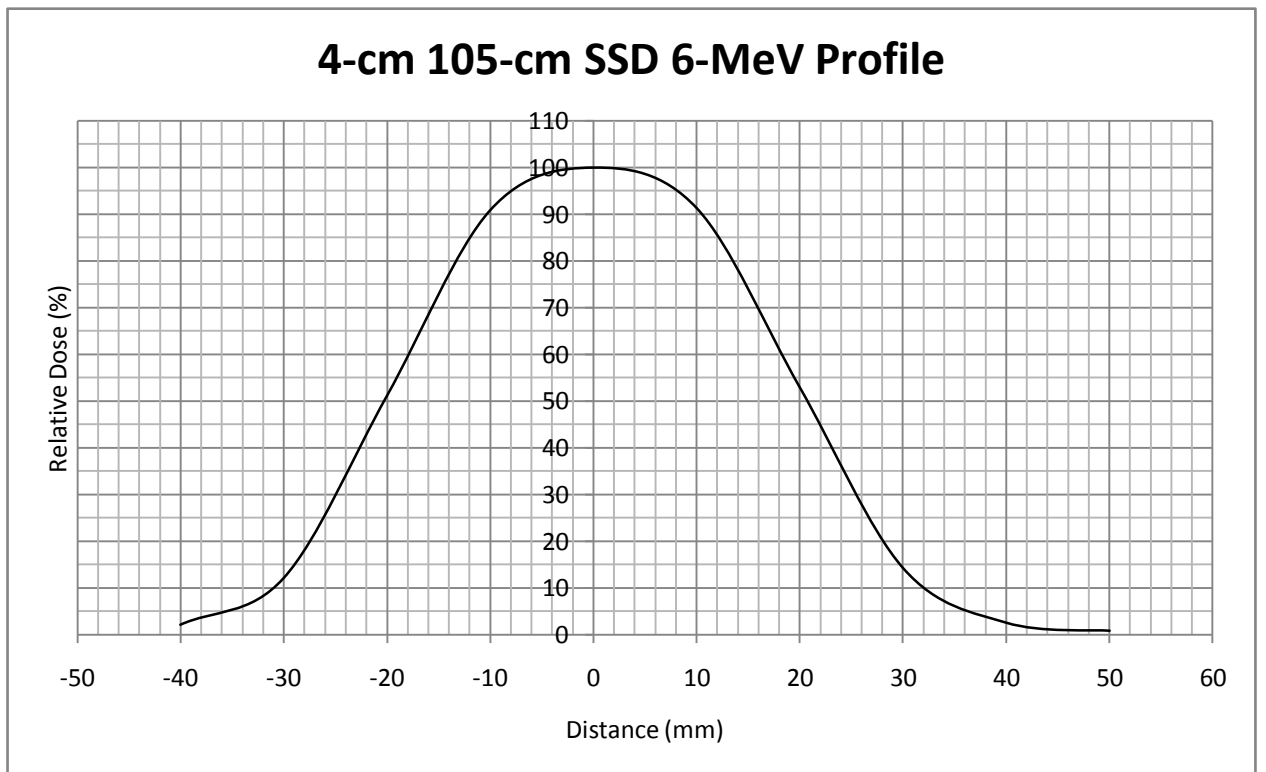
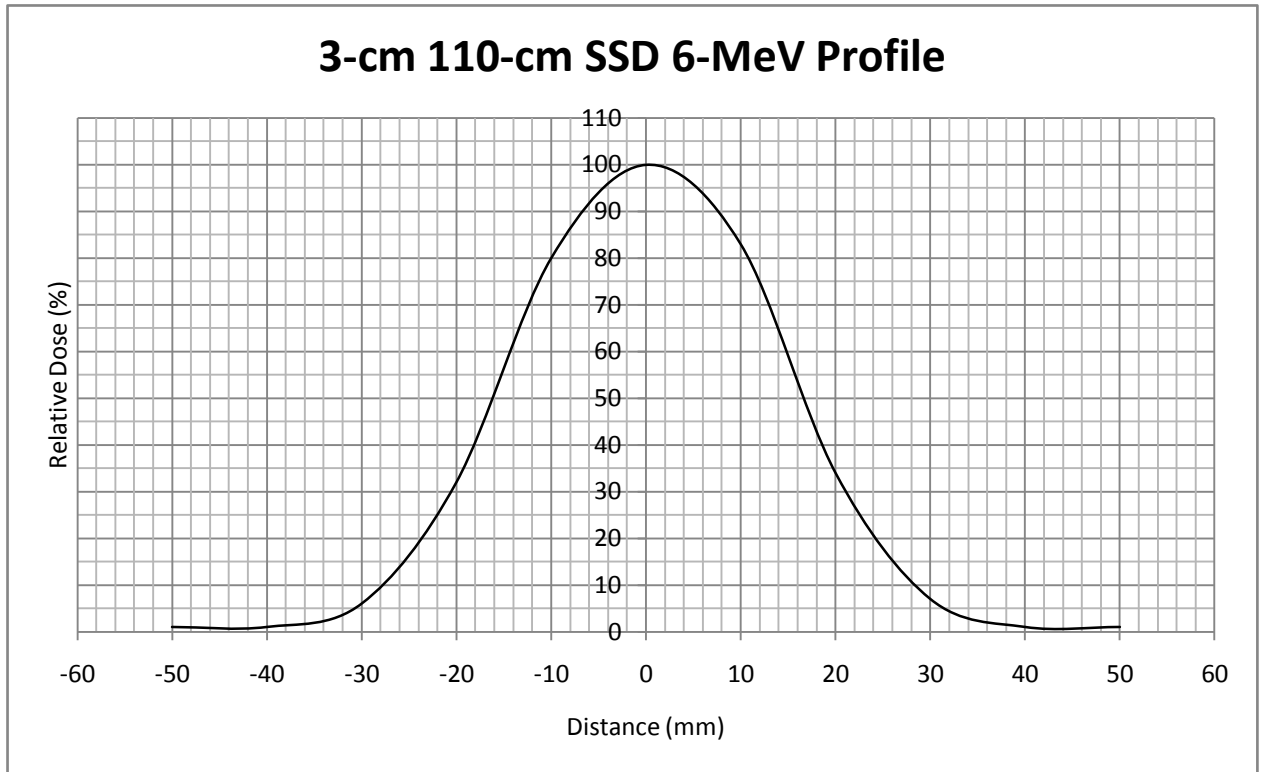
3-cm x 5-cm 105-cm SSD 15-MeV Profile



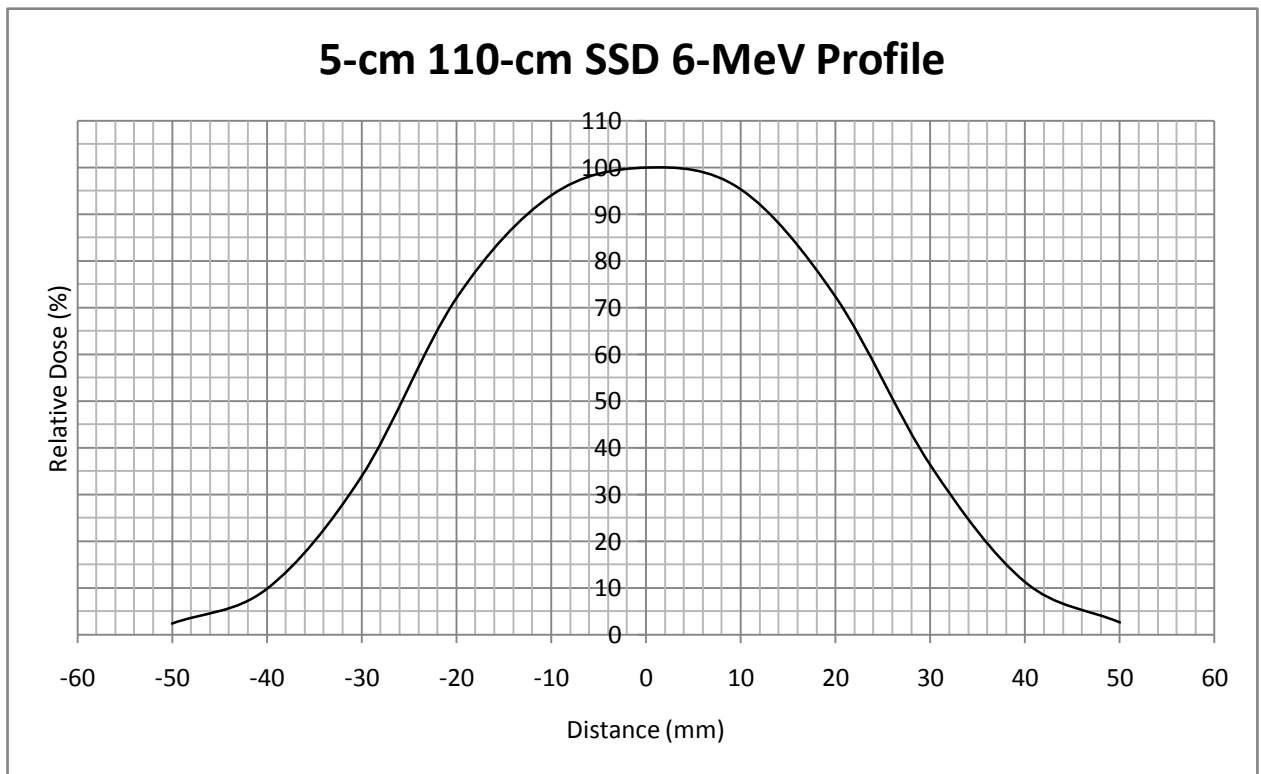
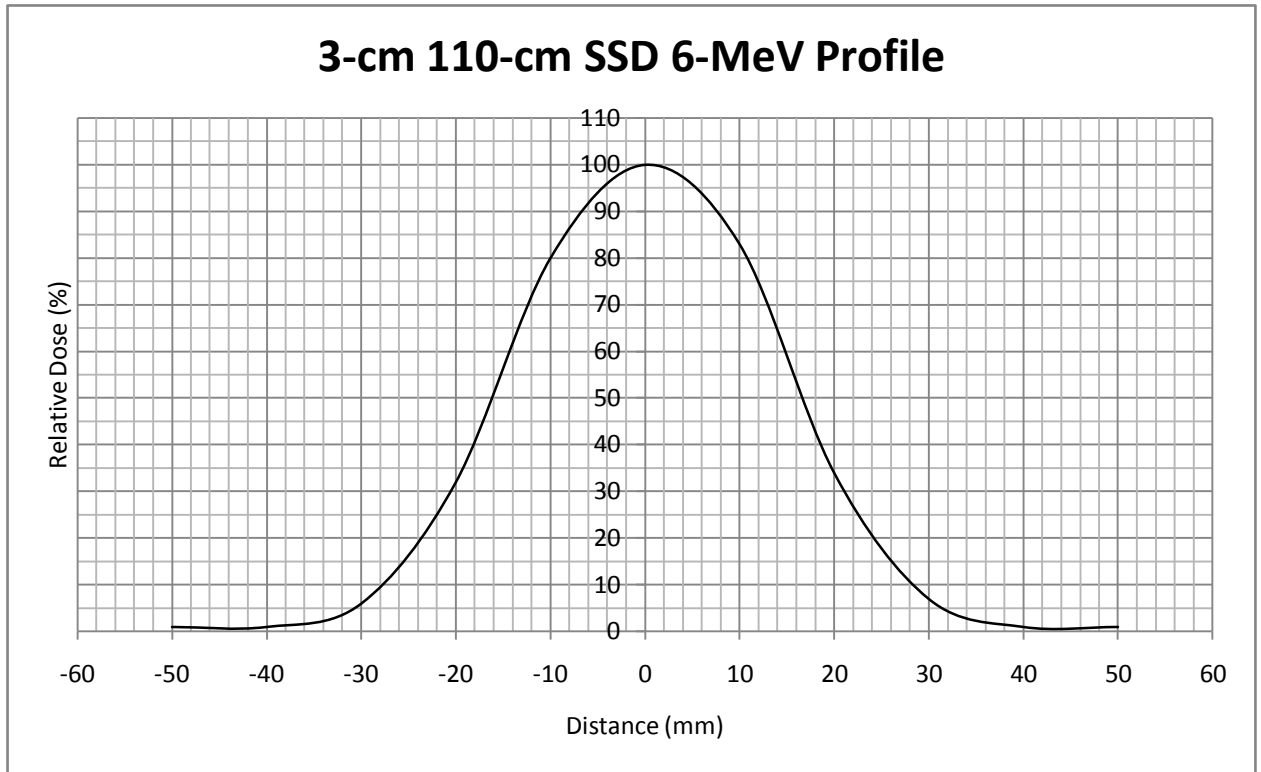
4-cm x 5-cm 105-cm SSD 15-MeV Profile



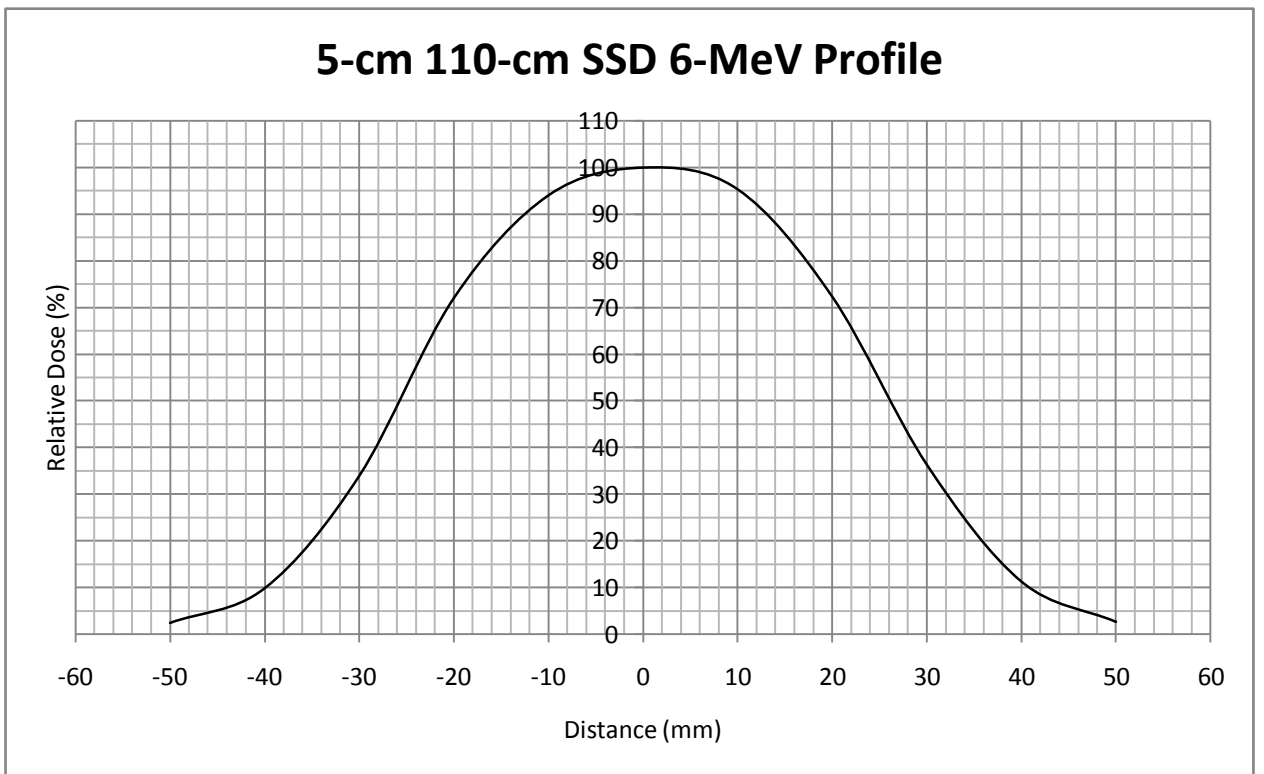
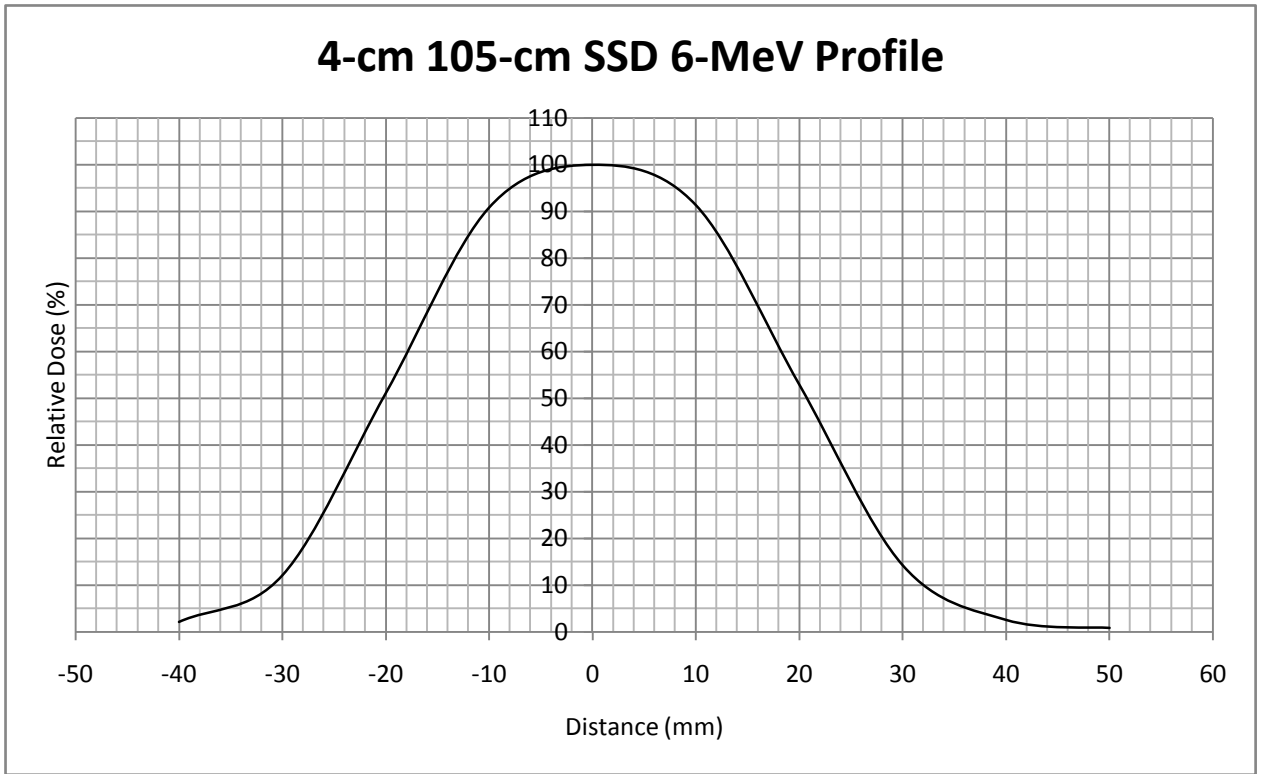
3-cm x 4-cm 110-cm SSD 6-MeV Profile



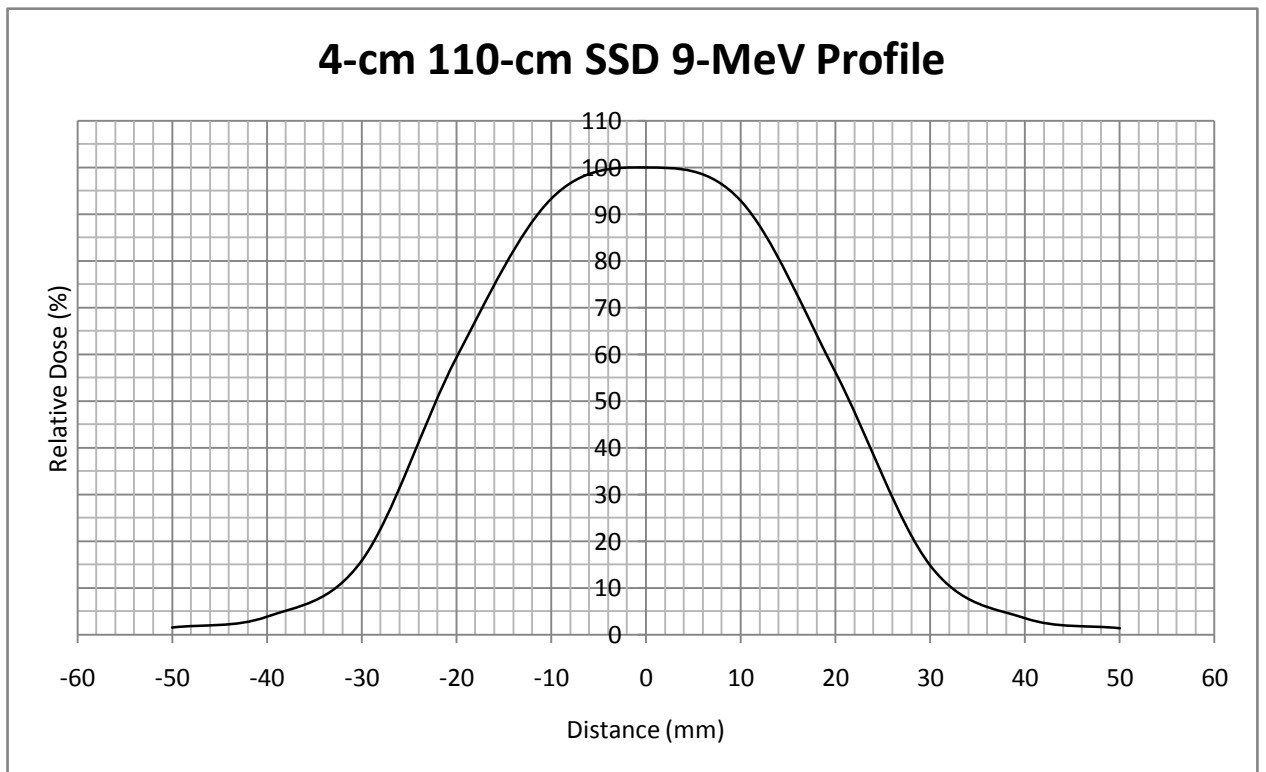
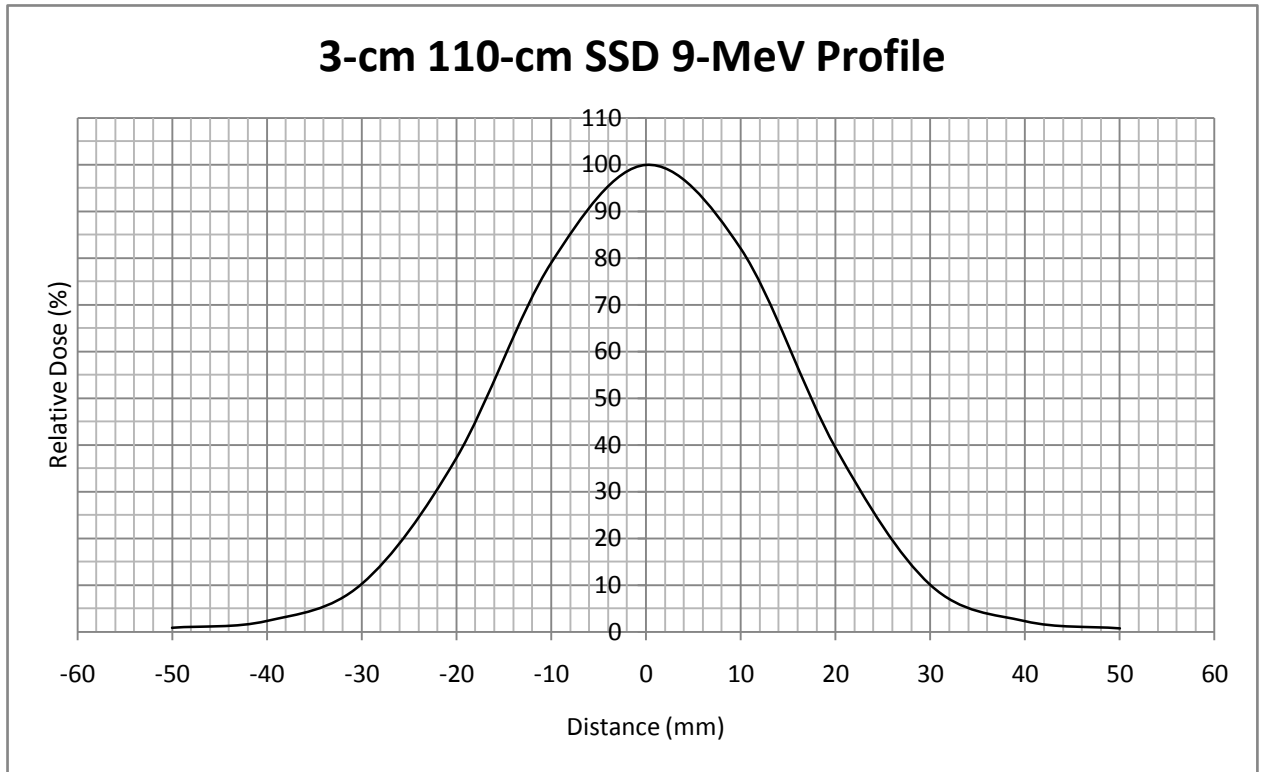
3-cm x 5-cm 110-cm SSD 6-MeV Profile



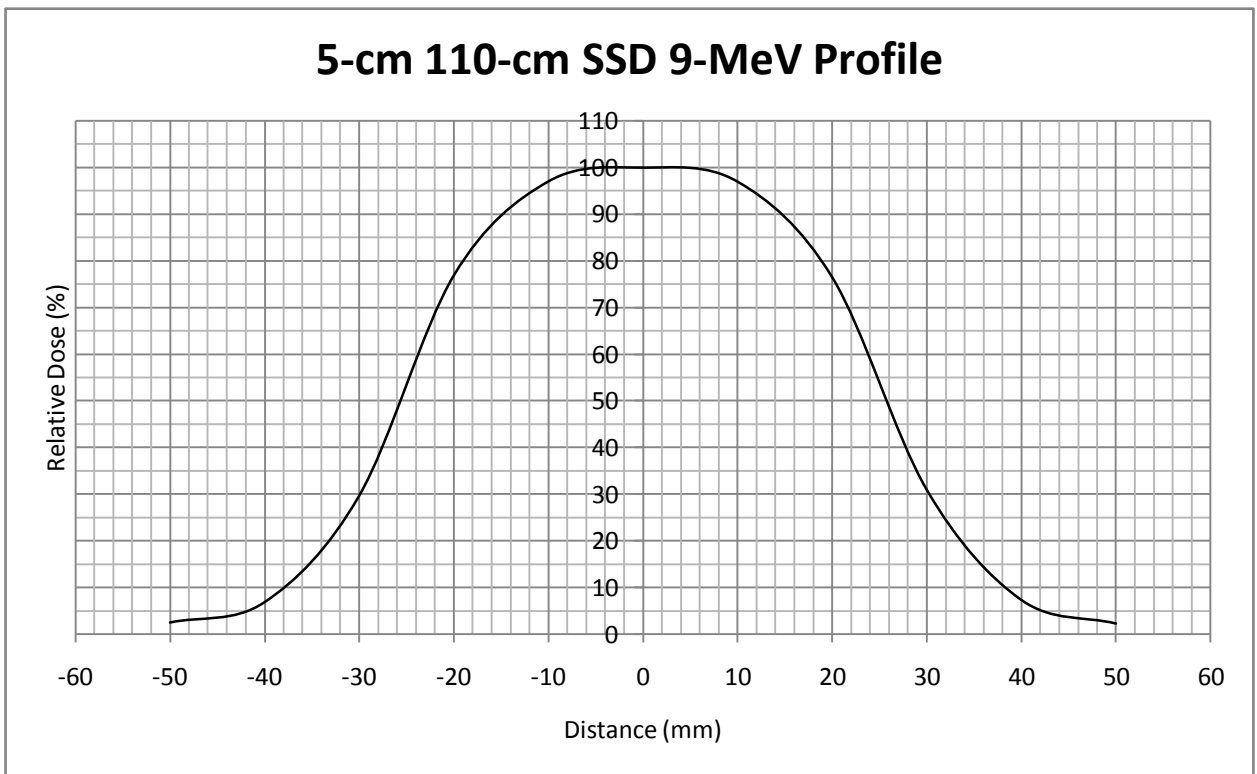
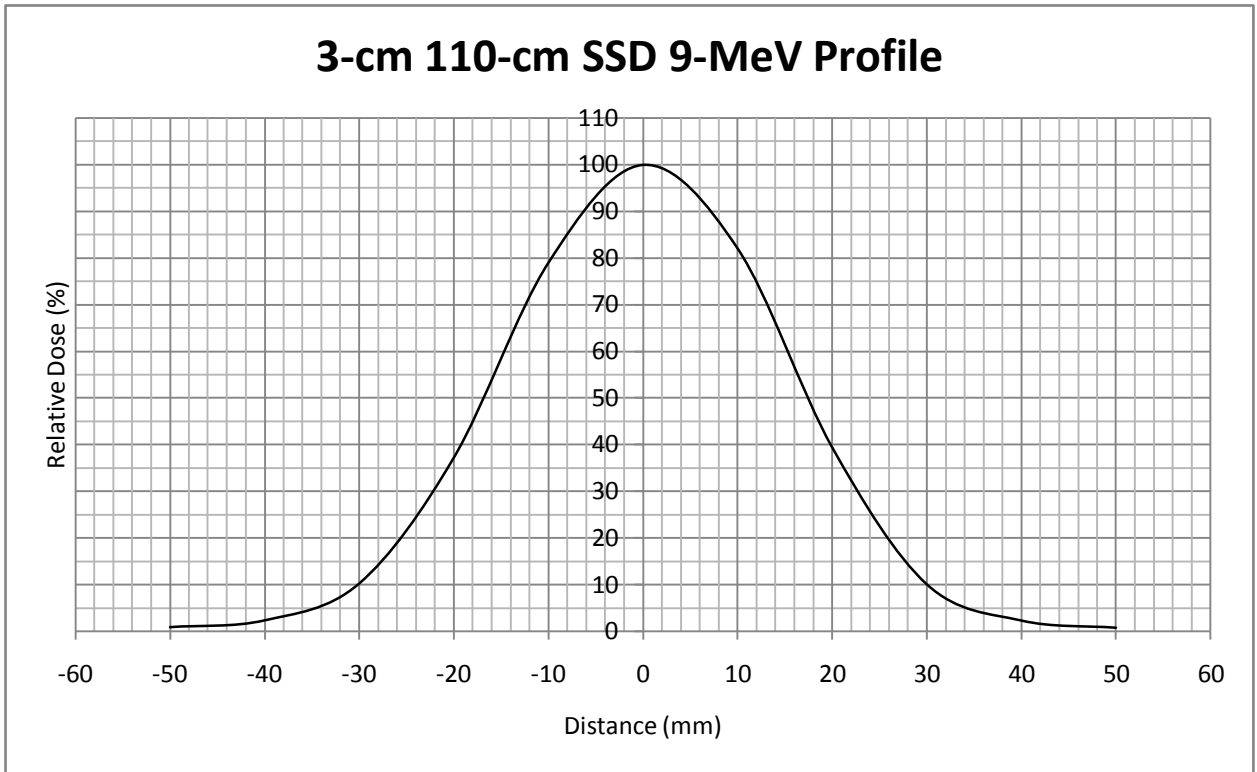
4-cm x 5-cm 110-cm SSD 6-MeV Profile



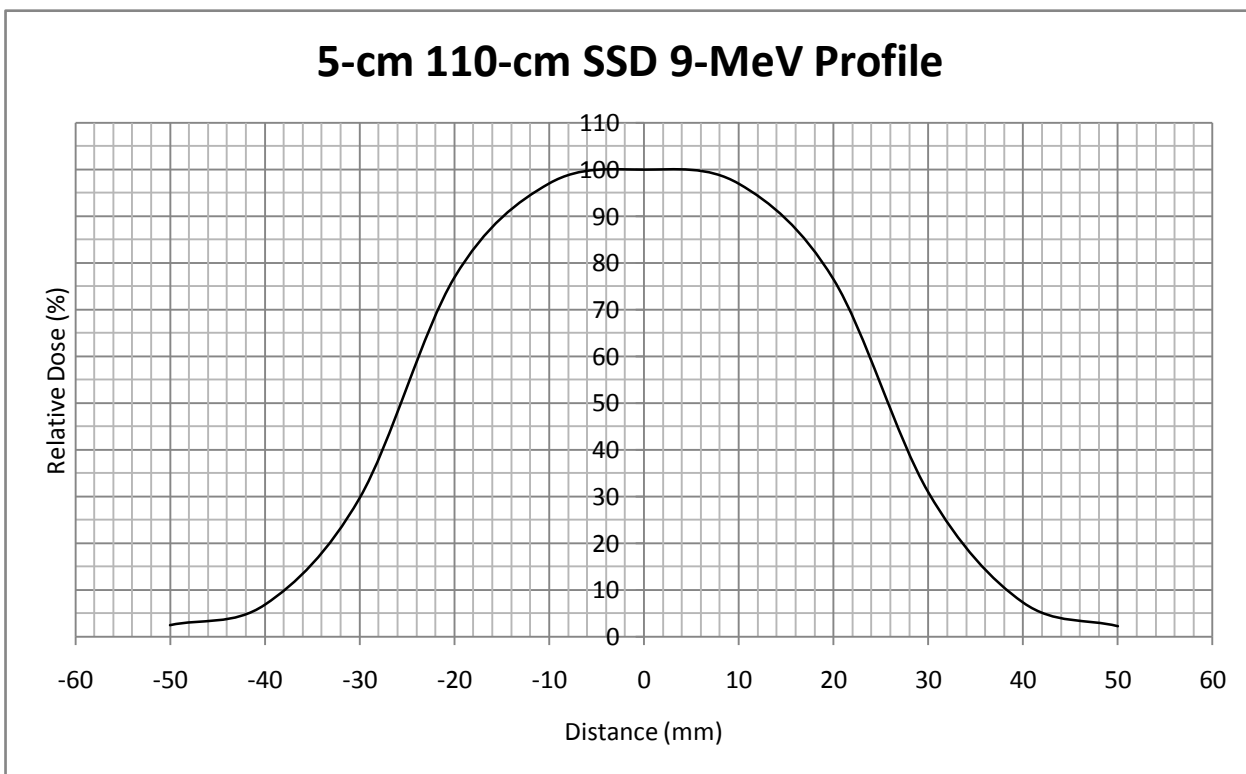
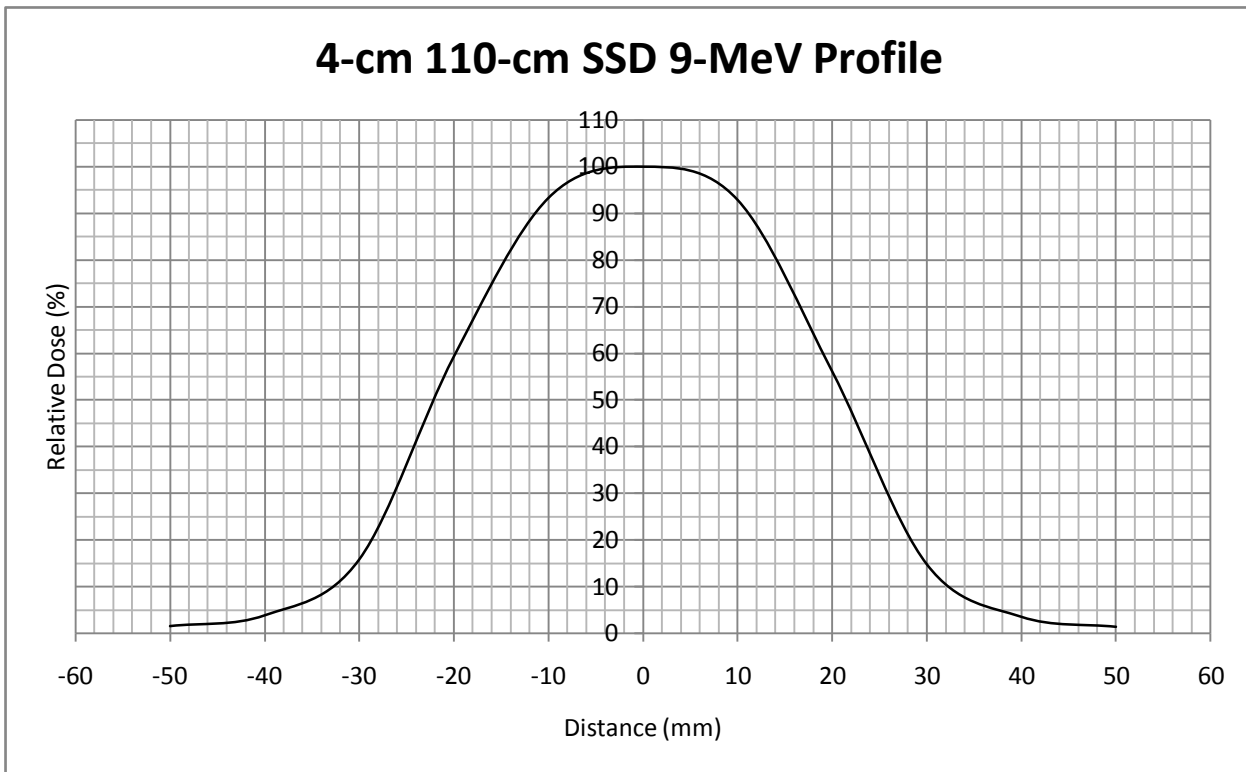
3-cm x 4-cm 110-cm SSD 9-MeV Profile



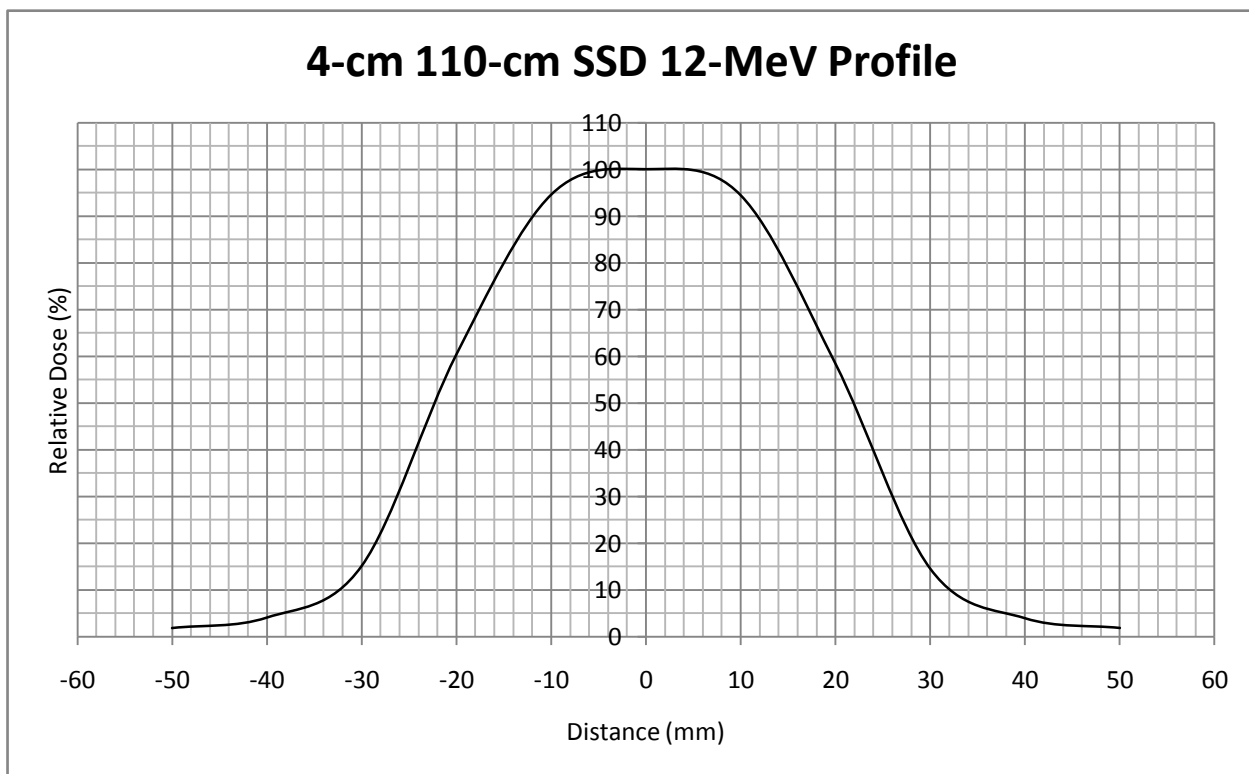
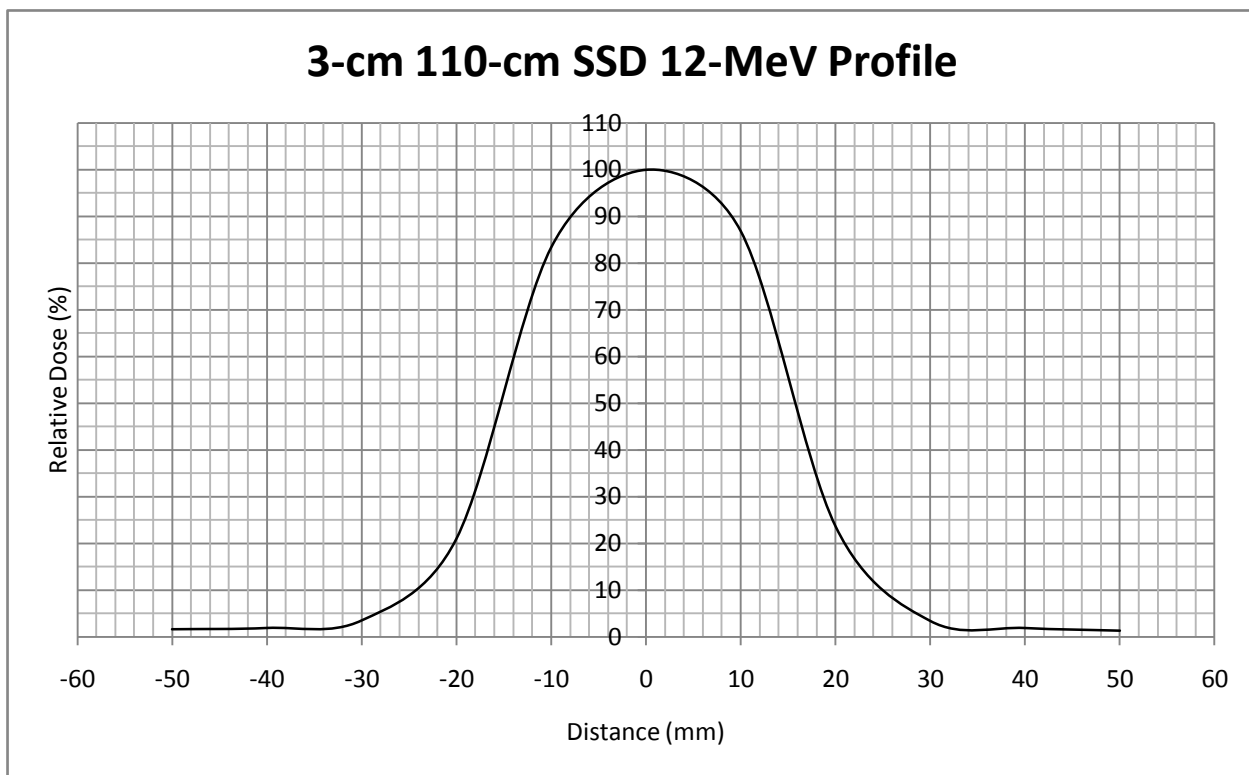
3-cm x 5-cm 110-cm SSD 9-MeV Profile



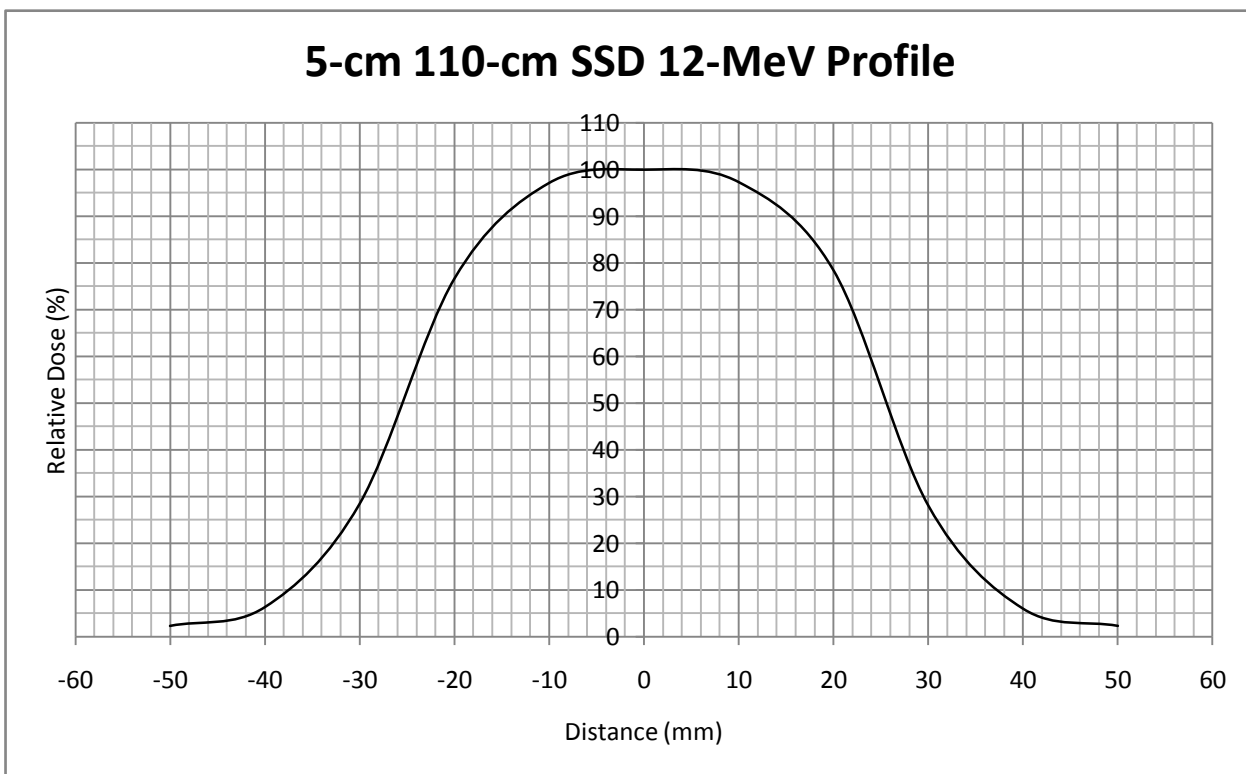
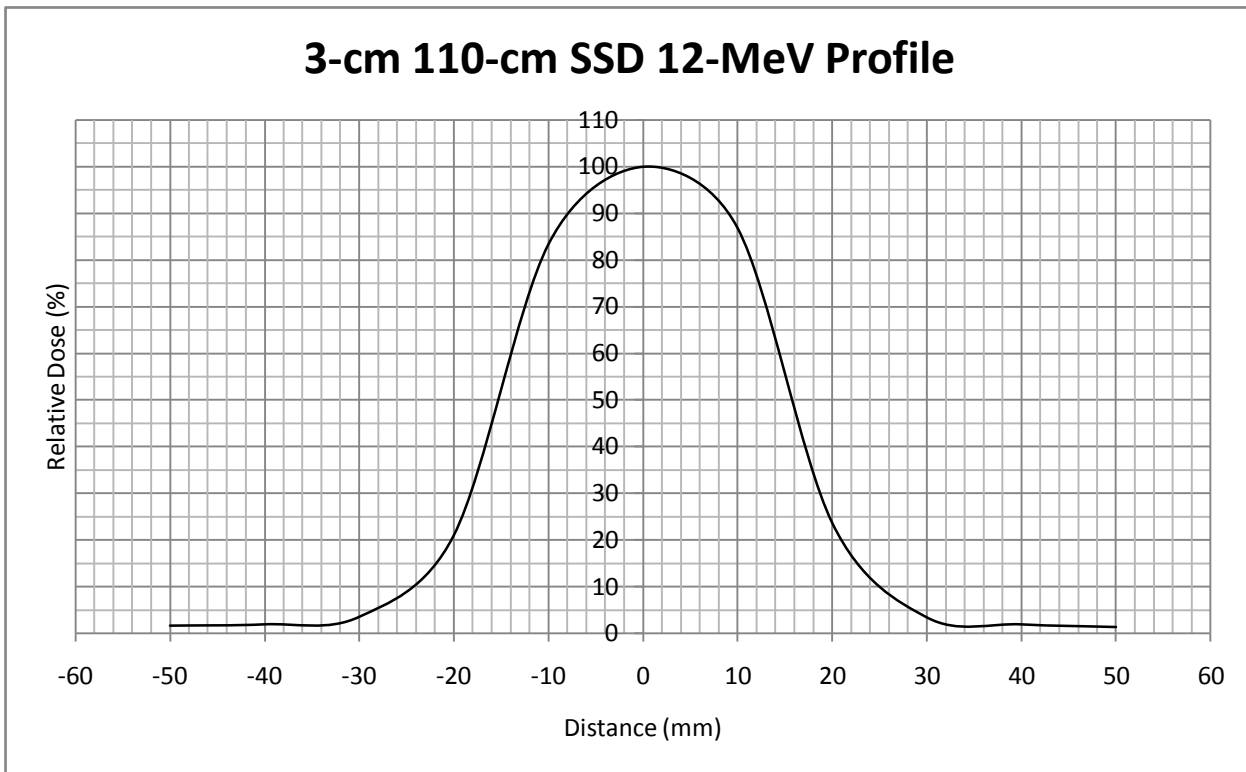
4-cm x 5-cm 110-cm 9-MeV Profile



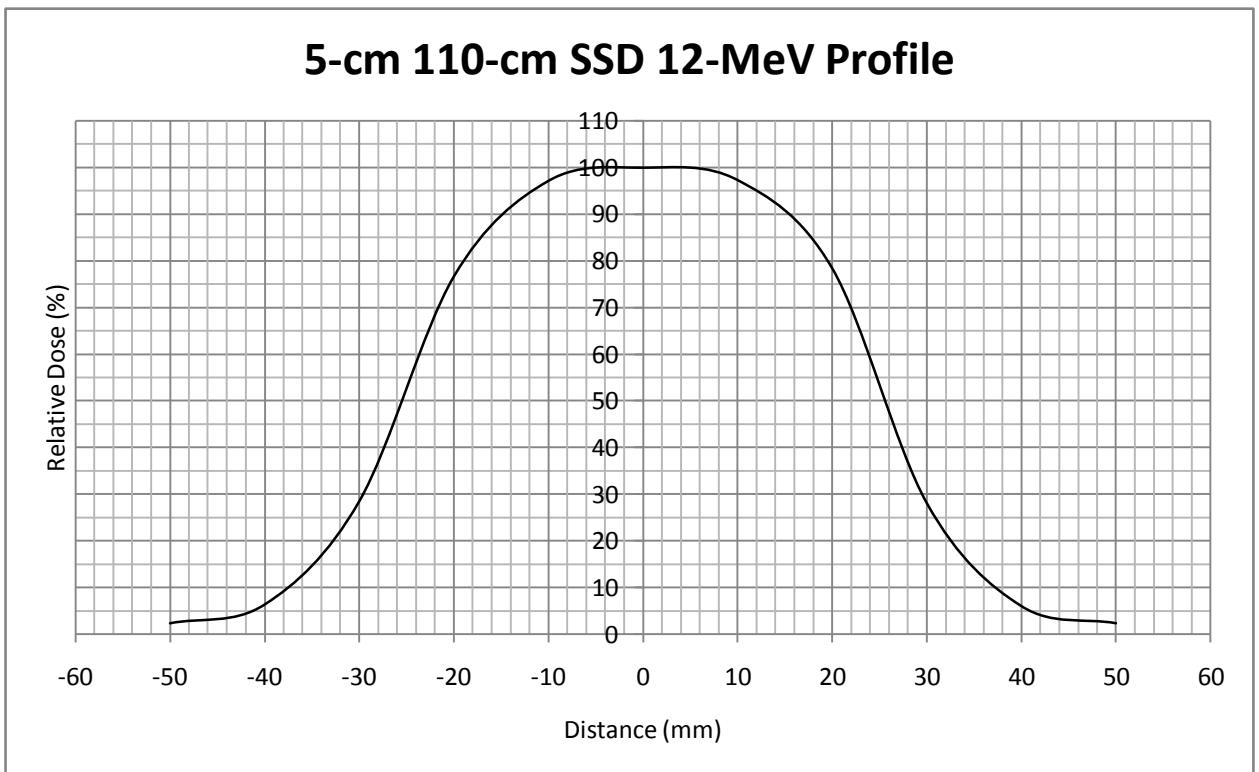
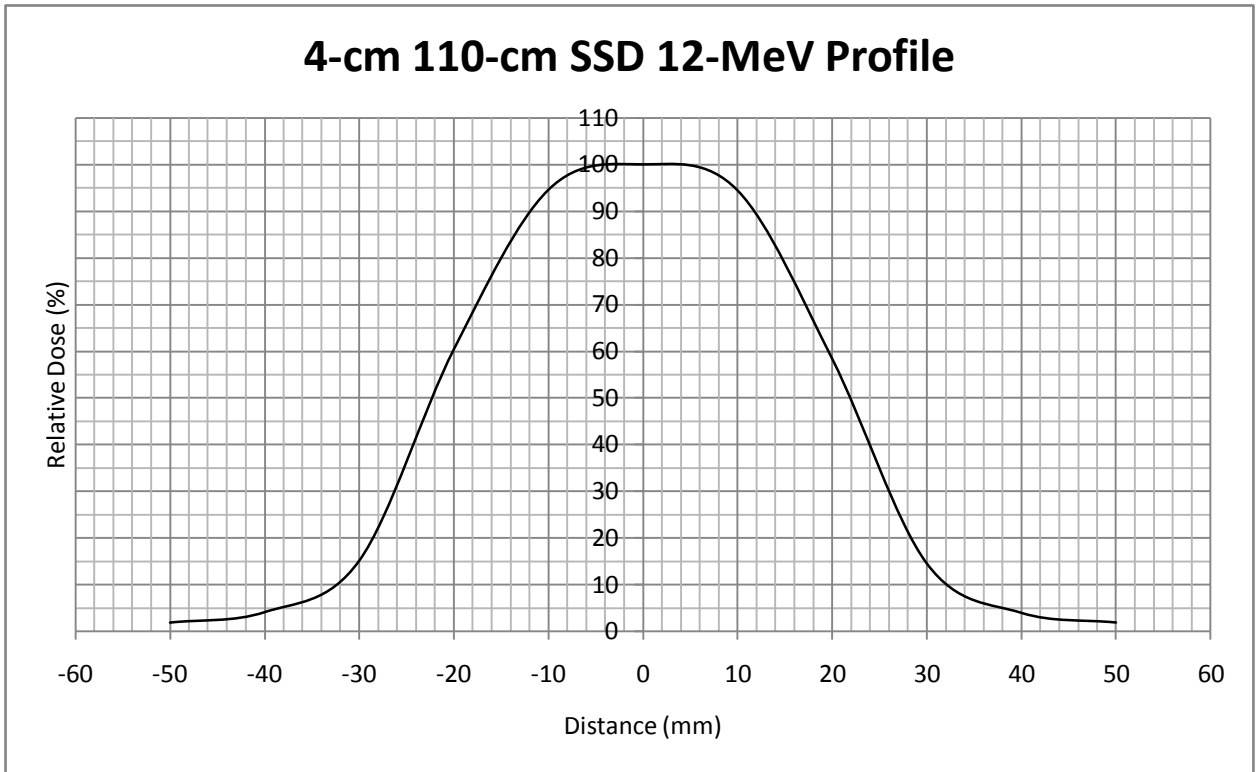
3-cm x 4-cm 110-cm SSD 12-MeV Profile



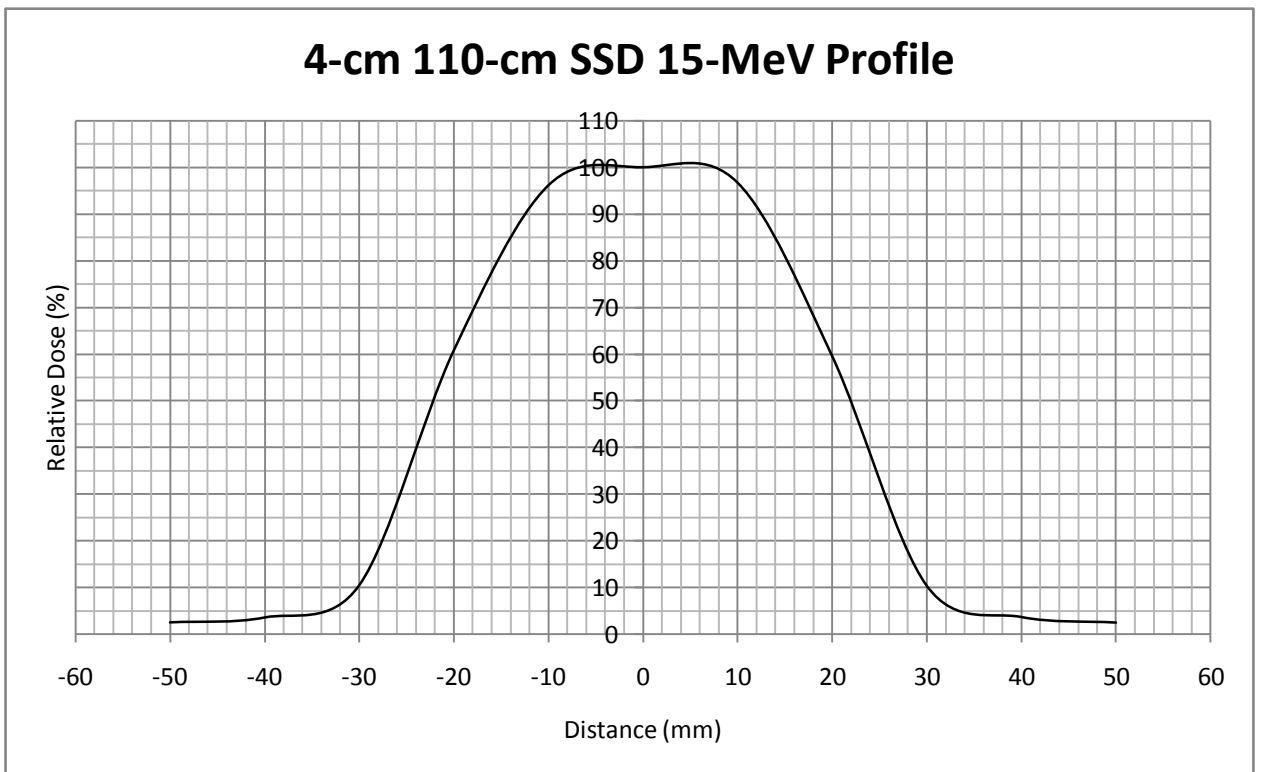
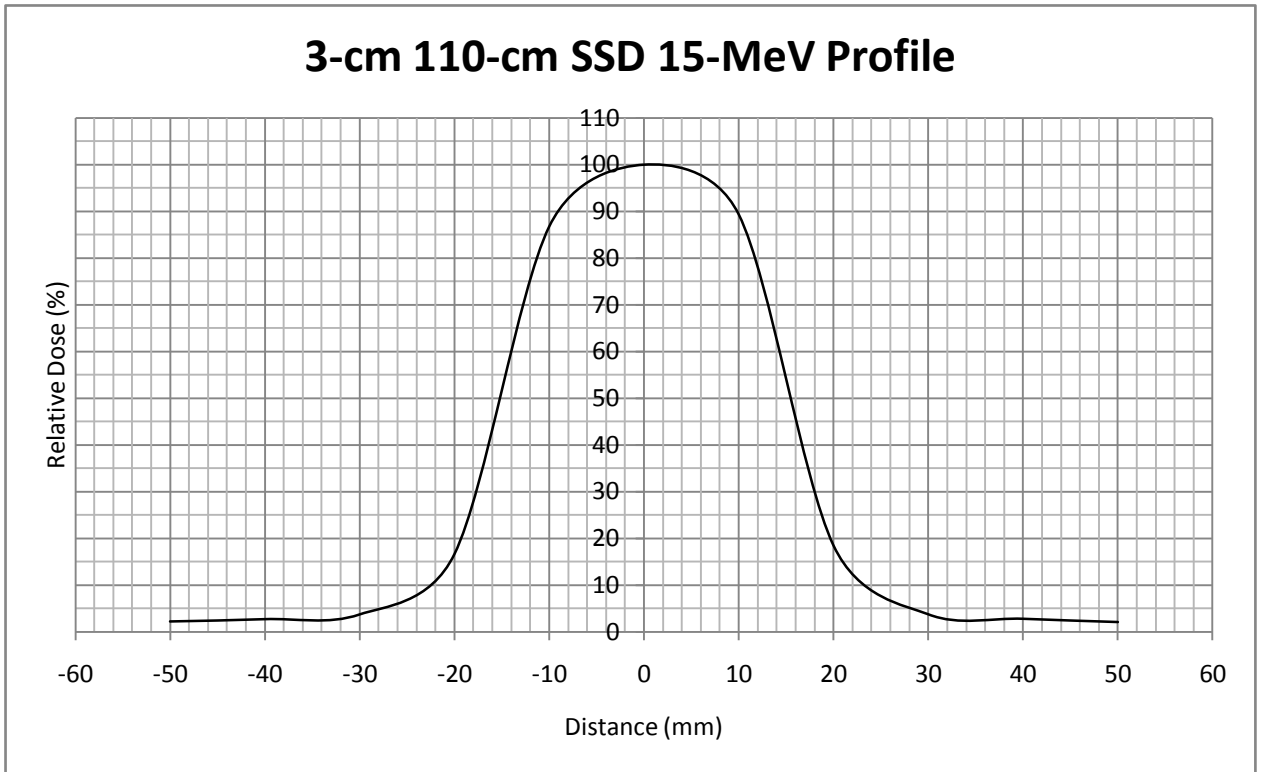
3-cm x 5-cm 110-cm SSD 12-MeV Profile



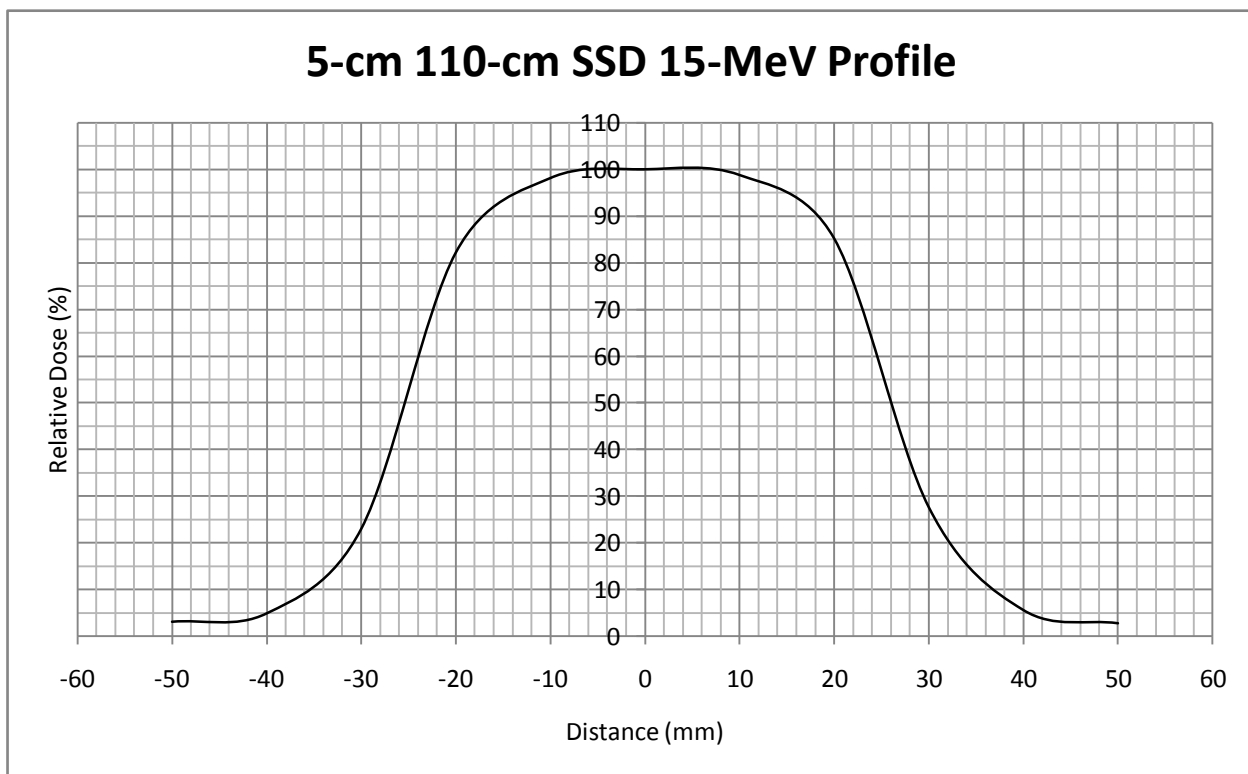
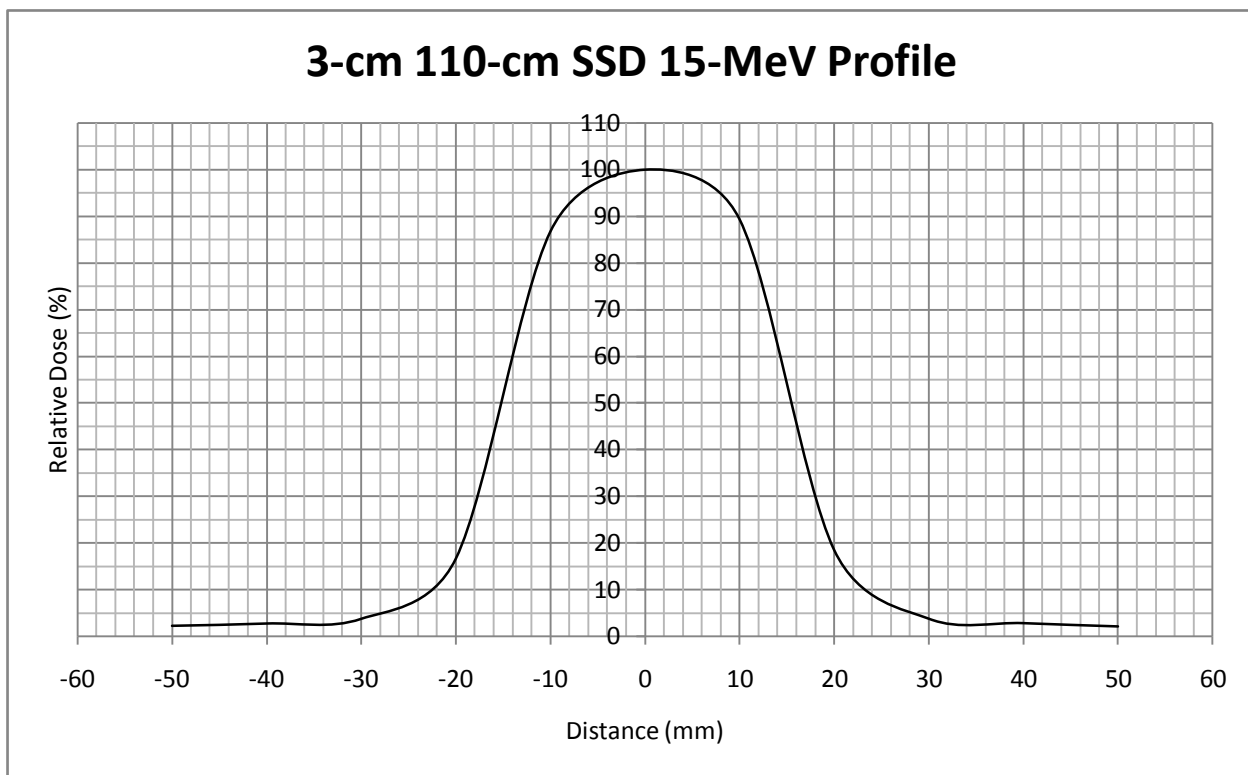
4-cm x 5-cm 110-cm SSD 12-MeV Profile



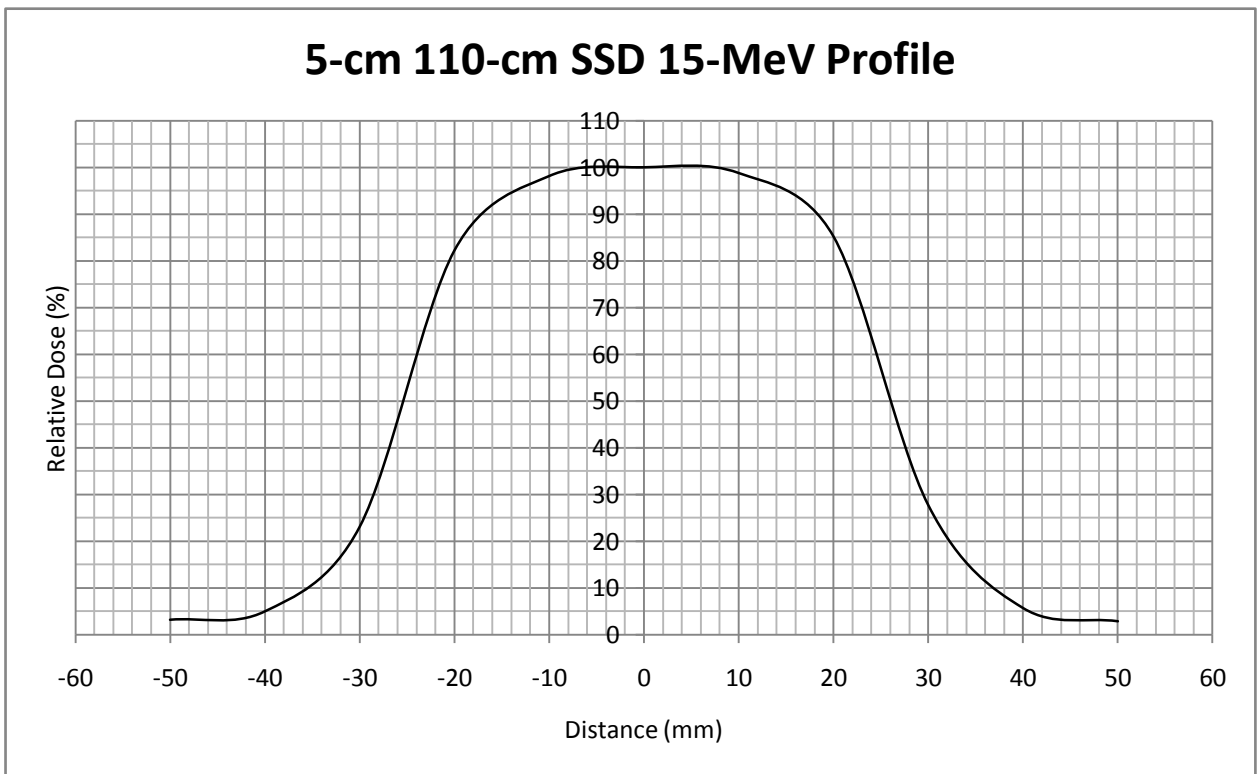
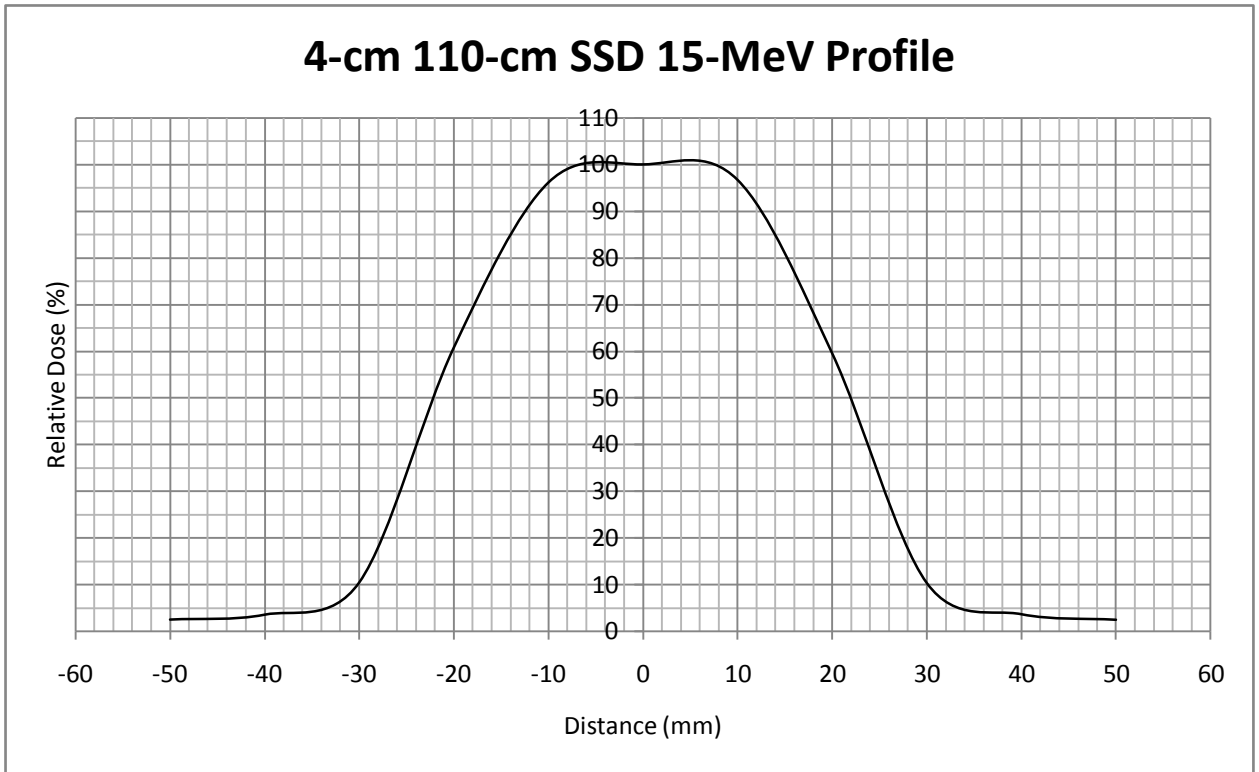
3-cm x 4-cm 110-cm SSD 15-MeV Profile



3-cm x 5-cm 110-cm SSD 15-MeV Profile



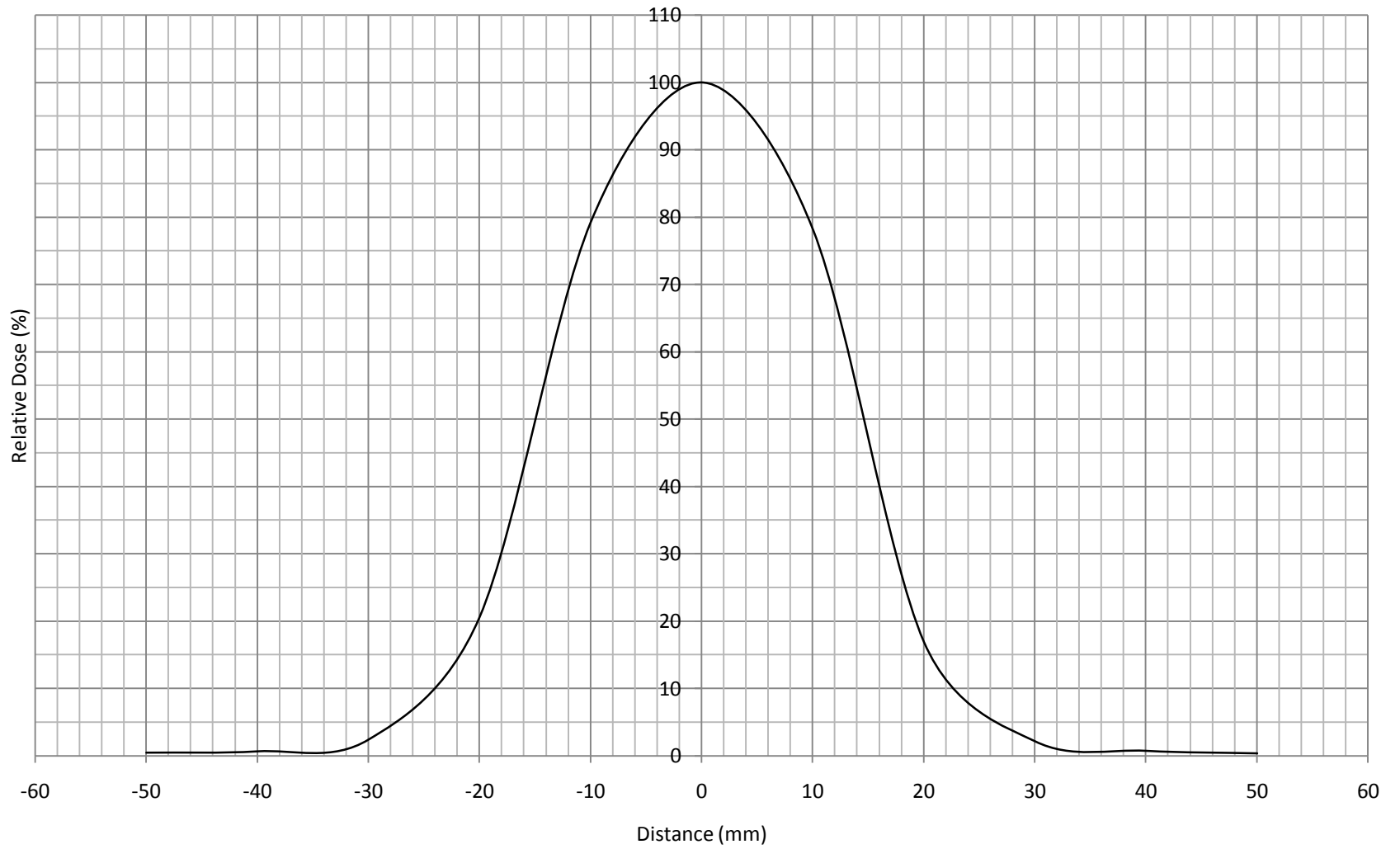
4-cm x 5-cm 110-cm SSD 15-MeV Profile



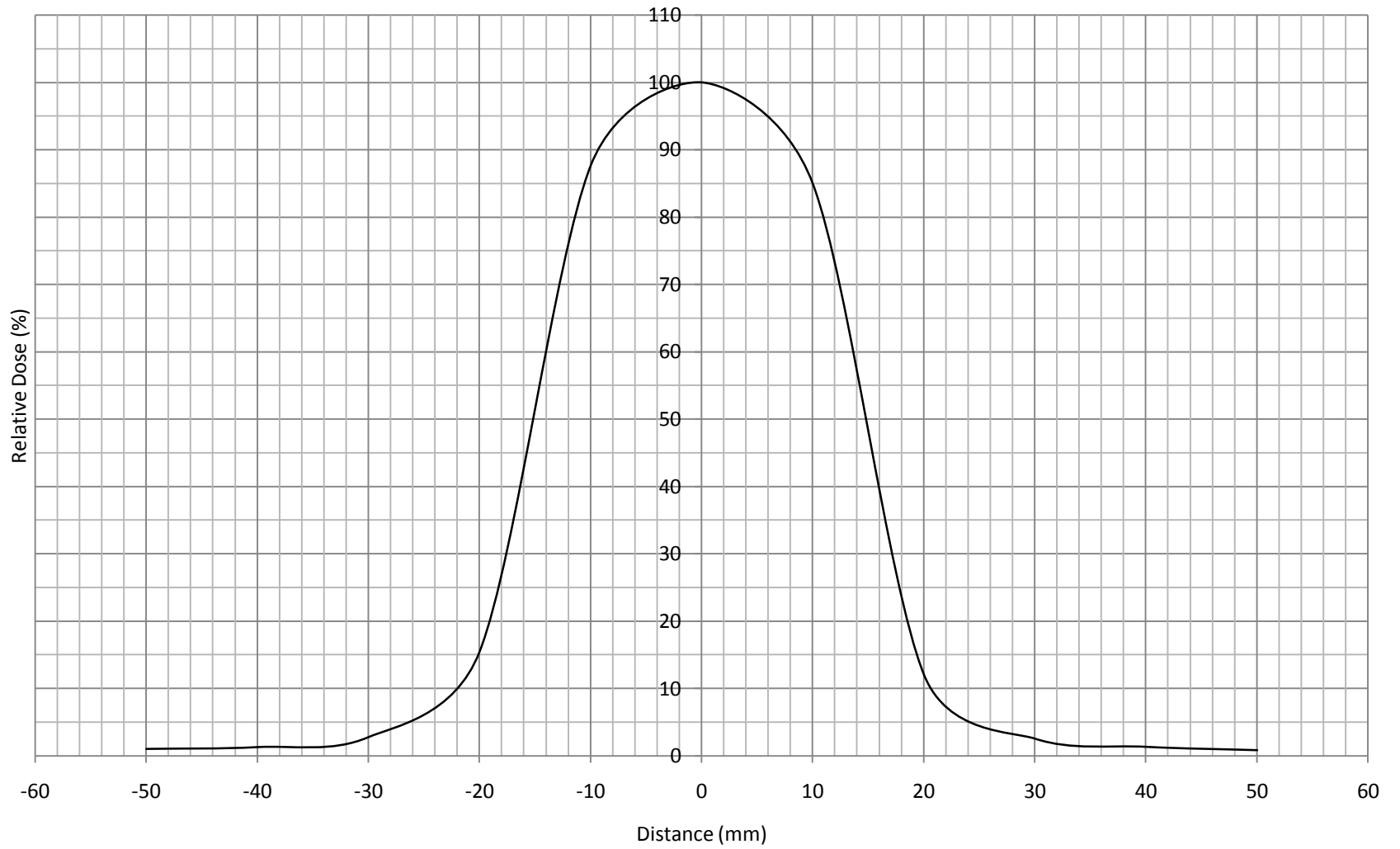
Appendix C

Beam Profiles of Small-Electron Circular Fields

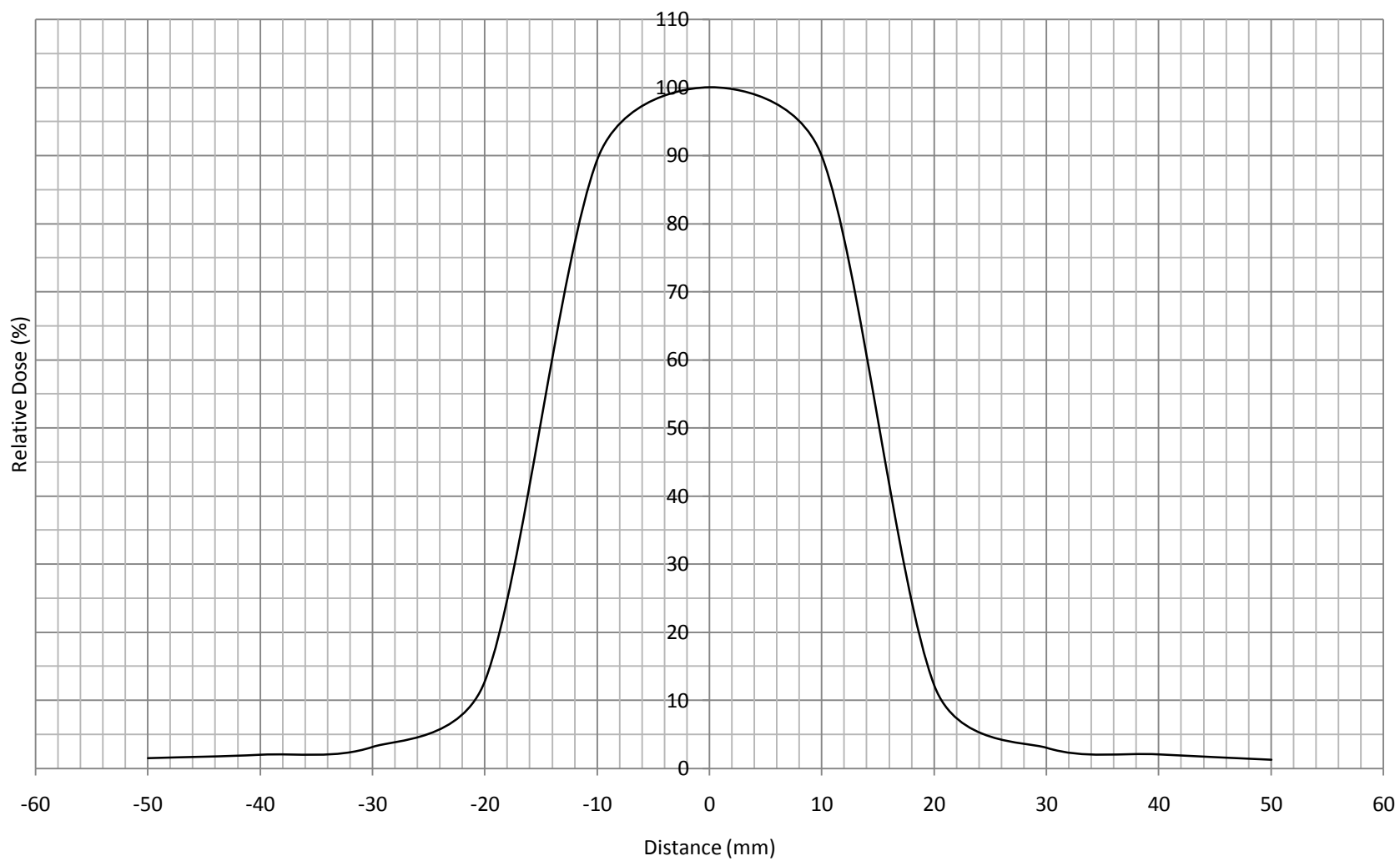
3-cm 100-cm SSD 6-MeV Profile



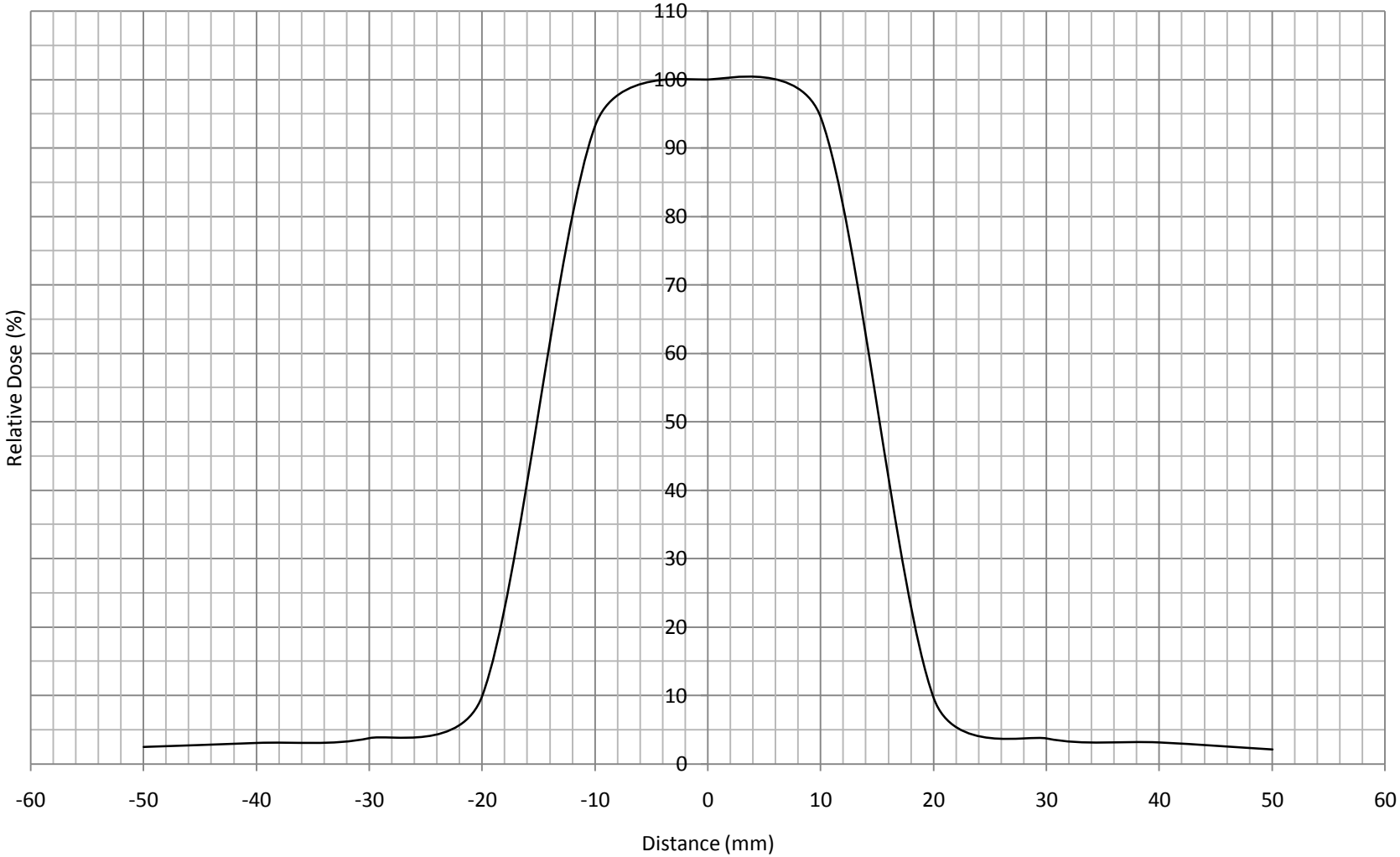
3-cm 100-cm SSD 9-MeV Profile



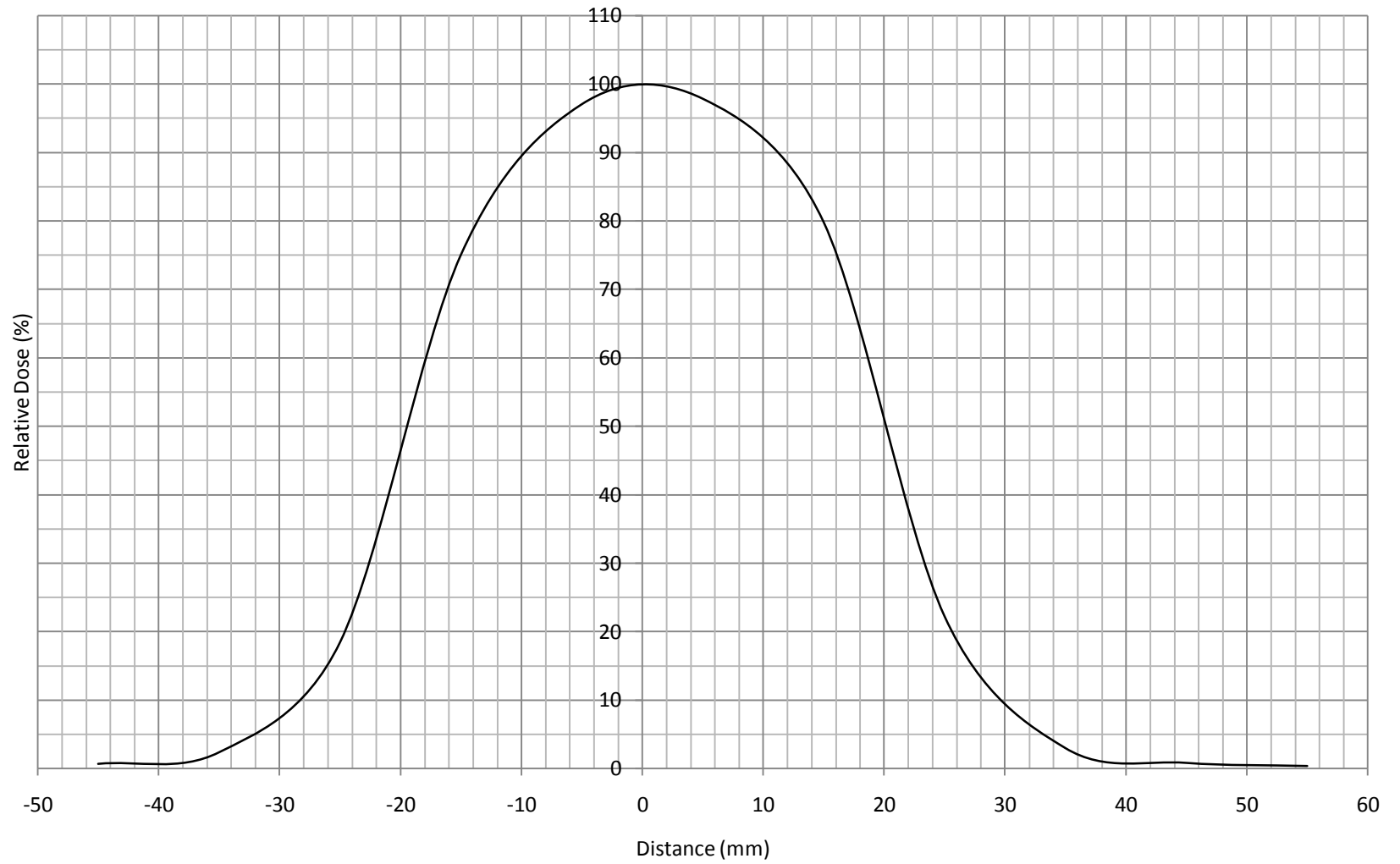
3-cm 100-cm SSD 12-MeV Profile



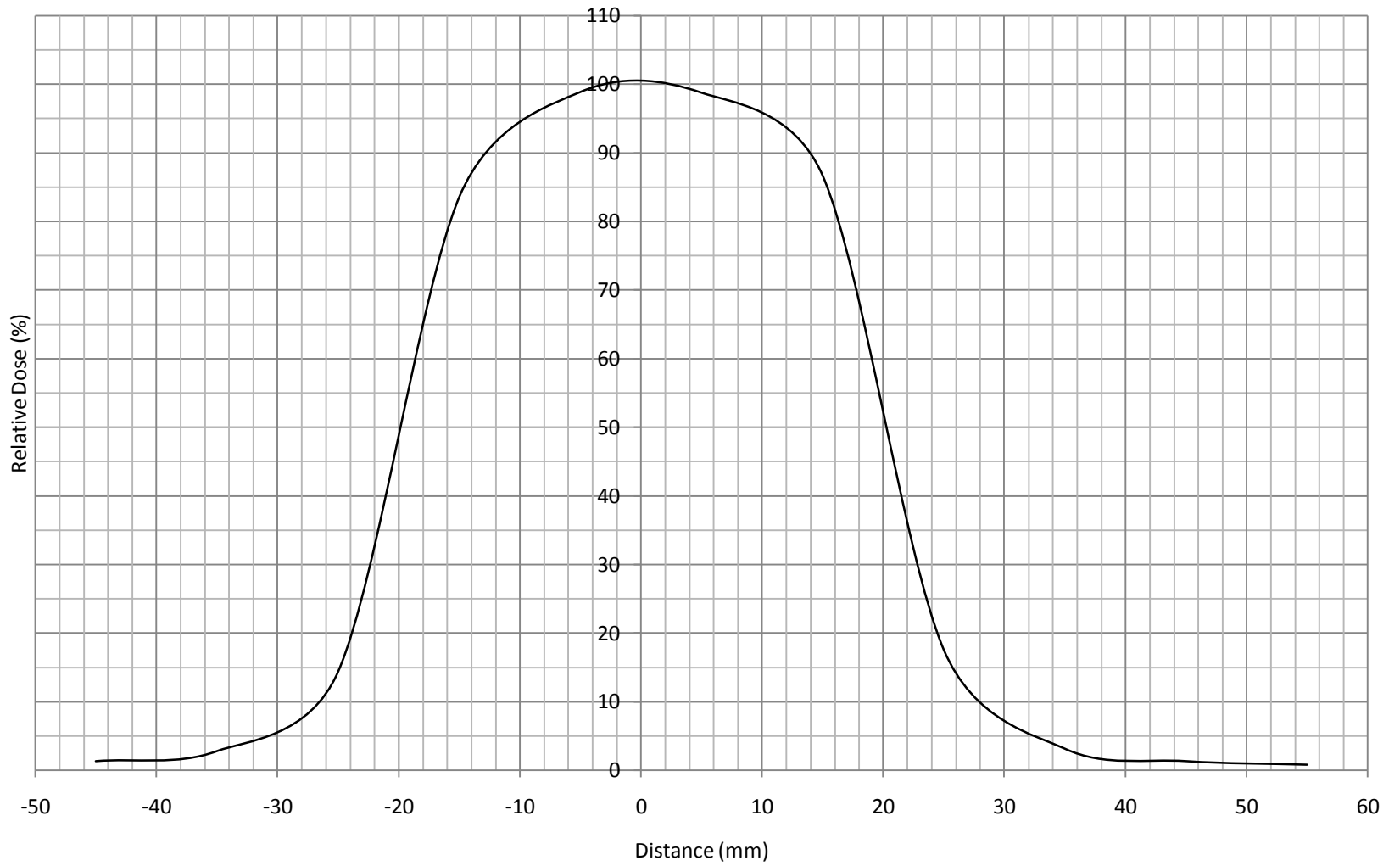
3-cm 100-cm SSD 15 -Profile



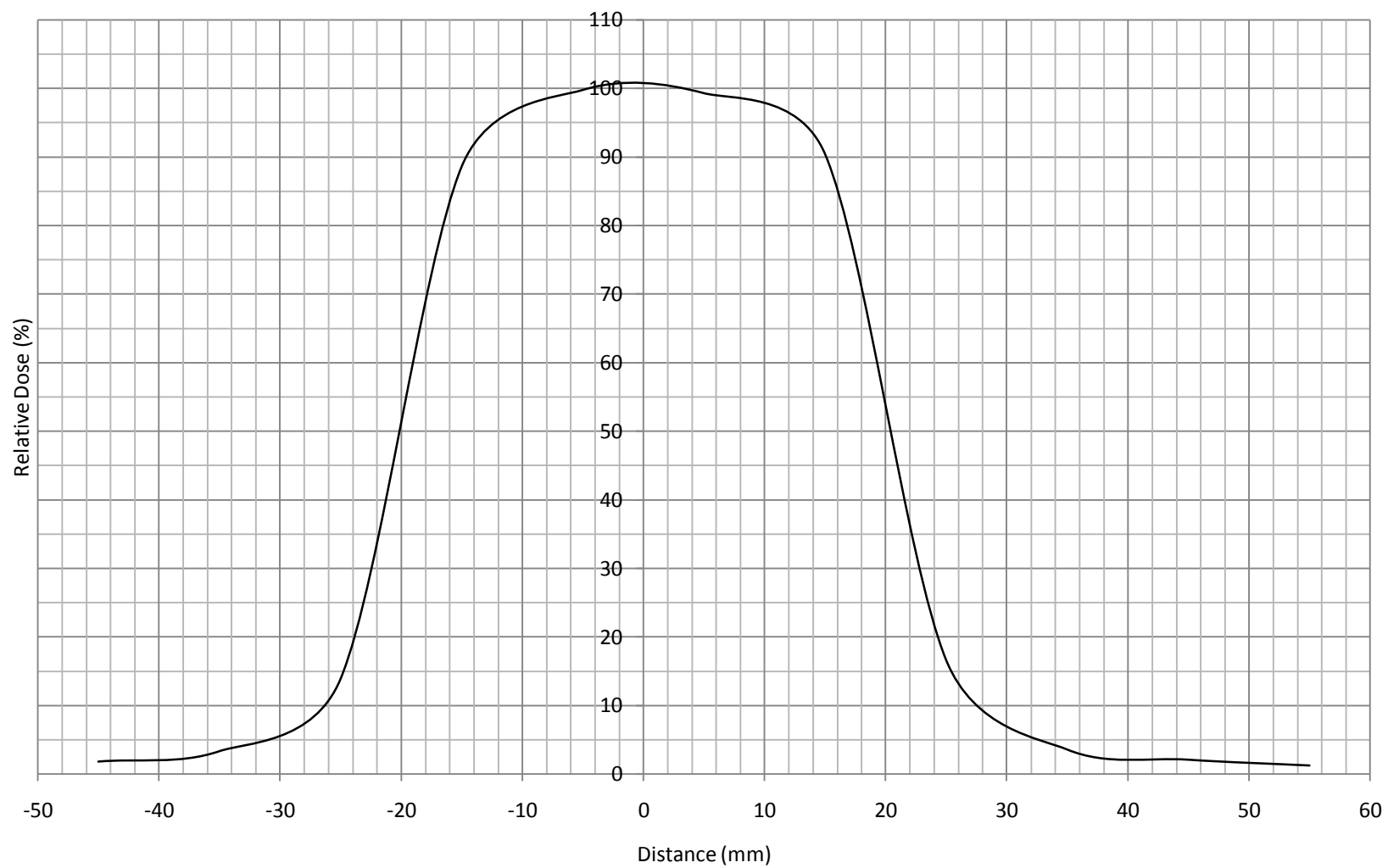
4-cm 100-cm SSD 6-MeV Profile



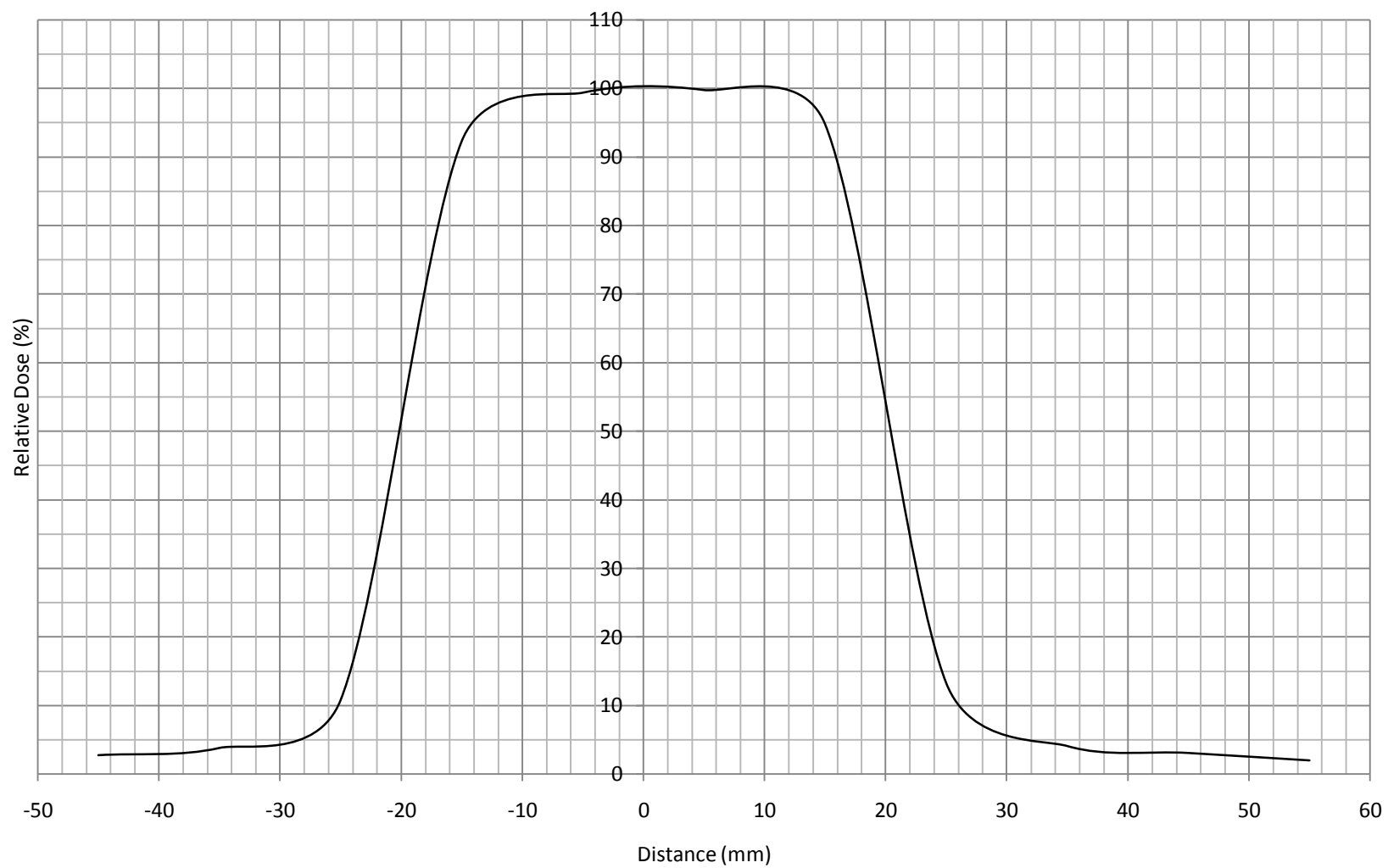
4-cm 100-cm SSD 9-MeV Profile



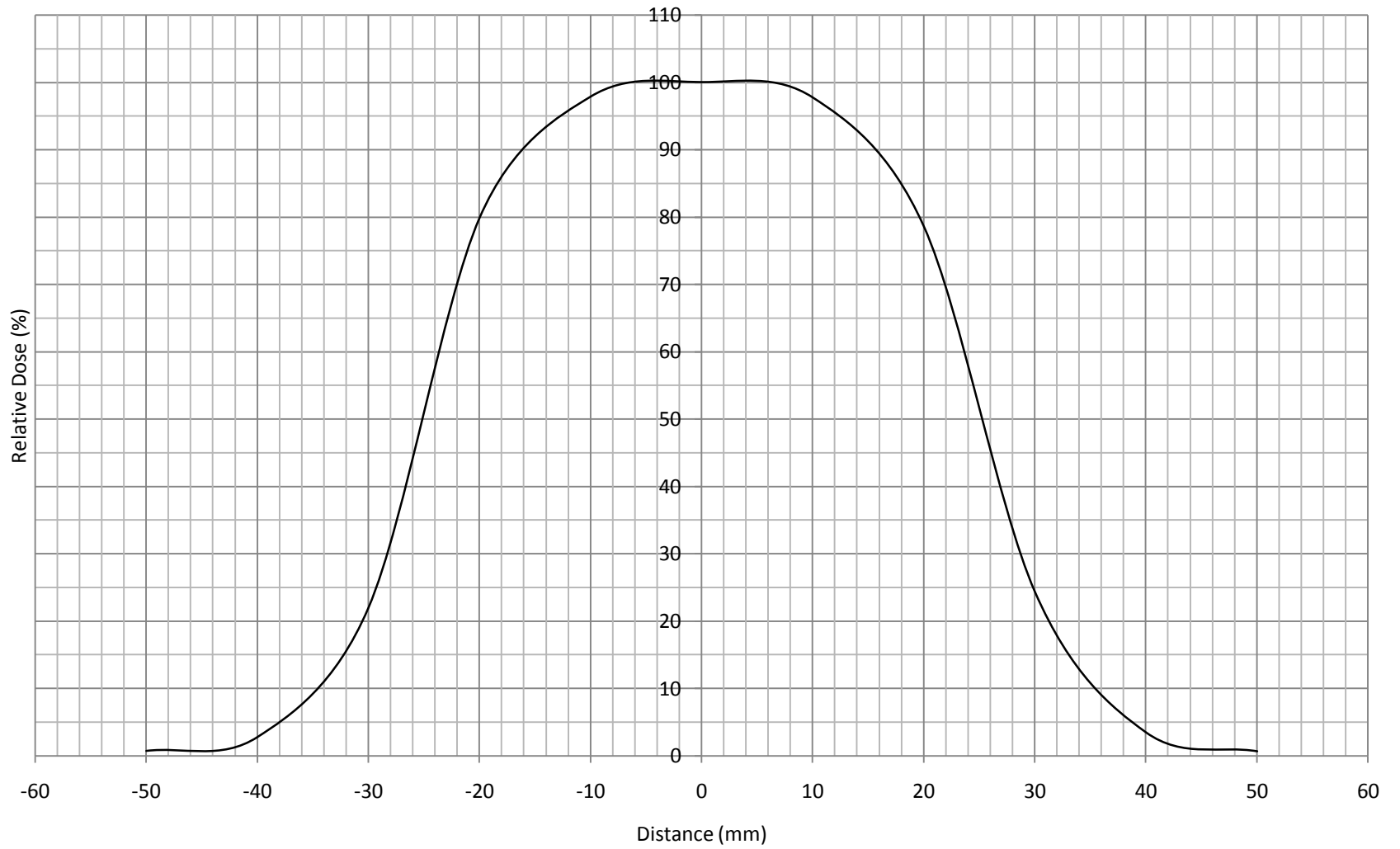
4-cm 100-cm SSD 12-MeV Profile



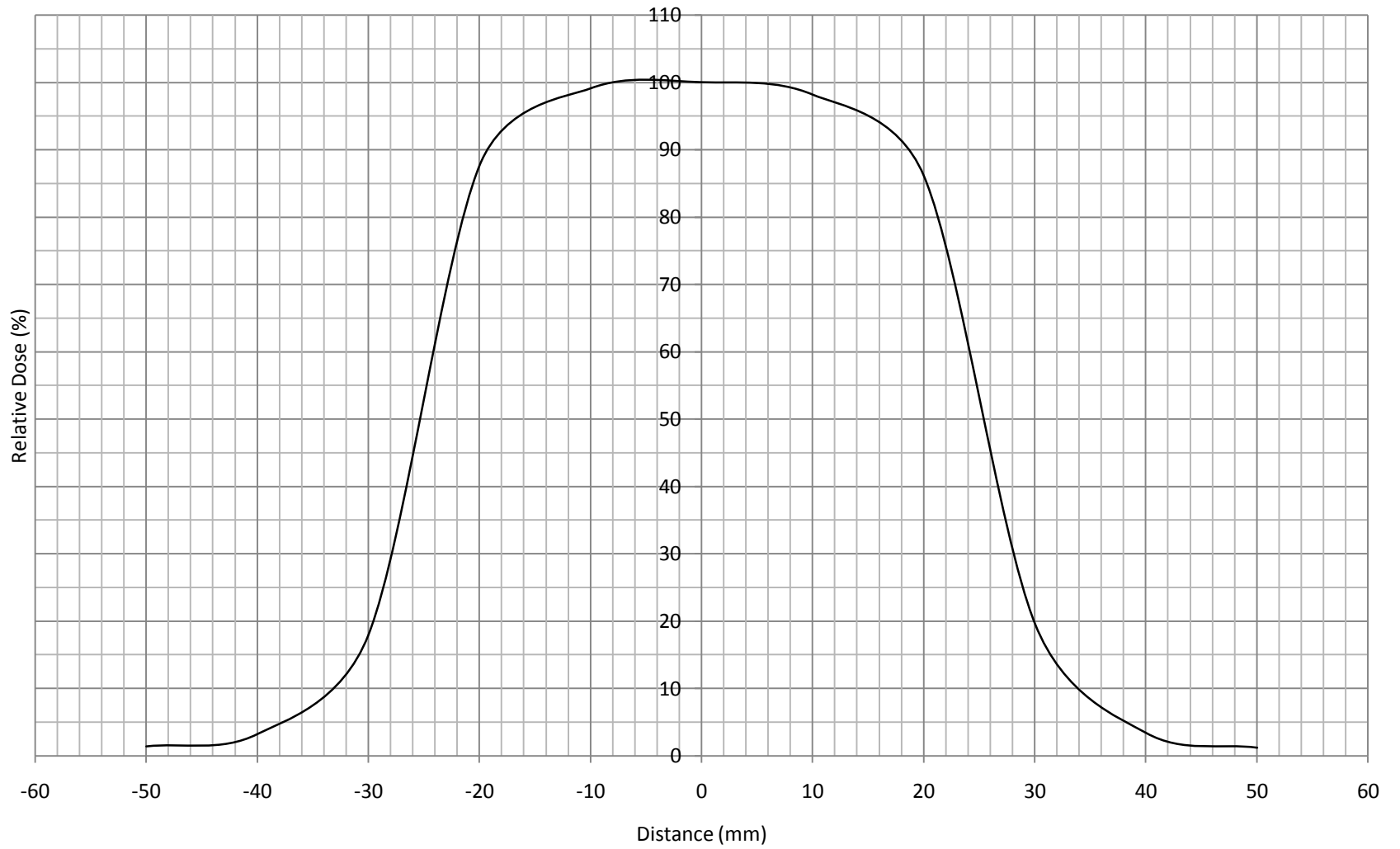
4-cm 100-cm SSD 15-MeV Profile



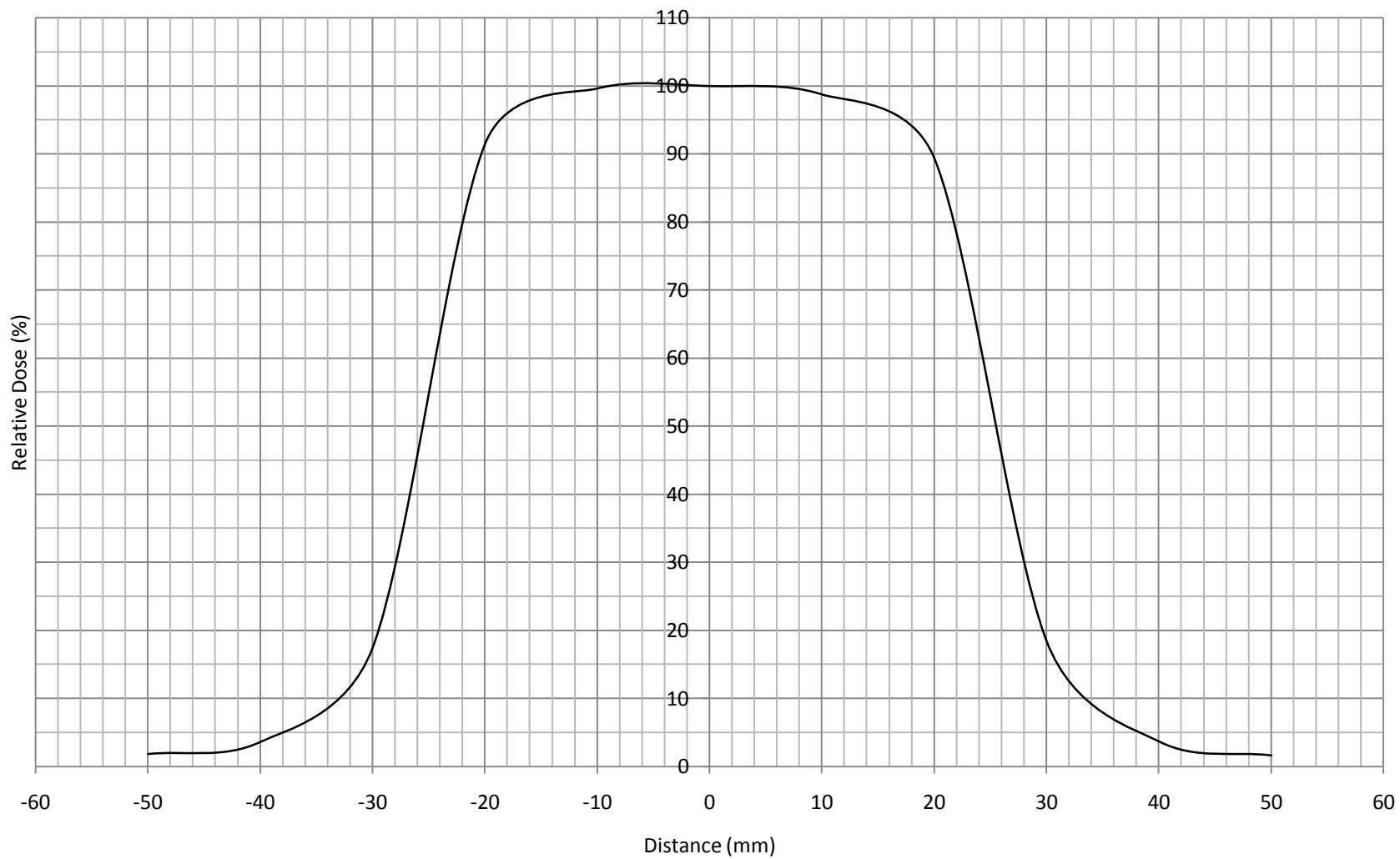
5-cm 100-cm SSD 6-MeV Profile



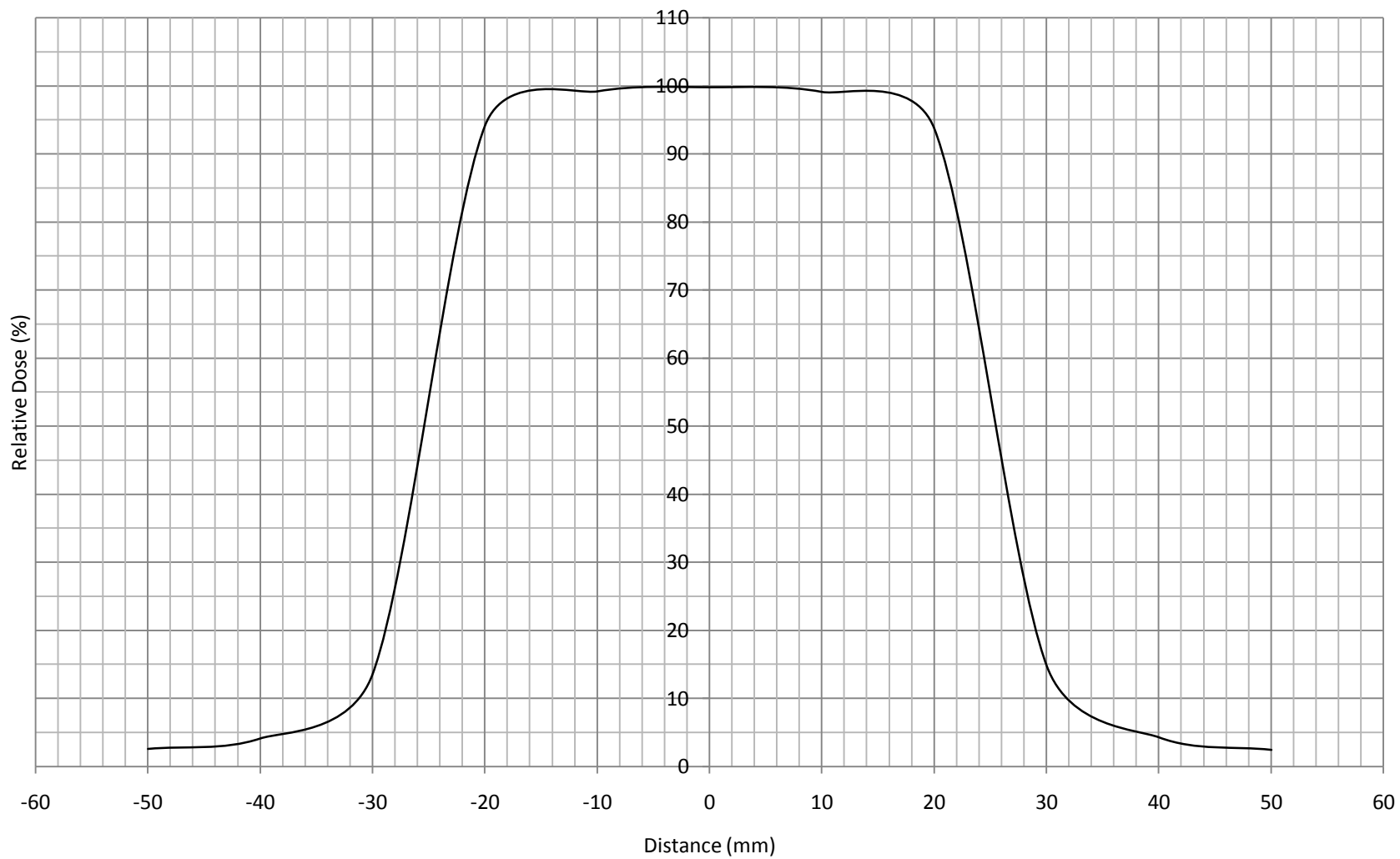
5-cm 100-cm SSD 9-MeV Profile



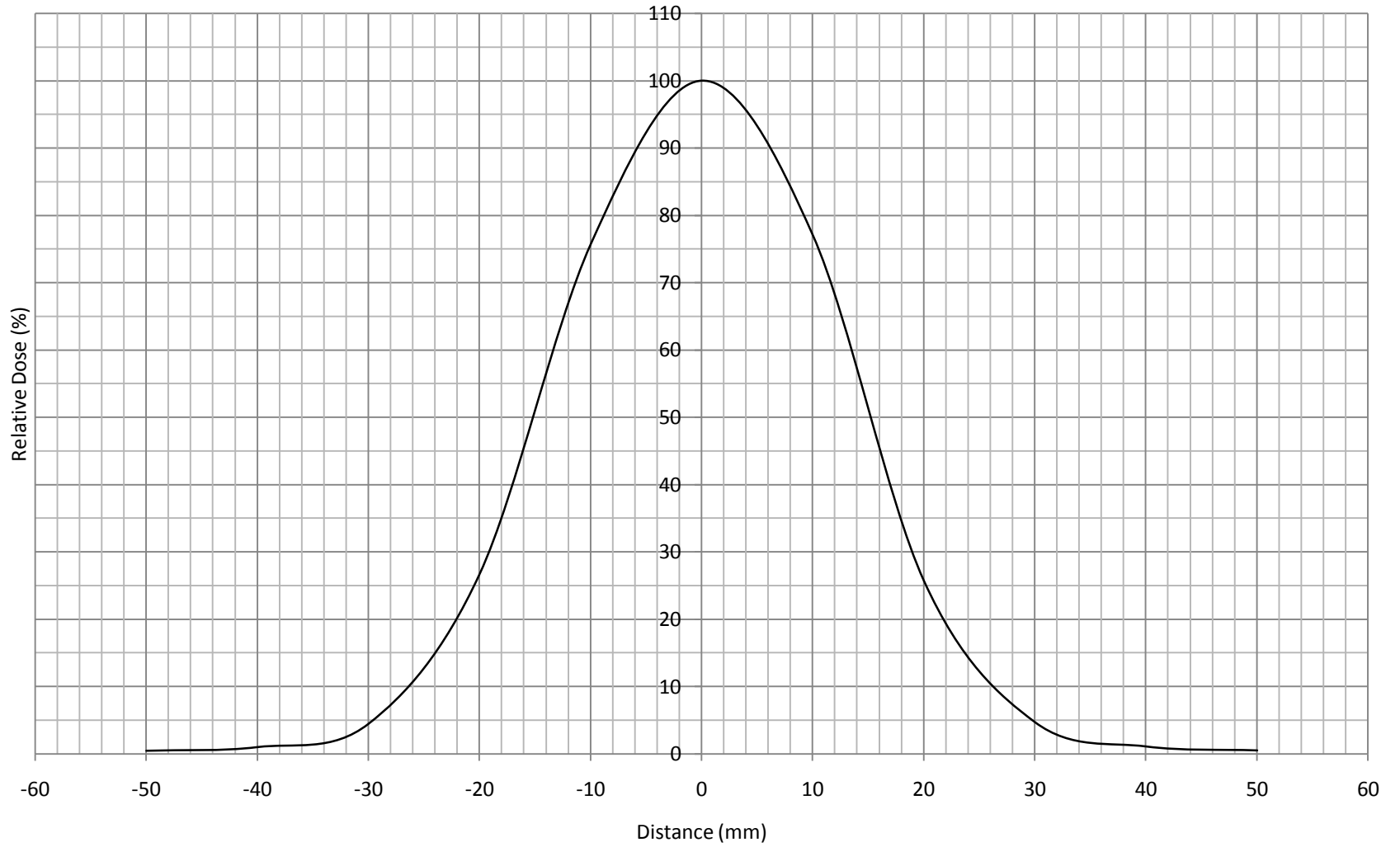
5-cm 100-cm SSD 12-MeV Profile



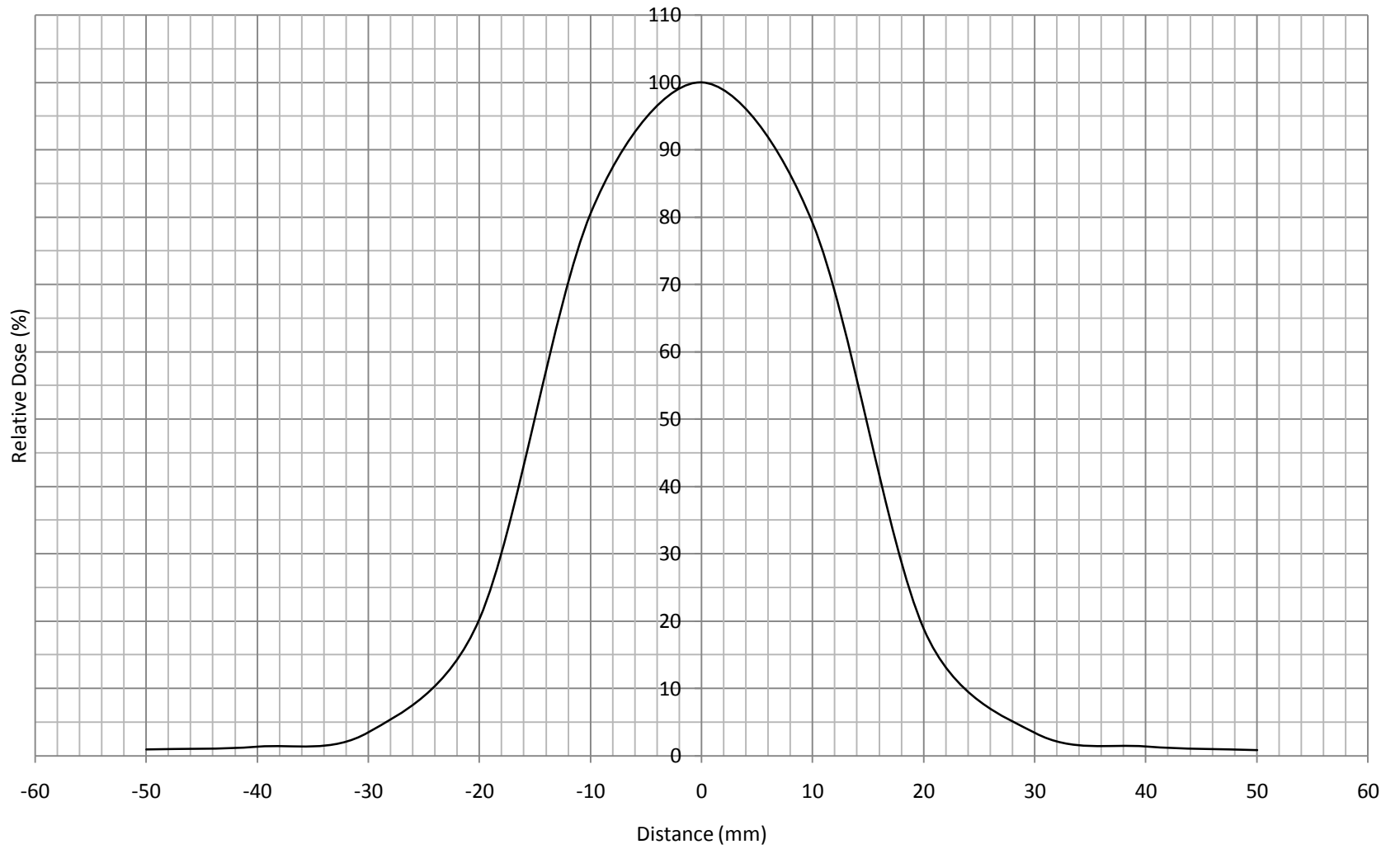
5-cm 100-cm SSD 15-MeV Profile



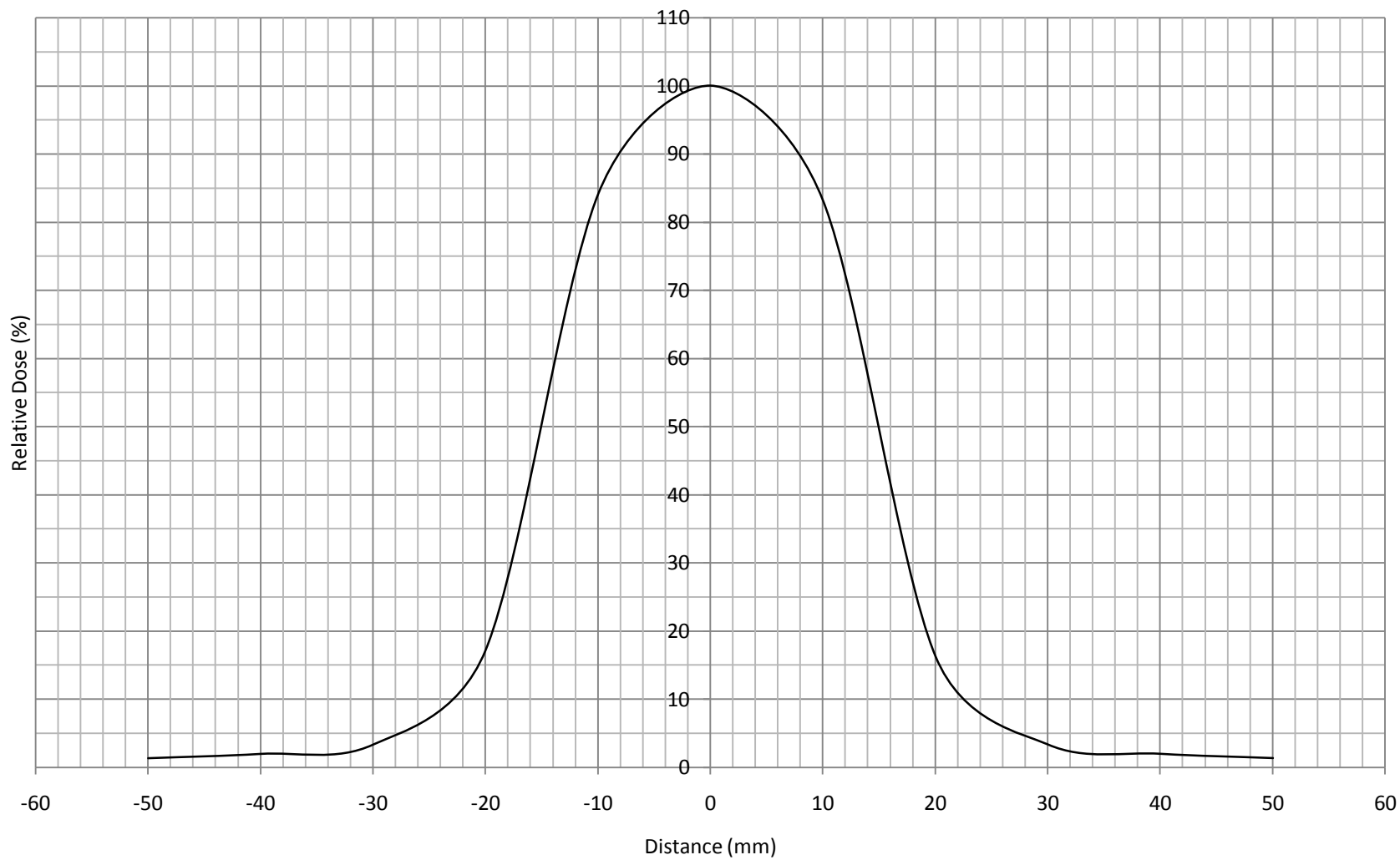
3-cm 105-cm SSD 6-MeV Profile



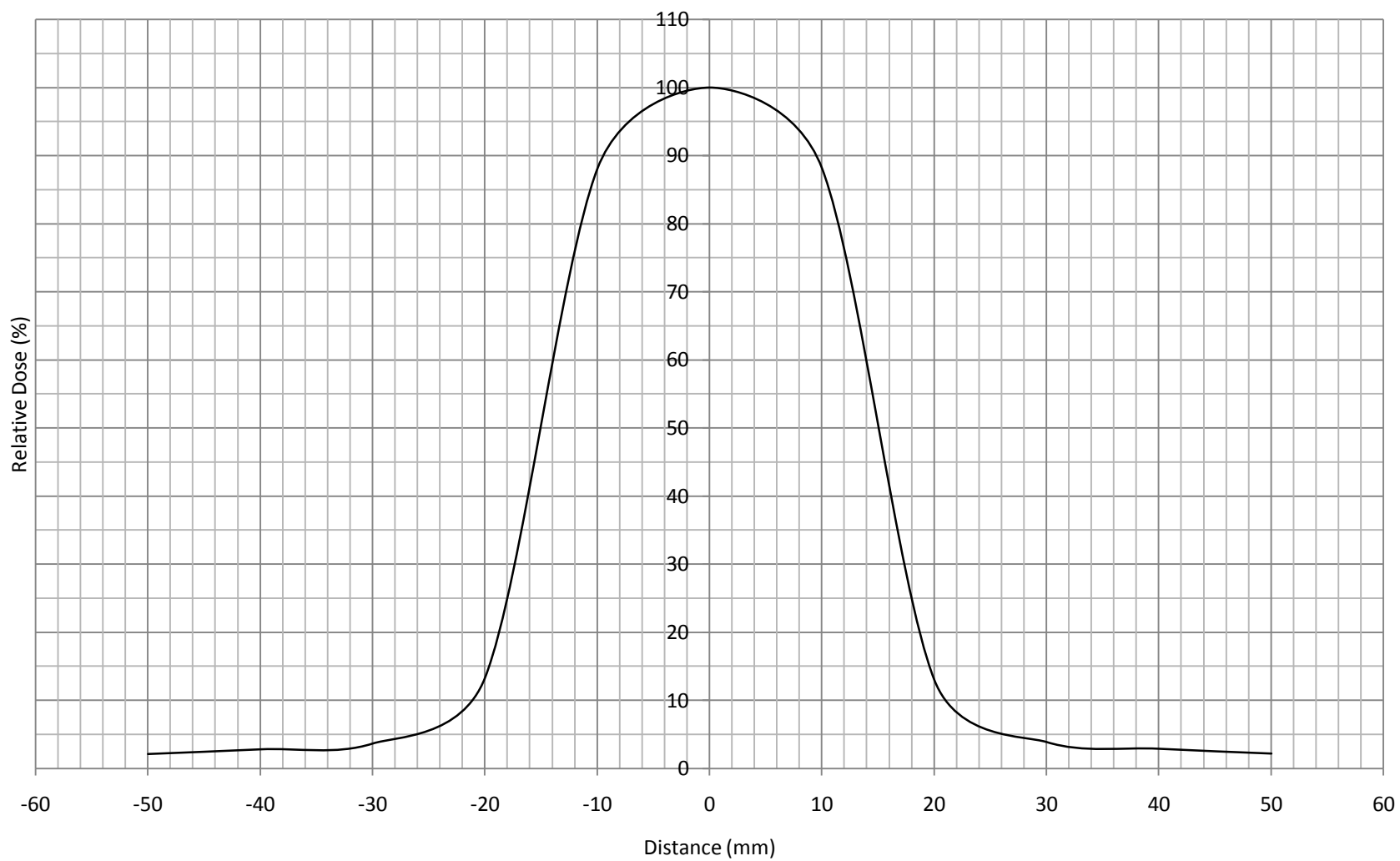
3-cm 105-cm SSD 9-MeV Profile



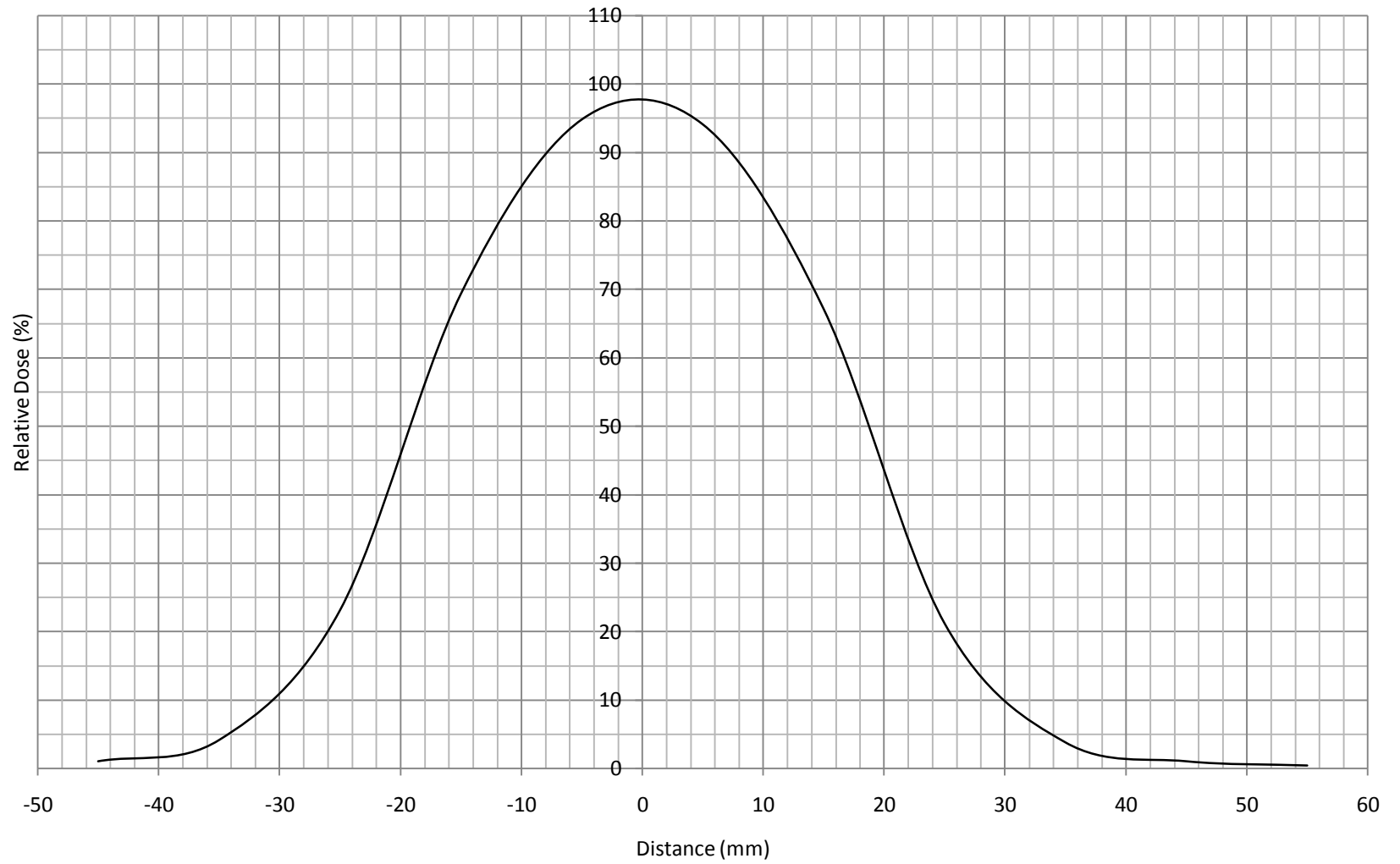
3-cm 105-cm SSD 12-MeV Profile



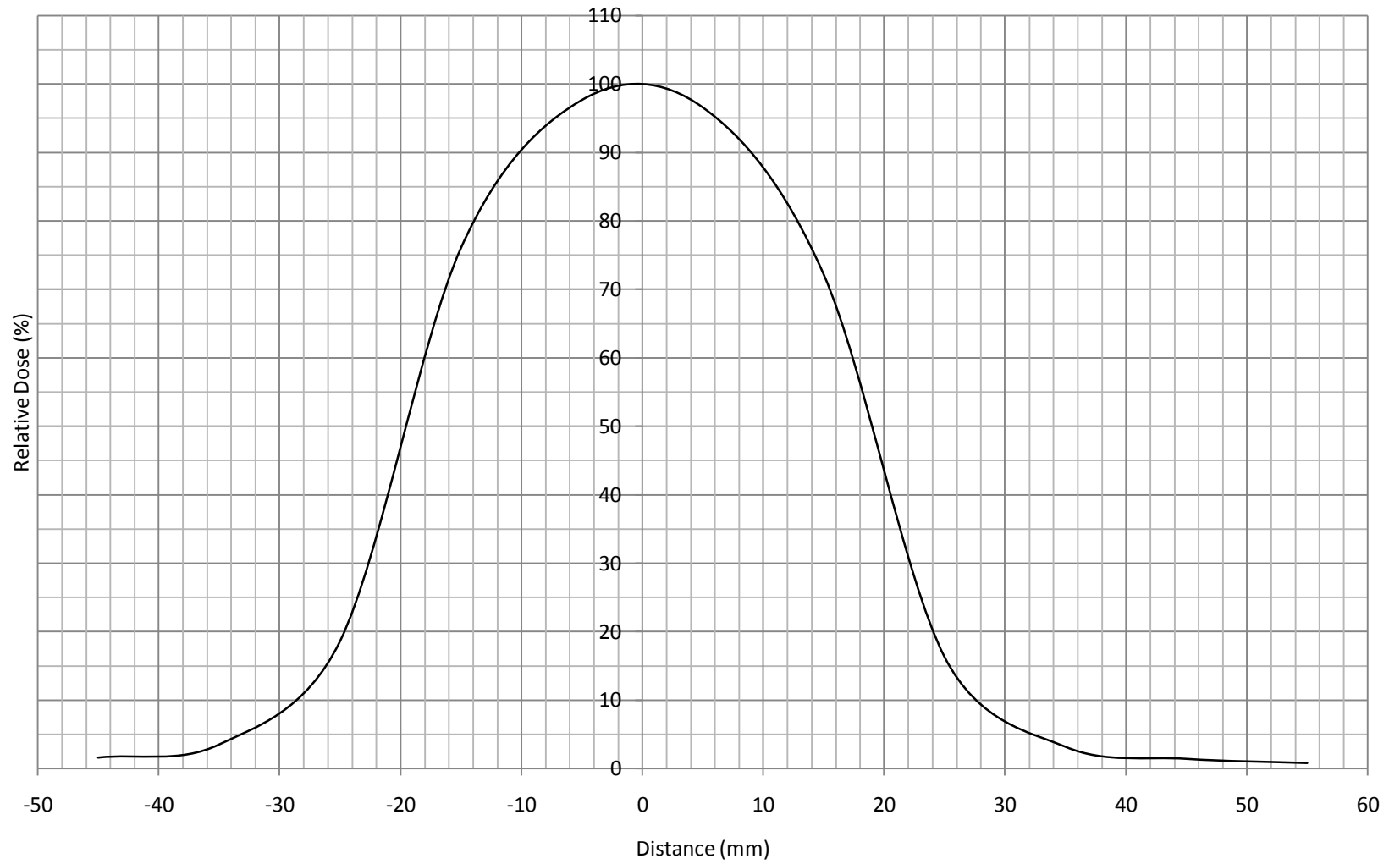
3-cm 105-cm SSD 15-MeV Profile



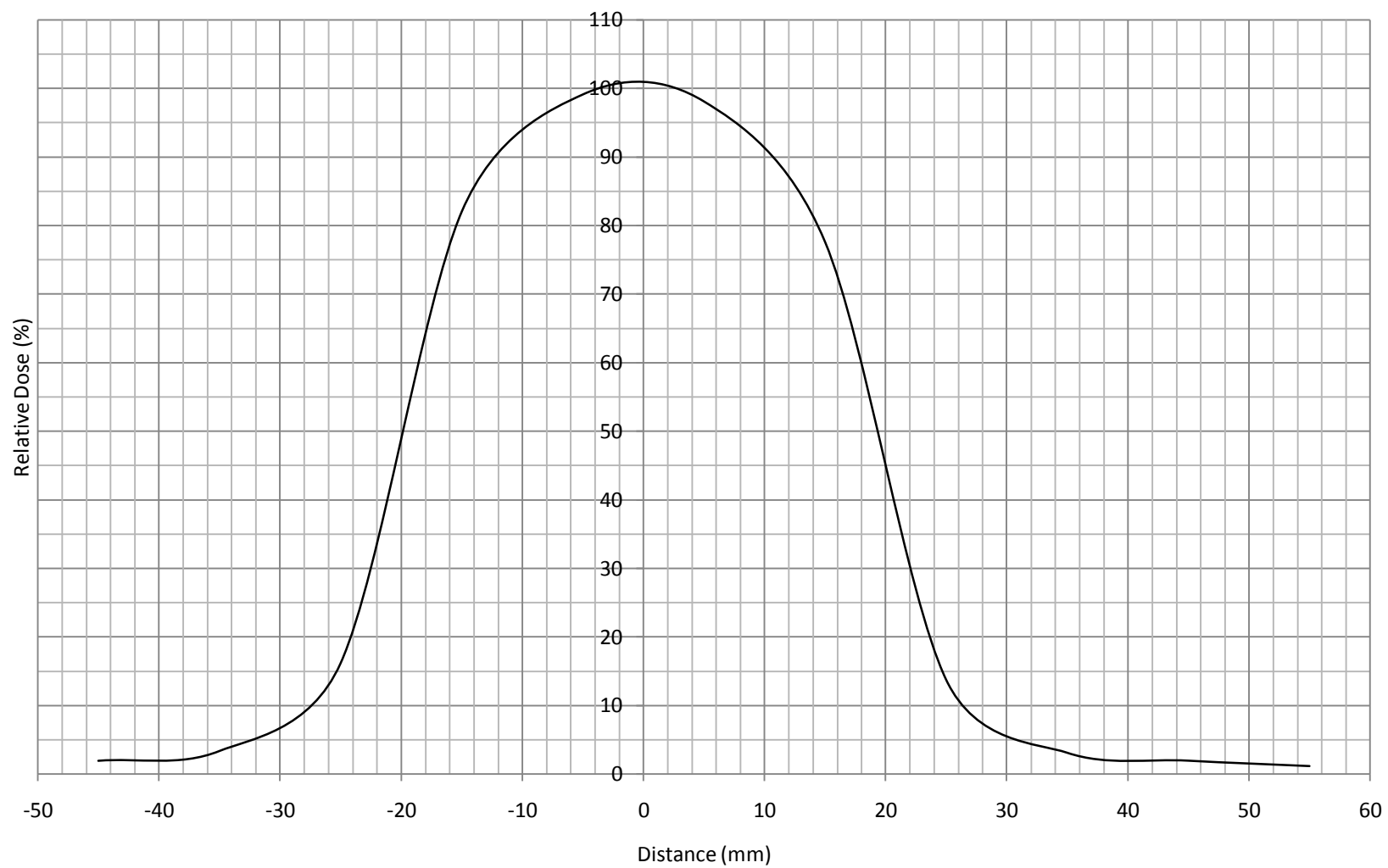
4-cm 105-cm SSD 6-MeV Profile



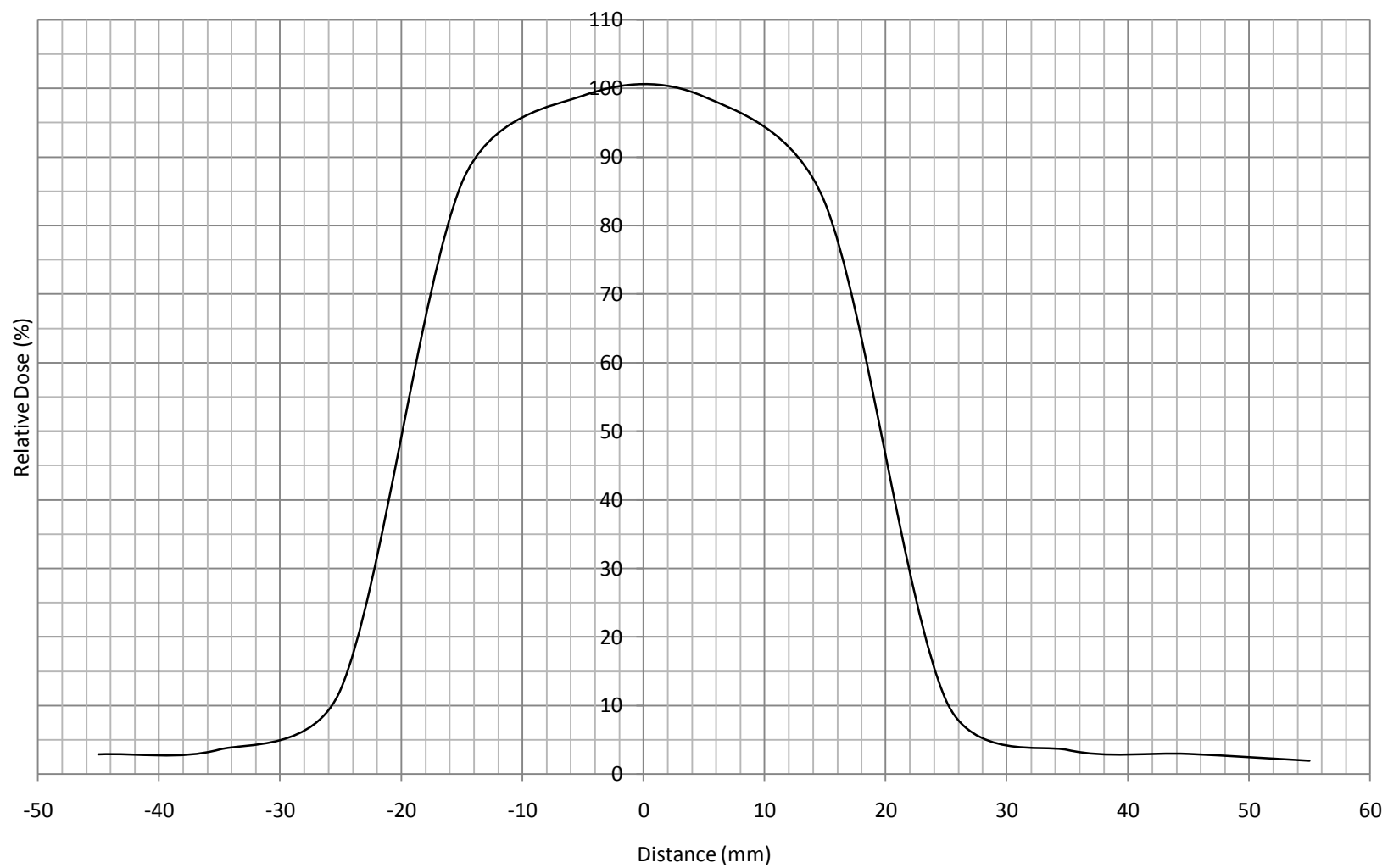
4-cm 105-cm SSD 9-MeV Profile



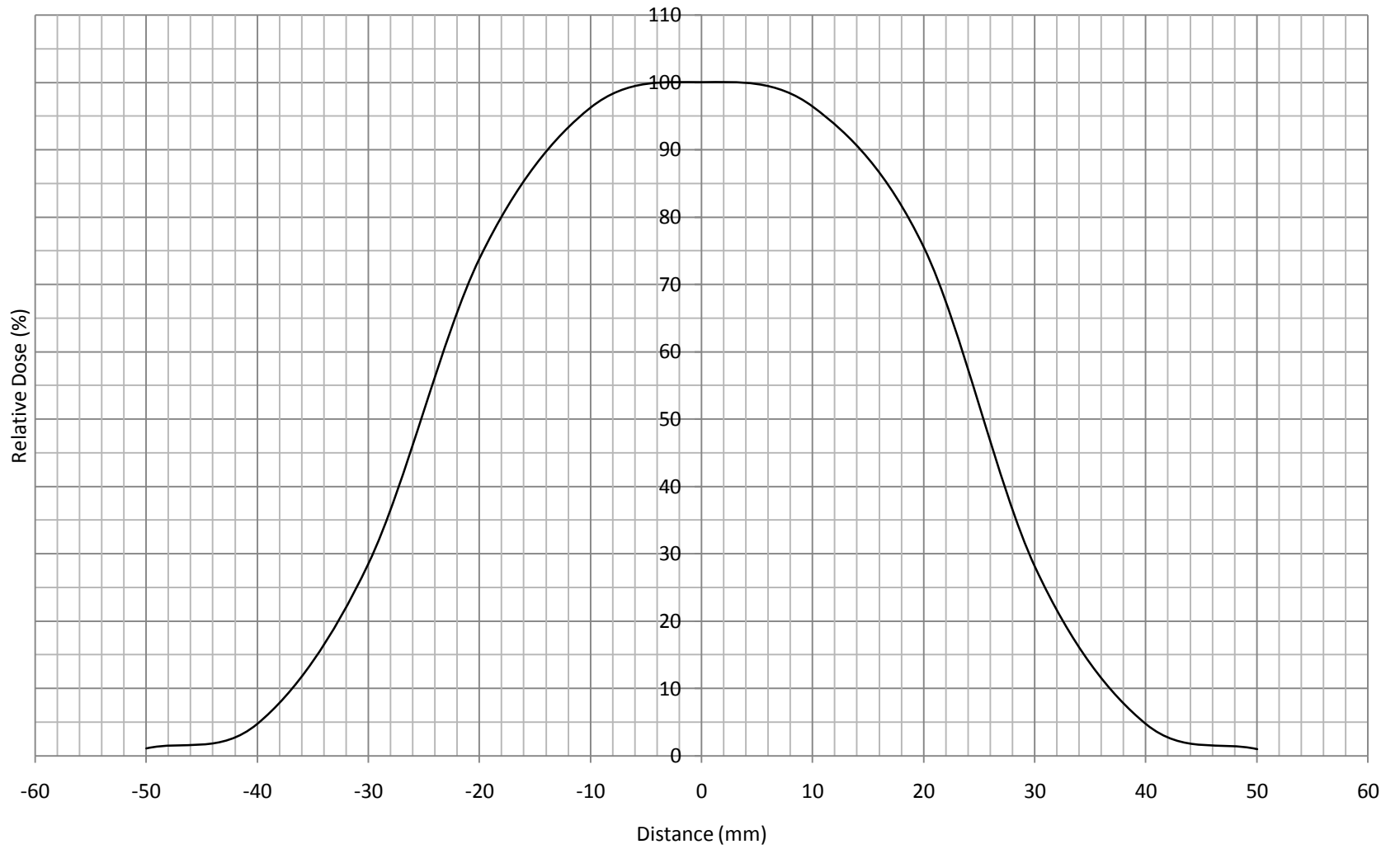
4-cm 105-cm SSD 12-MeV Profile



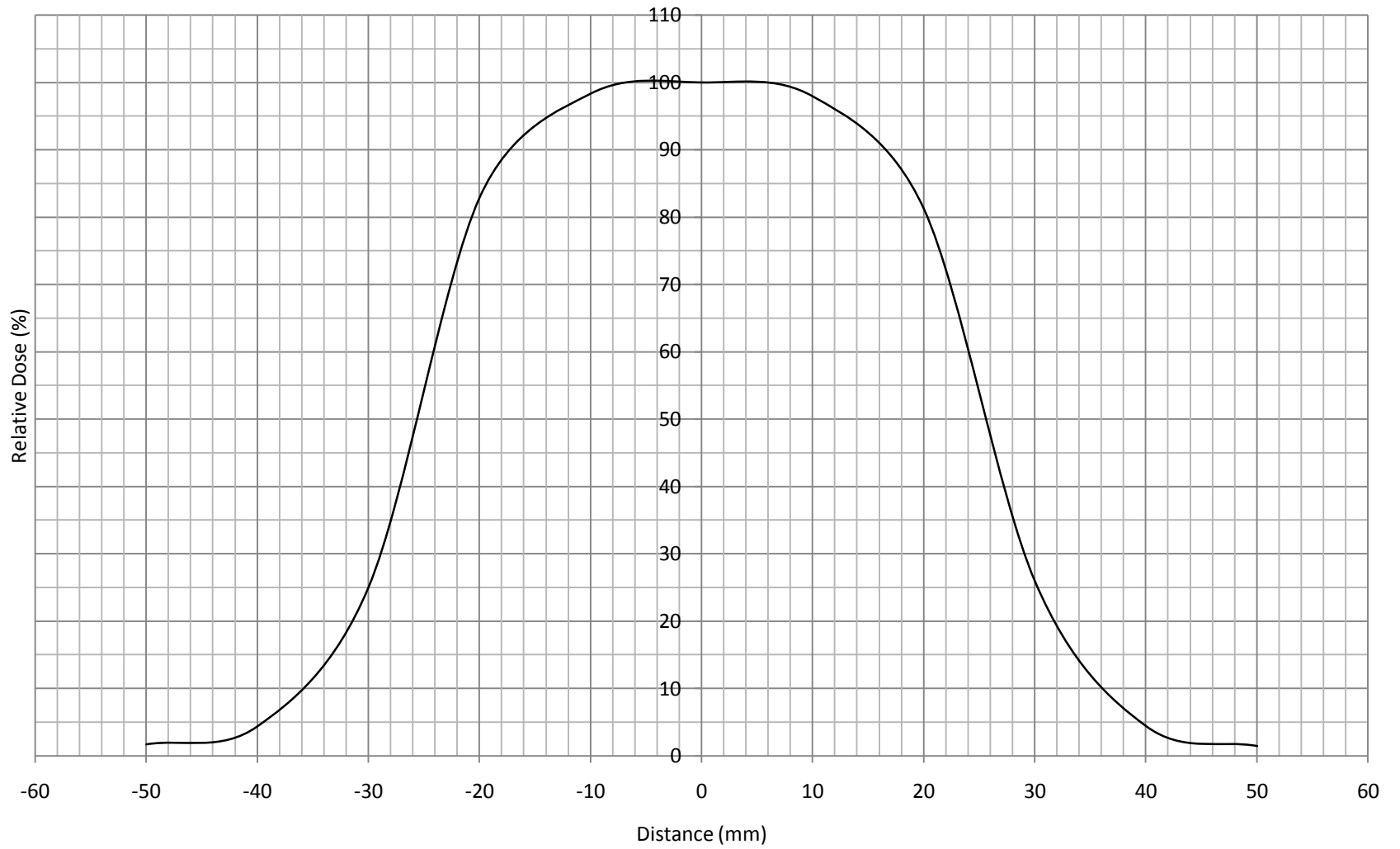
4-cm 105-cm SSD 15-MeV Profile



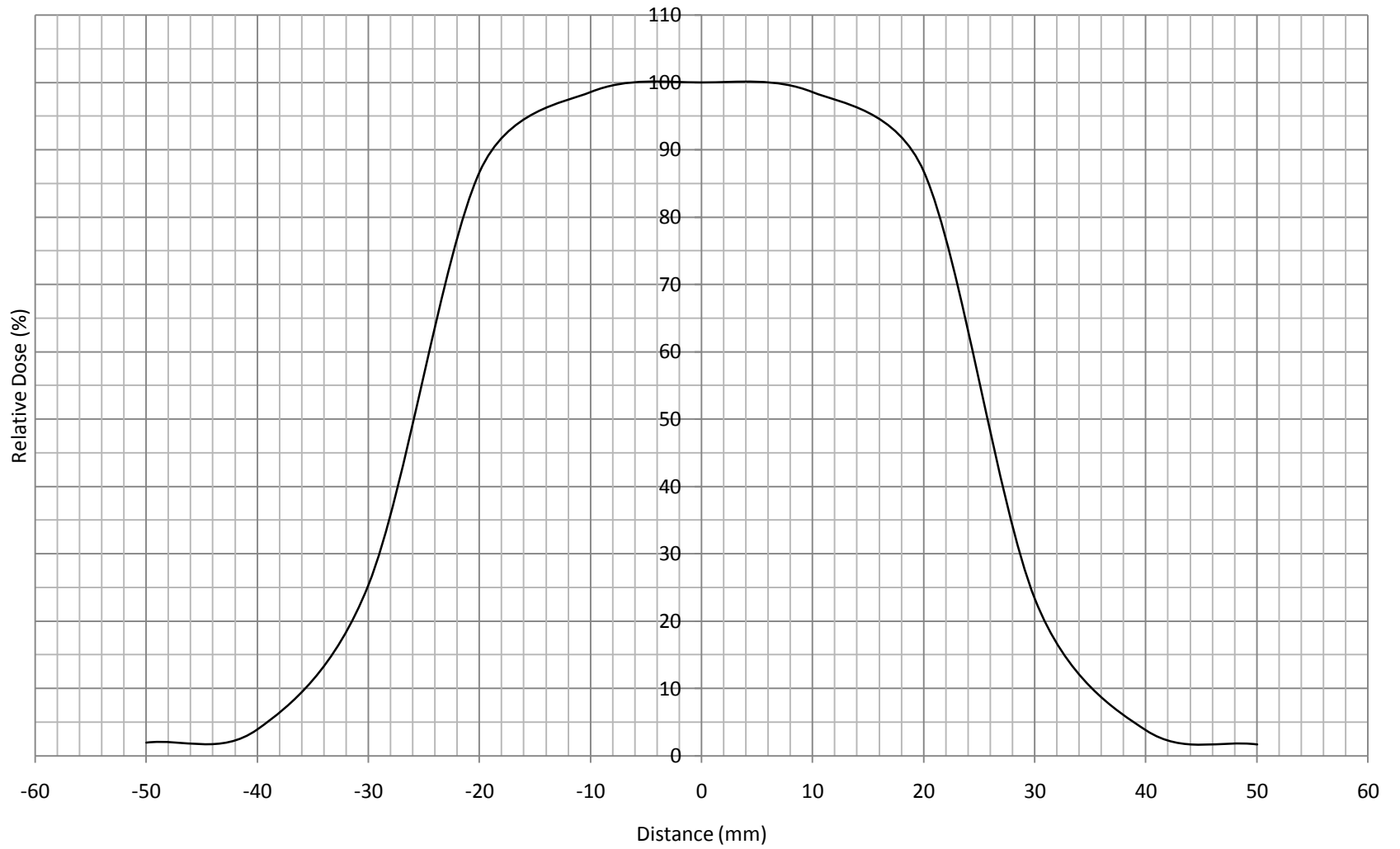
5-cm 105-cm SSD 6-MeV Profile



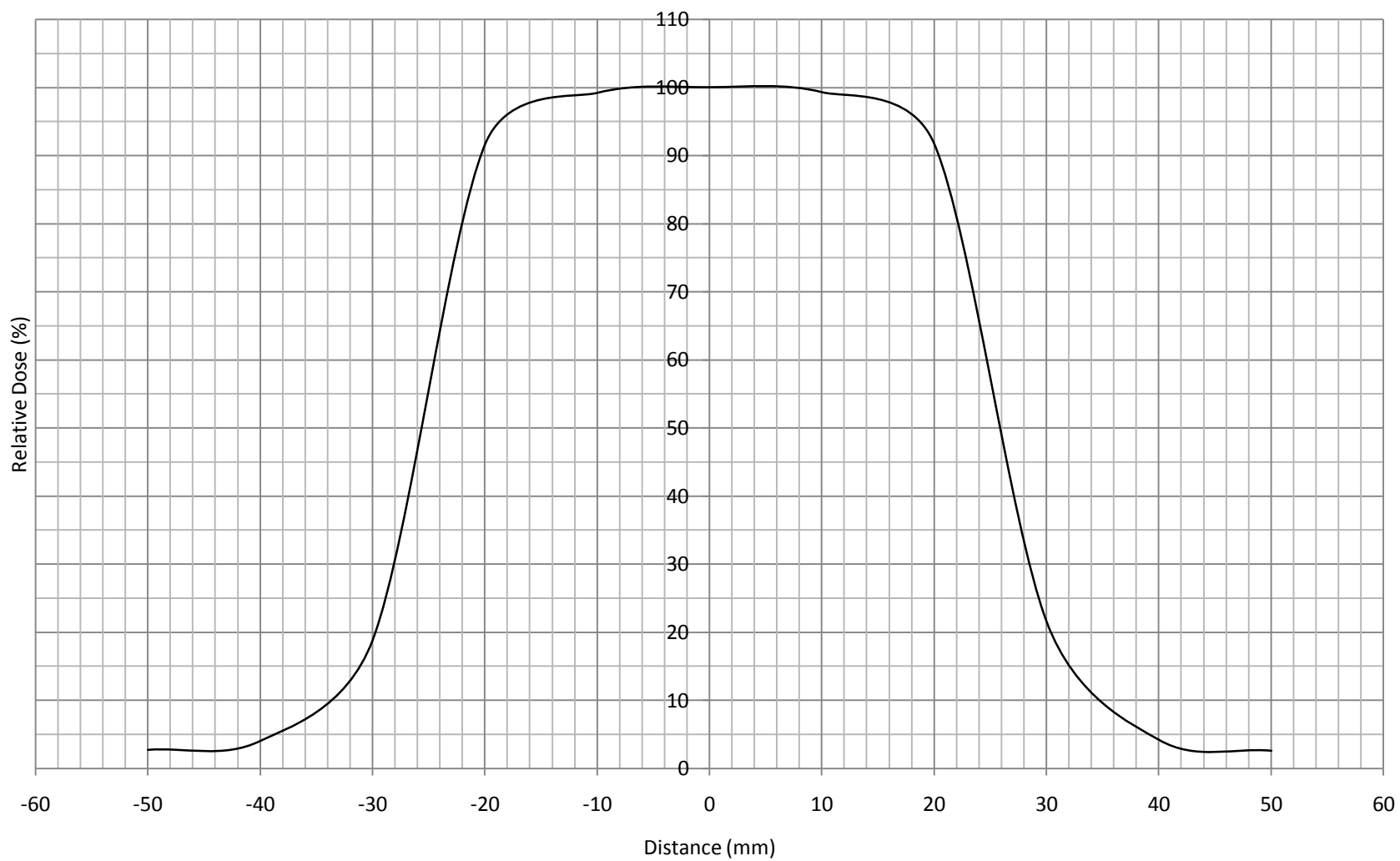
5-cm 105-cm SSD 9-MeV Profile



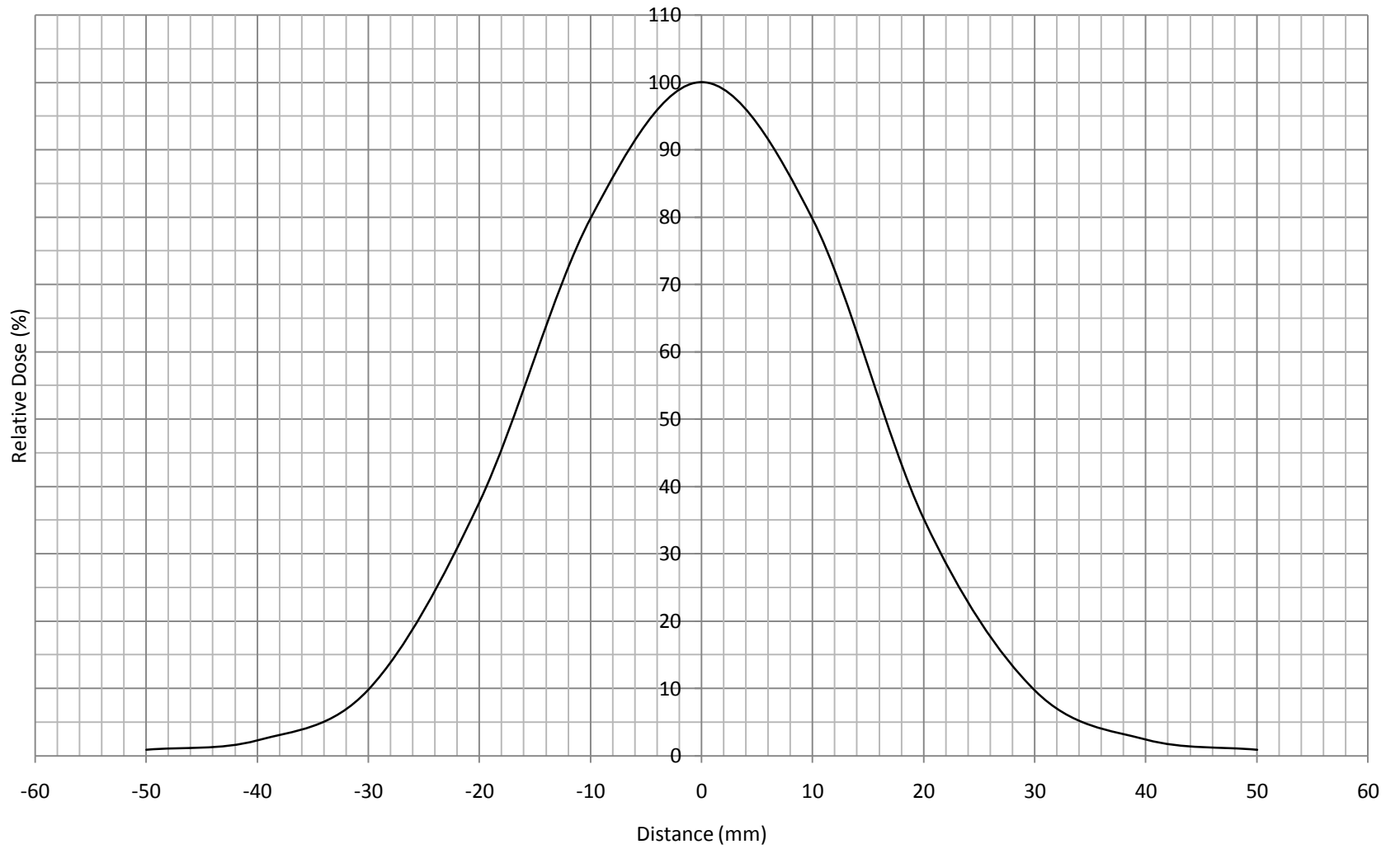
5-cm 105-cm SSD 12-MeV Profile



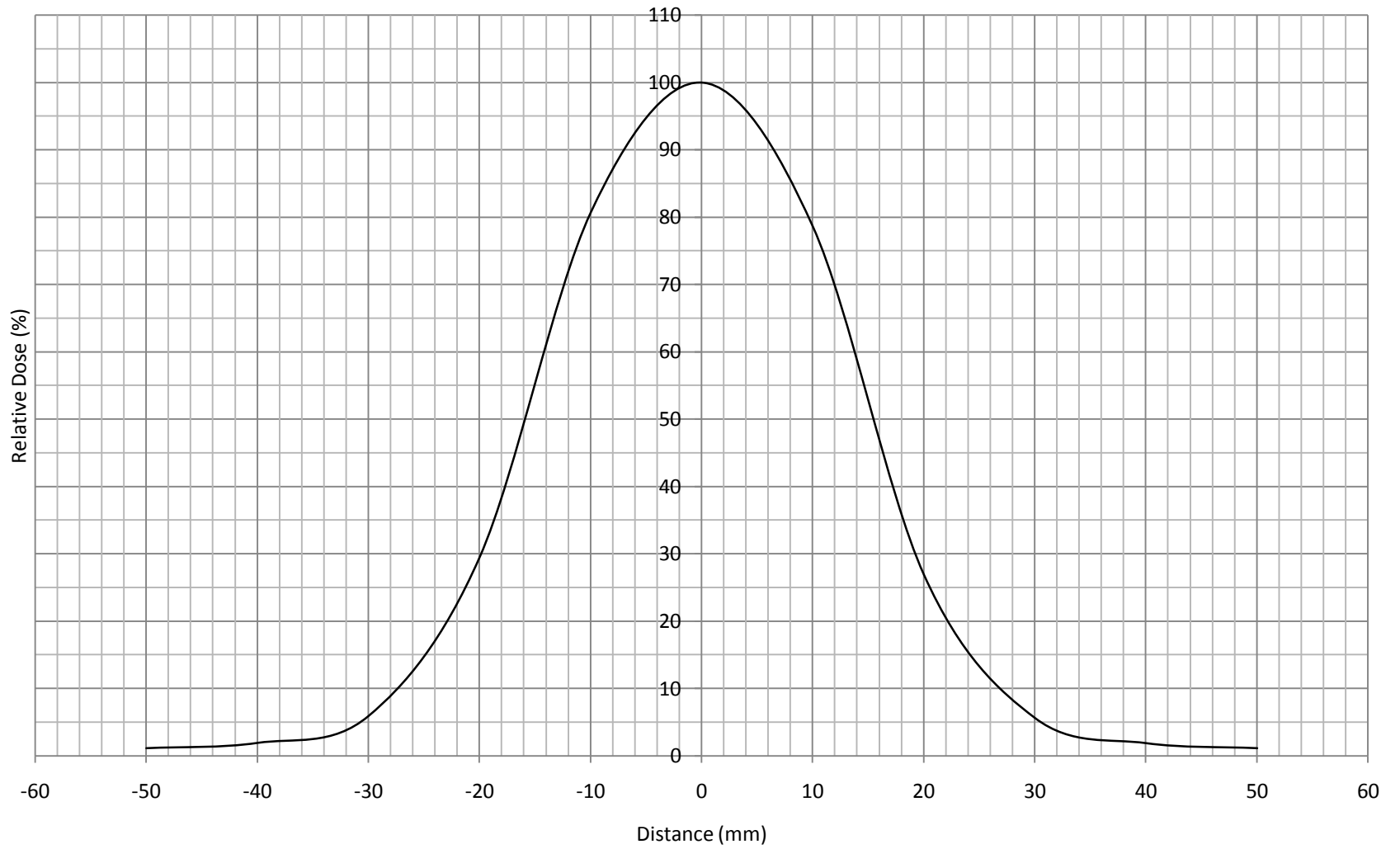
5-cm 105-cm SSD 15-MeV Profile



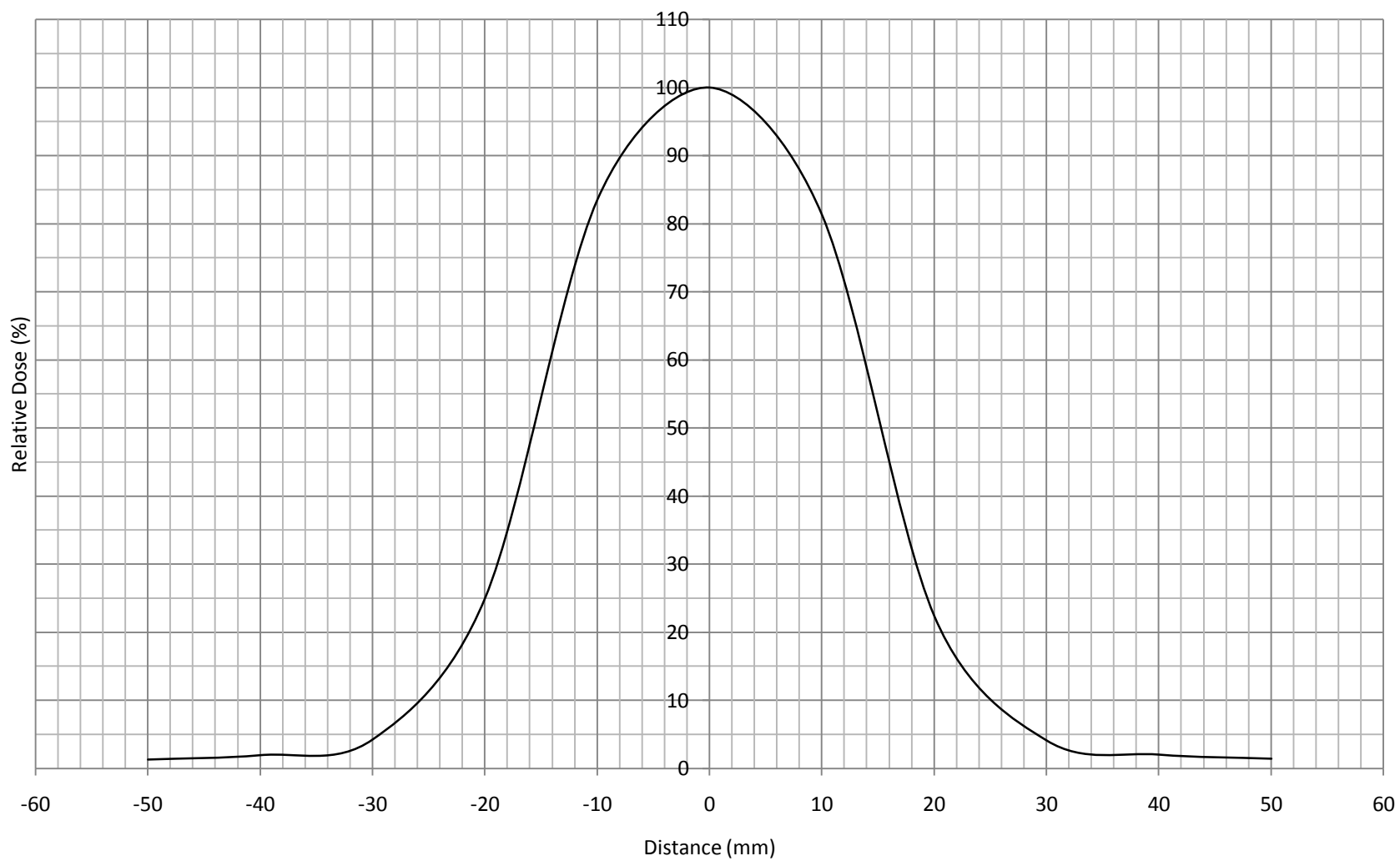
3-cm 110-cm SSD 6-MeV Profile



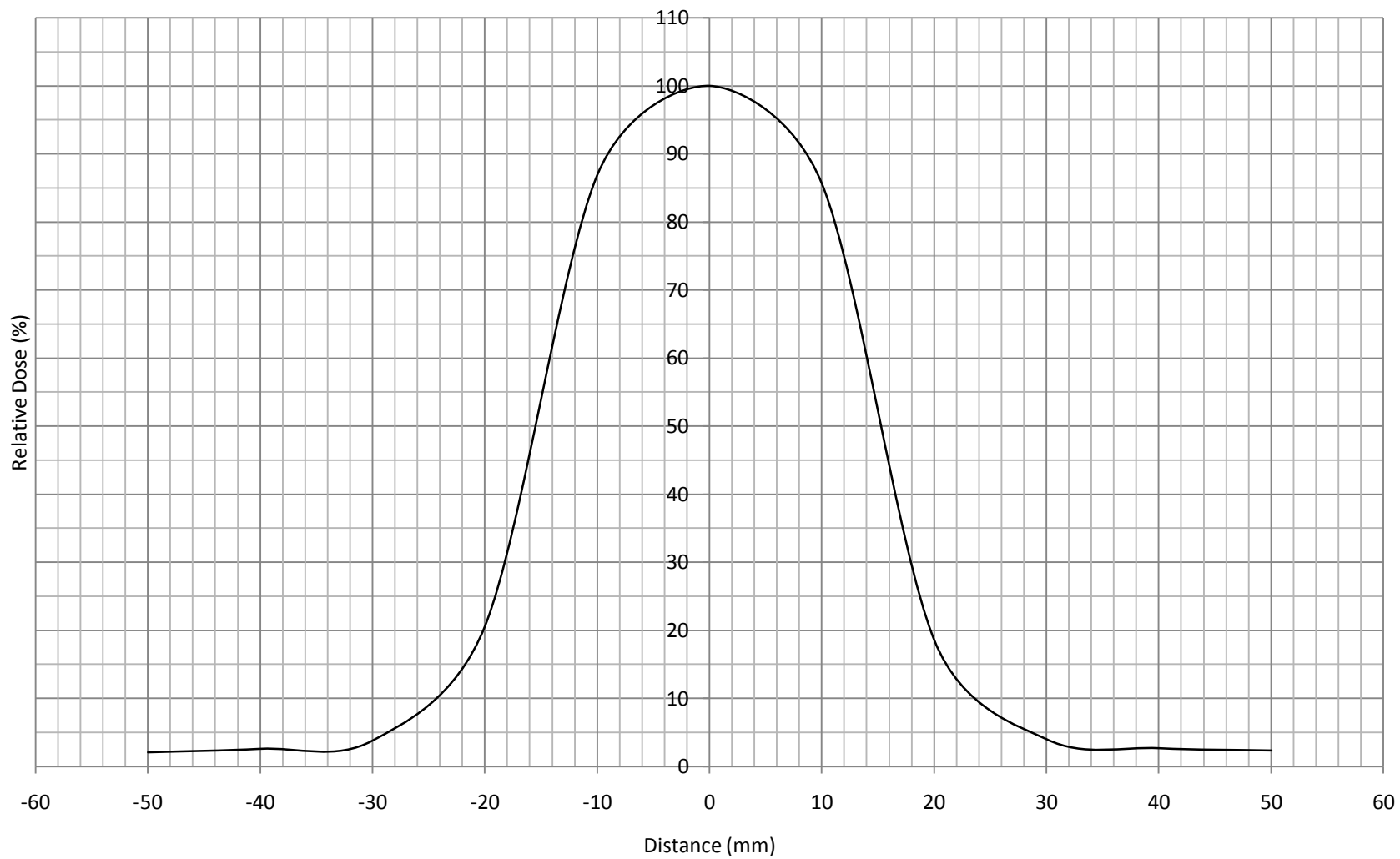
3-cm 110-cm SSD 9-MeV Profile



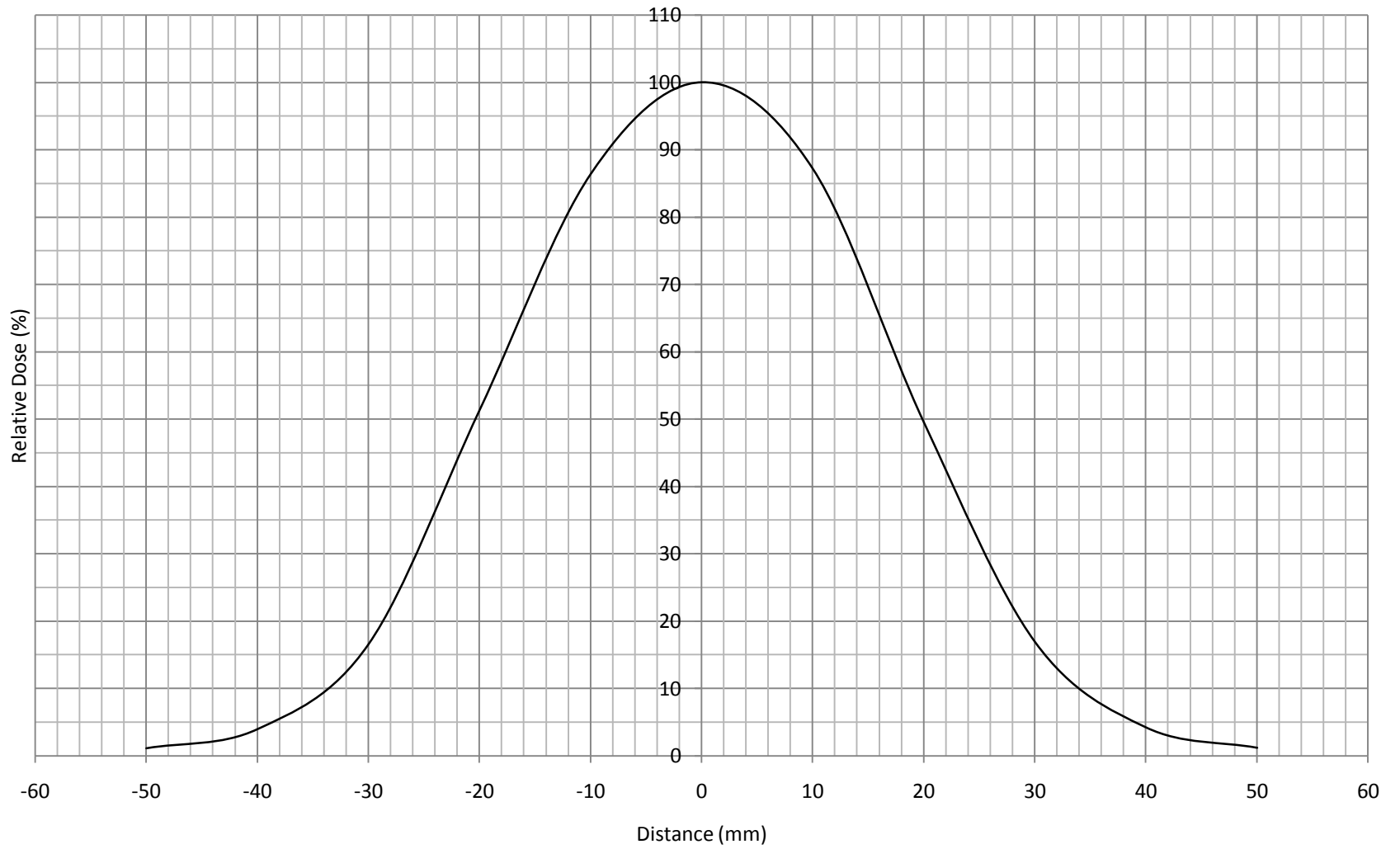
3-cm 110-cm SSD 12-MeV Profile



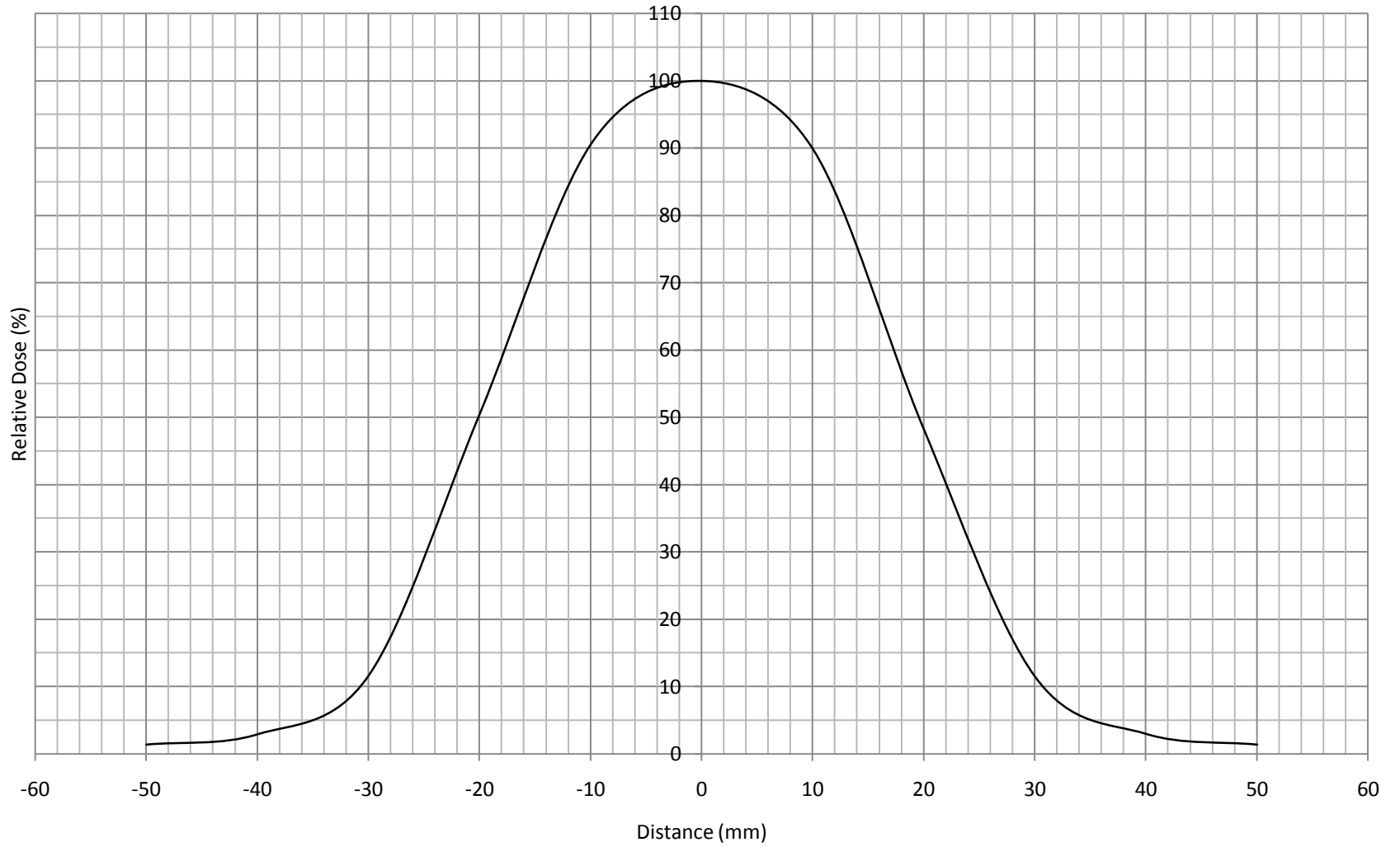
3-cm 110-cm SSD 15-MeV Profile



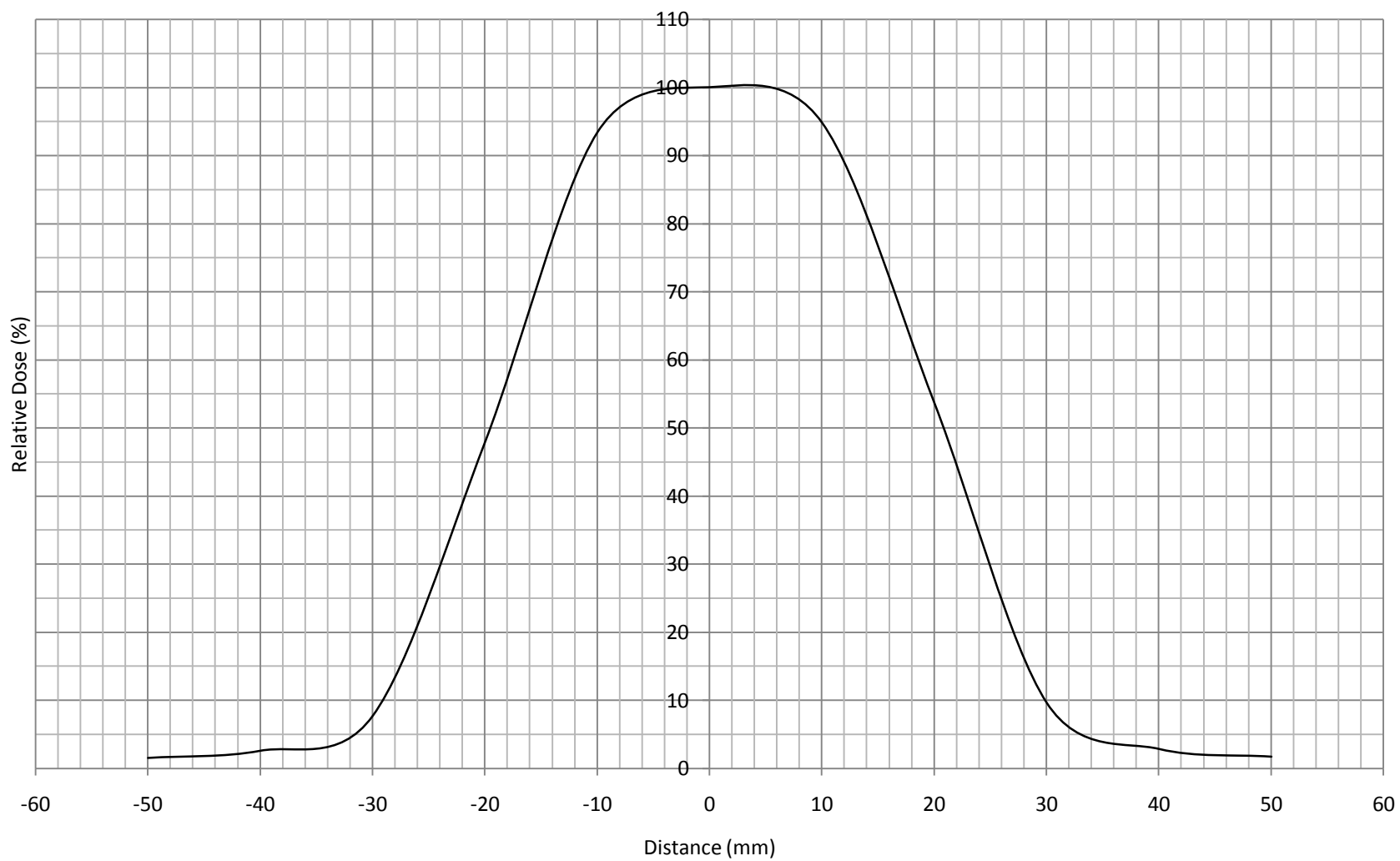
4-cm 110-cm SSD 6-MeV Profile



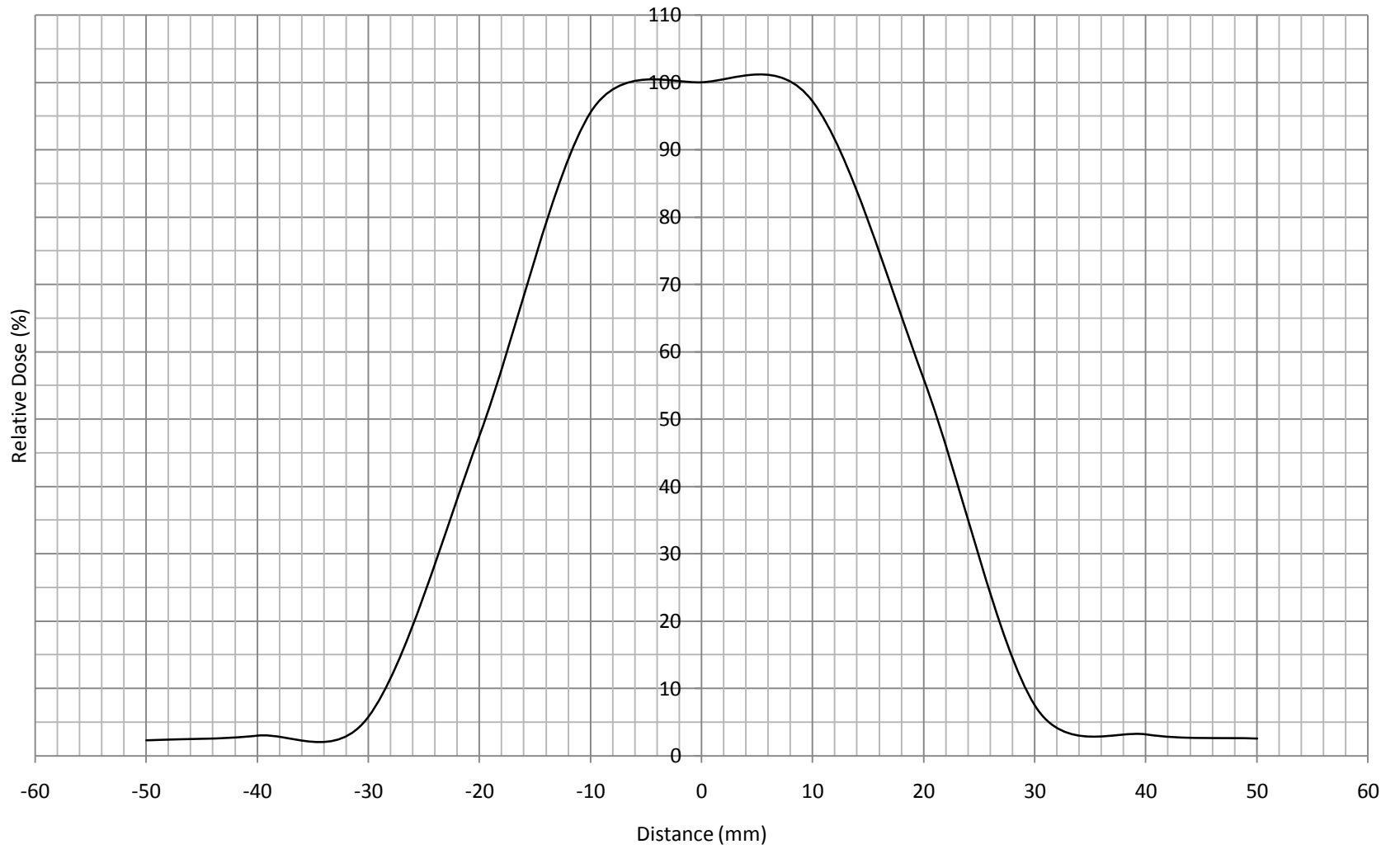
4-cm 110-cm SSD 9-MeV Profile



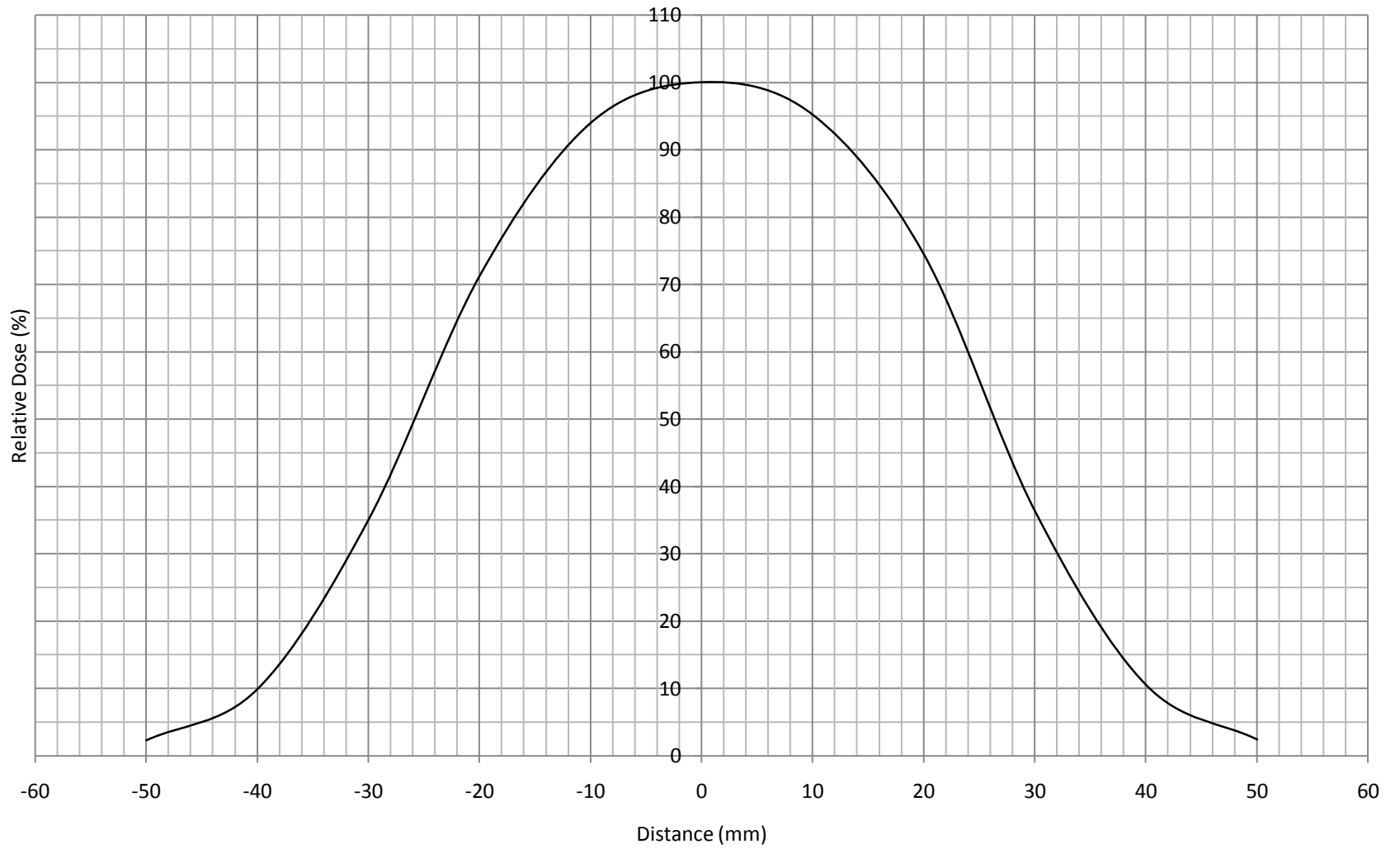
4-cm 110-cm SSD 12-MeV Profile



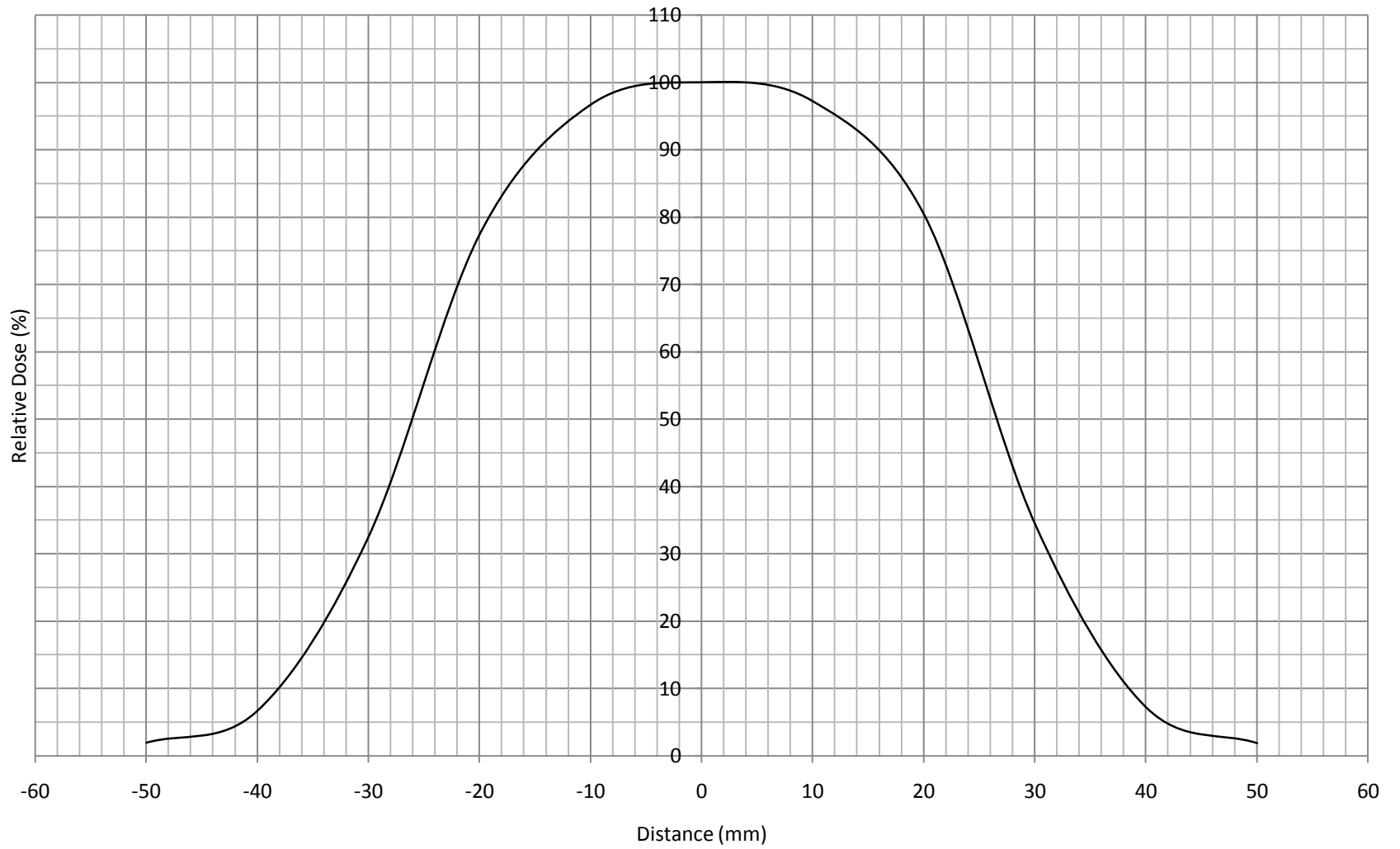
4-cm 110-cm SSD 15-MeV Profile



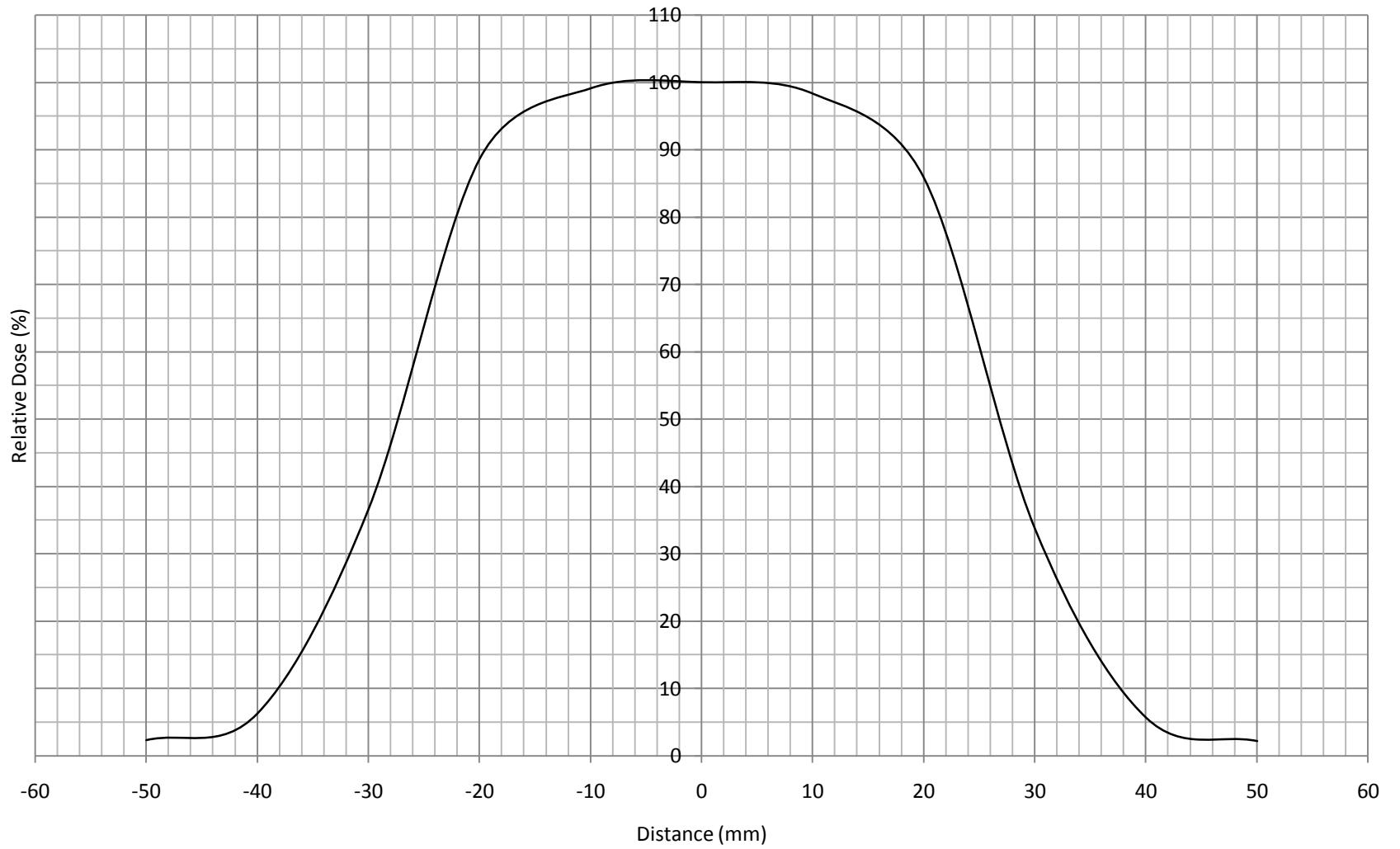
5-cm 110-cm SSD 6-MeV Profile



5-cm 110-cm SSD 9-MeV Profile



5-cm 110-cm SSD 12-MeV Profile



5-cm 110-cm SSD 15-MeV Profile

